UNIVERSITY OF LEEDS

Predicting Stiffness and Stress Variation of Saturated Clay Improved with Vibro Stone Columns and Evaluating its Effect on Improving Reinforced Foundations

Kareem Al Ammari
(200517914)

Submitted in accordance with the requirements for the
degree of
Doctor of Philosophy

University of Leeds
School of Civil Engineering

June
2016

Papers

Ammari, K. ; Clarke, B. (2016), 'Predicting the Effect of Vibro Stone Column Installation on Performance of Reinforced Foundations ', World Academy of Science, Engineering and Technology, International Science Index 110, International Journal of Civil, Environmental, Structural, Construction and Architectural Engineering, 10(2), 111 - 117.

ACKNOWLEDGEMENTS

I

Abstract

Vibro stone column techniques create an improved composite foundation in fine grained soils because of: (1) the installed load bearing columns of well-compacted, coarse-grained material and (2) the improvements to the surrounding soil due to the construction of the stone columns consolidating the surrounding soil. Extensive research work has been carried out over the last 20 years to understand the improvement in the composite foundation performance due to the consolidated soil. Few of these studies have quantified the changes in the stiffness and stress state of the treated soil, or have considered the impact that these changes have upon the performance of the composite foundation. Consequently, empirical and conservative design methods are still being used by ground improvement companies leading to a significant range of results in engineering practice. Based on cylindrical cavity expansion theory, two-dimensional finite element study to develop an axisymmetric model of a single stone column reinforced foundation was performed using PLAXIS 2D to quantify the effect of the vibro installation of this column in soft saturated clay by producing the load settlement response of the foundations. An updated mesh was used to cope with the large deformation of the soft clay around the installed column caused by the lateral expansion due to the Vibro technique. Different amounts of lateral expansion were simulated to determine the change in the stress state, stiffness and load settlement response. It was found that the radial expansion increases the pore pressure in the clay that starts to dissipate immediately after finishing the column installation leading to a permanent improvement of the stiffness of the soil which decreases with distance from the column. The radial stress acting on the column also changes creating a new coefficient of lateral earth pressure K, a key design parameter. The effect of these altered soil characteristics were assessed by applying a load to the composite foundation and calculating the resulting settlement.

The previous model results have been validated and applied for a well-documented field case of stone column groups using Plaxis 3D after adopting a conceptual model for accumulating the installation effect of two adjacent stone columns. A very good agreement between the recorded and simulated load-settlement curves was achieved after performing few calculation cycles of different degrees of expansion cavity. A simplified design framework base on numerical analysis in how to account for the stone column installation and the recommended degree of applied radial cavity during stone column installation was the main output of this research to achieve more efficient composite foundations.

Table of Contents

IV

VII

List of Tables

List of Figures

XI

XII

XIII

XV

XVII

Nomenclature

Unless otherwise stated, the following abbreviations and symbols are used in this thesis. However, when referring to specific publications, the original notation has been used.

Abbreviations:

CCET Cylindrical Cavity Expansion Theory

FEA   Finite Element Analysis

FEM   Finite Element Method

HS   Hardening Soil model

MC   Mohr Coulomb model

PWP   Pore water pressure

Symbols

α Slope of s/s_{uc} versus B/L line

β Settlement reduction factor (= $S_{treated}/S_{untreated}$)

γ Bulk unit weight

$\varepsilon_y, \varepsilon_h$ Vertical and horizontal strain, respectively

Δ_r Expansion cavity degree

κ Slope of unload/reload line on plot of υ versus $\ln(p')$ (Cam clay swelling index)

κ^* Modified swelling index

XIX

λ	Slope of isotropic normal compression line on plot of u versus $\ln(p')$ (Cam clay compression index)
λ^*	Modified compression index
$\boldsymbol{\nu}$	Poisson's ratio
σ_c	Stress on a stone column
σ_s	Stress on the soft soil
σ, σ'	Total and effective normal stress, respectively
$\sigma_1, \sigma_2, \sigma_3$	Major, intermediate and minor principal stress, respectively
$\sigma'_{col}/\sigma'_{soil}$	Stress concentration ratio
$\sigma'_{y,0}$, $\sigma'_{y,max}$	In situ and maximum vertical effective stress, respectively
τ	Shear stress
ϕ	Friction angle
ψ	Angle of dilatancy
A	Tributary area of soil per column in a large grid
A_C	Area of the stone column
A_S	Area of soil around stone column in unit cell
A/A_C	Area ratio
a	Width of square footing
b	Unit cell radius
C_C, C_S	Compression and swelling indices, respectively
C_k	Hydraulic change index (= $\Delta e/\Delta\log(k)$)

c	Cohesion
c_u	Undrained shear strength
c_r, c_v	Coefficients of consolidation in radial and vertical direction, respectively
D	Diameter of circular footing
D_c	Diameter of stone column
d_e	Unit cell diameter (= 2b)
E_i	Initial stiffness
E	Young's modulus
E_{oed}	Oedometer modulus
E_{ur}	Unloading and reloading stiffness (Young's modulus for unload-reload)
E_{50}	Secant modulus at 50% of the material strength
E_{col}/E_{soil}	Modular ratio
e_0	Initial voids ratio
F_c	Cavity expansion factor (Vesic, 1972)
F_q	Cavity expansion factor (Vesic, 1972)
f_d	Depth factor (Priebe and Grundbau, 1995)
g	Gravitational acceleration
G	Shear modulus
H	Thickness of soil deposit
I_L	Liquidity index

I_P	Plasticity index
I_r	Rigidity index (Vesic, 1972)
K	Coefficient of earth pressure
K_A, K_P	Coefficient of active and passive earth pressure, respectively
K_0	Coefficient of earth pressure at rest
K'	Bulk modulus
k_{vert}, k_{horz}	Coefficients of vertical and horizontal permeability, respectively
L	Column length
m	Power for stress-level dependency of stiffness
m_v	Modulus of volume compressibility
m_1	Ultimate bearing pressure improvement factor
m_2	Allowable bearing pressure improvement factor
N	Diameter ratio (= d_e/d_c)
N	Number of elements
n	Number of variables
n	Number of nodes in the element
n	Settlement improvement factor (= untreated/streated)
p, p'	Mean principal total and effective stress, respectively
p_A	Applied pressure
p_{ref}	Reference pressure (Hardening Soil model)
p_{lim}	'Limit pressure' at which indefinite expansion of a cavity occurs

XXII

q	Deviatoric stress
q	Discharge
R_f	Failure ratio (Hardening Soil model)
R_{inter}	Strength reduction factor (Hardening Soil model)
R_c	Stone column radius
s	Column spacing
s	Settlement of a finite group of stone columns
s_{uc}	Settlement of an infinite grid of stone columns
s/s_{uc}	Settlement ratio
t	Time
u	Vertical displacement
u	Pore water pressure
V	Soil volume
v_{ur}	Poisson's ratio for unloading
w	Strain energy or work done
w	Water content
Y	Yield
z	Depth of the soil element

1   Chapter 1: Introduction

1.1 General

Vibro stone columns, which enhance the bearing capacity and stiffness of soft soils, are a common technique for improving ground. They might be used to assist different loading combinations ranging from small footings to the loadings of large areas. Soft soils undergo significant deformation when subjected to small loads. So the main purpose of composite systems is to reduce its settlement.

Several methods of stone column installation have been developed over the last four decades to achieve well-compacted and efficient stone columns that work with the surrounding clay as composite system. All installation methods of stone columns involve partial to full radial displacement of the clay surrounding the vibro stone column. So the effect of this degree of lateral expansion on the response of the surrounding clay should be taken into consideration in the design process of the reinforced ground (Kirsch, 2006). In this study the dry bottom-feeding system for stone column installation, which is the most common, was used to model vibro stone column installation process. This system allows the feeding of granular material from the bottom of the poker by supplying these materials through the nose cone of the vibrator after reaching the required depth and without the need to use a water jet. Vibro compaction displaces the clay as the stone column is formed and, with time, the clay around the column consolidates and gains strength (Kirsch, 2004). The installation produces a variation in lateral stress and increase the pore water pressure within the clay, which leads to additional confinement for the stone column. An equilibrium state is eventually reached as the excess pore pressure dissipates, resulting in an increased stiffness of the surrounding soil. The stone column accelerates the rate of consolidation as enhanced drainage path (Munfakh, et al.,1984; Kirsch, 2006; Castro, 2007 and Gäb, et al.,2007).

The current design protocols of stone column reinforced foundations are generally based either on theories that were developed for single stone columns or on theories that consider the composite system of the stone column reinforced ground as a homogeneous medium, ignoring the effect of the column/soil interaction. They ignore changes in the stiffness and stress state that occur after column installation and consolidation, on the effect on the performance of this reinforced system. In this research, numerical modelling is applied to the three stages of stone column reinforced foundation construction, namely vibro installation of stone columns, radial consolidation to formed vertical stone column and consolidation after applying construction loading, in order to predict the stiffness and stress variation within the improved soil and evaluate its effect on improving the reinforced foundations.

1.2 Research Scope and Objectives

The scope of this research is to build upon previous studies and use cavity expansion theory to predict the variation of stiffness and stress state in the soft soils due to the installation of stone columns in short and long term. Commercial software was used to estimate the effect of variation of stiffness and strength on the performance of the improved ground, taking into account soil-column interaction of the soil adjacent to the column, and use it in design calculations of the foundation system. To achieve this aim, an in-depth study to build a model based on expansion cavity theory was developed to estimate the change of stiffness and stress state at various distances from the expanding cavity. An engineering design framework was developed to account for the stone column installation effect in an infinite group.

The objectives of this study can be summarized as follows:
- To develop a numerical model to simulate the case of axisymmetric single stone column that supports a rigid foundation. Realistic boundary conditions including restraints, ground water table, applied loads, columns installation methods were modelled.

2

- To use the numerical model in analysing large deformation due to the cavity expanding made by stone column installation and then assesse the changes in both the stress state and improved stiffness within the improved soft soils due to the column installation in both short term and long term, and quantify these changes with different degrees of cavity expansion. Plaxis 2D with the right input parameters of the physical and mechanical properties of both stone column material and soft saturated clay taken from case studies was used.

- To examine the material models that represent both soft saturated clay and stone column material and find the best representative ones. The calculation processes was carried out under the successive calculation phases that match the best field recorded data.

- To study and quantify the installation effect of single stone column on the settlement and bearing capacity performance of the treated ground after applying vertical loads using PLAXIS 2D.

- To develop a simplified numerical technique framework that designed for infinite group of stone column based on the single stone column case, which accounts for the improvements due to a certain degree of expansion, according to installation method, soft soli properties and columns spacings.

- To validate the single stone column model with a well-documented stone column group field case. Using the original ground properties, the geometry of the stone columns and the settlement records of the ground when subjected to loading after stone columns had been installed. This validation will be carried in two stages; Firstly, Use an axisymmetric homogenization method to simulate the installation of another stone column adjacent to the first one in Plaxis 2D. Then study stress interactions between the two columns for all the inter spacing cases and assess the accumulative improvement effect of stiffness and confinement for the applied expansion cavity degrees. Secondly, to use Plaxis 3D to simulate the actual geometry of the infinite installed stone columns in selected field case after applying the accumulated resulted lateral pressure coefficient and the stiffness

3

from the last step. Then compare the results with the field load-settlement records.

- Many degrees of expansion cavity during the installation process are to be carry out to achieve the most satisfactory agreement between the recorded and simulated load-settlement carves.

1.3 Structure of Thesis

The content of this thesis is organised into six chapters;

Chapter 1 provides general introduction with the research scope and objectives. **Chapter 2** provides a full detailed literature review of the stone column soil improvement technique, including historical development, advantages, construction methods and previous research works and design methods (analytical, experimental and numerical) that study the settlement performance of these foundations. Moreover, challenges related to the installation effect of the vibro stone columns are covered by the same chapter, which identifies the knowledge gap.

Chapter 3 presents a background of available numerical methods in general concentrating on the Finite Element Method that adopted in this research. Plaxis software was selected as an efficient available codes for this study. Material models, boundary conditions, mesh options and more features of Plaxis software are explained. Implementation of the principles of the finite element method using Plaxis has applied this chapter in the process of building the axisymmetric model of single stone column installed of well documented Bothkennar soft clay soil. Validation process has been carried out to check the use of Plaxis 2D and the selected Hardening Soil Model parameters to be Adequate for representing the soft soil. Finally, primary analysis checks have performed to establish the final Geometric dimensions and mesh specification for the finite element model to be ready for studying the stone column installation effect next chapter.

Chapter 4 presents a series of stone column construction simulation with different cavity expansion degrees. Then, the process of loading them to get the settlement response. The primary results generated by the finite element

model have revealed the changes that happen in the soft soil (stress state and stiffness) due to the installation of the stone column. Consequently, the relationship between the cavity expansion degree caused by stone column installation and settlement performance has been established. A simplified design framework base on numerical analyses to account for the increase of soft soil stiffness and lateral stresses after stone column installation in the design of the improve soil/stone columns system is presented

Plaxis 3D is used to validate the previous model results in **Chapter 5**. A well-documented field cases, namely wastewater treatment plant in Santa Barbara, California, US is utilised for this purpose. Ground profile, soil properties and the geometry of the stone columns are presented. The field load–settlement measurement curves are compared to the results of numerical load test using Plaxis 3D. Plaxis 3D proves to be able to capture the soil settlement behaviour. Then, the settlement of stone column group are studied after accumulating the effect of stone columns installations based on a conceptual stress-stiffness relationship. The predicted settlement of the improved ground after loading is compared with the actual settlement. Many degrees of expansion cavity during the installation process are carried out to achieve the most satisfactory agreement between the recorded and simulated load-settlement carves. The findings raise the importance of considering the impact of the installation methods of stone column on the performance of the system. Finally, 3D numerical analysis results is compared with settlement performance results of three previous studies for the same field case and all used numerical analysis techniques.

Finally, conclusions, discussion and future recommendations extracted from this research are presented in **Chapter 6,** highlighting its contribution to apply it in the engineering design and construction of stone column reinforced foundations. Figure 1.1 illustrates a brief research structure of this thesis.
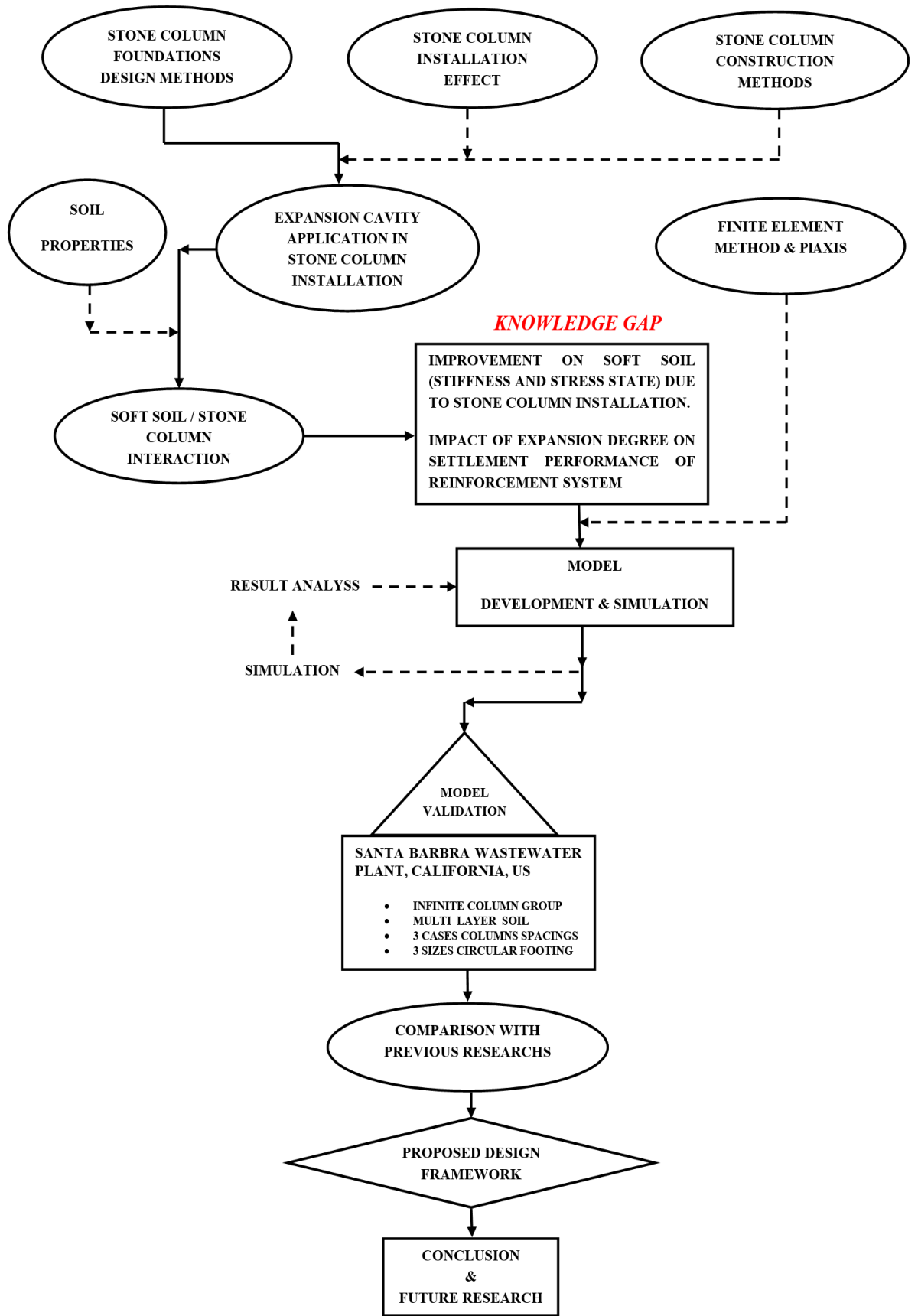
Figure 1.1 Illustration of research structure.

2 Chapter 2: Literature Review

2.1 Ground Improvement Techniques

The inevitable construction over soft and weak soils in urbanized and coastal areas has increased the demands to develop new construction techniques that overcome the poor ground conditions of these areas. As a result, a wide range of ground improvement techniques have been developed to be more economical modern alternatives to the traditional methods of construction that are usually based on transferring the loads to bearing strata using deep concrete piles. The main concepts of these ground improvement options usually involve one or more of the following processes; densification, drainage, cementation and reinforcement (McKelvey, 2002). These ground improvement techniques have become of great importance in the last three decades, giving more applications in practice (Simpson and Tatsuoka, 2008).

The development of the technology of these techniques will be critically important for the future of geotechnical practice for the following reasons:

- Low effective cost construction of infrastructure, with better balance of cut and fill (Simpson and Tatsuoka, 2008);

- Reduction of CO_2 emissions and construction energy (Simpson and Tatsuoka, 2008);

- Effective solutions for environmental issues using recycled industrial wastes and using demolition materials of old structures (Aqil et al., 2005);

- Remediation techniques for polluted ground and soils (Simpson and Tatsuoka, 2008);

- Maintenance and rehabilitation of decaying structures due to ageing (Simpson and Tatsuoka, 2008);

7

- Effective use in the protection of natural slopes and embankments, which become more unstable due to weather events and climate changes (Simpson and Tatsuoka, 2008).

Numerous ground improvement techniques are known involving mechanical and chemical stabilization, and hydraulic and electrical techniques. The selection of a suitable method is based on a number of factors. For example ground conditions, available material close to the site, and cost and effectiveness of the adopted method. Table 2.1 illustrates the classes of the known ground improvement techniques according to the improvement principle and the place of application.

Deep ground improvement techniques are methods that involve deep treatment of the ground mass by installing columns of stiffer material to reduce the settlement under applied loads. These could be considered "soft" piles because they are either formed of uncemented granular material, or weakly cemented soil mixed with lime or cement or soil columns stiffened by dewatering. These soft piles include vibro stone columns, lime compaction piles, deep mixing columns and compaction grouting.

Some of these columns simply modifies the soil in situ (the deep mixing columns) or replace the soil (replacement stone column); others displace the soil in order to increase the lateral resistance in order to support the column or produce a column in which the water content varies radially with distance from the column (displacement stone column and compaction grouting). A consequence of that every type has a different effect on the surrounding soil (Shen et al., 2005, Priebe and Grundbau, 1995). A full replacement column has no displacement impact on the surrounding soil. So less support is derived from it to the column compared to the case of full displacement column. However the full displacement column also consolidates the surrounding soil increases its strength to support more load. This increase in soil capacity, which is not taken into account in design considering yet, must contribute to the overall capacity of ground improvement system.

Table 2.1 Classification of Ground Improvement Techniques.

Classes of Ground Improvement Techniques	Improvement Method	Place of Application				Principle of Technique		
		Soil Mass	Soil Surface	Soft Pile	Tensioned Nail	Ground Reinforcement	Ground Improvement	Ground Treatment
Mechanical Techniques	Stone Columns			Θ		Θ		
	Deep Dynamic Compaction	Θ					Θ	
	Vibro Concrete Columns			Θ		Θ		
	Surface Compaction		Θ				Θ	
	Compaction Grouting			Θ			Θ	
Chemical Techniques	Surface Mixing		Θ					Θ
	Deep Soil Mixing			Θ		Θ		
	Lime Columns			Θ		Θ		
	Jet Grouting	Θ					Θ	

Category	Technique	1	2	3	4	5	6	7
	Permeation Grouting	Θ					Θ	
	Blasting	Θ					Θ	
Tension Techniques	Soil Nails				Θ	Θ		
	Geosynthetics		Θ	Θ		Θ		
	Ground Anchors				Θ	Θ		
	Deep Soil Nailing				Θ	Θ		
Electrical Techniques	Electro-osmosis		Θ		Θ		Θ	
Hydraulic Techniques	Preloading	Θ					Θ	
	Drainage/Surcharge		Θ	Θ			Θ	
	Vertical Drains			Θ		Θ		
	Dewatering	Θ						Θ
Heating/Freezing Techniques	Freezing	Θ						Θ
	Heating	Θ						Θ

2.2 Vibro Stone Columns

Vibro stone columns is one of the most common soil improvement techniques, which is utilized worldwide to increase bearing capacity and reduce the total and differential settlements of superstructures constructed on soft and weak soils (Mitchell, 1981). The method is an application of the vibro compaction technique, which was first used in the 1930s to treat loose cohesionless soils by densification. The application of this technique was performed by pushing a vibratory poker into the ground. This vibration helped to rearrange the particles of soil, increasing the density and consequently increasing the stiffness and bearing capacity of the soil mass (McKelvey, 2002). In the 1950s, engineers tried to apply this technique to improve fine-grained soils such as silts and clays, but unfortunately, these fine-grained soils did not respond to deep vibration. However, it was found that the best way to utilize the vibro technique to improve these kinds of soils was to install a column of granular material using a deep vibrator to create a column/soil system in which the columns are confined by the soil with the columns acting as the foundations. Since the technique displaces the fine soil, and increases the pore pressure in the soil. This PWP dissipates radially because of the stone columns, increasing the stiffness of the composite system.

2.3 Application of Stone Columns

There are numerous benefits of using stone columns as an improvement technique for soft fine soils, including:

1. Substantial increase in the shear strength of the original ground (Cooper and Rose, 1999);

2. Enhanced drainage of excess pore water, because stone columns have high permeability compared to clay (Wood et al., 2000);

3. Higher shear strength and stiffness than soft clay, i.e., they behave more like a pile foundation;

2.4 History of Stone Column Foundations

The first use of stone columns was possibly for military purposes in Bayonne, France in the 1830s (Ayadat et al., 2008). Crushed aggregate columns of 0.2 m diameter and 2 m length were installed in soft estuarine deposits to support the heavy foundations of artillery bases. It was reported that the use of these stone columns resulted in a significant reduction of settlement and large improvement in the stability of the foundations (Hughes and Withers, 1974).

This technique was not mentioned again until the 1930s when Serzey Steuerman, an employee of the Keller Company in Germany, revolutionized this technique by inventing a simple vibratory machine that could improve the ground by using a poker vibrator. The first fully reported field project using this vibro compaction technique was in 1937 when it was used to densify a 7.5 m depth of loose sand *in situ* beneath a building in Berlin, and the result was a 45–80% increase in density and a doubling of the bearing capacity (Slocombe et al., 2000).

The vibro compaction technique was transferred to the United States (USA) after Serzey Steuerman formed his own company for vibro flotation foundations (VFC) in Pittsburgh, USA. The development of this technique was continued in both Germany and the USA during the 1940s and 1950s, and the treated depth was increased to about 20 metres. By the end of the 1950s, this technique was introduced into Great Britain and France, where there was a need to treat finer and more cohesive soils, which are very common in Great Britain, in particular. Therefore, the challenge for VFC and Keller was to develop a means to install stone column materials into fine-grained soils. In 1956, an advance of the vibro replacement technique solved the limitation of vibro compaction in cohesive soils. In this technique,

a borehole is created in the soil by a vibrating poker. Then, coarse aggregate is poured into the created borehole and the poker is used to compact the backfill. This creates stone columns that form a tight inter-lock with the soil that surrounds them. McKelvey et al. (2004b) states that the length of these columns can easily reach 15m and in typical cases the column would occupy the place of 10–35% of the soil in the location. How the soil types that can be treated by deep vibratory techniques are extended by the vibro replacement technique is demonstrated in Figure 2.1.
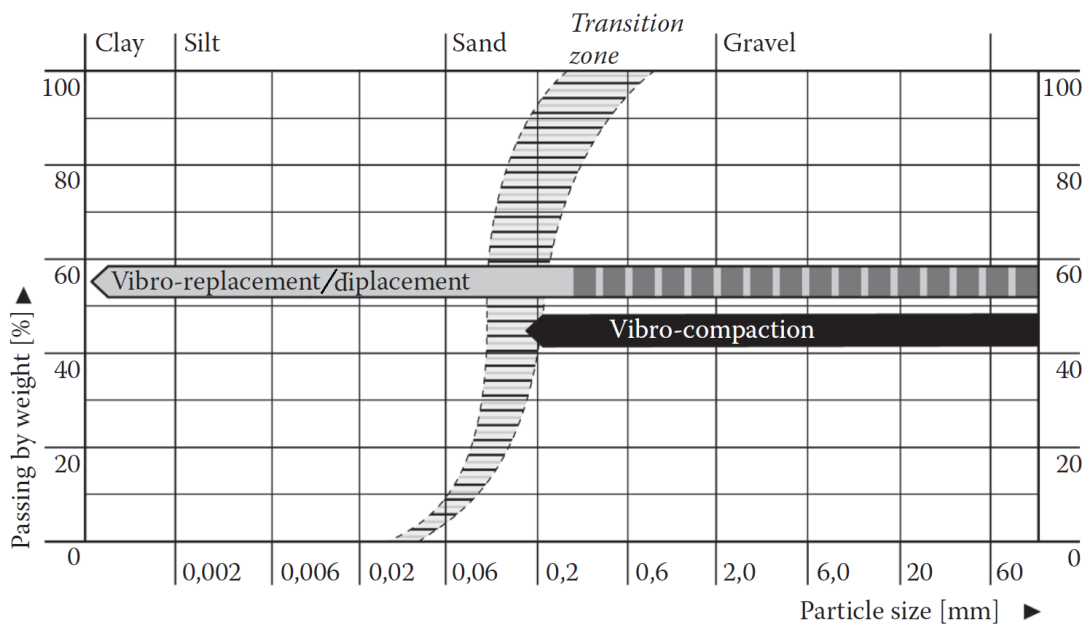
Figure 2.1 The types of soils that can be treated through the vibro replacement and compaction techniques (http://keller-foundations.co.uk, 2011).

According to the strength of the fine-grained soils and the on-site ground water conditions, two different methods were developed to meet the design requirement of treating fine-grained soils, namely the wet method and the dry method. These methods are described in more detail later in this chapter. In 1955, the stone column technique started to spread to Japan and then later on to China and many other countries (Greenwood, 1975).

In 1972, due to the development of drill rigs and poker vibrators and the need for a faster method for stone column installation, a new drill rig was developed that could penetrate and discharge stone simultaneously,

13

allowing the concept of bottom feeding of stone column formation (Greenwood, 1975).

2.5 Equipment Used in the Vibro Stone Column Technique

The main equipment used in the construction of a vibro stone column is the poker (vibrator) Figure 2.2. It has a torpedo shape with a diameter ranging from 0.30–4 m, a length from 2–5 m and a weight varying from 2–4 tonnes, according to the purpose and size of the project. The poker vibrator is facilitated with an eccentric weight attached to a shaft near the bottom of the vibrator. When the vibrator rotates around its vertical axis, the eccentric weight emits a horizontal vibration that is applied directly to the ground. This vibrator is connected to the follower tubes. They in turn are suspended from a crane, Figure 2.3. Fins are fixed on the head of the vibrator to prevent it from rotating in the hole. The vibrator is linked to an electrical or hydraulic motor in the crane. The power and flush supply pipes are accommodated within follower tubes located on the side of the vibrator. Figure 2.2 presents the detail of a typical vibrator. More developed rigs are purposed built with facilities for penetration, feed delivery system, digital data acquisition systems and modems to transmit data from site to office (Slocombe et al., 2004). Additional details about vibro stone column equipment can be found in Brauns (1978), Baumann and Bauer (1974) and Greenwood and Kirsch (1983).
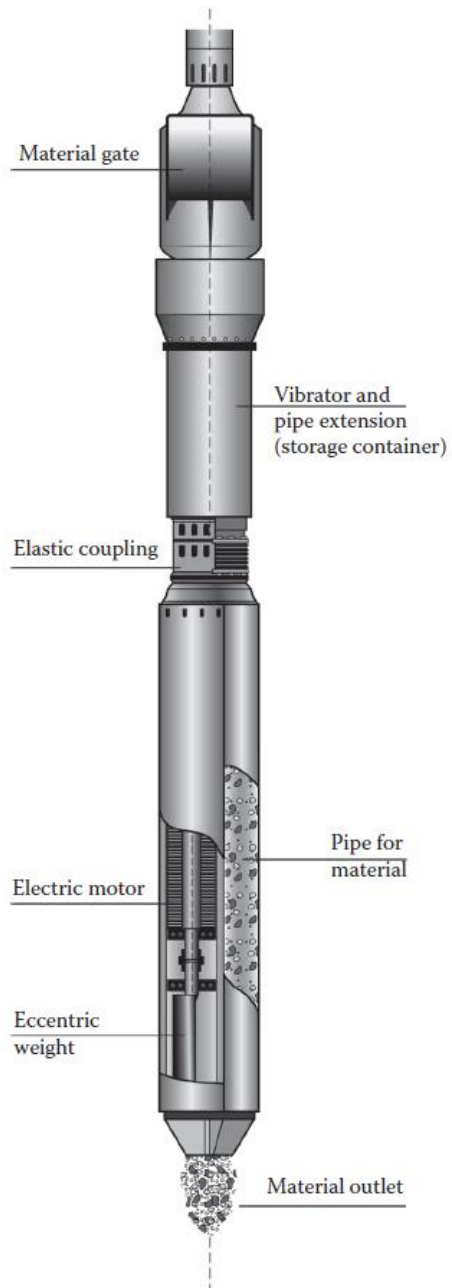
Figure 2.2 The poker (vibrator) (http://keller-foundations.co.uk, 2011).

Figure 2.3 Dry bottom feed system using 'vibrocat' (http://keller-foundations.co.uk, 2011).

2.6 Vibro Stone Column Construction

Many methods of stone column installation have been developed over the last four decades to achieve well-compacted and efficient stone columns that work with the surrounding clay as one composite system. Using the right material for the stone column is the first important step. This material must not break down during installation or under loading, must be free of fines (clays and silts), inert to any chemical reaction with the minerals of the surrounding clay and clean from any contamination that could affect the ground water (Hu, 1995). The particle size of the stone column material varies from 20–75 mm depending on the method of installation and the type of vibrator. Uniformly graded gravels are preferable in practice (McKelvey et al., 2004). There are two conventional methods of stone column installation based on the treated soil conditions: the dry top-feeding method and the wet top-feeding method.

2.6.1 Vibro Displacement by Dry Top-Feeding Method

In Dry Top-Feeding method, compressed air is used to help in the penetration process in addition to the vibration and self-weight of the vibrator. Compressed air also releases the suction forces as the vibrator is withdrawn from the hole. The hole is formed by displacing the *in situ* soil laterally without any soil removal, (a in Figure 2.4). When the vibrator reaches the required depth, it starts to withdraw thereby allowing a charge of stone material, which has already been placed on the top of the hole, to be introduced into the annulus between the borehole sides and the vibrator, (b in Figure 2.4). This process is carried out in stages and at every stage the vibrator is reintroduced into the borehole to compact the stone material already in place,(c in Figure 2.4) until the stone column is finished, (d in Figure 2.4).

Dry Top-Feeding method is usually used for stable cohesive soils with undrained shear strengths exceeding 30 kPa (McKelvey, 2002), and when the ground water level is beneath the treatment depth to ensure that the

borehole sides do not collapse during withdrawal of the vibrator. The stone column diameters formed by this method usually range between 0.4–0.8 m.
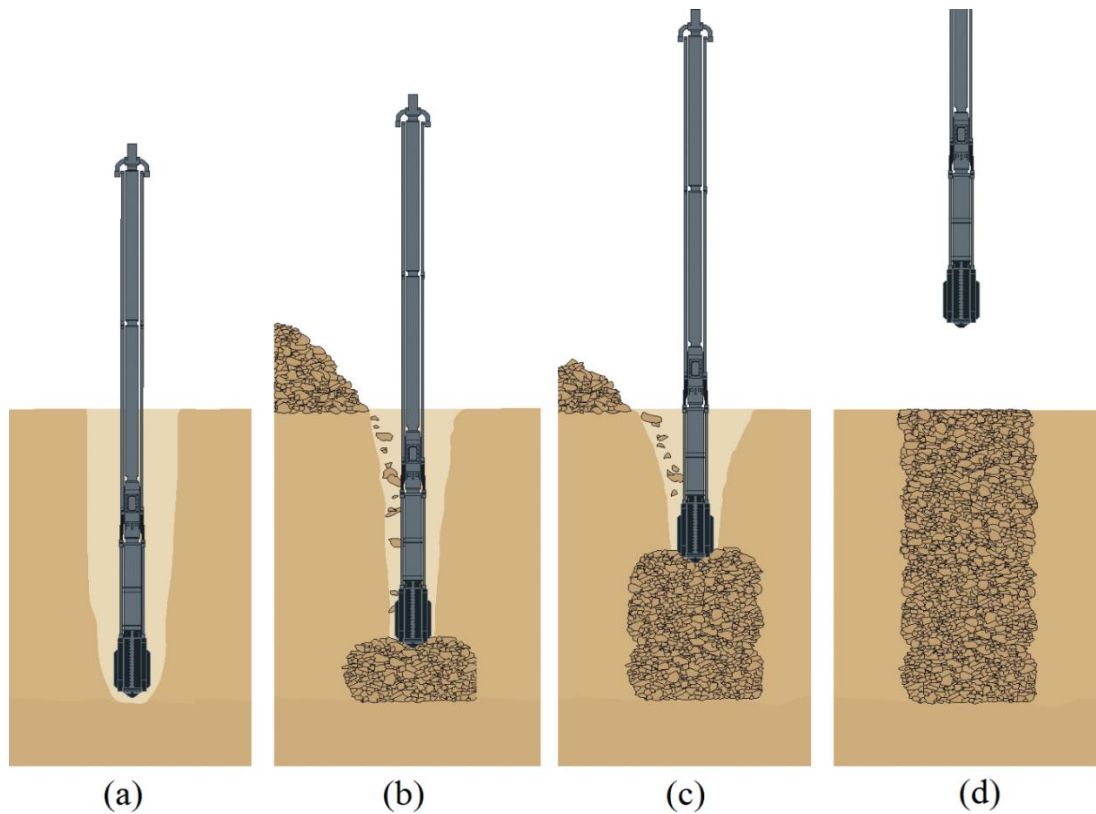
Figure 2.4 Vibro displacement by dry top-feeding method (http://keller-foundations.co.uk, 2011).

2.6.2 Vibro Replacement by Wet Top-Feeding Method

Wet Top-Feeding method is usually used for soft, cohesive soils with a high ground water table and undrained shear strength of less than 30 kPa. In these kind of soils, the side walls of the borehole could collapse and therefore there is a need for continuous support during the stone column installation process. To present this, a current of water is jetted from the nose of the vibrator to aid the penetration the soft soil, (a in Figure 2.5) and this water current keeps the side walls of the borehole stable as shown in (b in Figure 2.5). When the vibrator reaches the desired depth, backfill is introduced into the hole through the annulus between the borehole and the vibrator, (c in Figure 2.5), and the poker is moved up and down in the borehole to compact the stone column material and push it against the walls

of the borehole, (d in Figure 2.5). The diameter of the stone column in this method usually ranges between 0.8–1 m.
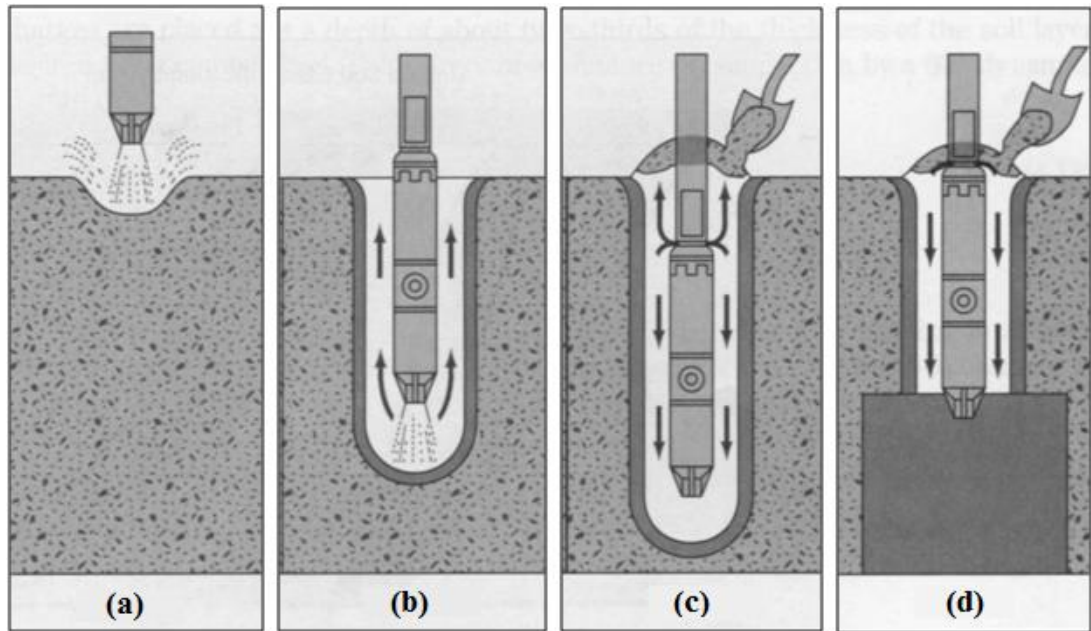
Figure 2.5 Vibro replacement by wet top-feeding method (McKelvey, 2002).

2.6.3 Vibro Displacement by Dry Bottom-Feeding Method

In both of the previous methods, the need to remove the vibrator to introduce a charge of stone column material and then reintroduce the vibrator again to compact the stone slows the installation process and can cause collapse of the borehole walls. A new system of vibro equipment was developed in Germany to overcome these problems. This system allows the feeding of granular material from the bottom of the borehole by supplying these materials through the nose cone of the vibrator after reaching the required depth and without the need to use a water jet. This system is called the dry bottom-feeding system; Figure 2.6. In this method the installation process is unaffected by the presence of ground water and it is suitable for a wide range of soft soil conditions and strengths ($Cu=15-50$ kN/m^2) (McKelvey, 2002). It is now the most commonly used method for vibro stone column installation. More detail about the methods of vibro stone column installation

can be found in Jebe and Bartels (1983), Greenwood and Kirsch (1983) and Watts et al. (1989).
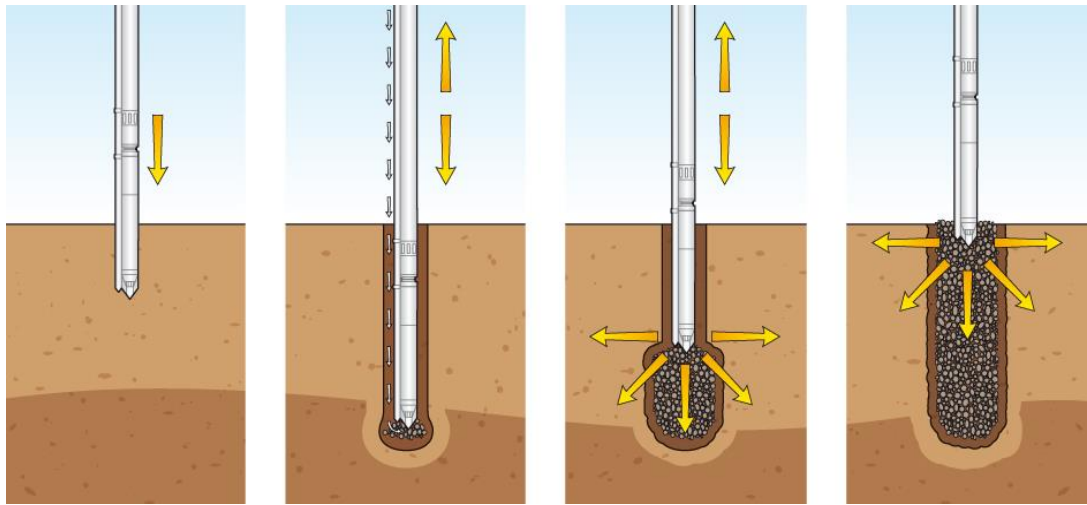
Figure 2.6 Vibro displacement by dry bottom-feeding method (http://keller-foundations.co.uk, 2011).

A compozar method is another technique to construct stone columns which has been developed in Japan, as shown in Figure 2.7. The principle of this technique is to drive a steel casing pipe into the ground until the desired depth is reached by using a vibratory hammer. Then the stone is placed inside the pipe and the pipe is withdrawn gradually while the sand is driven into the borehole and compacted using an air compressor (Aboshi et al., 1979).
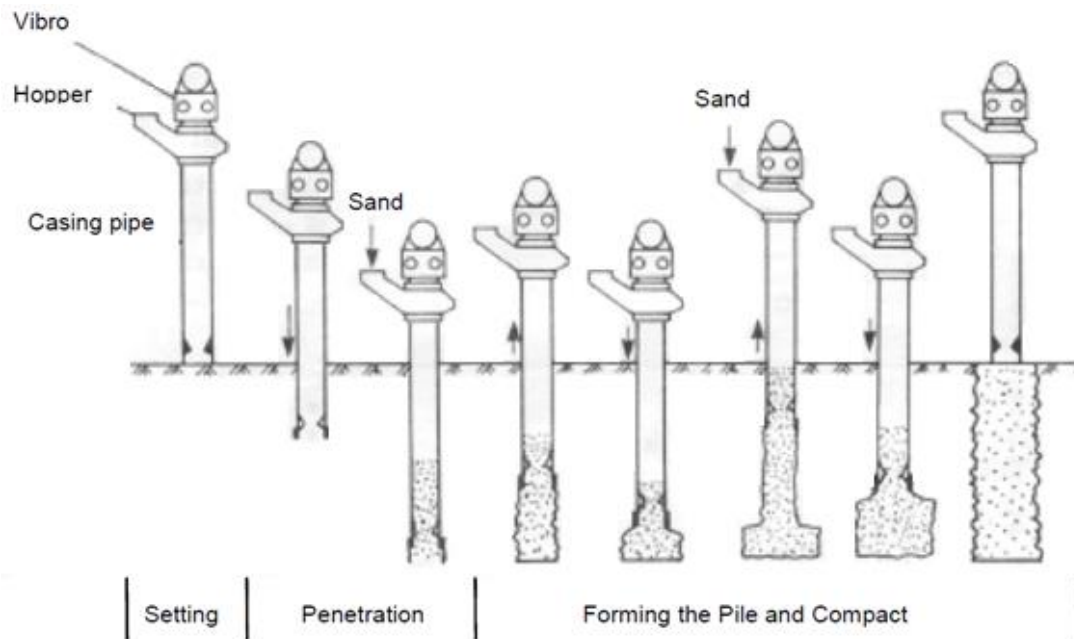
Figure 2.7 Compozar method (Aboshi et al., 1979).

2.7 Mechanism of Stone Column Performance

Soil improvement through vibro stone column techniques consists of two main parts: (1) the installed load bearing columns of well-compacted, coarse-grained backfill material (Mitchell, 1981) and (2) the improvements to the surrounding soil due to vibro compaction (Priebe and Grundbau, 1995). However, the second part of the vibro stone column performance is difficult to assess, both in terms of settlement reduction and enhanced load bearing capacity (Hassen et al., 2010).

Two major effects can be distinguished due to the installation of stone columns: the displacement of the ground due to the creation of the stone columns and changes within the soil due to movements of the vibration poker (Kirsch and Sondermann, 2003). This increases the lateral stress within the clay which provides additional confinement for the stone column. An equilibrium state is eventually reached when the horizontal stress in the stone column equals that in the soil adjacent to the column. This increase in lateral stress increases the pore pressure, which dissipates with time. The stone columns accelerate the rate of consolidation of soft clays, providing a

drainage path and relieving excess pore water pressures (Munfakh et al., 1984).

2.8 The Performance of Stone Columns

Soft clayey soils, which have poor characteristics in terms of stiffness, strength and drainage, can be treated by vibro stone columns. As a result of these poor characteristics, foundations on such type of soils are subjected to large settlement even under relatively low loads. So, settlement is considered as the main governing criterion in the design of these stone columns foundations. Significant cost impact of the time of consolidation can be noticed in soft soils, stone column soil improvement technique can minimize the time of the consolidation. Consequently, this strengthens the soil more quickly and, therefore, less time would be required to complete construction projects such as embankments.

Before reviewing the literature of the research in this subject, it is important to define some concepts.

2.8.1 Stone Column Patterns

Figure 2.8 shows typical arrays of stone columns used to support pad foundations (a), strip foundations (b) and line loads (c, d and e).
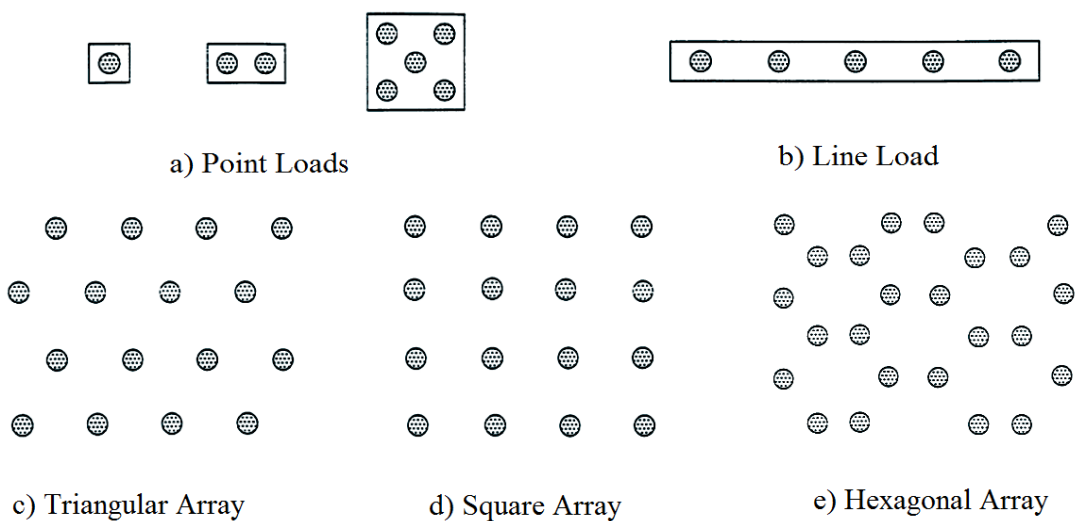
Figure 2.8 Stone column patterns (after Mitchell, 1981).

2.8.2 Unit Cell

The unit cell in a stone column reinforced foundation system can be defined as a stone column with its tributary area of soil (Hu, 1995), as explained by the following equation (2-1):

$$A = A_c + A_s \qquad (2\text{-}1)$$

where A is the unit cell area;

A_C is the stone column section area;

A_S is the stone column tributary area of soil.

The real shape of this unit cell is a regular polygon area, but using a finite element method. Balaam and Poulos (1978) have proved that the unit cell area can be approximated, accurately enough, as an equivalent circle to ease the studying of the behaviour of stone columns. Figure 2.9 illustrates the equivalent diameter, d_e, of the unit cell for the three types of arrays used, in which the columns are spaced, s, apart.

This is the physical definition of the unit cell, but the more important use of this term is as a concept or theory to calculate and design the stone column reinforced foundations. See section 2.10.1.
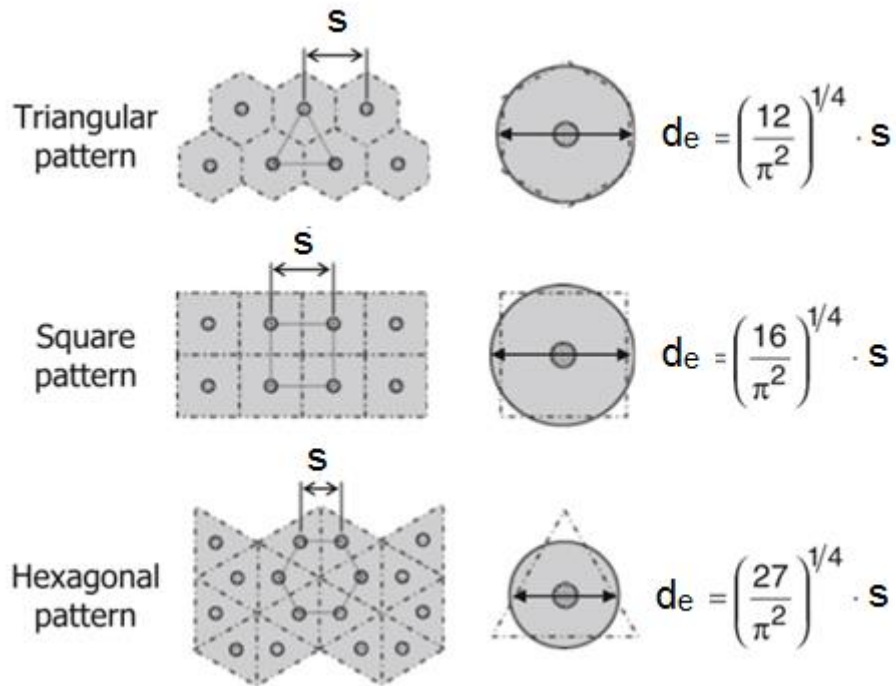
Figure 2.9 The equivalent unit cell for different types of stone column patterns (after Balaam & Poulos, 1978).

2.8.3 Area Ratio (μ_s)

The area ratio is the ratio of the area of a stone column section to the area of its unit cell of soil, which is explained by the following equation (2-2):

$$\mu_s = \frac{A_C}{A} = \frac{A_C}{A_C + A_S} \tag{2-2}$$

Figure 2.10 shows both the area of stone column and its equivalent soil area in triangular pattern.
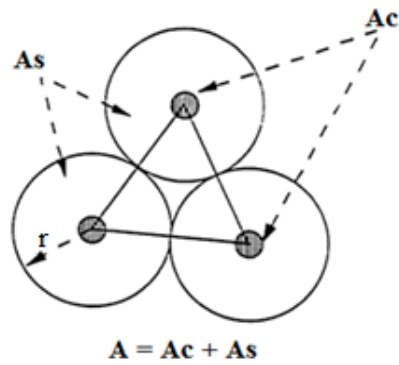
Figure 2.10 Area definition of unit cell.

It is important to mention here that, according to the installation procedure of the stone column, the area ratio may be called a replacement ratio or a displacement ratio.

2.8.4 Stress Concentration Ratio (n)

The stress concentration ratio (n) is defined as the ratio of the uniform average vertical stress on a stone column (σ_c) to that applied on the surrounding soil (σ_s) within the unit cell (Hu, 1995), as illustrated in Figure 2.11 and by the following equation (2-3):

$$n = \frac{\sigma_c}{\sigma_s} \qquad (2\text{-}3)$$
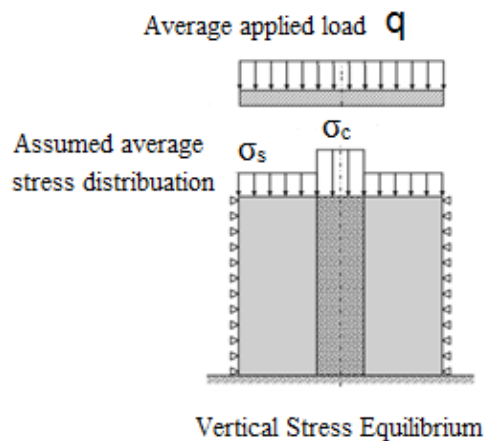
Figure 2.11 Stress concentration ratio definition (after Saadi, 1995).

Based on the concept of the unit cell, the relationship between the stress concentration ratio (n) and the ratios of stresses in both clay and stone column, a_s and a_c respectively, can be defined as follows:

$$\sigma = \sigma_s \mu_s + \sigma_c(1 - \mu_s) \tag{2-4}$$

$$\sigma_c = \frac{\sigma}{1+(n-1)\mu_s} = a_c\sigma \tag{2-5}$$

$$\sigma_s = \frac{n\sigma}{1+(n-1)\mu_s} = a_s\sigma \tag{2-6}$$

Due to the discrepancy of the stiffness between the clay and the stone material, the column normally carries more load than the clay, especially in the initial stages of loading. This ratio is important to express the changes in stiffness and stress state of the treated clay during loading and after consolidation.

2.8.5 Settlement Reduction Ratio β (Improvement Factor)

The settlement reduction ratio for a given load level is defined as the ratio between the settlement of soil reinforced by stone columns at this load level and the corresponding settlement of the unreinforced soil (μ_s = 0). Many researchers use the term "Improvement Factor" to express this ratio. The value of this factor is ranged between 1 and 6.

$$\beta = \frac{S}{S_t} \tag{2-7}$$

2.9 Laboratory Studies

Laboratory-based analyses of stone column behaviour were very few before 1974 compared to experimental fieldwork studies, but the need to validate the theoretical solutions and simulate the field monitoring data has encouraged many researchers to become involved in the analytical aspect of the work. Based on the foci of previous laboratory research, the studies can be divided into isolated column studies and column group studies.

2.9.1 Isolated Column Studies

One of the most fundamental laboratory models used to understand the behaviour of a single stone column under loading was carried out by Hughes and Withers (1974). A Leighton Buzzard sand column was installed in one dimensionally consolidated clay (kaolin) bed. The length of the column was 150 mm and the diameter ranged between 12.5–38 mm in order to examine the influence of area replacement ratio on the behaviour of this column. A stress-controlled loading procedure was used in these tests and loads were applied only to the column area. Figure 2.12 shows the equipment used.
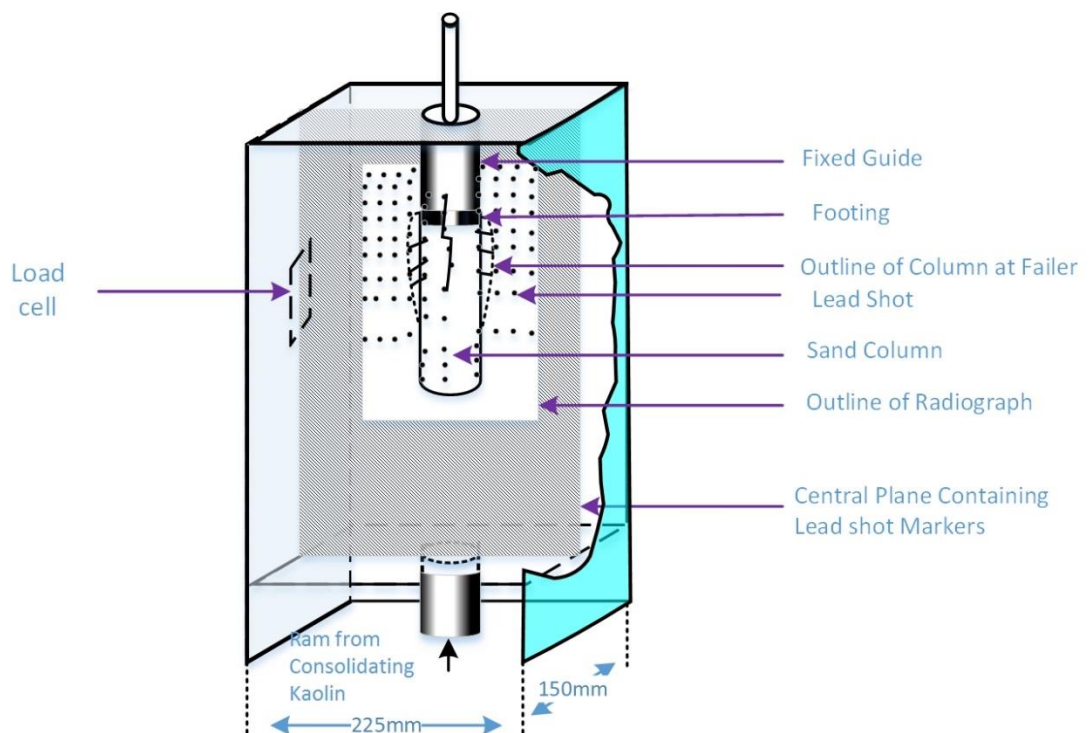
Figure 2.12 The single stone column laboratory model (after Hughes & Withers, 1974).
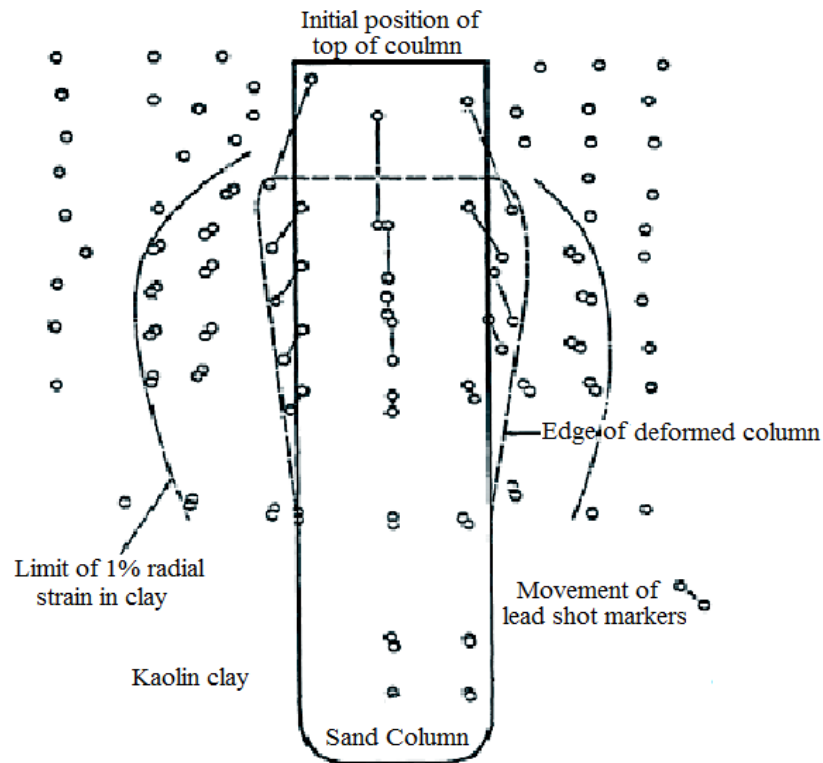
Figure 2.13 The displacement of lead markers due to loading using radiographs (after Hughes & Withers, 1974).

A radiographic technique was used to monitor the pre-placed lead shot markers and investigate the behaviour of the stone column under this load, as shown in Figure 2.13.

The authors monitored the behaviour of the stone column after gradual loading and found that the column started to bulge near the upper part, as shown in figure 2.14. This bulging, in turn, increased the lateral confinement of the surrounding clay around this zone thereby reducing the settlement by the factor of six times compared to the unreinforced clay and increasing the bearing capacity significantly, as shown in Figure 2.15. The ultimate strength is mainly controlled by the lateral confinement of the surrounding clay in the bulging zone. This is similar to the behaviour of the pressuremeter with the radial resistance of the surrounding soil reaching its limiting value when the bulge is about four diameter lengths from the top (Hughes and Withers, 1974). This length is defined as the critical length at which end bearing and bulging failure will occur simultaneously in a single column.
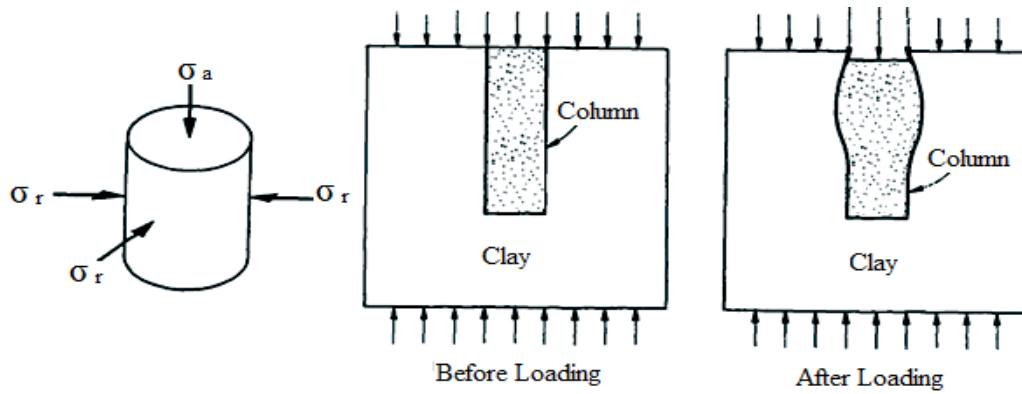
Figure 2.14 Load bearing mechanism of single stone column (after Hughes & Withers, 1974).
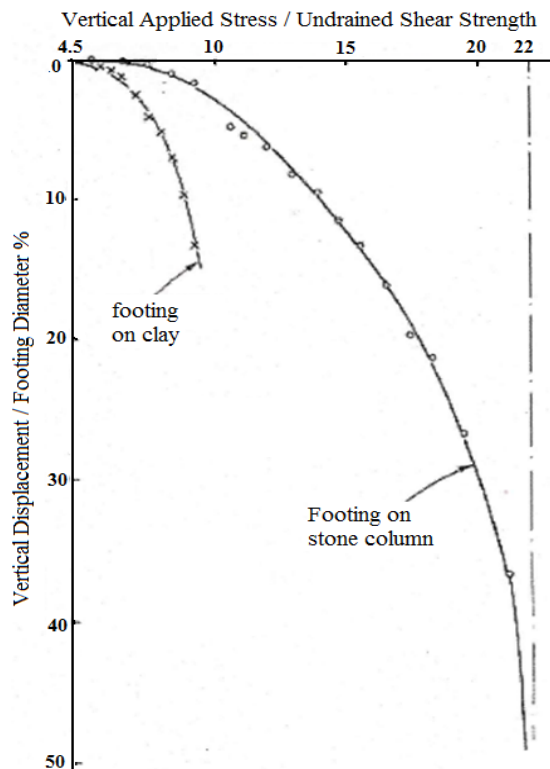
Figure 2.15 Load settlement curves for a stone column reinforced footing and an unreinforced one (Hughes & Withers, 1974).

Due to the similarity between the behaviour of a stone column and the pressuremeter test, Hughes and Withers adopted Gibson and Anderson (1961) expression for the expansion of the cylindrical cavity to assess the ultimate capacity load for a single stone column. This simple method will be explained in detail in section 2.10.3.

Greenwood (1991a) states that the bulging occurs in the upper part of the stone column because of the high stresses transferred directly to this part, while the confining radial stress of the surrounding clay is relatively low, due to the low overburden pressures at this level.

Although, Hughes and Withers' laboratory model was essential in describing the procedure of stone column bulging, they missed an important aspect of this behaviour when they applied the load just to the stone column and ignored the surrounding clay. This is because the surrounding clay reduces the interaction between the clay and the columns and increases the interface shear. Christoulas et al. (2000) confirmed that this is the case by conducting a laboratory test model using pressure cells and electronic piezometers to monitor the pore water pressure and lateral stresses in the treated clay. They found that the length of the bulging zone is 2.5–3 times the column diameter, whereas Hughes and Withers found this length to be four times the column diameter because they just applied the load to the stone column.

Charles and Watts (1983) examined the effect of the replacement ratio of a single stone column on the vertical drained displacement of reinforced clay under a rigid foundation load by installing single stone columns with different diameters in remoulded clay, using a large oedometer 1.0 m diameter and 0.6 m high, as illustrated in Figure 2.16.
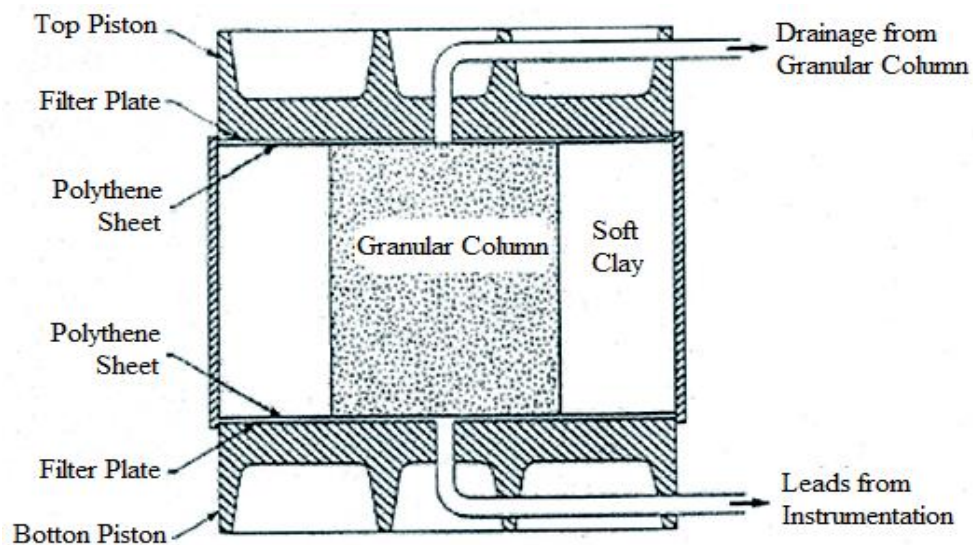
Figure 2.16 Large oedometer test used for a single stone column (Charles and Watts, 1983).

This large-scale oedometer was provided with earth pressure cells to measure the changes in stresses within the column/clay system, with electrical piezometers to measure the changes in pore water pressure within the clay and with linear variable differential transducers (LVDTs) to assess the changes in the stone column diameter and vertical movement.

Charles and Watts (1983) found that increasing the stone column diameter has a significant effect on reducing the compressibility of the clay layer. Figure 2.17 illustrates the effect of the replacement ratio on the bearing capacity of reinforced soil. They recommended a 30% replacement ratio to get a satisfactory settlement reduction.
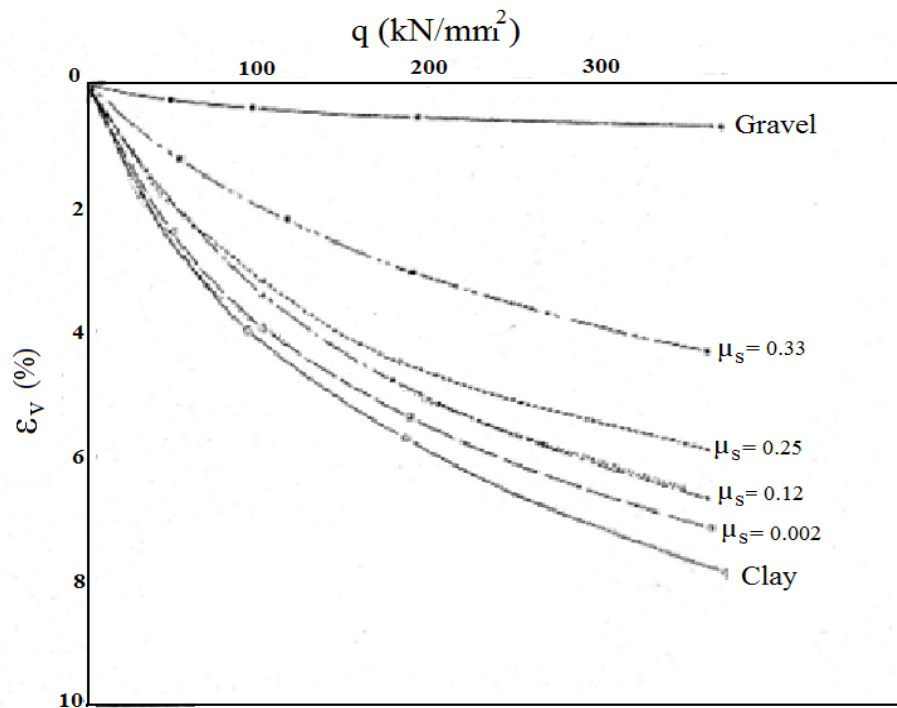
Figure 2.17 Replacement ratio effect on the load-settlement relationship (Charles & Watts, 1983).

In 1983, Barksdale and Bachus conducted a series of drained vertical load tests with single end bearing columns using a physical unit cell chamber (108 mm diameter and 305 mm high, Figure 2.18, to study the behaviour of uniform loading over an infinite system of stone columns.
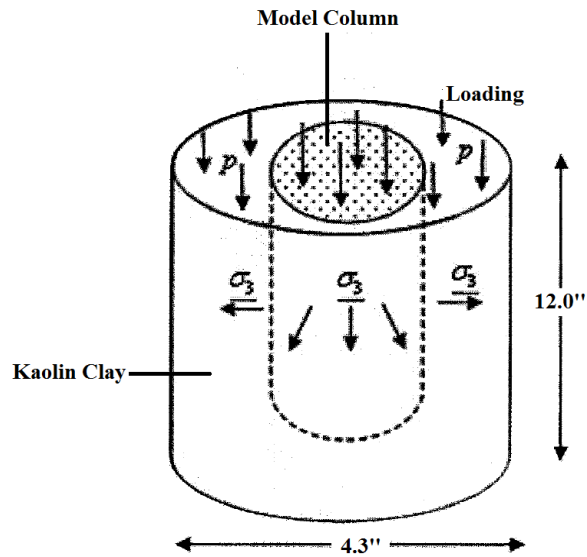
Figure 2.18 Idealization of physical unit cell (after Barksdale & Bachus, 1983).

A one-dimensional load using a rigid piston was applied in increments to the column and the surrounding clay. The settlements were recorded for different replacement ratios. The results of these unit cell tests showed that as the replacement ratio increases, the settlement reduction ratio reduces. Figure 2.19 illustrates these results.
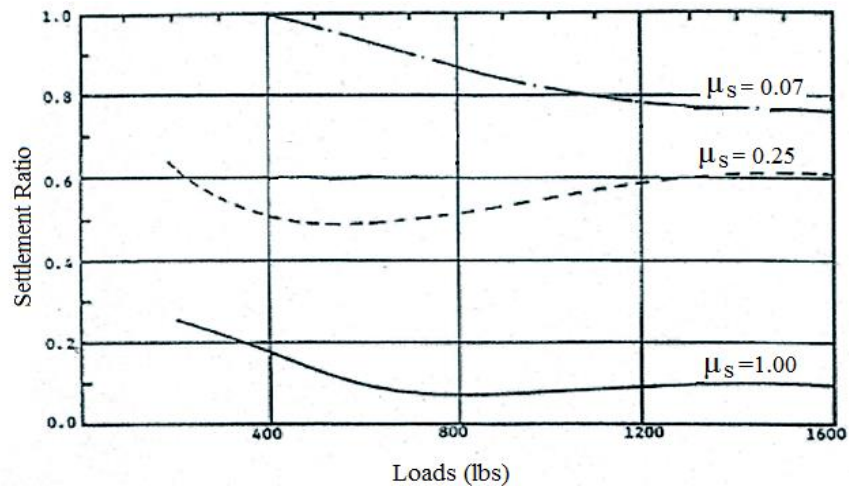
Figure 2.19 The effect of the replacement ratio on the settlement reduction ratio. Physical unit cell model (after Barksdale & Bachus, 1983).

Barksdale and Bachus (1983) found irregular settlement reduction with increasing the applied load for the replacement ratio of 0.25%. They recommend μ_s = 40% to achieve satisfactory settlement reduction. They also

mention that the stress concentration ratio (n) decreases slowly with time and load level from 4.2 to 2.8. Although the authors did not pay enough attention to the last result, which is related to the stress concentration ratio (n), it is considered to be more important than the other ratios because it expresses the permanent change of stress state and stiffness within the stone column-soil system that confines the bearing columns.

Juran and Guermazi (1988) designed a modified triaxial cell with 100 mm diameter specimens and performed a series of laboratory tests to study the effect of replacement ratio, loading rate, loading process and partial consolidation on the performance of granular column reinforced soft soils. The results showed qualitatively that the parameters have a significant influence on the settlement reduction and the vertical stress concentration ratio in the reinforced soil foundation.

The significant influence of the studied parameters on the vertical stress concentration ratio supports the research idea of this report that the changes of the stiffness and stress state of the clay after column installation (short term) and consolidation (long term) have an important influence on the performance of ground reinforced with stone columns.

Narasimha Rao et al. (1992) studied the effect of the length and the diameter of the stone columns under loading by conducting a set of tests on an isolated column. The result showed that when the stone column length increases, the bulging zone becomes shorter and the confinement stress of the surrounding clay reduces. This usually continues until the ratio of the column length to the diameter is more than 8, after which there is no significant benefit of increasing the stone column length to attempt to increase the bearing capacity.

2.9.2 Column Group Studies

Much of the early research in the field of stone column reinforced foundations such as Thorburn and MacVicar (1968), Thorburn (1975), Greenwood (1970), Hughes and Withers (1974) and Hughes et al. (1975)

showed that the unit cell concept governs the behaviour of the stone column group system, which means that every column, within its unit cell, acts independently from the neighbouring units, ignoring any interaction between these columns and the accumulative confinement of the surrounding clay. These authors state that the bearing capacity of a group of stone columns that supports a foundation is equal to the bearing capacity of single column unit cell multiplied by the number of these columns, considering that the failure of a stone column group is as a result of bulging, as in the case of the isolated column, as shown in Figure 2.20.
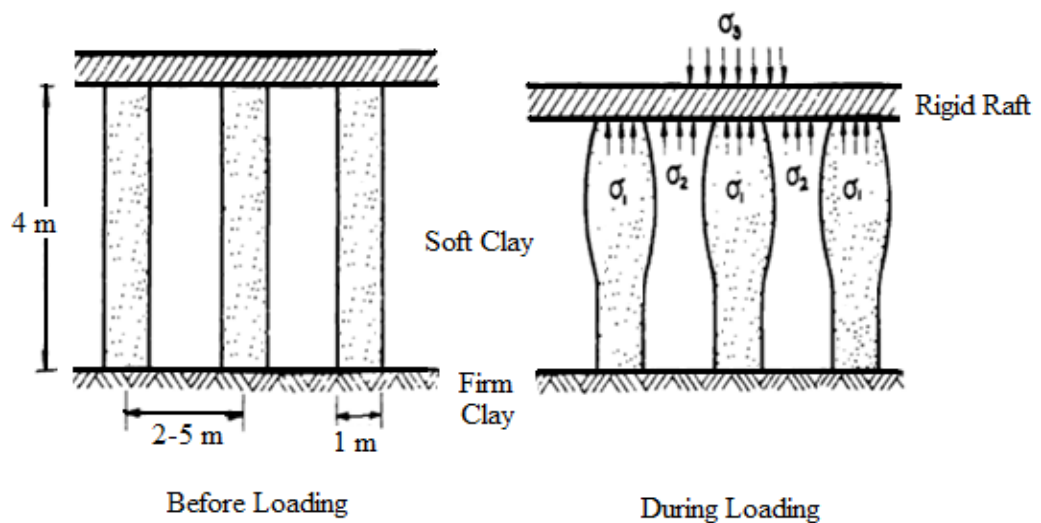
Figure 2.20 Load bearing mechanism of small group of columns under a rigid footing load (after Hughes & Withers, 1974).

This is a conservative approach to design of stone column reinforced foundations because it ignores the effect of adjacent columns in increasing the confinement. Many attempts have been made to take into account the interaction between the columns within the stone column group and to study the effect of increasing the confinement pressure due to the existence of the group on transferring the load to a greater depth and changing the mechanism of failure.

One of these attempts was made by Barksdale and Bachus (1983), who performed a series of vertical loading tests on a group of stone columns that reinforced a clay medium within a testing box. The vertical rigid load test

results showed clear evidence of the interaction effect between two adjacent columns, which restrained the bulging of the interior sides of the columns, as shown in Figure 2.21. (Barksdale and Bachus, 1983) reported stress concentration ratios higher than those found in the results of unit cell tests, which means that the confinement around the columns increases, enabling them to carry a higher proportion of load. The increase in bearing capacity in this case reached 70% compared to unreinforced clay.
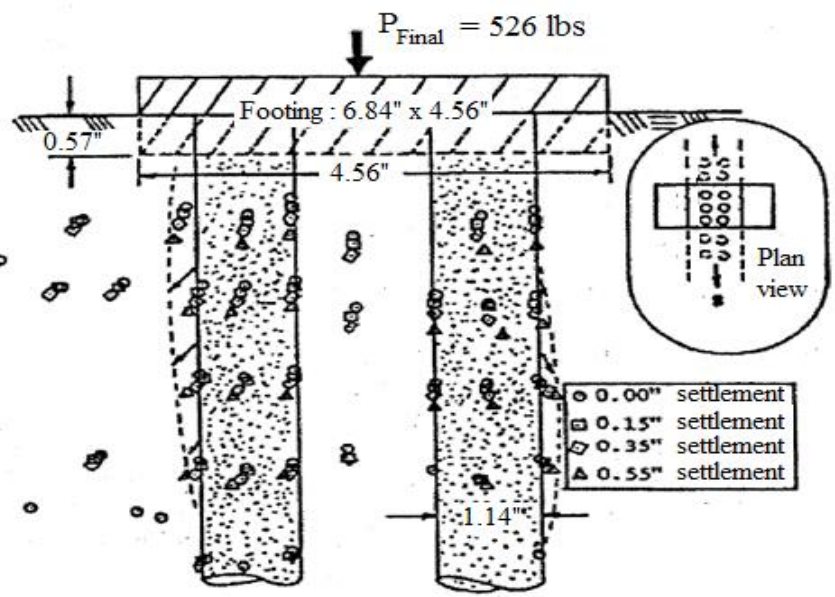
Figure 2.21 Bulging of stone columns within the group (after Barksdale and Bachus, 1983).

However, at that time, the authors did not pay enough attention to this interaction and they concluded that the effect of the interaction of the columns in the group on the bearing capacity of every column of the group is limited, as Figure 2.22 shows that there is only a 10% increase in capacity.
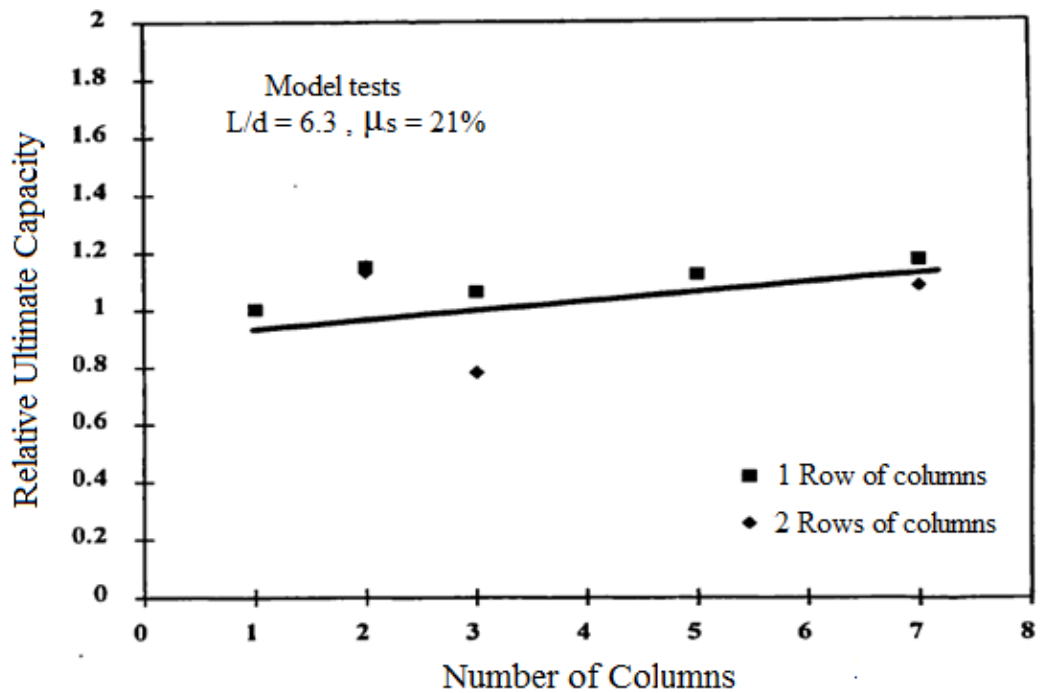
Figure 2.22 Increase in load bearing capacity per column with increase in total number of columns (after Barksdale & Bachus, 1983).

In Japan, the Japanese Port and Harbour Research Institute (PHRI) conducted a set of centrifuge tests on large diameter stone columns, which were installed using the compozar method, in order to study the performance of these stone columns on the bearing capacity of reinforced soft soil and the failure mechanism. Toyoura sand and kaolin were used in this model and the load was applied at a constant displacement rate of 17.5 mm/min under 50 g gravity conditions, achieving an undrained situation (more details can be found in Terashi and Kitazume (1990) and Hu (1995). The geometry of this model is illustrated in Figure 2.23.
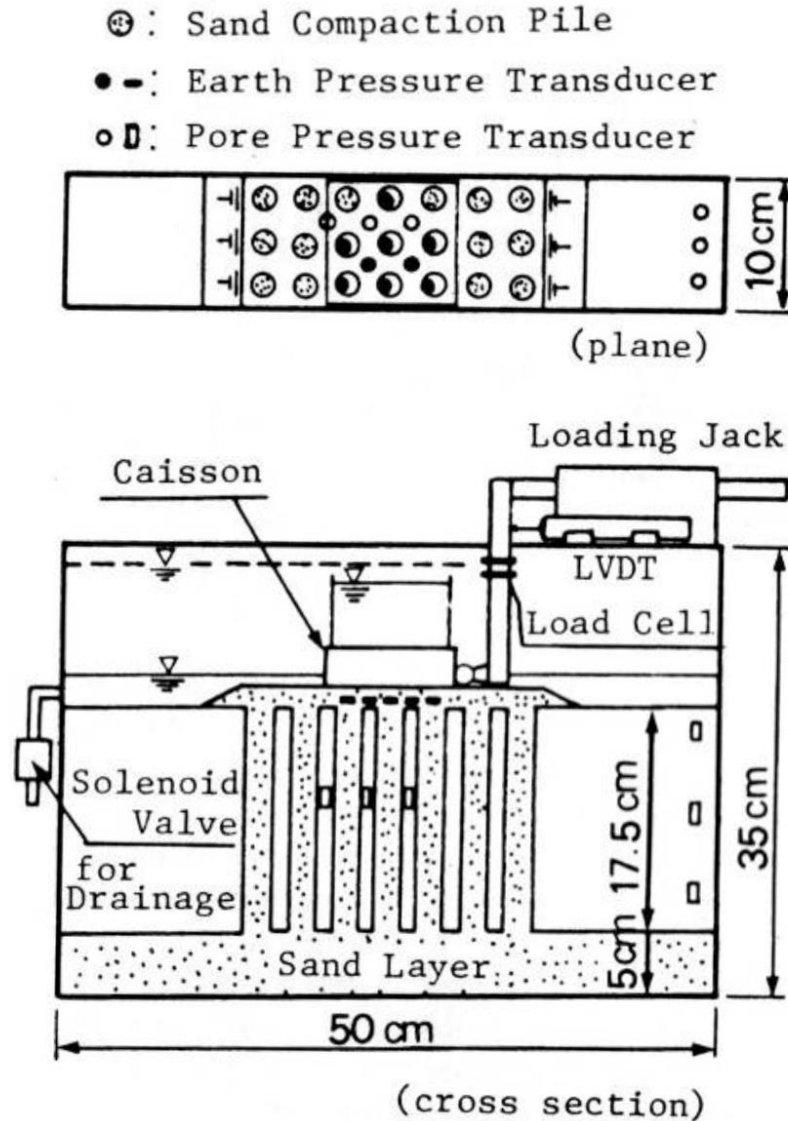
Figure 2.23 centrifuge experimental set-up of the model test using the compozar method (after Terashi and Kitazume (1990).

The results of these tests showed the importance of using the stone columns technique in increasing the bearing capacity of soft soils and revealed the deformation patterns and failure mechanism of this group, as shown in Figure 2.24.

Figure 2.24 Deformation pattern and failure mechanism of sand compaction piles group (after Terashi and Kitazume, 1990).

There was no mention at that time of the interaction between the stone columns. Terashi and Kitazume (1990) restudied the results of these centrifuge laboratory tests and reported that the deformation patterns and failure mechanism of a group of stone columns are different from those described by unit cell theory. Hu (1995) also used the result of the centrifuge model to validate his conclusion, which will be explained later.

The Tokyo Institute of Technology (TIT) undertook another centrifuge model of stone columns to investigate the effect of increasing the width of the compaction pile reinforcement area outside the footing limits on the performance of the column/soil system. Using Toyouta sand for the compaction and Kawasaki clay for the soft soil, undrained displacement controlled tests with an applied rate of 0.1mm/min under a 50 g gravity condition were performed. Area ratios of 23% and 36% were studied for three reinforcement areas: B, 2B, 3B, where B was the width of the footing. The results showed that there is a clear improvement in bearing capacity as the reinforced area increases. Increasing the width of the reinforcement area and a higher area ratio leads to a significant increase in bearing capacity

compared to the same width with a smaller area ratio, but the effect of this increase becomes negligible after a certain limit. Figure 2.25 presents this effect. This behaviour was interpreted by Hu (1995) as follows: as the a_s value increases, the load transfers deeper into the ground.
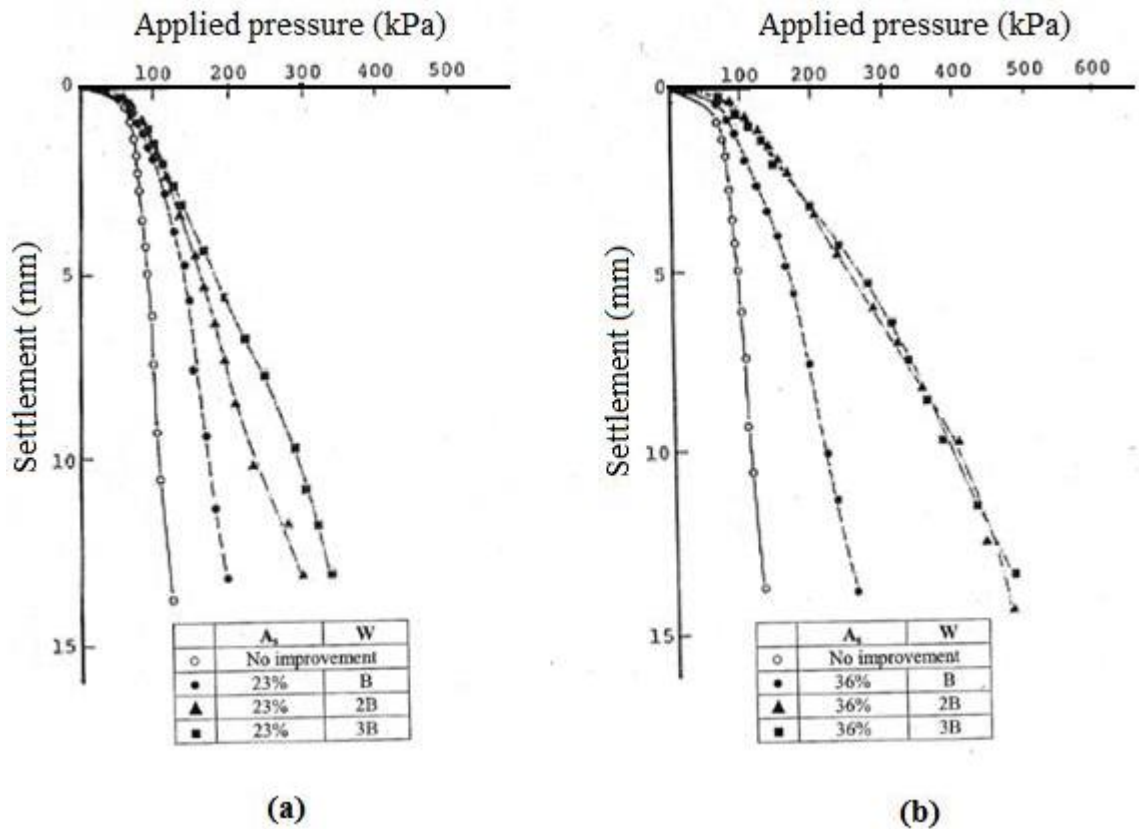
Figure 2.25 The effect of reinforced area width on improved system performance for as=23% and as =36% (after Terashi and Kitazume, 1990).

In order to create a clear physical model that would capture the column/soil and column group interaction, Hu (1995) carried out an extensive series of tests concentrating on area replacement ratio, column length, method of installation, initial strength of treated soil and flexibility of applied footings. The tests were conducted by applying the load on a 300 mm diameter area of one-dimensionally consolidated kaolin that was reinforced with a group of fine sand columns under fully drained conditions.

In qualitative terms, the findings of Hu's study can be summarized by the following points:

- Increasing μ_s results in an improvement in bearing capacity and settlement performance. Figure 2.26 shows the settlement of the ground surface adjacent to the footing for different rates of μ_s. Hu (1995) recommends an area ratio greater than 24% to achieve a significant improvement in reinforcement foundation systems.
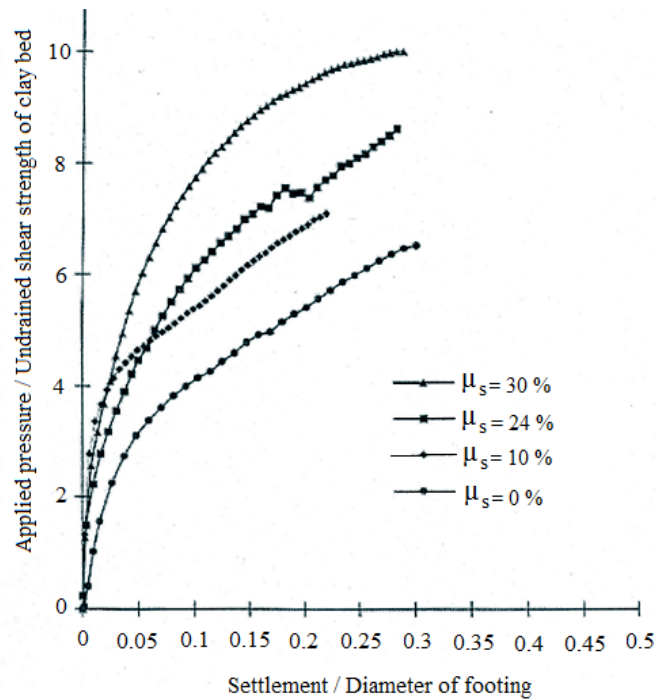
Figure 2.26 Effect of area ratio, As, on the settlement performance of a stone column group (after Hu, 1995).

- As the area replacement ratio increases, the stress concentration ratio (n) increases.

- Increasing the ratio L/d (column length to column diameter) causes an increase in bearing capacity. This continues to a limiting L/d ratio. However, after that limit there is no noticeable improvement when this ratio increases. These results are presented in Figure 2.27.
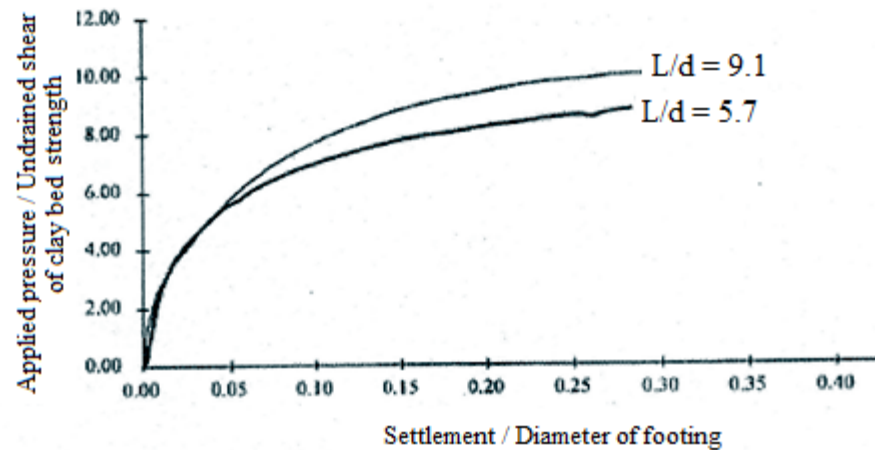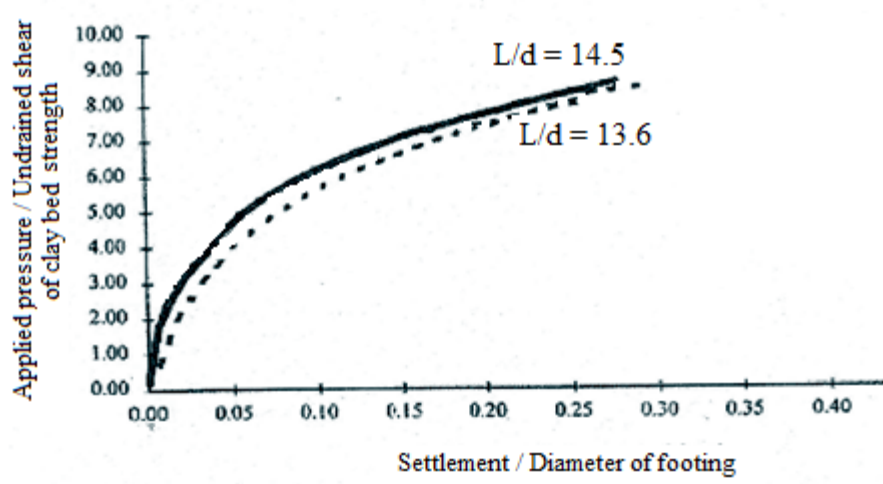
Figure 2.27 Effect of column length on the performance of reinforced clay (after Hu, 1995).

- An important contribution of Hu's study was the analysis of the deformed shape of the columns during and after the loading process. He concluded that the columns usually deform by bulging, punching, shearing and bending. This deformed shape happens within a conical region directly beneath the footing. This conical shape interacts with the neighbouring columns preventing bulging in the upper part of the internal columns, while the bulging in the outer columns remains in the upper part as shown in Figure 2.28. Figure 2.29 illustrates the deformed shape of the stone column group. Hu mentioned that the depth of the failure wedge increases as the a_s ratio increases.

(a) Before overall failure

(b) After overall failure

(c) Horizontal movement deduced from centrelines of columns
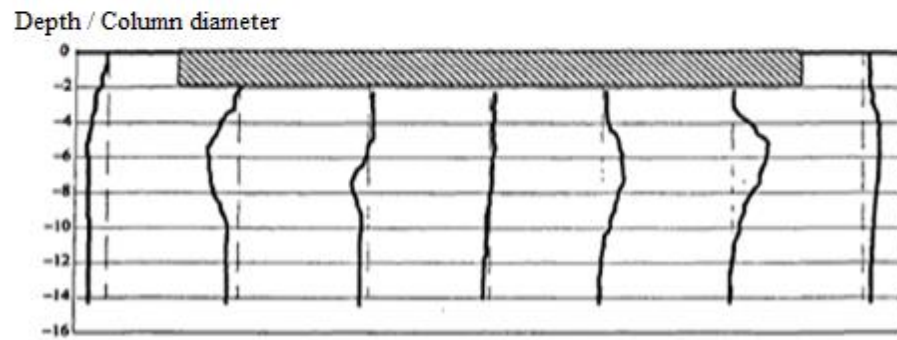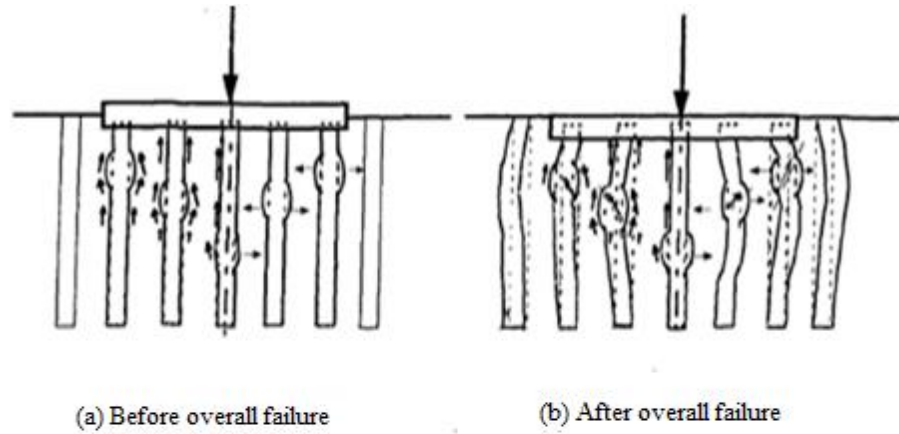
Figure 2.28 Interaction between the stone columns before and after failure (after Hu, 1995).
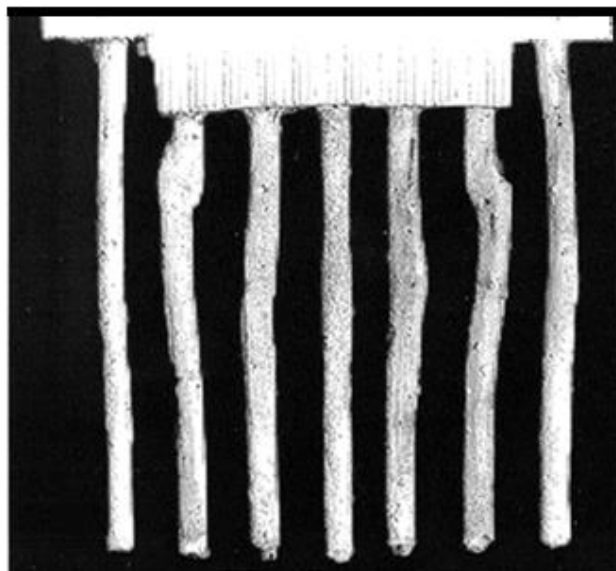
Figure 2.29 Deformations for stone column group under loading suggested by Hu (Hu, 1995).

- Hu (1995) proposed that the mode of failure for a group of stone columns is a general shear failure with four parts that are schematically presented in Figure 2.30.
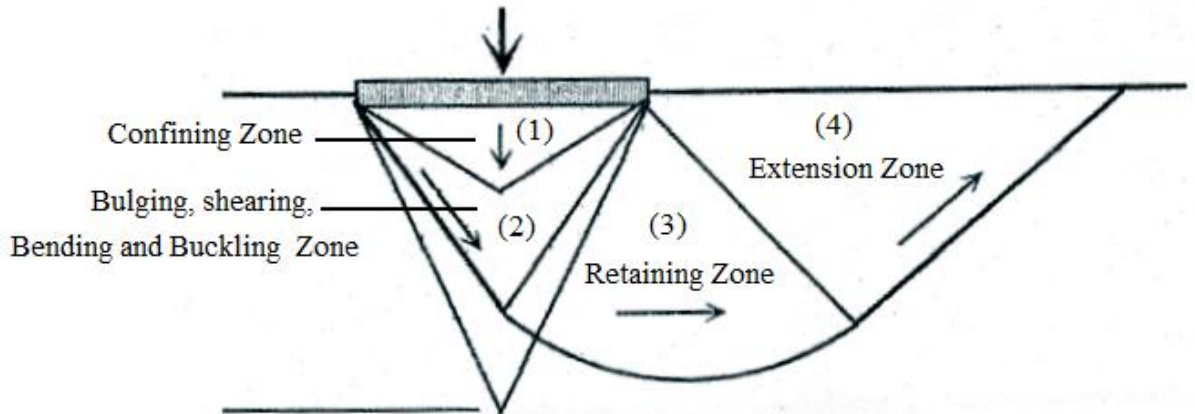
Figure 2.30 Failure mechanism of stone column group proposed by Hu (1995).

Hu's laboratory model is considered to be one of the most successful models in capturing the behaviour and deformation of a stone column group, but there was no qualitative description of the important role that the clay between the columns plays in increasing the bearing capacity and determining the failure mode of the stone column group.

In 2002, McKelvey (2002) studied the performance of rigid footings supported on a partially penetrating small stone column group (floating stone column group). One of the main purposes of this study was to monitor reinforced group deformations and the failure mechanism for different column group patterns and lengths. So, McKelvey conducted two series of tests. In the first one, she used a transparent material that has mechanical properties similar to clay and can easily view the deformation and failure mechanism of the small stone column group. In the second series of model tests, kaolin clay was used. Interaction of the stone columns in the group were observed for both model test series, as presented in Figure 2.31.
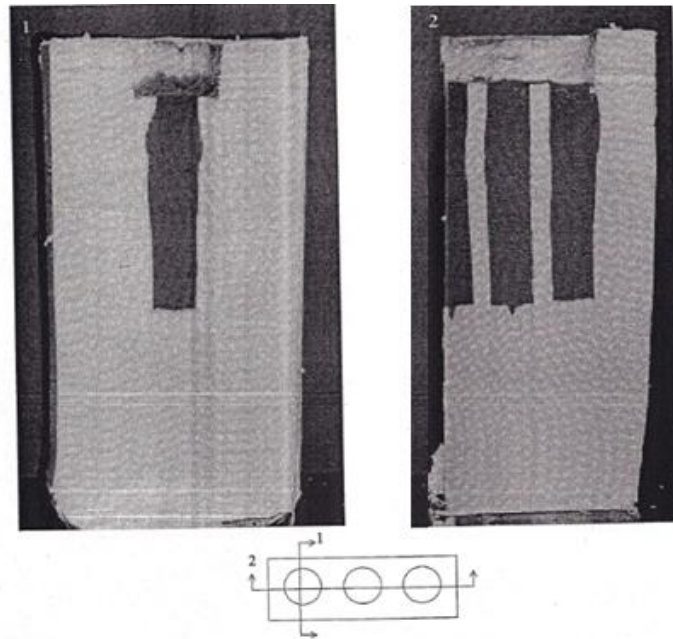
(a) Photograph of 2-dimensional slices of deformed columns
after test TS-05

TS -11

Direction of location of
photographs
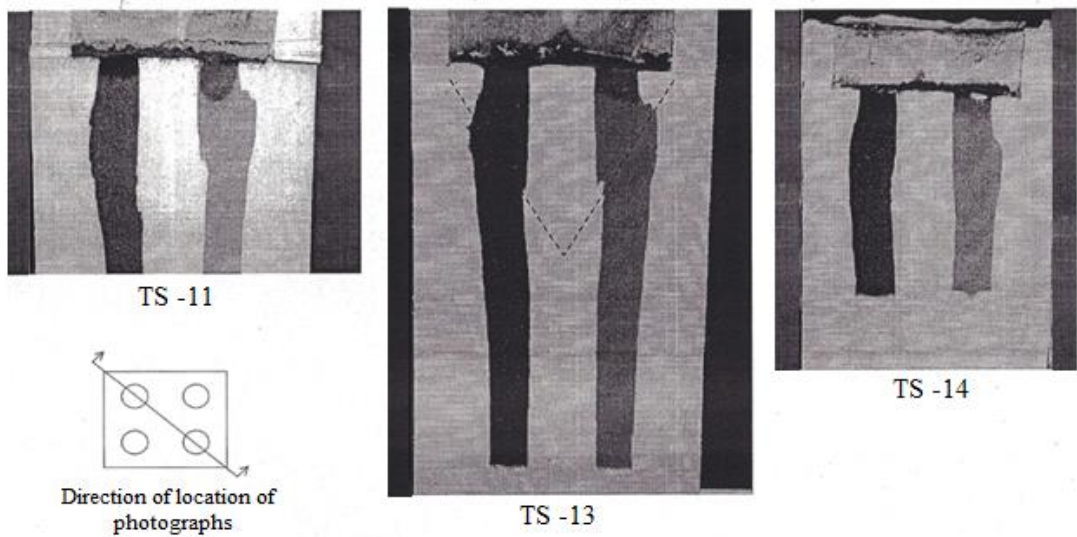
TS -13

TS -14

(b) Comparison between deformed shapes in TS-11 (L/d =10),
TS-13 (L/d =10) and TS-14 (L/d =6)

Figure 2.31 Deformed shapes of different patterns and lengths in the stone
column groups under loading (after McKelvey, 2002).

Black et al. (2006) use small scale laboratory tests to examine the behaviour
of single stone columns of large diameter and small groups of columns
beneath a circular footing (diameter = 60 mm). The following two area ratios

were assumed: $A/A_C = 2.5$ and 3.6. Through varying the length ($L = 125$–400 mm), an investigation of the impact of the length of the column was conducted. Results in Figure 2.32 showed that the stiffness of single columns is double that of the group stone columns, which indicates under-performance in the group of stone columns. The cause of this might be a 'block failure' manifested in column groups. Acting together, columns exhibit punching in the soil underlying them and to the length of the reduced shoulder between the footing edge and the column edge (Figure 2.33).

It was found that the length of the column and arrangement are determinants of the pattern of deformation. Punching into the soil was exhibited in group and single columns, which had a length of 125 mm and the ratio of the length to diameter (L/d) ranged between 3 and 5. With the increase in the length to 250 mm, while the group of columns (with length to diameter ratio = 11–14) kept punching in the soil beneath them, bulging was found in single columns (with length to diameter ratio = 7–10). Nevertheless, groups of columns perform as a 'block' and assuming that the group diameter (d = 60 mm) is more suitable, the length to diameter ratio is re-defined as 4 and 6. While no punching occurred for the end- bearing columns, it was found that all the columns, which had a length of 400 mm, experienced bulging. It was suggested by Black (2006) that the cross-over from punching to bulging failure is defined by an approximate length to diameter ratio of 8.
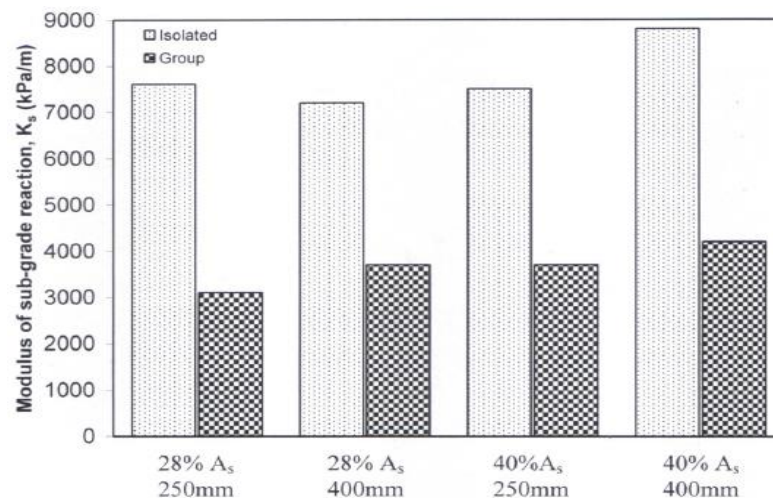
Figure 2.32 Isolated and group formation Ks comparison (Black, 2006).
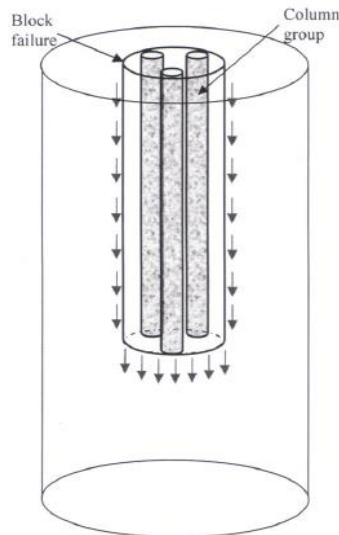
Figure 2.33 Illustration of group columns block failure (Black, 2006).

In short columns, it was found that the vertical stress did not increase as no more stress could be endured by columns failing by end-bearing. Nevertheless, it was found that as the columns got longer, the ratio of the stress concentration became greater and this was a reflection of the maximum capacity of bulging columns. In groups of columns, the pressure recorded in the columns was observed to be lower than the pressure under the footing centre. The higher and increasing pressure in the footing centre supports the surrounding columns with a lateral force and, hence, they experienced bulging in an outward manner getting farther from the columns beside them. This could be an explanation of why group columns underperform in settlement in light of the performance of the single columns that are located under the footing centre.

2.10 Theoretical Analysis and Design Methods

The design of a vibro stone column foundation needs to take into account the combined response of both materials (gravel and clay) to the applied load, but the different stress-strain relationships for granular material and

soft clay makes the analysis of this problem complex and difficult unless so some idealizations and theories for these materials are considered (Hu, 1995). The early research by Hughes et al. (1975), Baumann and Bauer (1974) and Priebe (1976) idealized the granular material behaviour as elastic and the clay as material as elastio plastic, while the modern stone column design methods are based on plasticity theory.

The main goals of the design procedure can be summarized by the following (Watts, 2000):

1. Estimation of the bearing capacity of the composite stone/soil system incorporating a suitable factor of safety against failure;

2. Determination of suitable geometry of the reinforced ground system (column length, column spacing, column diameter) depending on the treated ground conditions and the intended applied load;

3. Assessment of the equivalent treatment depth for the reinforcing system;

4. Prediction of the settlement of the treated ground under loading.

Most of the design methods in the last four decades have been either empirical or semi-empirical and have been based on approaches that will be discussed in the following subsections.

2.10.1   Unit Cell Concept

The unit cell is an idealization of a single stone column and its surrounding soil within an infinite spacing large arrays of stone columns using many assumptions and idealizations, which can be summarized as follows (Balaam and Booker, 1985):

- Load is applied uniformly on the unit cell and causes equal settlement for both column and clay;

- Both column material and clay are homogeneous materials;

47

- The influence of the boundary conditions is negligible (there should be no shear stresses or radial displacements in the sides of the influence zones);

- The principal stresses in the unit cell are vertical, radial and tangential stress.

The adopted arranging of the column decides the shape of the influence zone. The behaviour of each stone column and its surrounding influence zone is identical in a large array. Hence, the analysis of one column and its surrounding influence zone can be generalized to other columns. It is possible here to approximate the influence zone into a circle of equivalent area by applying the concept of unit cell (Section 2.8.2). Such a concept can be used with interior columns under wide loaded areas, which has a proportion that increases with any increase in the size of the group, such as large floor slabs or embankments. However, the concept of unit cell cannot be applied to groups of columns under strip/pad footings or under wide loaded areas because the loss of lateral confinement.

2.10.2   Cylindrical Cavity Expansion Theory

Cavity expansion theory has been used early in practical geotechnical problems related to *in-situ* soil testing such as the interpretation of pressuremeter test (Gibson and Anderson, 1961); (Meyerhof, 1961) and (Clarke, 1990). It was subsequently developed to cover more geotechnical applications of pile foundations, tunnelling and underground excavations to analyse the relationship between cavity expansion pressure and displacement, taking into account the stress-strain behaviour of soil (elastic, elastic-plastic, strain hardening/hardening, critical state) (Shien 2011). The displacement of soil during the stone column installation process is a cavity expansion problem. The alteration in the surrounding soil caused by the stone column installation process is commonly not considered in the design.

However the installation process changes the properties of the soil around the stone column, increasing the horizontal pressure on the column and

increasing the stiffness of the surrounding soil. This means the capacity of the stabilised ground increases.

In 1972, Vesic developed a cylindrical cavity expansion theory for both cohesive and cohesiveless soils by considering the unit cell concept and the bulging failure mode in order to calculate the ultimate cavity resistance of the treated soil from equation (2-8):

$$\sigma_3 = CF_c + qF_q \tag{2-8}$$

Where F_c and F_q are dimensionless cavity expansion factors, which are functions of the friction angle of the treated soil and the Rigidity Index (Ir). F_c and F_q can be directly obtained from the charts in Figure 2.34.
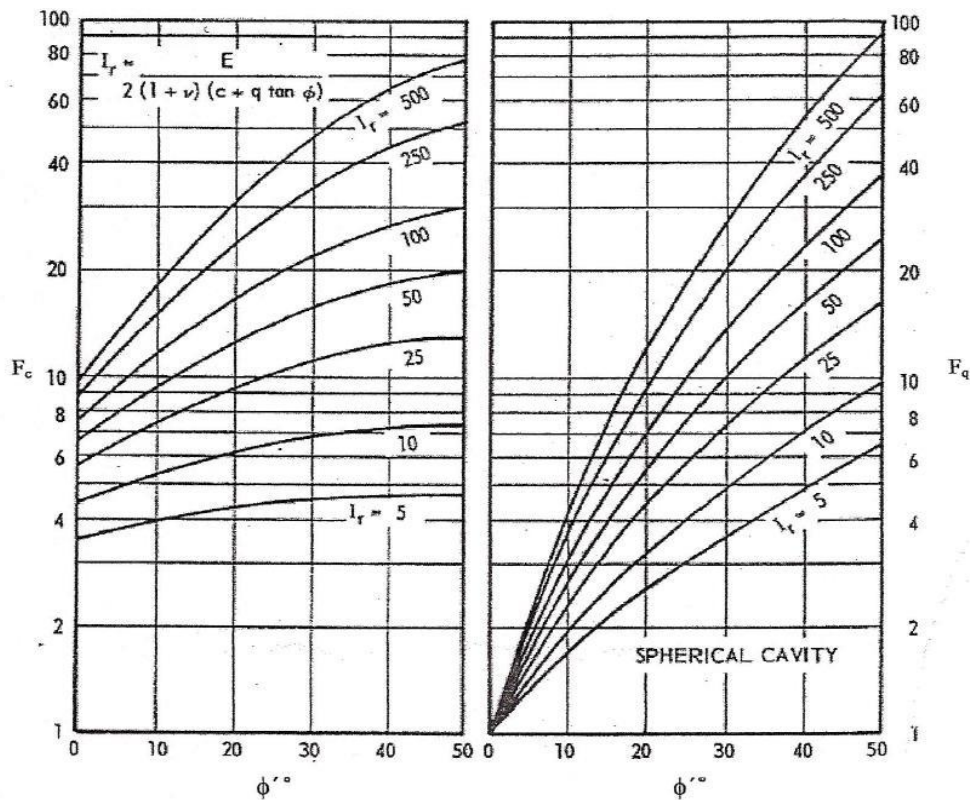
Figure 2.34 Determination of Vesic's cavity expansion factors, Fc and Fq (Vesic, 1972).

The Rigidity Index (I_r) given as:

$$I_r = G / (C_u + P' \tan\emptyset') \tag{2-9}$$

where C_u is the cohesion of the soil; q is the stress at the failure depth (the depth of the bulging); G is the shear module of the treated soil; and P' is the mean isotropic effective stress at the equivalent failure depth.

Based on equation (2-8) the ultimate bearing capacity of one column is expressed as:

$$q_{ult} = k_p(cF_c + qF_q) \qquad (2\text{-}10)$$

An interesting approach based on the similarity between the behaviour of a stone column while bulging and the pressuremeter test was proposed by Hughes and Withers (1974), who also adopted the elastic plastic theory that had been developed by Gibson and Anderson (1961) to interpret the pressuremeter test results using the expansion of cylindrical cavity. They applied it to calculate the lateral ultimate stress as follows:

$$\sigma_{rl} = \sigma_{r0} + c_u[1 + log_e \frac{E}{2C(1+v)}] \qquad (2\text{-}11)$$

where σ_{r0}, E, v and c_u are the total lateral stress, the elastic modulus, Poisson's ratio and the undrained shear strength of the soil, respectively.

Hughes and Withers state that equation (2-11) can be approximated to the following equation:

$$\sigma_{rl} = \sigma_{r0} + 4c_u \qquad \text{or} \qquad \sigma_{rL} = \sigma_{r0}^{`} + 4c_u + U \qquad (2\text{-}12)$$

Therefore, the ultimate load that the single stone column (bulged laterally) can endure can be calculated from equation (2-13) (Hughes and Withers, 1974):

$$\sigma_v^{`} = \frac{1+\sin\phi^{`}}{1-\sin\phi^{`}}(\sigma_{r0} + 4c_u - U) \qquad (2\text{-}13)$$

where $\phi^{`}$ is the friction angle of the stone column material; σ_{r0} the total *in situ* lateral stress; c_u the undrained shear strength; and U the pore water pressure. Although bulging is not the predominant deformation mode of the stone column group, Greenwood and Kirsch (1983) state that, due to the simplicity of this method, it is still widely used.

Randolph et al. (1979) made a detailed study of the application of cylindrical cavity expansion in modelling the installation of driven piles. Randolph's

solution made use of the analysis developed for the interpretation of pressuremeter test in estimating the stress changes within the plastic zone, R (where R is the radius of plastic zone) after the undrained cavity expansion for pile driving in clay and is given by Randolph et al. (1979).

$$\Delta\sigma_r = c_u \left[1 + ln\left(\frac{G}{c_u}\right) - 2ln\left(\frac{r}{r_0}\right) \right] \tag{2-14}$$

$$\Delta u = c_u \left[ln\left(\frac{G}{c_u}\right) - 2ln\left(\frac{r}{r_0}\right) \right] \tag{2-15}$$

Egan et al. (2009) used the elastic plastic theory that had been developed by Gibson and Anderson (1961) on undrained cavity expansion to predict the pressure in the cavity, when a penetrating vibro poker starts with an initial radius is zero and it expands to radius (a) and an infinite boundary condition is valid the lateral ultimate stress (σ_{lr}) is expressed as:

$$\sigma_{rl} = \sigma_{r0} + c_u \left[\frac{E}{2c_u(1+v)} \right] \tag{2-16}$$

where; σ_{r0}, E and v are the initial total horizontal stress, Young's modulus and Poisson's ratio respectively. For this case, the radial stress, σr in the plastic zone (r>R) and the elastic zone (r >R) are given by Eq. (2-17) and Eq. (2-18) respectively.

$$\sigma_r = \sigma_{r0} + c_u \left[\frac{R}{r}\right]^2 \tag{2-17}$$

$$\sigma_r = \sigma_{r0} + c_u - 2c_u ln\left[\frac{r}{R}\right] \tag{2-18}$$

The excess pore water pressure (Castro and Sagaseta, 2007), is shown in Eq. (2-19).

$$\Delta u = 2c_u ln\left[\frac{r}{R}\right] \tag{2-19}$$

The zone of soil near to the cavity turns into a plastic state while the soil beyond remains in an elastic state. The plastic radius, R, can be calculated as:

$$R = a e^{\frac{P-\sigma_r}{2c_u}} \tag{2-20}$$

Where; a is the radius of poker, p is the cavity pressure, σ_r is the radial total stress at radius r, and c_u is the undrained shear strength.

2.10.3 Ultimate Bearing Capacity

2.10.3.1   Single Column Analysis

The simplest method to calculate the ultimate bearing capacity of a single stone column reinforced footing was proposed by Bell (1915), who relied on the maximum lateral support of the cohesive clay to determine the increase in the capacity of a granular column at a certain depth z, as illustrated in Figure 2.35.
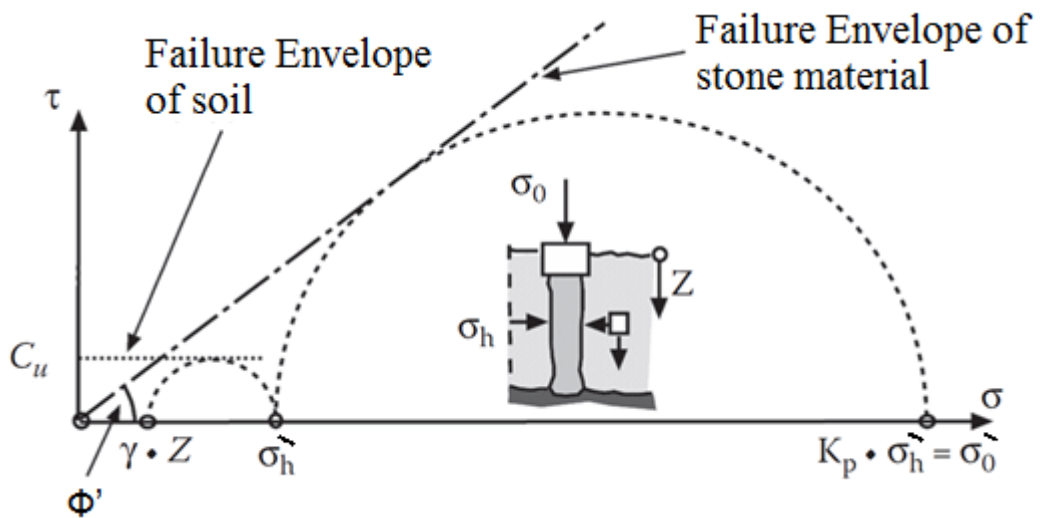
Figure 2.35 Influence of lateral support on column stress (Brauns, 1978).

$$\sigma_h = \gamma z + 2C_u \tag{2-21}$$

To estimate the maximum vertical column stress from Φ' equation (2-22):

$$\sigma'_0 = K_p(\gamma Z + C_u) \tag{2-22}$$

Where K_p is the passive earth pressure coefficient, which can be calculated from equation (2-43):

$$K_p = tan^2(\pi/4 + \phi/2) \qquad \text{or} \qquad K_p = \frac{1+\sin\phi}{1-\sin\phi} \tag{2-23}$$

where φ' is the angle of internal friction of column material and Cu is the cohesion of the *in situ* clay. Despite limiting the rule of the clay by just confining the equation to the columns and neglecting the clay's share in

carrying part of the load, Greenwood (1970) suggested the use of Bell's theory to calculate the preliminary design for the bearing capacity of a stone column reinforced foundation.

As discussed before in this chapter, Hughes and Withers (1974) carried out a series of tests on single stone columns. As is shown in Figure (2.6), there was observation of negligible strain below 4d of the column depth and clear deformation in the supper sections of the columns, which is idealised as uniform bulging. Gibson and Anderson (1961) developed Cylindrical Cavity Expansion Theory for predicting the limiting radial stress. According to the results of the quick expansion tests, Gibson & Anderson (1961) approximated the limiting radial stress (σ_{rL}) as follows:

$$\sigma_{rL} = \sigma_{r0} + 4C_u + U \tag{2-24}$$

where σ_{r0} = total in situ lateral stress

c = undrained cohesion

u = pore water pressure

Suppose that columns are in a critical state, then the relation between ultimate vertical stress (σ_v') and the limiting radial stress can be expressed as follows:

$$\sigma_v' = \left(\frac{1+sin\varphi\prime}{1-sin\varphi\prime}\right)\sigma_r' \tag{2-25}$$

where $\sigma r'$ = lateral effective stress

φ' = angle of internal friction of column material

Hence, the ultimate vertical stress for column bulging is:

$$\sigma_v' = \left(\frac{1+sin\varphi\prime}{1-sin\varphi\prime}\right)\sigma_{r0} + 4c + U \tag{2-26}$$

It is worth mentioning that column punching might appear if vertical forces exceed the ultimate bearing capacity at the base and the shear resistance on the sides of the column.

Approach developed by Brauns (1978) assumed that the upper part of the stone column, in which the failure normally happens, behaves like a triaxial

compression of cohesionless soil and that the failure is shearing on a plane that inclines $(45 + \frac{\phi'}{2})$, as shown in Figure 2.36.
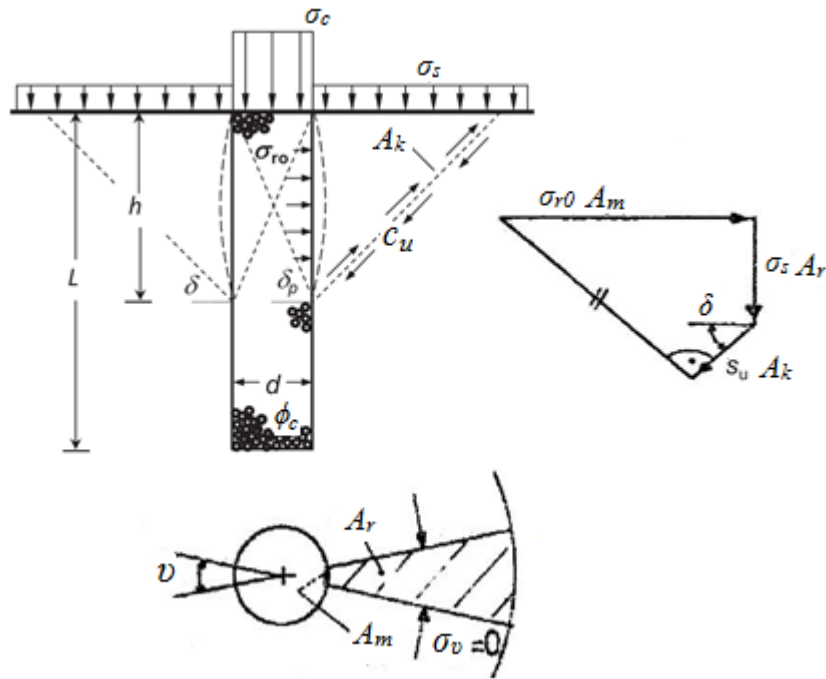
Figure 2.36 Simplified analysis of the bearing capacity of a single stone column (after Brauns, 1978).

Brauns assumes in this method that the treated clay is purely undrained cohesive $\phi_s = 0°$, weightless ($\gamma = 0$) and has no shear resistance ($\tau = 0$). By calculating the cone angle δ, using a trial and error procedure from equations (2-27) and (2-28), the ultimate load for a single column can be calculated as follows:

$$\delta_p = 45 + \frac{\phi'}{2} \tag{2-27}$$

$$\tan \delta \ (tan^2 \ \delta - 1) = 2 \tan \delta_p \tag{2-28}$$

$$\sigma_{vc} = \frac{2}{sin2 \ \delta} \ \frac{\tan \delta_p}{\tan \delta} . K_p \tag{2-29}$$

A comparison of the above mentioned methods was carried out by Brauns (1978) to find the differences in estimating the ultimate capacity of a single stone column. It is clear from Figure 2.37 that due to the different adopted

theories, idealizations and assumptions in these studies, the estimated ultimate bearing capacities trend to have a large scatter.
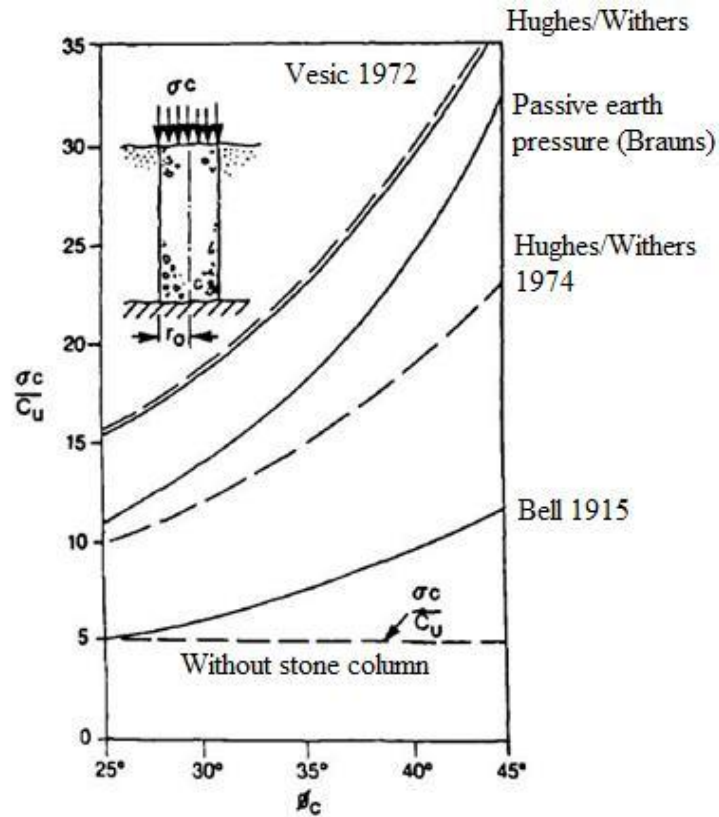
Figure 2.37 A comparison of some different methods to estimate the ultimate capacity of a single stone column (after Brauns, 1978).

Greenwood (1975) used the passive resistance theory to calculate the ultimate bearing capacity of a stone column unit cell. He considered that the maximum load that the unit cell can bear is achieved when the ratio of the applied vertical stress on the column to the passive lateral stress reaches the peak of the passive earth pressure coefficient, as in the following:

$$q_{ult} = K_{ps}(\gamma Z K_{pc} + 2C_u\sqrt{K_{pc}} + XqK_{pc}) \tag{2-30}$$

where γ is the bulk unit weigh of *in situ* soil; k_{ps} and k_{pc} are the passive pressure coefficient for stone and soil, respectively; C_u is the undrained cohesion of soil; Z is the depth of soil; and X is the critical depth (where bulging and end bearing failure occur simultaneously).

The most recent approach for the design of an end bearing individual stone column within a group was suggested by Barksdale and Bachus (1983). It is an approximate method that needs good engineering judgement in addition to the following equation:

$$q_{ult} = C_u . N_c \tag{2-31}$$

where q_{ult} is the ultimate bearing capacity of the stone column; C_u is the undrained shear strength of the treated soil; and N_c is a bearing capacity factor of the stone column material. N_c is dependent on the stiffness of the *in situ* soil and the method of installation for the stone column and can be taken as the following:

N_c = 18 and 22 for low to high soil stiffness, respectively.

$N_c = 25-30$ for vibro-replacement stone columns (Datye, 1985).

$N_c = 40$ for vibro-displacement stone columns (Datye et al, 1982).

2.10.3.2   Group Columns Analysis

All the methods that have been mentioned above, (Hughes & Withers, 1974; Vesic, 1972; Brauns, 1978; Greenwood, 1975 and Barksdale & Bachus, 1983) assumed that each column in the group behaves similarly to a single isolated column on its own, as they consider the unit cell theory in their designs. This means that the ultimate bearing capacity for the whole stone column system foundation is the predicted q_{ult} for a single column unit multiplied by the number of columns in the group. However, practically, the stone columns and the treated clay between them always work together as one system under the applied foundation. So, neglecting the interaction in the soil/columns system will not lead to a true design of the stone column reinforced foundation.

Barksdale and Bachus (1983) recognized this issue in estimating the ultimate bearing capacity of a group of stone columns and according to the undrained shear strength of *in situ* soil, they recommended the following:

- If the undrained shear strength of *in situ* soil *Cu* is less than 30 kPa, which means the treated soil is soft enough to make the deformation and failure of the columns occur as bulging (ductile failure), then the ultimate bearing capacity can be predicted depending on unit cell theory by using Equation (4-31) to calculate q_{ult} for one column and multiply this by the number of the whole group.

- If the undrained shear strength of treated soil is greater than 30 kPa, then the reinforced soil can be considered as one block beneath the rigid foundation and it is more likely that this composite system will fail on a straight shear failure plane that inclines with ζ angle of the vertical (brittle failure), as shown in Figure 2.38.
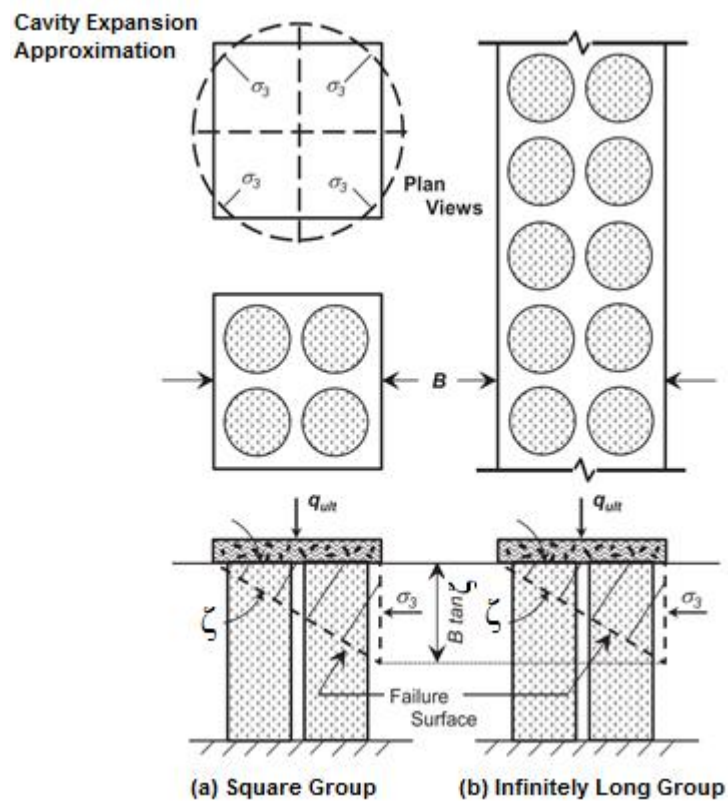
Figure 2.38 Shear failure mechanism for group of stone columns (after Barksdale & Bachus, 1983).

The total bearing capacity of the reinforced ground can be calculated from the equilibrium of the soil block as follows:

$$q_{ult} = \sigma_1 = \sigma_3 \tan^2 \zeta + 2C_{avg} \tan \zeta \qquad (2\text{-}32)$$

$$\sigma_3 = \frac{\gamma_s \, \zeta \, \tan \zeta}{2} + 2Cu \qquad (2\text{-}33)$$

$$C_{avg} = (1 - \mu_s)Cu \qquad (2\text{-}34)$$

$$\zeta = 45° + \frac{\phi^{`}_{avg}}{2} \qquad (2\text{-}35)$$

$$\tan \phi^{`}_{avg} = \alpha_s \mu_s \tan \phi_s \qquad (2\text{-}36)$$

where σ_3 is the lateral resistance of the reinforced soil block; B is the width of the foundation; γ_s is the unit weight of the soil; Cu is the undrained shear strength of the *in situ* soil; μ_s is the area replacement ratio; C_{avg} and $\phi^{`}_{avg}$ are the average cohesion and average friction angle of the reinforced soil block, respectively; and α_s is the stress concentration ratio of stone.

Using the same homogenization technique concept (by assuming that the stone columns reinforced ground works as one block under the footing and that general shear failure occurs), Priebe (1991) developed two methods (using the German standards) to estimate the ultimate bearing capacity of the footings reinforced with a limited number of stone columns.

In the first method, the ultimate bearing capacity of the footing can be calculated from the following equation:

$$P_{ult} = A_F(C^{`}_{avg} \, N_c \, v_c + \gamma_s \, d \, N_d v_d + \gamma \, BN_B v_b) \qquad (2\text{-}37)$$

Where A_F is the area of the footing, γ_s is the unit weight of the soil, d is the footing depth, B is the footing width; N_c, N_d and N_b are bearing capacity factors (functioned to $\phi^{`}_{avg}$), $v_c$, $v_d$ and $v_b$ are shape factors for the treated ground and $\phi^{`}_{avg}$ and $C^{`}_{avg}$ the equivalent internal friction angle and equivalent cohesion of the reinforced soil block, respectively.

In the second method, the design bearing capacity of the supported footing is calculated using all untreated ground parameters (bearing capacity factors N_c and N_d shape factors v_c and v_d, internal friction angle $\Phi^{`}_c$ and cohesion C_u), with an equivalent footing width $\bar{B}$ in equation (2-38) to increase the failure line under the supported footing; Figure 2.39:

$$P_{ult} = A_F(c'N_c \, v_c + \gamma_s \, d \, N_d v_d) \qquad (2\text{-}38)$$
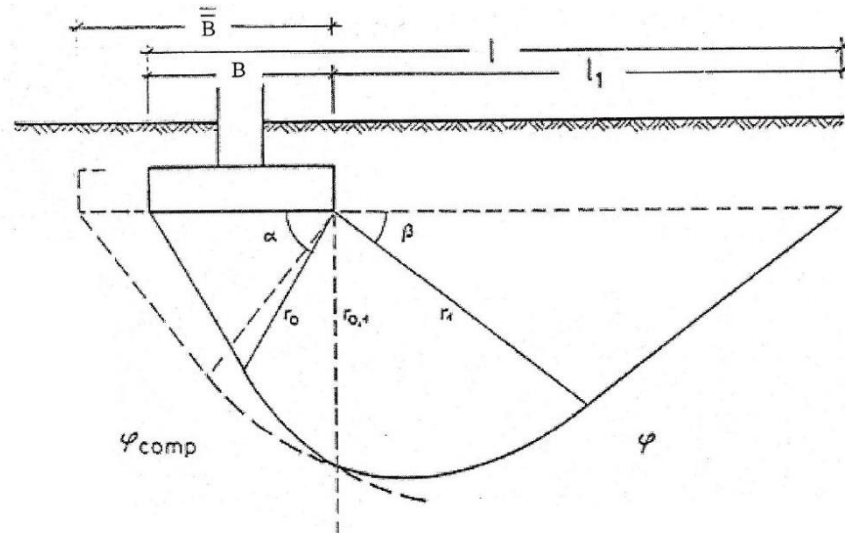
Figure 2.39 Approximate ground failure line in order to determine the assumed footing width, $\bar{B}$ (Priebe, 1991).

Priebe (1993) developed design curves for a foundation supported with an infinite grid of stone columns. These curves determine the proportion of load carried by the stone columns (m) using the area ratio and the friction angle of column material; Figure 2.40.
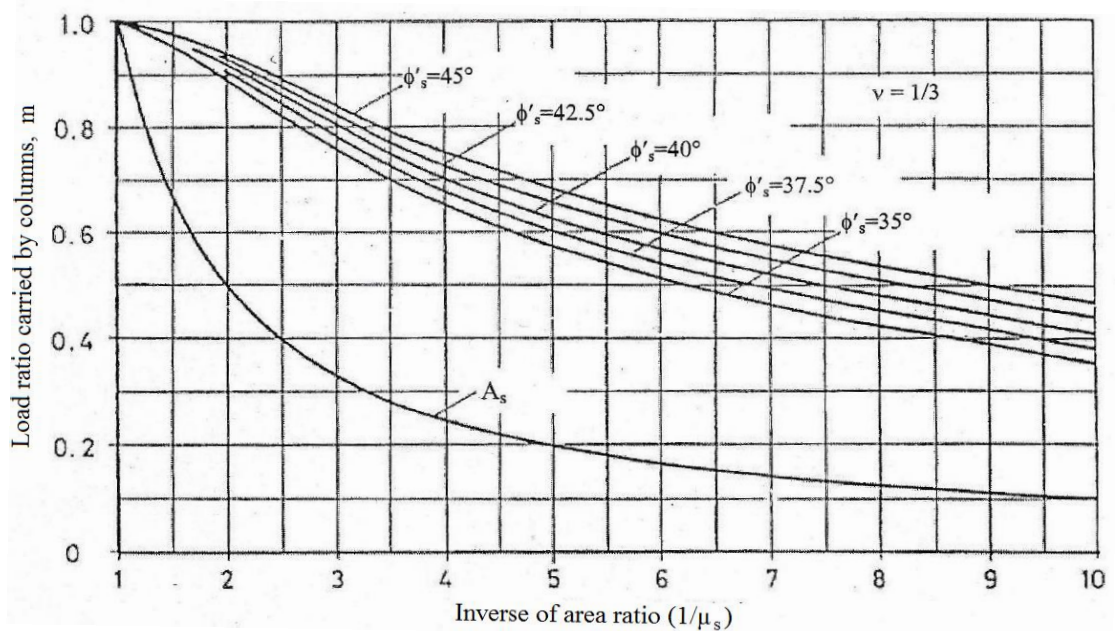
Figure 2.40 Design charts to determine the proportion of load carried by the stone columns (after Priebe, 1993).

Based on the foregoing regarding the use of the ultimate bearing capacity in the design of stone column reinforced foundations, it can be recognized that there are two main concepts in calculating the ultimate capacity of stone column group systems; the first assumes that each column in the group behaves similarly to a single isolated column on its own, as this concept considers the unit cell theory in their design. The second concept is the homogenization approach, (Barksdale & Bachus, 1983; Priebe, 1991) that idealizes the reinforced ground as one block which has high stiffness and low compressibility to fail under loading on a straight shear surface, regardless of any local failure of individual columns. Although the homogenization approach has a main advantage compared to that based on the performance of single columns (the unit cell), i.e., taking into account the footing size in the design, the former ignores the local bulging of columns in soft cohesive soils and both field observations and laboratory tests have proved that the stone column reinforced foundation does not fail in shear but remains in a state of plastic equilibrium (Vautrain, 1977). So, any realistic and sufficient design needs to consider the effect of the properties of the *in situ* soil and its stiffness response to the column installation and consolidation process.

2.10.4   Settlement and Consolidation Analysis

Most soft soils, which are the focus of this research, reach the allowable settlement well before reaching the ultimate bearing capacity. Nevertheless, sufficient bearing capacity of the ground foundation is considered to be one of the important criteria in geotechnical design. So, many researchers have found that it is more effective to design stone column reinforced foundations by using settlement analyses.

The simplest method to estimate settlement of an isolated floating stone column was proposed by Mattes and Poulos (1969) using linear elasticity theory as follows:

$$\delta_p = I_p \frac{P_p}{E_s L_p} \tag{2-39}$$

where δ_p is the settlement of the stone column, P_p is the axial load applied on the stone column, L_p is the column length, I_p is a displacement influence factor related to the relative stiffness between column material and treated soil usually taken between (30 and 50), and E_s is the elasticity modulus of the treated soil. Balaam (1978) stated that using this method to calculate the settlement gives underestimated values.

Empirical design curves were proposed by Greenwood (1970) to estimate the reduction of ground settlement due to the consolidation of the clay after installing the vibro-replacement stone columns rested on a good bearing layer. The aim behind the development of these curves was to address the issues of dry and wet methods of construction. It was observed that there was better settlement performance in the installed columns that depend on the wet method. Yet, this can be ascribed to the larger diameters of the columns, which happens when this construction technique is applied. This reduction is a function of the undrained shear strength of the clay and the column spacings, as presented in Figure 2.41.
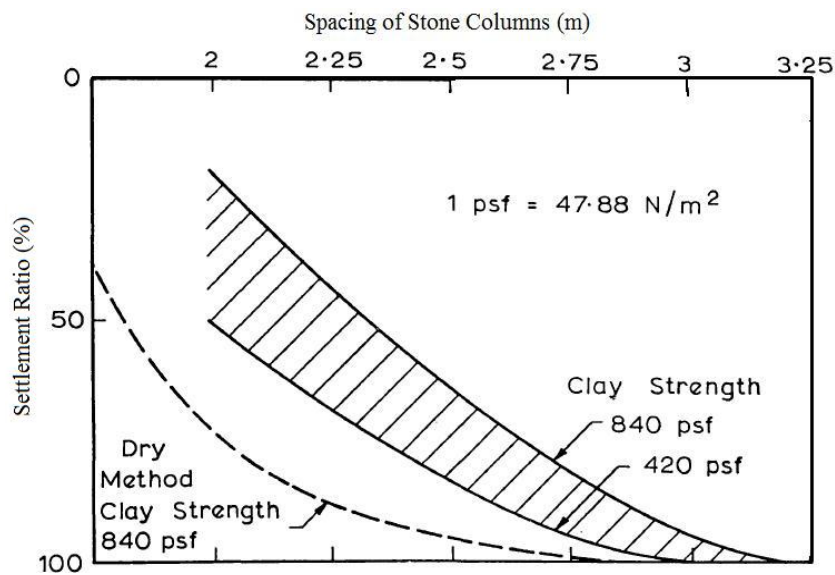
Figure 2.41 Design chart to determine the settlement reduction in stone column reinforced foundations (after Greenwood, 1970).

Greenwood recommends adhering to the indicated range when using this method. Although Greenwood's method is a simple empirical one, Balaam and Booker (1981) and Barksdale and Bachus (1983) compared it with their theoretical and numerical approach and they found acceptable agreement.

In 1979, Aboshi et al. proposed a simple method to predict the settlement of composite ground reinforced with large diameter vibro stone columns under a flexible footing. This method is based on maintaining an equilibrium condition between the stone/clay interface during one-dimensional consolidation caused by loading, taking into consideration the stress concentration factor (n) and the ratio of stresses in both stone column and clay, α_c and α_s respectively, which were given in equations (2-4), (2-5) and (2-6). Aboshi *et al.* (1979) show stress concentration ratios measured at several construction sites which range from 1.6–11.5. Barksdale and Bachus (1983), however, claim that the typical range of stress concentration ratios is 2.5–5.0. This method is called the equilibrium method and based on one-dimensional consolidation theory, settlement can be expressed for unreinforced and reinforced ground as follows:

$$\Delta S = m_v . \sigma . H \tag{2-40}$$

$$\Delta S_t = m_v . \sigma_c . H = m_v . \alpha_c(\sigma_c) . \sigma . H \tag{2-41}$$

$$\beta = \frac{\Delta S}{\Delta S_t} = \alpha_c(\sigma_c) = \frac{1}{1+(n-1)\mu_s} \tag{2-42}$$

Where μ_s is the ratio of replacement, m_v is modulus of volume compressibility of untreated ground; and H is the thickness of the treated clay. Alternatively, Aboshi et al (1979) provided design curves for this method, as shown in Figure 2.42. This suggested design method depends on an infinite grid of columns.
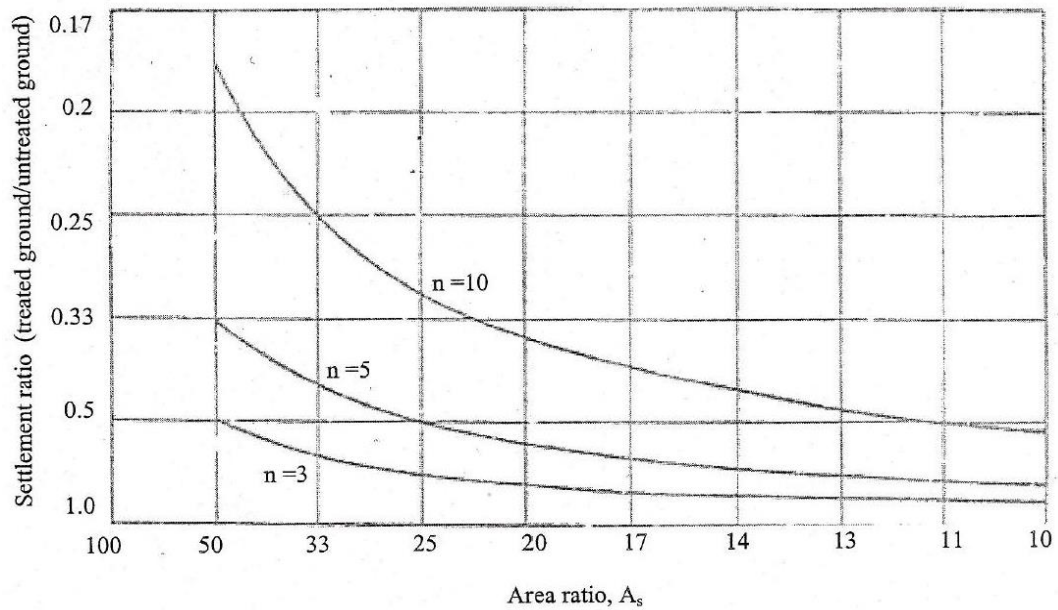
Figure 2.42 Design curves of settlement reduction ratio using the equilibrium method (Aboshi et al, 1979).

Aboshi et al (1979) readressed some of the shortcomings of the equilibrium method by adding two recommendations: (Du Yanjun and Nenghe, 2010) I that μ_s should be less than 30%, otherwise the effect of column replacement cannot be neglected and as a result the method will give overestimated settlement and (2) that field values of the stress concentration ratio (n) should be used because this term is essential for accurate settlement estimation.

Again, the unit cell concept is assumed to use in this method to assess the settlement for a group of stone columns without any consideration of columns/soil stiffness or columns/column interactions assuming that there are no shear stresses between the *in situ* soil and stone columns and the vertical stresses remain constant with depth.

An analytical solution was proposed by Balaam and Booker (1981) to decide the settlement of an infinite array of end-bearing stone columns. Both of the surrounding soil and the stone backfill are idealised as linear elastic materials, which can be defined by Poisson's ratio (*v*) and Young's modulus (E). Appropriate values selection should consider the stress level which might be encountered under the foundation. The analysis here can be done

by compressing a cylindrical body between rough (substratum) and smooth (raft) plates and restraining a smooth wall. The researchers undertook an axisymmetric FEA and found a triaxial state of stress in the column. The researchers also found that field quantities, which are remote from the substratum, are not sensitive to a rough or smooth boundary condition that is assumed at the substratum. In this case, a smooth substratum can be assumed and an exact analytical solution, which depends on Cylindrical Cavity Expansion Theory, can be reached.

The assumption in the first approximation (Solution A) is that the column is laterally restrained. The researchers found that this assumption has good results, but stress discontinuity ($\Delta\sigma_r$) might occur at the column-soil interface. The column will attract more load because it is stiffer than the surrounding soil. Therefore, the wall, not the surrounding soil, will develop a higher radial stress. The discontinuity of this stress shows itself as a bugling column in reality; it is very important to account for this. Because of the issues discussed in the first solution, a second solution (Solution B) is developed with a lateral expansion of the column and a zero vertical movement of the raft. This conveys a radial stress equal and opposite to $\Delta\sigma_r$ at the column-soil interface, as is shown in Figure 2.43.
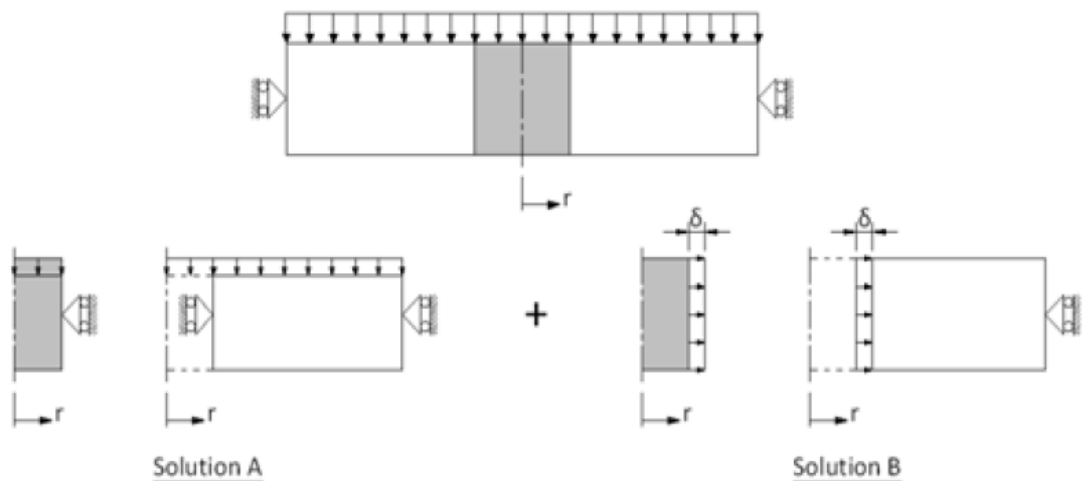
Figure 2.43 Boundary conditions for solutions A & B proposed by Balaam & Booker (1981).

Super-imposing solutions A and B are the final solution (see Table 2.2). Integrating the vertical stresses across the soil surface determines the relationship between the average applied stress q_A and strain.

Table 2.2 Final solution for stresses and strains in column and soil (Balaam & Booker, 1981).

	Region 1	Region 2
	Stone column	Clay
ε_z	ε	ε
y	$Fr\varepsilon$	$\left[F \dfrac{a^2}{r} \dfrac{(b^2 - r^2)}{b^2 - a^2} \right] \varepsilon$
σ_r	$[\lambda_1 - 2(\lambda_1 + G_1)F]\varepsilon$	$\left[\lambda_2 + \dfrac{2a^2 F}{b^2 - a^2}\left(\lambda_2 + G_2 + G_2 \dfrac{b^2}{r^2} \right) \right] \varepsilon$
σ_θ	$[\lambda_1 - 2(\lambda_1 + G_1)F]\varepsilon$	$\left[\lambda_2 + \dfrac{2a^2 F}{b^2 - a^2}\left(\lambda_2 + G_2 - G_2 \dfrac{b^2}{r^2} \right) \right] \varepsilon$
σ_z	$[\lambda_1 + 2G_1 - 2\lambda_1 F]\varepsilon$	$\left[\lambda_2 + 2G_2 + 2\lambda_2 \dfrac{Fa^2}{b^2 - a^2} \right] \varepsilon$

$$Lame's\,parameters: \lambda = \frac{vE}{(1 - 2v)(1 + v)} ; G = \frac{E}{2(1 + v)}$$

$$and\ where\ F = \frac{(\lambda_1 - \lambda_2)(b^2 - a^2)}{2[a^2(\lambda_2 + G_2 - \lambda_1 - G_1) + b^2(\lambda_1 + G_1 + G_2)]} \tag{2-43}$$

$a = radius\ of\ stone\ column$

$b = radius\ of\ unit\ cell$

Relationship between strain and average applied stress, q_A:

$$q_A b^2 = [(\lambda_1 + 2G_1)a^2 + (\lambda_2 + 2G_2)(b^2 - a^2) - 2a^2(\lambda_1 - \lambda_2)F]\varepsilon \tag{2-44}$$

$$q_A = [(\lambda_1 + 2G_1)(A_c/A) + (\lambda_2 + 2G_2)(1 - A_c/A) - 2(A_c/A)(\lambda_1 - \lambda_2)F]\varepsilon$$

$$(2\text{-}45)$$

$$\varepsilon = q_A / [(\lambda_1 + 2G_1)(A_c/A) + (\lambda_2 + 2G_2)(1 - A_c/A) - 2(A_c/A)(\lambda_1 - \lambda_2)F]$$

$$(2\text{-}46)$$

The settlement reduction factor (β) is defined as:

$$\beta = \varepsilon / q_A m_{v2} \qquad\qquad (2\text{-}47)$$

$$\beta = E_{oed} / [(\lambda_1 + 2G_1)(A_c/A) + (\lambda_2 + 2G_2)(1 - A_c/A) - 2(A_c/A)(\lambda_1 - \lambda_2)F]$$

$$(2\text{-}48)$$

Under specific circumstance, many researchers found that it is possible for the elastic analysis to overestimate the efficiency of stone columns in minimizing foundation settlement. In this regard, an interaction analysis proposed by Balaam and Booker (1985) has some simplifying assumptions which account for the yielding of the column. In this analysis, the major principle stresses are closer to vertical and there might be important column yielding, with little yielding in the surrounding clay. Consequently, (Balaam and Booker, 1985) assume the following (Killeen and McCabe, 2014):

(i) stone columns are in a triaxial stress state

(ii) yielding may occur in columns and no yielding occurs in the surrounding soil

(iii) no shear stress develops along the stone-soil interface that might cause any slipping between them.

(iv) the behaviour of stone columns is idealised as an elasto-plastic material satisfying the Mohr-Coulomb yield criterion

Such assumptions were incorporated in one solution that was compared with FEA to check the validity of the proposed solution. To have a non-associated flow rule and satisfy the criterion of Mohr-Coulomb yield, the materials of the column and the clay were treated as dilatant materials. The validity of the assumptions was tested by selecting geometrical materials and appropriate material parameters. The solution suggested by Balaam & Booker (1985) is an accurate and effective solution for the calculation of the decrease in

settlement because of stone columns. This solution is effective because of the noticeable agreement that was found between the methods used.

One of the most applicable methods of estimating the settlement improvement factor in practice was developed by Priebe (1976) and corrected by him in 1993. Based on unit cell analysis and the division of the unit cell into discrete horizontal slices an, then, taking the sum the estimated settlement for all of these slices. This method considers that the total settlement comes from two parts (Du Yanjun and Nenghe, 2010): the immediate settlement of the stone materials S_1 (considering no volumetric strain) and (2) the consolidation settlement S_2 of reinforced clay adopting Terzaghi's classical one-dimensional consolidation theory.

Priebe (1976) produced a series of design curves to predict the settlement reduction ratio β (improvement factor) of an infinite array of end-bearing stone columns supporting a rigid foundation by using the area replacement ratio and the friction angle of the column material. These curves, which are represented by equation (2-49), are presented in Figure 2.44.

It is assumed that such columns are in an active state, and they bulge consistently along their length. To account for the impacts of the installation of the column, the surrounding soil is idealised as an isotropic elastic material where the increased coefficient of lateral earth pressure is assumed ($K_0 = 1$). As is shown in Figure 2.44, the friction of the stone backfill (ϕ_c) and column spacing (A/A_c) significantly influence the factors of settlement improvement.
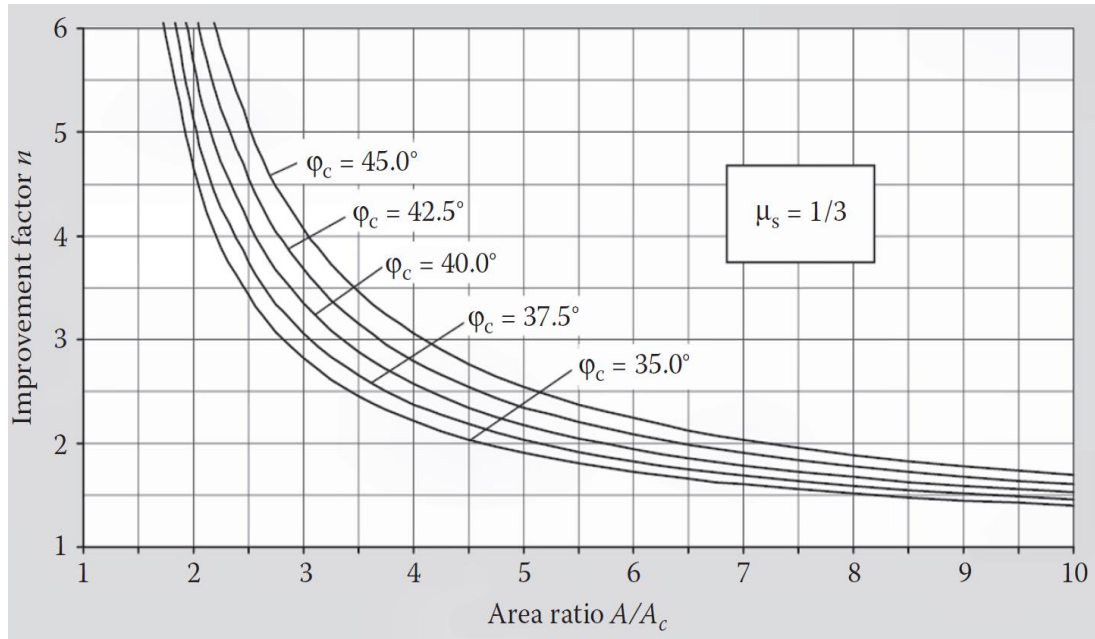
Figure 2.44 Design curves of basic settlement improvement factor n_0 for various strength of stone column material (after Priebe, 1995).

$$n = \frac{S}{S_t} = 1 + \mu_s \left[\frac{0.5 + 2v \frac{1-\mu_s}{v+\mu_s}}{K_{ac}.2v \frac{1-\mu_s}{v+\mu_s}} \right] \tag{2-49}$$

$$K_{ac} = tan^2 \left(45 - \frac{\phi_c}{2}\right) \tag{2-50}$$

where μ_s is the area replacement ratio; K_{ac} is the active earth pressure coefficient of column material; and v is Poisson's ratio = $^1/_3$.

In deriving the above method, Priebe assumed that the stone column works as a cylindrical incompressible material surrounded by an elastic medium (Clayton et al., 1992) and rested on a firm layer with no change in lateral stress with depth, and for more safety the effect of soil overburden was neglected.

In 1995, Priebe changed some of his assumptions to overcome the conservative results of his earlier approach and took into account the compressibility of the stone column material and the effect of overburden. The basic design curves assume the stone column material to be incompressible. So, Priebe (1995) allowed some adjustment (correction

factor) that can be added to the actual area ratio, Figure 2.45. Increasing the area ratio A/A_C by an amount $\Delta A/A_C$, which depends on the ration of compression moduli of the soil and column, accounts for the effect of column compressibility. If column compressibility is modified, it leads to lower settlement improvement factors (n_1).

The effect of overburden stress is also neglected by the basic settlement improvement factor. It is assumed that the pressure difference at the column-soil interface is constant with depth and it does not consider the difference between the unit weight of the surrounding soils and the column material. When depth increases, overburden stress increases as well. Hence, overburden stress should be considered in order to minimize column bugling and give better settlement improvement factors. A depth factor (f_d) which is defined as the ratio of the original pressure difference to the 'new' pressure difference is given here to account for the effect of overburden stress. There is a direct relation between the depth factor and the settlement of stone columns. The calculation of the modified settlement improvement factors is as $n_2 = f_d \times n_1$.
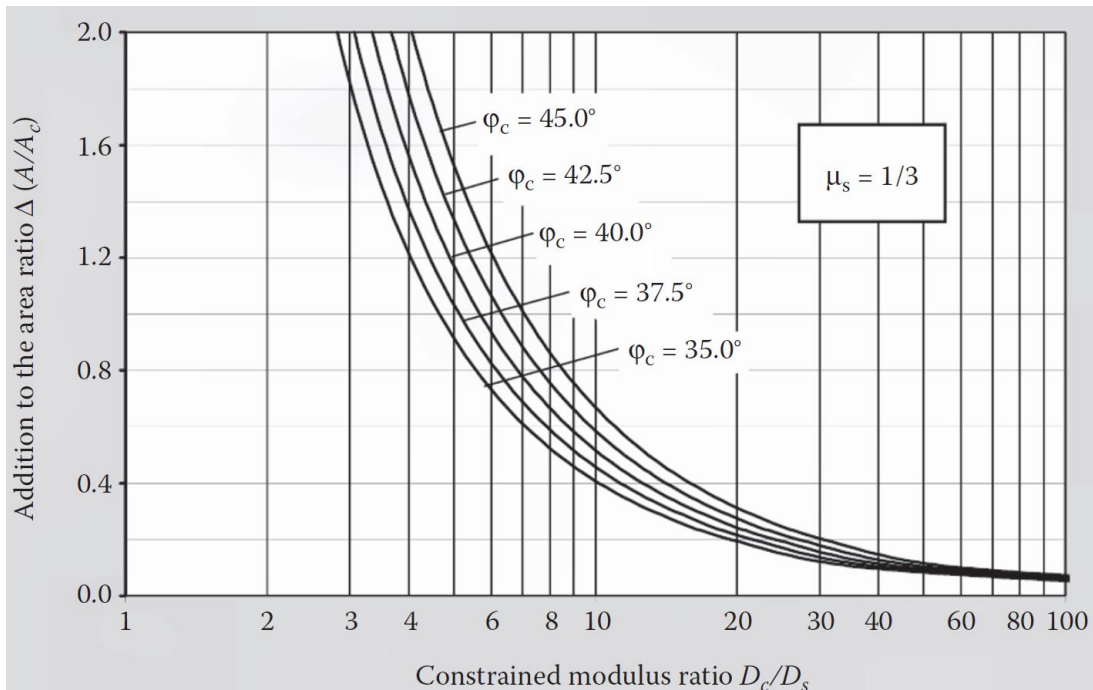
Figure 2.45 The correction factor of the area ratio addition (n_1) (after Priebe, 1995).

69

In practice, a foundation resting on soft soils may be supported by a small number of columns, so the previous design charts are not sufficient to estimate settlement for a limited number of stone columns. Priebe and Grundbau (1995) developed further design curves, as presented in Figure 2.46 and Figure 2.47, to estimate the settlement of the pad and strip rigid foundation on a limited number of columns (including a single column) as a function of S_∞, the settlement of an unlimited column array supporting an infinite raft foundation.
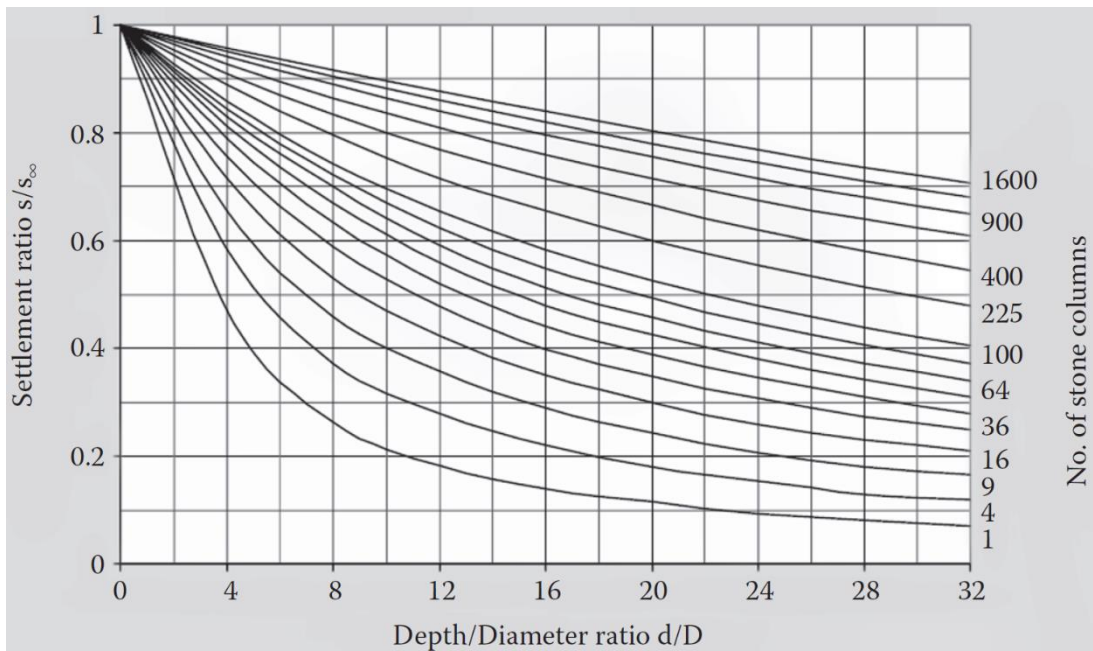
Figure 2.46 Design curves for predicting the settlement of a pad footing supported by a finite number of stone columns (after Priebe, 1995).
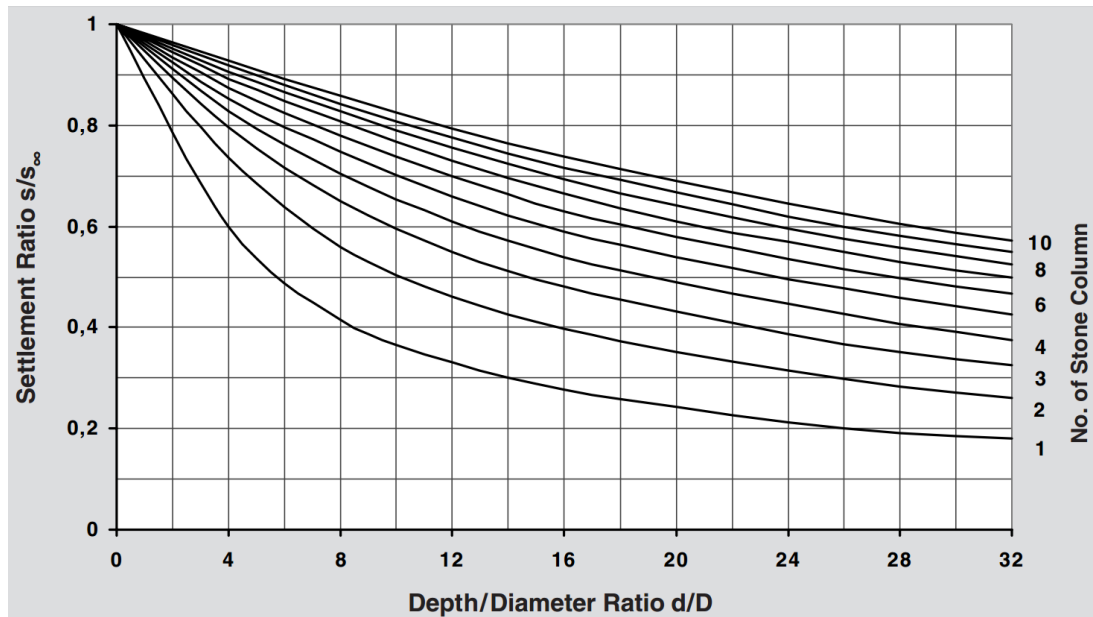
Figure 2.47 Design curves for predicting the settlement of a strip footing supported by a finite number of stone columns (after Priebe, 1995).

As show in figure 2.49, settlement ratio (s/s_∞) decreases quickly with depth. This is ascribed to a decay of vertical stress with depth beneath pad footings. Therefore, the effects of the depth factor (f_d) is decreased for pad footings. In this case, a suggestion by Priebe says that the subsoil can be divided into many layers and the settlement for every layer can be calculated separately in order to avoid the over estimation of the settlements of pad footings. The following formula can be used to calculate the settlement:

$$\Delta s = \frac{P}{D_s n_2} [(S/S_\infty)_L d_L - (S/S_\infty)_U d_U] \tag{2-51}$$

where d_L and d_U are the upper and lower bound depths of the layer.

Although Priebe's method is considered to be a reliable method for using in stone column reinforced foundations design. It is widely used in the USA by (for example) Hayward Baker and in the UK by the Keller Foundation and Cementation, Barksdale and Bachus (1983) compared it with some field results and found that using this method leads to an overestimation of the results of the beneficial effect of stone columns in reducing settlement.

71

To summarize the settlement performance of stone e column in the previous reviewed studies it can be said that; many important factors were identified to affect the stone column settlement performance including the length of the column and area ratio. The columns can be arranged to obtain the desired settlement performance. Large groups of close columns were more affected by the length of the column. It was also found that to obtain the same settlement performance, less stone is needed for long columns that are widely spaced than short columns which are closely paced. A further finding was that when the columns length is less than $L/h ≤ 1⁄4$ (where h is soil deposit thickness) and its area ratio is more than $A/A_C > 25$, negligible settlement improvement factors arise.

2.10.5   Summary of Theoretical Analysis and Design Methods

Cylindrical Cavity Expansion Theory (CCET) and the unit cell concept have been the basis for a large number of design methods for settlement performance and ultimate bearing capacity of stone columns. An infinite wide load area is supported by an infinite grid of columns is assumed in using the unit cell concept. This is based on the assumption that the behaviour of every column in grid is the same, and hence the analysis of one column and its surrounding zone will be overgeneralized to other columns. Therefore, this concept can be only used with interior columns in large groups. CCET can be used to determine the strains and stresses developing in the expanding cylindrical shell and the surrounding soil.

The previous sections discussed the analytical and empirical design methods which are applied to decide the ultimate bearing capacity of columns. In this discussion, it is indicated that ultimate bearing capacity of stone columns largely depends on the passive resistance of the surrounding soil, particularly in the upper section of the column.

Previous sections presented a range of design methods, analytical to empirical, to decide the settlement magnitude for stone columns. For example, a semi-empirical design method was developed by Priebe (1995)

who simplified the assumptions. These assumptions state that uniform bugling happens along the columns which are in the active state. Also, overburden stresses and column compressibility were accounted for by modification factors. Compared to Priebe (1995), a more strict theoretical solution was developed by Balaam and Booker (1981) who modelled the surrounding soil and stone columns as linear elastic materials. However, this solution failed to explain column yielding, which overestimates the efficiency of stone columns in decreasing foundation settlement. To address this issue, other researchers, such as Balaam and Booker (1985) and Pulko and Majes (2005), developed this solution to explain column yielding via an interaction analysis and analytical design method. Similarly, Rowe (1962) proposed a dilation theory which addresses column yielding and idealises the behaviour of stone columns as elastic rigid plastic.

Since stone columns have high permeability that allows vertical drains and stress concentrations, they are considered as an effective method for increasing consolidation rate. A solution was simplified by Han and Ye (2001) for computing consolidation rate for reinforced foundations of stone column. Castro and Sagaseta (2009) developed this solution and modelled stone columns as an elasto-plastic dilatant material, and they explained lateral expansion. The importance of such a method is that it can decide the time and depth of yielding, which makes it possible to precisely determine the strains and stresses that happen at different stages of the loading history in columns.

2.11 Numerical Analysis of Stone Columns

Over the last 20 years, numerical analysis has been the preferred method in studying and designing stone column foundation systems. Numerical analysis is a powerful technique that can be used to understand the complexity of these systems due to the different behaviours and responses of clay and granular material. It is capable to perform very complex calculations in a relatively short time with very flexible tools in finding the

solution. Similar to the analytical solutions, different concepts, assumptions and idealizations have been adopted in numerical analysis to study the behaviour of reinforced ground.

According to the ability of the finite element codes that are used in analysing stone column reinforced foundations and the simulation methods, previous numerical studies can be divided into the following:

- Single Isolated stone column studies;

- Stone column group studies.

  numerical methods of analysis still provide solutions to complicated equations. If such numerical methods of analysis are correctly applied, they are expected to give a reasonable prediction of the ground behaviour. This chapter describes how these solutions are achieved and the underlying principles.

2.11.1 Isolated Replacement Stone Column

Balaam and Poulos (1978) used the finite element method to model a flexible footing (uniform vertical pressure) supported by a single stone column. They studied the settlement of this unit cell by adopting the Mohr-Coulomb failing criterion and by treating both clay and stone as elastic, perfectly plastic materials in one analysis and as ideal elastic in another; Figure 2.48.
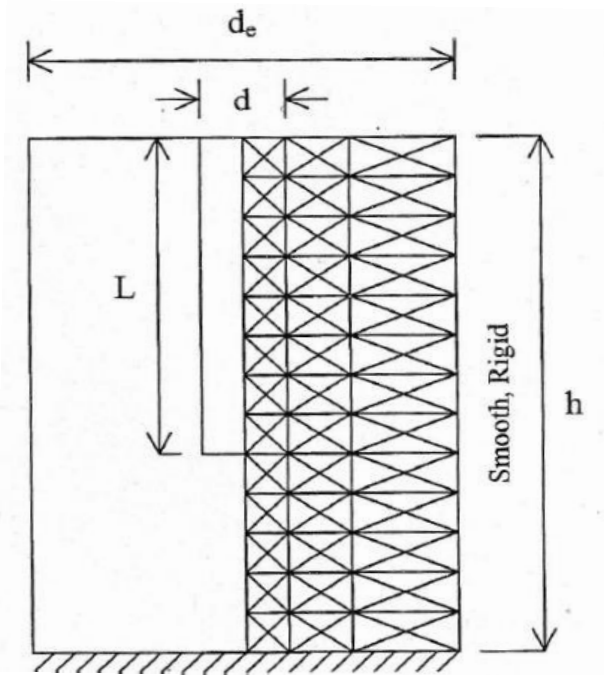
Figure 2.48 Finite element mesh of unit cell (Balaam, 1978).

Balaam found, as expected, that the settlement decreases dramatically as the replacement ratio, column length or E_c'/E_s' increases; Figure 2.49.
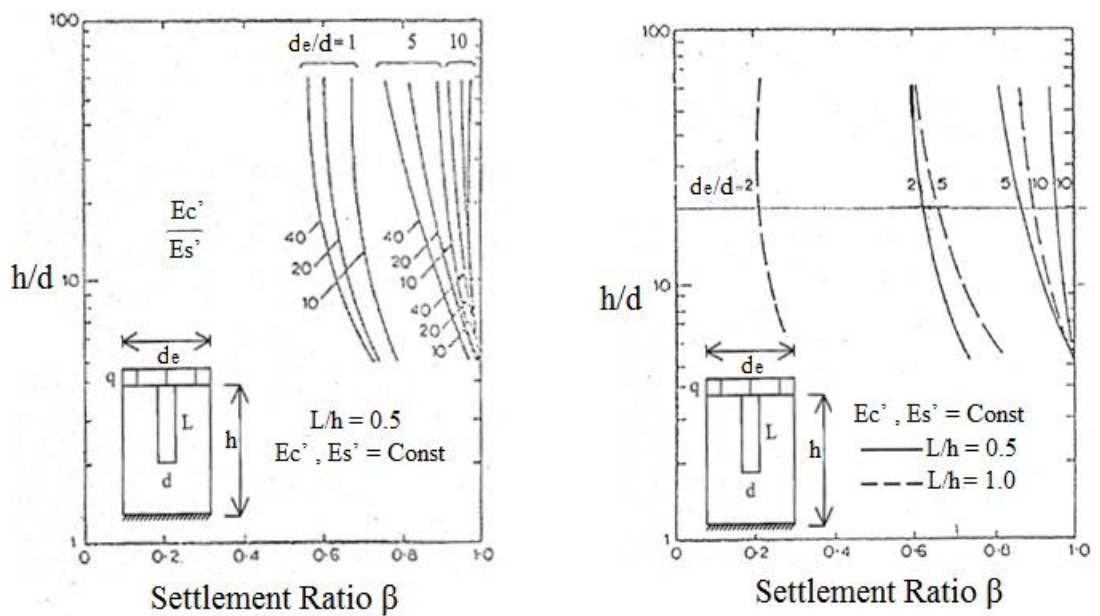
Figure 2.49 The effect of column length and E_c'/E_s' on the settlement reduction ratio (Balaam and Brown, 1977).

They also found that the resulted settlement when modelling materials as elastic is just 6% different from the elasto-plastic modelling results.

Balaam and Booker (1985) studied the behaviour of a large array of stone columns under a rigid raft foundation using the unit cell concept. They assumed a fully drained loading condition and that the clay was an elastic material, while the stone material was allowed to yield to incorporate the interaction between the stone column and the surrounding clay while loading. They also adopted Biot's theory of consolidation analysis, which assumes that dissipation of pore water pressure mostly happens in the radial direction and ignores the vertical direction of drainage. A parametric study was also performed to investigate the effect of column spacing, Poisson's ratio of the clay, internal friction angle of column material, dilatancy angle and $E_c^`/E_s^`$.

The interaction results showed that when the column diameter to spacing ratio exceeds 5, the reduction in settlement due to reinforcement is negligible. The result is in agreement with Hughes and Withers' (1974) laboratory model.

Again, the unit cell concept was used to simplify the problem with many assumptions, which meant that the assumed behaviour was totally different from the real behaviour of both clay and column materials. Some of these assumptions were related to the materials, such as using a fully elastic model to represent the clay and considering it as a purely cohesive material. Other assumptions based on the simulation method and the ability of the finite element code, such as the restrictions of boundary conditions in the unit cell method and the modelling of the stone column as a replacement column without taking into consideration the installation procedure and the applied radial displacement to the surrounding clay which, in turn, alters the stress state within the clay and improves the stiffness after dissipation of pore water pressure. These neglected changes are believed to have a positive effect on improving the performance of reinforced ground. All of

these simplifications and idealizations are believed to affect the outcomes of the numerical analysis.

2.11.2 Full Replacement Stone Column Group

Due to the complexity of the stone column group in terms of both geometry and stress distribution under the applied footing, it is very difficult to capture the real behaviour without studying the problem in three dimensions by using 3D finite element codes that incorporate the changes in stresses and strains in all directions. However, most of the finite element codes that were used by previous researchers to conduct their numerical analyses were 2D codes with axisymmetric or plain strain analysis. In the case of single stone column (unit cell method) the problem is easy to simulate in axisymmetric analysis, but in the stone column group case it is impossible to simulate it as a real geometry using 2D finite element programs. So, to consider a three-dimensional stone column model as plain strain or axisymmetric, homogenization techniques were adopted to model the column group using 2D finite element codes; this homogenization technique is based on the assumption that the distribution of the material of the stone columns is uniform within the whole reinforced zone.

There are two approaches of homogenisation;

1. Mixture Homogenization Method

This method is based on the assumption that the columns' granular material is scattered homogeneously throughout the treated soil as a volume ratio to get new mixed material (Etezad-Borojerdi, 2007); Figure 2.50.
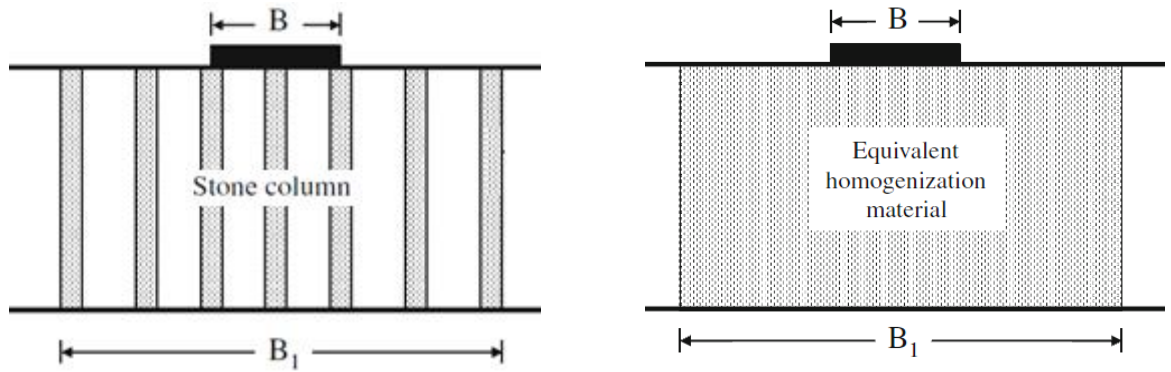
Figure 2.50 Simulation of reinforcement system in the mixture homogenization method (Choobbasti et al., 2011).

The main parameters (for Mohr–Coulomb model) of this new equivalent of soil/columns system can be determined form equations 2.52, 2.53 and 2.54 (Choobbasti et al. 2011).

$$\gamma_{com} = \rho.\gamma_s + (1-\rho)\gamma_c \tag{2.52}$$

$$c_{com} = \rho.c_s + (1-\rho)c_c \tag{2.53}$$

$$\Psi_{com} = \rho.\Psi_s + (1-\rho)\Psi_c \tag{2.54}$$

where γ_{com}, C_{com}, ψ_{com} are the composite unit weight, cohesion, and dilation angle of the equivalent reinforced soil. C_s, C_c, γ_s, γ_c, ψ_s, and ψ_c are cohesion, unit weight, and dilation angle of the column material and clay, respectively. The cohesion for stone column (C_s) and dilation angle for clay (ψ_c) are assumed to be zero. composite angle of friction is calculated from equation 2.55 (Cooper and Rose, 1999; Christoulas et al., 2000; Mestar and Riou, 2004).

$$\phi'_{com} = \rho.\phi'_s + (1-\rho)\phi'_c \tag{2.55}$$

where ϕ_s and ϕ_c are the angle of friction of the stone column material and the soft soil, respectively.

Gerrard et al. (1984) conducted one of the first research studies using this homogenization technique to investigate the stone column group. They modelled the soft clay and stone column with a constitutive model that combined the elasto-plastic behaviour of both the clay and the column materials. They used the Mohr-Coulomb yield criterion to analyse the

settlement of this homogeneous material under an equal applied vertical strain. Figure 2.51 presents the result of this settlement analysis for different area replacement ratios.
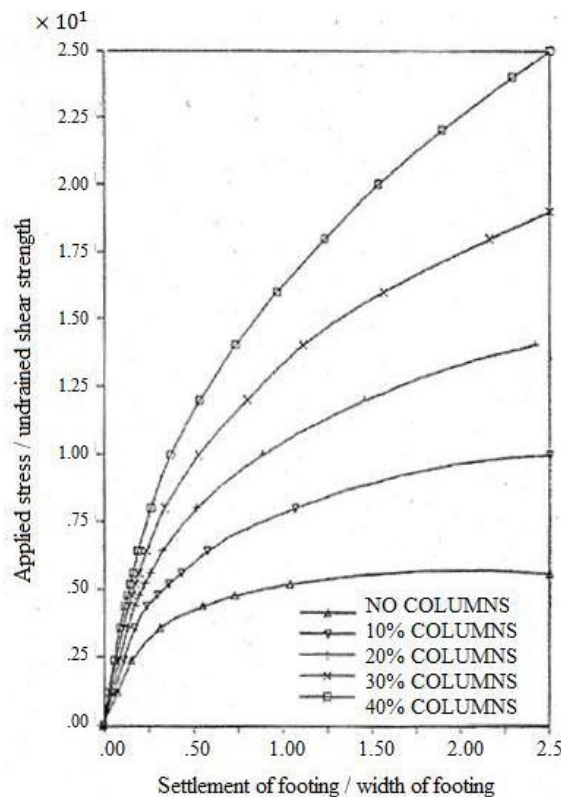
Figure 2.51 Load-settlement relationship for different area replacement ratios (Gerrard et al., 1984).

Schweiger and Pande (1988) utilized the homogenization method to model the reinforced soft clay under a road embankment. They state that their results are realistic.

It is clear that using the homogenization method provides a very simple engineering solution for analysing the behaviour of stone column reinforced foundations. It might be acceptable in a preliminary estimation of ultimate bearing capacity, but the principle of superposition assume that stone column and surrounding soil behave elastically, and the fact that stiffness is constant does not take into account the radial variation in stiffness which is shown by cavity expansion theory. So, the solution is far from reality because it ignores the basic concepts in geotechnical engineering when two contrasting materials are dealt with as a homogeneous one.

This material may meet the mechanical properties of the composite system, but it ignores the drainage properties and resulting consolidation. It also neglects the progressive consolidation process and the effect of this process on the performance of the system.

2. Axisymmetric and Plane Strain Homogenization Methods

Both of these homogenization methods are dimensional changing processes to create a three-dimensional distribution of stone columns within the treated clay in a way that considers these stone columns modelled as axisymmetric or plane strain. The new dimensions of the stone column distribution are calculated to keep the replacement ratio of the area, the distance between the columns and total surface area as in the original situation. Figure 2.52 and Figure 2.53 illustrates the calculation process of both cases.

Stone column area $= \pi R^2$
Number of stone columns in the first ring $= 8$
Total area of the first ring $= 8 \pi R^2$
Radius of the first ring (Rr) $=$

$$\sqrt{\frac{2.S \times 2.S}{\pi}}$$

Thickness of the first ring (Tr) $=$

$$\frac{8\pi R^2}{2\pi.Rr}$$
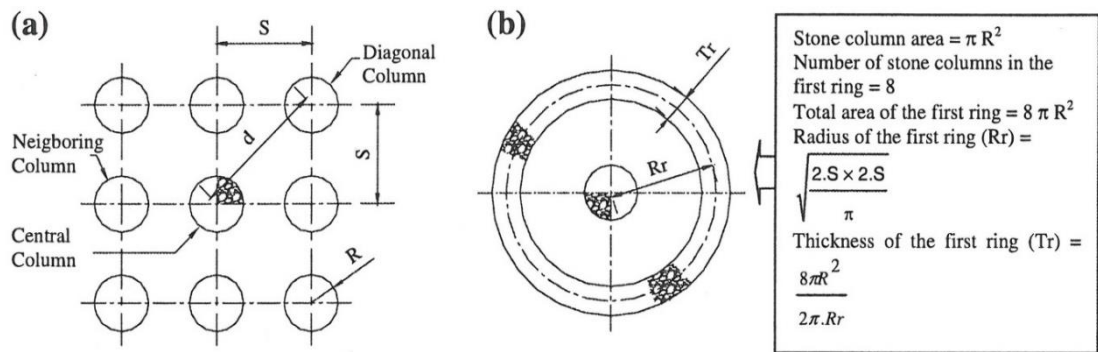
Figure 2.52 Idealization of concentric rings: (a) stone column grid with respect to a reference column; (b) calculation of the first concentric ring dimensions (Elshazly et al., 2008a).

$$\frac{\pi.d^2}{4} = t_e.S$$

$$t_e = \frac{\pi.d^4}{4S}$$
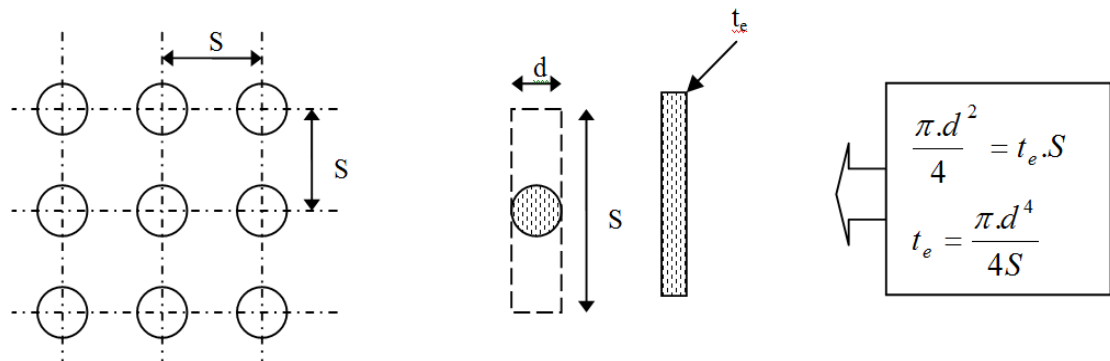
Figure 2.53 Idealization of stone columns in plane strain (Zahmatkesh & Choobbasti, 2010).

Mitchell and Huber (1985b) were the first to adopt the axisymmetric homogenization technique, utilizing the axisymmetric finite element model developed by Duncan and Chang (1970) at the University of California. They compared the load-settlement relationship, which resulted from the field loading tests carried out in a Santa Barbara waste water treatment plant in California, with the predictions resulting from an axisymmetric finite element model. The finite element mesh is illustrated in Figure 2.54. The result of the comparison show that the predicted settlement is greater than observed real settlement, as is shown in Figure 2.55.
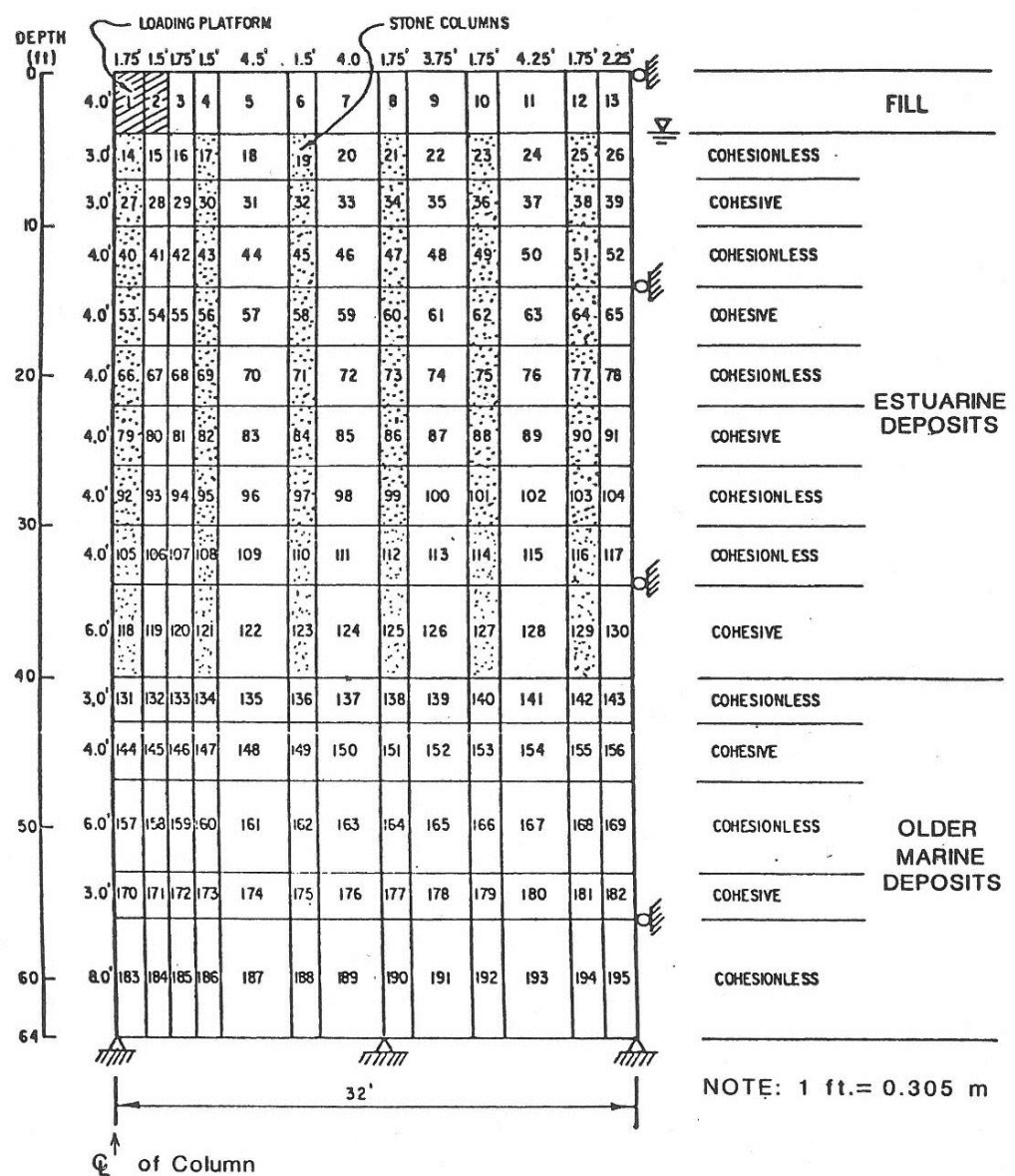
Figure 2.54 Finite element mesh used by Mitchell and Huber (1985b) to model the stone column reinforced ground at Santa Barbara waste treatment plant.

81
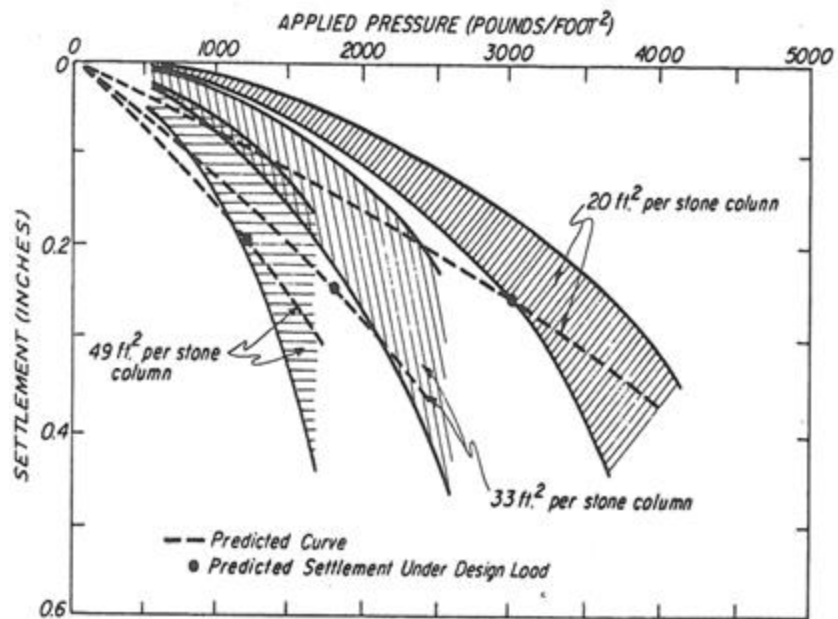
Figure 2.55 Predicted load settlement response using finite element analysis compared with observed results for various stone column spacings (Mitchell and Huber, 1985).

Mitchell and Huber (1985) state that this overestimated settlement may relate to incomplete consolidation during each step in the field and the exclusion of the general horizontal expansion of the ground while loading. This interpretation of the difference between the numerical analysis and the field records did not take into account the new geometry of the stone column distribution in the simulation model. It is obvious that the new geometry shortens the drainage path of the pore water pressure and speeds the consolidation process. As a result, the estimated settlement may be overpredicted.

Elshazly et al. (2007) carried out a numerical analysis to prove the importance of taking into consideration the changes of the stress state and stiffness of the treated clay in the reinforced foundation design. This change starts after the installation of vibro-replacement stone column installation and continues during clay consolidation. They re-studied the field loading tests carried out on a single column within an extended group in the Santa Barbara waste water treatment plant, using non-linear finite element code.

They applied the axisymmetric homogenization method and adopted the same soil profile and geometric idealizations used by Mitchell and Huber (1985). This calibration was performed using a fine mesh as presented in Figure 2.56 and a hyperbolic hardening soil model for the clay and the column materials and a Mohr-Coulomb failure criterion with fully drained conditions.
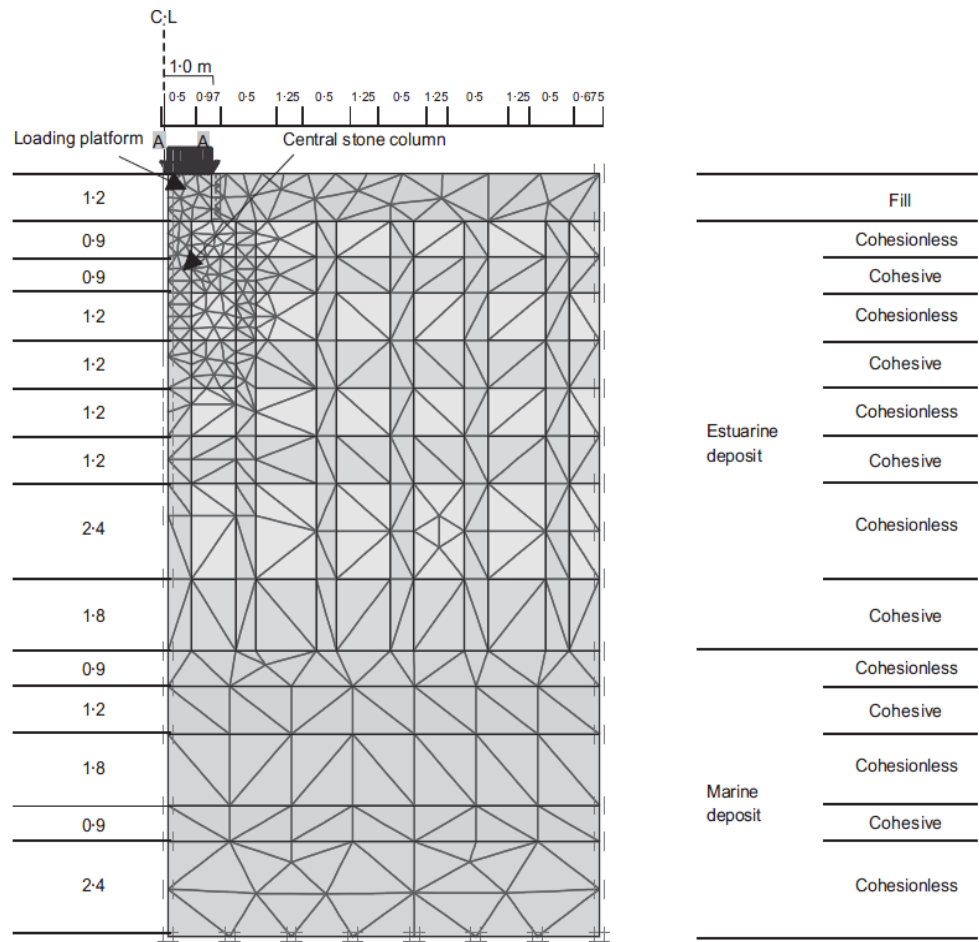
Figure 2.56 Finite element mesh used by Elshazly et al to model the stone column reinforced ground at Santa Barbara waste treatment plant (Elshazly et al., 2007).

They found that installing the vibro-replacement stone columns significantly alters the soil stress state, which can be represented by the lateral earth pressure ratio (*K*). They calibrated this parameter utilizing the back-analysis method and found that the horizontal to vertical soil stress ratio K of the clay surrounding the stone columns increases from the original value of untreated

clay to the range [1.1 to 2.5] according to the layer. This study is considered to have been the first step to quantify the change in the *in situ* soil after vibro stone column installation and consolidation, which leads to improvement in the design of the foundation.

Elshazly et al. (2007) continued their numerical analysis of calibrating the results of Santa Barbara field case, by carrying out two other analyses. The first was in 2007 when they studied the effect of stone column length and applied flexible foundation diameter on the settlement performance of the reinforced ground for two different applied loads (30 and 60 kPa). The result is illustrated in Figure 2.57.
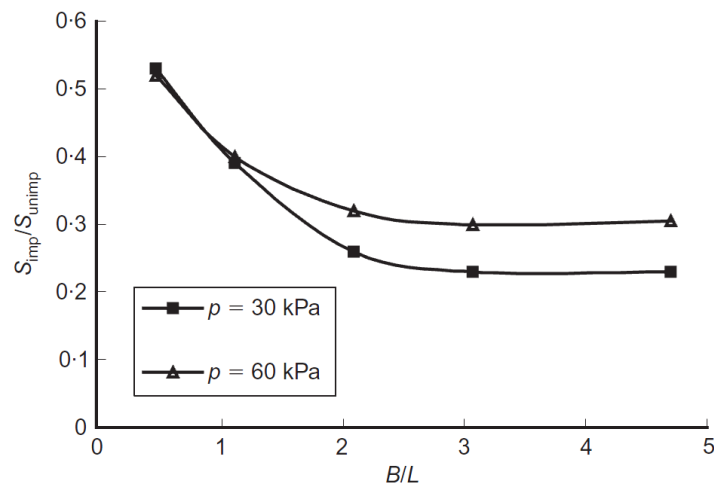
Figure 2.57 The effect of stone column length and applied flexible foundation diameter on the settlement reduction ratio (Elshazly et al., 2007).

In the second numerical analysis, Elshazly et al (2008) looked for the relationship between the inter-column spacing and the corresponding alteration of soil stress state of the clay around the stone columns. He found; that the confinement stress around the stone columns which is expressed by the coefficient of lateral earth pressure reduces with the increasing of the inter-column spacings, Figure 2.58.
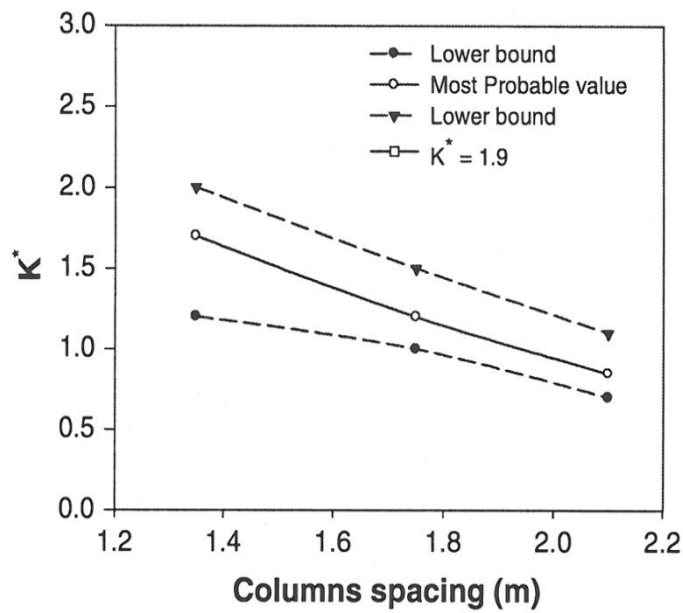
Figure 2.58 The effect of the column spacing on the soil stress state of the clay around the stone columns (Elshazly et al., 2008b).

Lee and Pande (1994) restudied the axisymmetric homogenization technique mentioned above and assumed an elastic plastic behaviour for both the clay and the stone column materials. They also adopted a Mohr-Coulomb yield criterion for the column material and a Modified Cam Clay to represent the clay. They applied their homogenization model using axisymmetric finite element code with the experimental data from the test results of Stewart and Hu (1993). Hu (1995) compared the typical load-settlement curve produced using Lee and Pandes' (1994) homogenization numerical analysis with his physical model results. Hu found that Lee and Pandes' (1994) homogenization technique overestimated the total bearing capacity by about 20% and the stiffness was also overestimated by a large proportion using this method, as is illustrated in Figure 2.59.
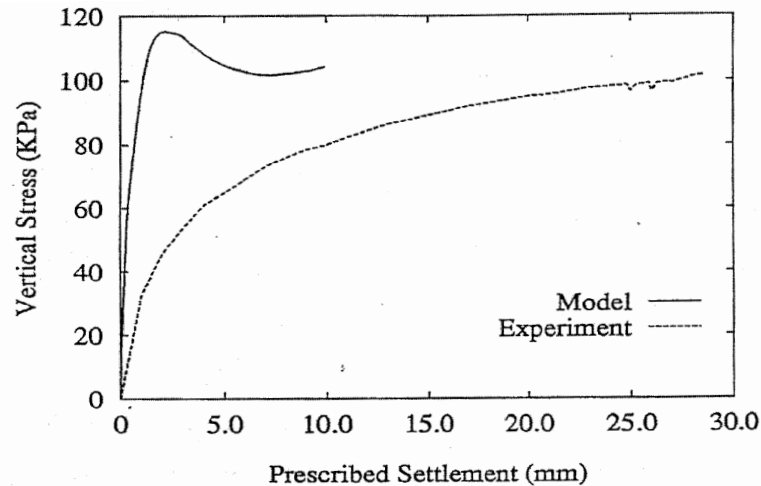
Figure 2.59 Comparison of the load-settlement curves produced using Lee and Pandes' (1994) homogenization numerical analysis and Hu's (1995) physical model.

The contradiction between Hu's physical model and Lee and Pandes' (1994) homogenization numerical model is that Hu (1995) found that to achieve a significant improvement in the bearing capacity of the stone column reinforced foundation, the area replacement ratio should be greater than 24%, whereas Lee and Pande recommend that the upper limit of this ratio should be 24% and state that there is no increase in bearing capacity beyond this value. It is clear that the homogenization method that assumes a fully drained condition with maximum area ratio 24% is not sufficient for this assumption and therefore it has some basic shortcomings.

Zahmatkesh and Choobbasti (2012) used the plane strain homogenization method (see Figure 2.53) in a series of drained numerical analyses to investigate the performance of stone columns within soft clay and to evaluate the settlement of a stone column reinforced system. Both the soft clay and stone material were assumed to have an elastic-perfectly plastic behaviour and follow the Mohr-Coulomb failure criterion.

Zahmatkesh and Choobbasti (2012) found from their numerical study that for different stone column area replacement ratios, the stress settlement behaviour with an entire area loaded is almost linear. This will allow the

equivalent stiffness of the improved ground to be found and thus the design of these foundations will become easier, as is shown in Figure 2.60.
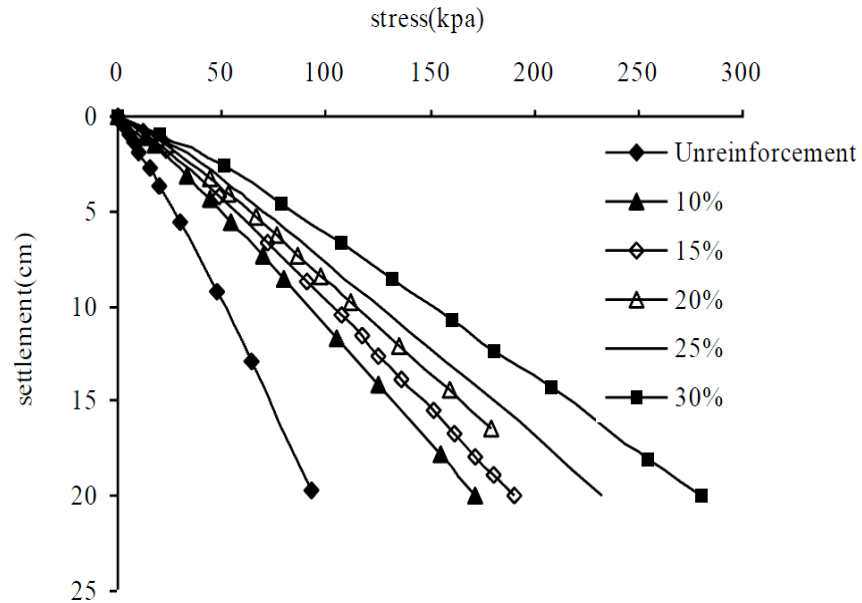
Figure 2.60 Stress settlement behaviour under loading for different area replacement ratios (Zahmatkesh and Choobbasti, 2012).

More importantly, Zahmatkesh and Choobbasti (2012) found that stress variation is caused in soft clay after column installation decreases with the distance from the column, as is illustrated in Figure 2.61.
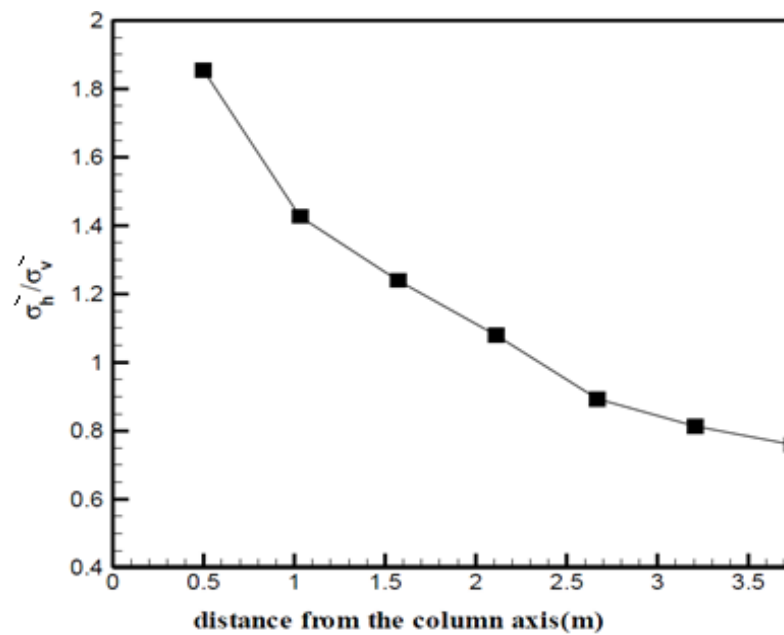
Figure 2.61 Variation of stresses in soft clay with distance from the column (Zahmatkesh and Choobbasti, 2012).

Wehr (1999) studied the deformations and stress distribution within three-dimensional stone column group model under loading assuming elasto-plastic behaviour for both the clay and stone column material. Wehr found that the deformation and failure shape of the reinforced clay mass is similar to what Hu (1995) found in his physical model; the outer columns were sheared while the central one was bulged, as is shown in Figure 2.62.
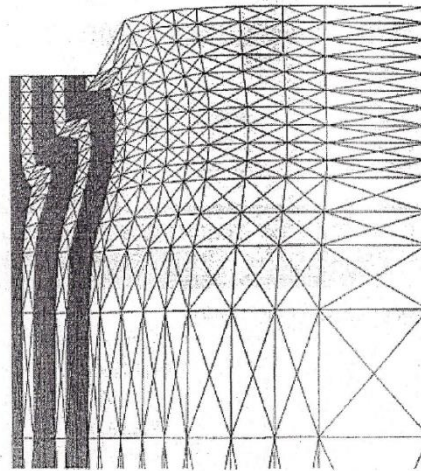
Figure 2.62 Deformed finite element mesh under 10 mm vertical displacement (Wehr, 1999).

Wehr (1999) also found that the distribution of the load between the columns and the surrounding clay during the loading process was similar to that presented in Figure 2.63. It can be noted from the behaviour of the outer range of the reinforced mass (3.clay) that the development in the clay stiffness due to consolidation increased the role of the clay in carrying a significant proportion of the load.
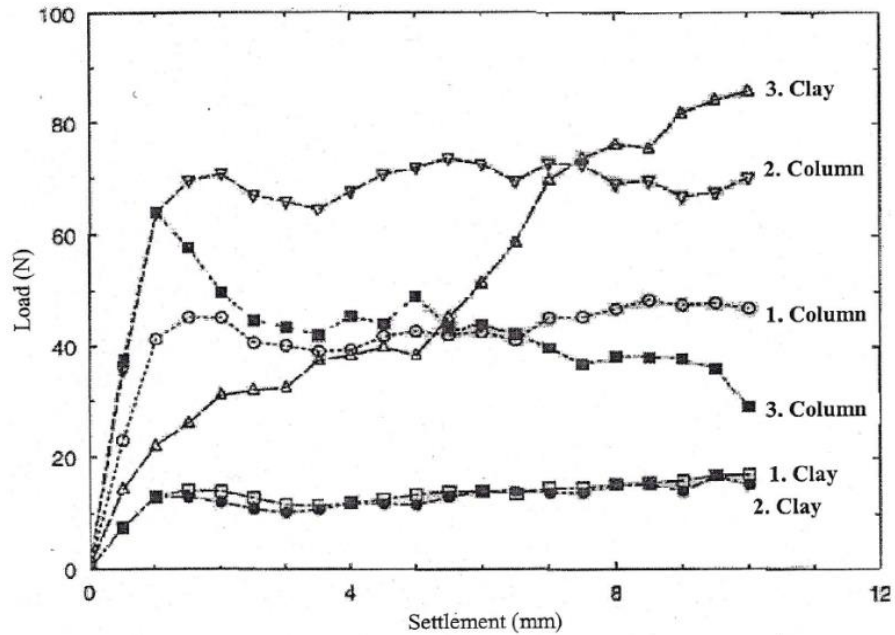
Figure 2.63 Load distribution between the columns and clay beneath the footing at various distances form the centre: (1) represents the centre; (2) represents the columns and clay at mid-radius; (3) represents the periphery of the footing (Wehr, 1999).

In a study by Kirsch (2008), a FEA was conducted on 2 footings supported by 25 columns. The FE model took into consideration the installation effects as they were measured previously in Kirsch (2006). A layer of sand on top of the stone columns was used to measure the ratio of the stress concentration (σ_c/σ_s). It was found that, under load, the ratio rose from 1.4 to 2.8 for the columns in the corner and from 1.4 to 1.6 for the columns in the centre. Upon reloading, the ratios also rose. Comparing the FEA to field data, it was observed that although the FEA over-predicted the columns maximum capacity, it was successful in predicting the settlement behaviour under loading. It was also found that the impact of the internal friction angle and the increase in the length of the column was more clearly apparent at low A/A_C. In addition, the stiffness of the column was not observed to have a noticeable effect on the footing settlement behaviour. It is held that because of stress concentrations, columns are deformed when they are subject to low loading, which leads them to lose sensitivity to the parameters related to elastic stiffness.

89

McCabe et al. (2009) reviewed a large number of these studies. In the aim of developing 'settlement improvement database', the authors collected a set of data points from more than 20 case studies. Due to insufficient provided data in the case studies, they assumed 40° for the angle of internal friction of the stone backfill as a typically embraced value in designs.

Wide area loadings were the focus of most data points. In Figure 2.64, a comparison is presented between the wide area loadings data points and the curve representing basic improvement, as suggested in Priebe (1995). Despite the scatter that can be observed, it is obvious that the trend represented by the measured data is similar to Priebe's (1995) predicted trend.
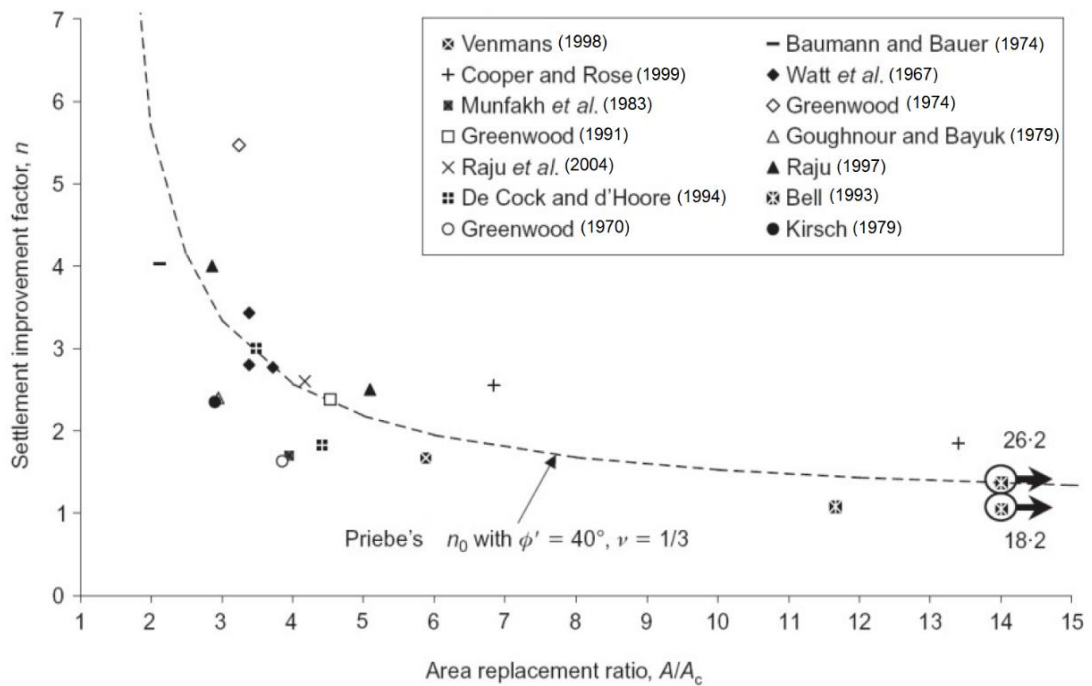
Figure 2.64 The factors of settlement improvement in comparison with the ratio of area replacement for widespread loading sites (McCabe et al., 2009).

2.12 The Effects of the Column Installation

Due to the vibrating poker penetration of the ground, the soil that surround the poker is imparted with horizontal vibratory forces. Fine particles attenuate the horizontal forces which change the stress state of the soft fine soils (Sondermann and Wehr, 2004). It is possible to predict the displacement of soil caused by the installation of a pile through a theory of cylindrical cavity expansion along the shaft of the pile and a theory of spherical cavity expansion along the pile tip and the soils situated at the surface of the ground would be impacted by the heave of the surface (Yu, 2000), as is shown in Figure 2.65

Zone A: displacement affected by ground surface

Zone B: displacement are mainly in the radial direction

Zone C: displacement affected by pile tip
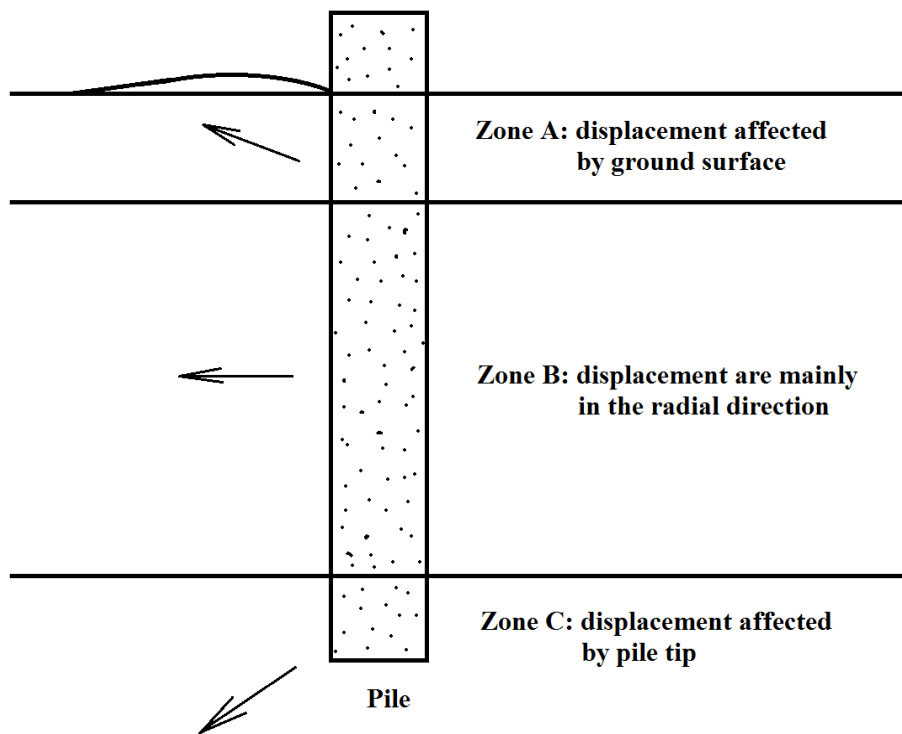
Pile

Figure 2.65 Displacement of soil because of pile installation (Yu, 2000).

2.12.1　　Laboratory Investigations

The patterns of soil displacement which are linked closed ended pile installation were investigated by Randolph et al. (1979a) through performing laboratory tests at a small scale.　As assumed in the theory of spherical cavity expansion, when the tip of the pile goes further, displacement of particles of soil occurs in outwards and downwards manner, but as soon as the tip surpasses the particles of soil, a radial displacement takes place. Furthermore, when the tip of the pile reaches a point beyond the particles of the soil at 4d–5d or more (d = pile diameter), soil displacement remains relatively static. The ultimate pattern of soil displacement would be similar to what happens in cylindrical cavity expansion.

Gill and Lehane (2001) adopted a method that employs a video camera in the aim of monitoring the displacement of soils that occurs during a flat bottomed penetrometer installation. This technique works through tracing dark beads as they move in front of a light background that is made of artificial material of a transparent nature. The features of this material resemble those of clay that is natural and lightly over-consolidated. Moreover, this material comprises of paraffin and particles of silica. It was observed that as the tip of the penetrometer got closer to the beads, soil displacement occurred in downward and outward manner, but as soon as the beads were surpassed by the tip, the displacement of the soils changed to become radial.

Jiun Liao et al (2006) developed a semi-empirical model to understand stone column behaviour and estimate the changes in undrained shear strength of *in situ* clay during and after installation of the column. Jiun Liao and colleagues believed that the clay around the vibro stone columns was subjected to lateral displacement during installation similar to that around the expanding cavity. So, based on the theory of the cylindrical expansion cavity in this study, they designed a large-scale laboratory model apparatus to take into account the changes in normally consolidated clay after installation of an expansion body. The diagram of this apparatus is shown in Figure 2.66.
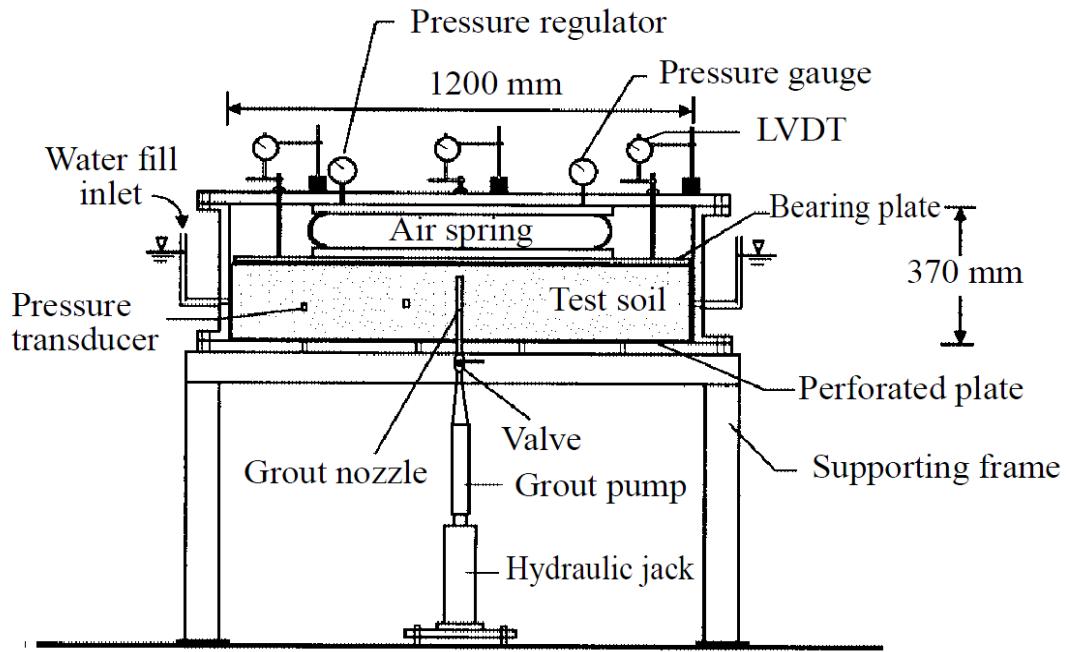
Figure 2.66 Laboratory model injection test apparatus used by Jiun Liao et al (2006).

To create the expansion body in the clay that would encounter the effect of a granular pile installation, Jiun Liao and colleagues injected a cement grout into the normally consolidated clay and generated grout bulbs that applied the required lateral displacement to the surrounding clay; Figure 2.67.

DGT1 ($\sigma'_p = 98$ kPa)   DGT2 ($\sigma'_p = 206$ kPa)
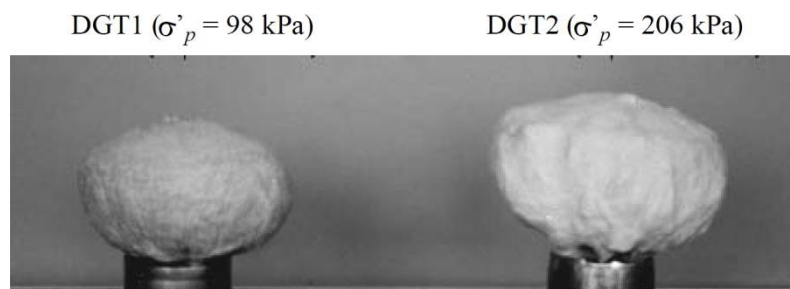
Figure 2.67 Injected grout bulbs used in laboratory model injection test (Jiun Liao et al, 2006).

The results of this laboratory model showed that, if the consolidation time for the excess pore water pressure, which initiates after grout injection, is sufficient to dissipate (t >3t_p, where t_p is the primary consolidation time), then the undrained shear strength increases around the pile within a distance up

to $7r_c$, where r_c is the radius of the expansion body. This increase in the undrained shear strength starts with a twofold increase adjacent to the pile and gradually decreases to the original undrained shear strength of clay at a distance $7r_c$ of the installed expansion body. Figure 2.68 illustrates these changes. This laboratory study shows the importance of changes in the stiffness and stress state of the clay, which extends to about $7r_c$ around the installed columns, on the performance of the reinforced ground.
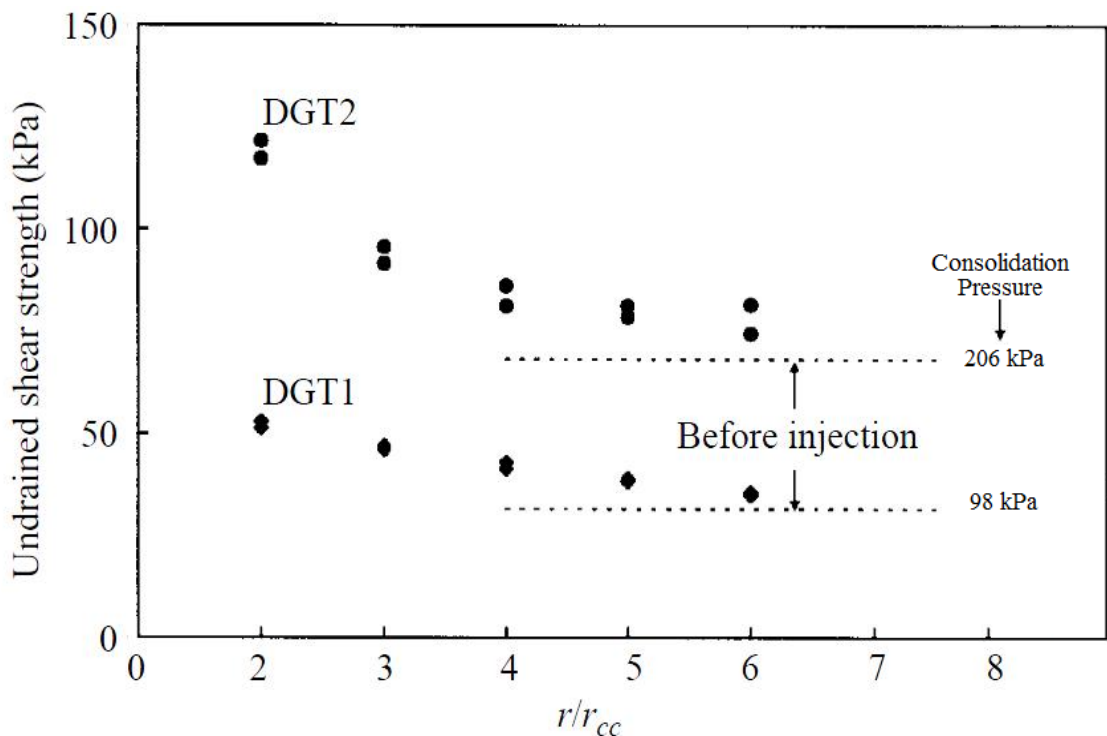
Figure 2.68 Undrained shear strength changes vs normalized radial distances (Jiun Liao et al, 2006).

2.12.2   Observed Field Measurements

In a study by Kirsch (2006), the author investigated the alterations that might occur in an in-situ stress regime in sandy silt as a result of installing two sets of 25 stone columns. With the aim of identifying the soil stress state after installing the columns, the author also studied the variations that might take place in soil stiffness, effective horizontal stress and pore water pressure. It was found that the pore water pressure increased soon after installing the

columns. The horizontal stress, presented in Figure 2.69, apparently rose within a region ranging between 4d to 8d from the column centre. A similar situation was attested in soil stiffness as shown in Figure 2.70. As the vibrating poker got closer to the positions set to be measured, both of the soil stiffness and horizontal stress increased. Nevertheless, the impacts of dynamic excitation and remoulding within a 4d distance compensate for this rise in soil stiffness and horizontal stress. Kirsch's (2006) statement about the role of the adjacent 4d cylindrical remoulded soil around the stone column was very controversial and needs more investigations because in most practical projects for stone column reinforcing foundation, the column spacing are less than 4d, more investigations were carried out about this point later in section 2.14 of this chapter.
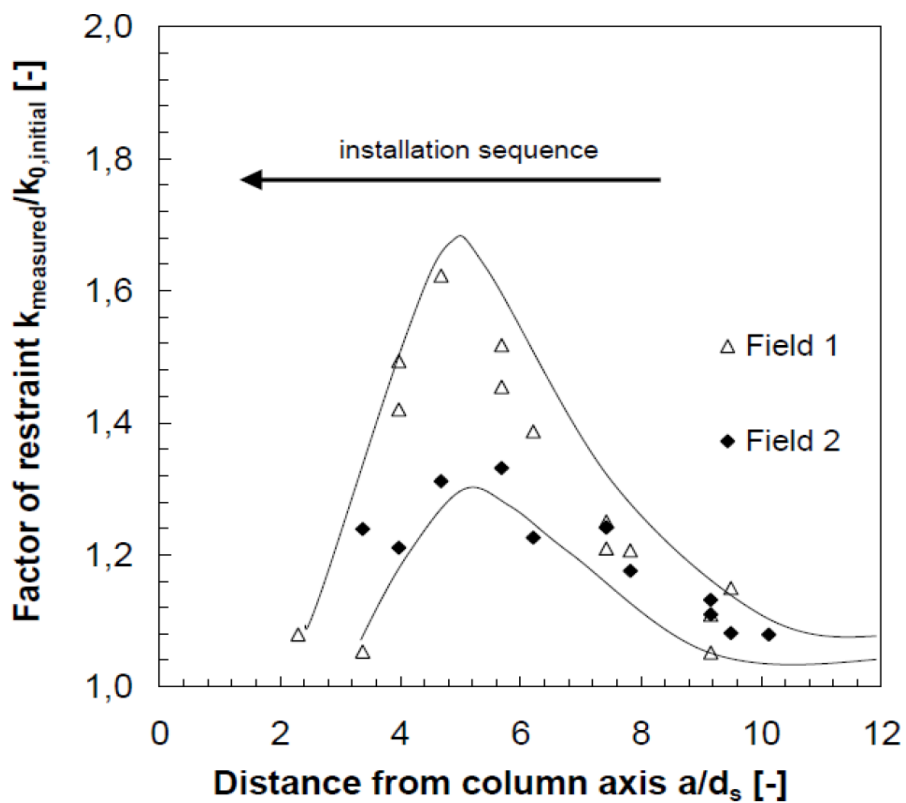
Figure 2.69 Measuring restraint factor during the stone columns installation (Kirsch, 2006).
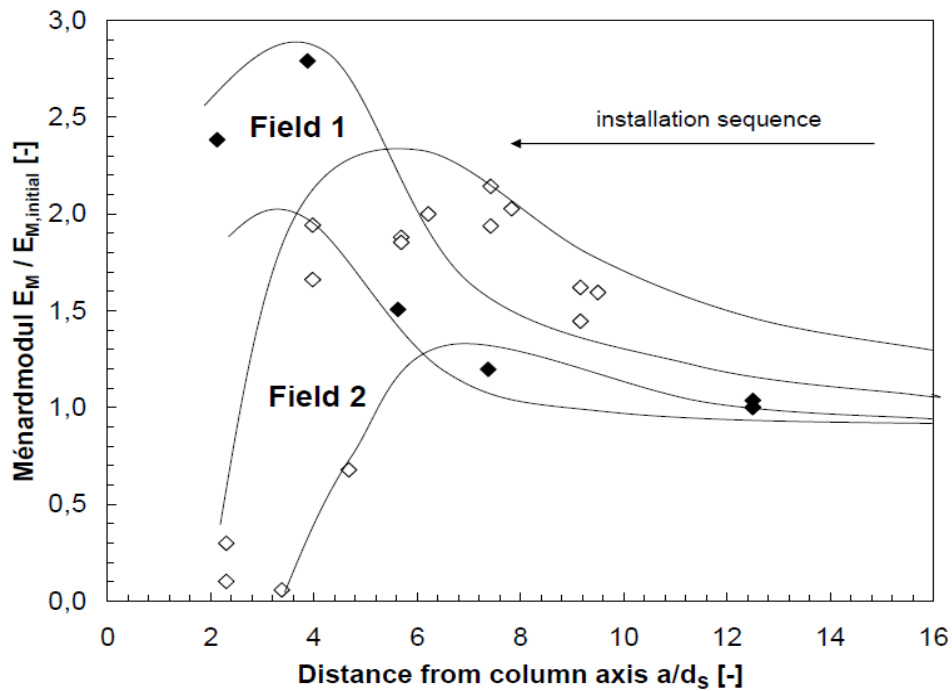
Figure 2.70 Development of the stiffness of ground during the installation of columns (Kirsch, 2006).

In Castro (2007), the increase and disperse of the excess pore water pressure arising from installing seven stone columns in a normally consolidated clay of was recorded. The poker penetration was topped by the pore water pressure, which also reached a peak when the tip of the poker surpassed the piezometers level. Although the surface of the ground experienced significant heave, the assumption that there were plane strain conditions was reasonable and, therefore, the theory of cylindrical cavity expansion could be used in the aim of simulating the installation of the poker. There was consistency between the theoretical values (determined based on Randolph et al.'s (1979b) analytical formula) and the development of the excess pore water pressure. As a result of the increase of excess pore water pressure that linked to installing a driven pile, it was assumed that there was a reduction in the undrained shear strength of the soil in the surrounding area. Nevertheless, as more columns are installed, the consistency between the theoretical and field values starts to disappear because of the violation of the assumed plane strain boundary conditions. The time it took to dissipate the excess pore water pressure was very short

(within 15 minutes) (Killeen, 2012). Compared with the theoretical disperse time (determined based on a finite difference method following Soderburg's (1962) theory), the actual dissipation time is 100 times less. This was because the clay fractures arising during the installation of the column work as drainage channels.

In Gäb et al. (2007), the settlement and pore water pressure in a large embankment construction were measured. The embankment was established on 11 m of loose-medium dense lacustrine sand with an underlay of 50 m of clayey silt. The installation of the stone columns was performed to 14.5 m. This was installed on a triangular grid at $A/A_C = 7.7$. The number of installed columns was 37 in a total of 4 rings. The installation started in an inward manner progressing from the outer edge to the centre. As the construction approached the piezometers, an increase in excess pore water pressure started to occur. The maximum level of this increase was observed just near the base of the column at 12 m, but it was even noticed at a deeper level at 20 m. The dissipation of the excess pore water pressure in the sand took a short time (< 1 day), but much longer in clay. Heave was also observed, at a slight level, though.

Based on data on stone column installation at different locations collated by Egan et al. (2008), it was found that heave could take place when stone columns are being installed, which is indicative of the presence of a relationship between the density of the column and the heave size. It was suggested by the authors that heave is a function of the method of construction, spacing and the size of the columns. The arrangement of footing also has an impact on the heave size; smaller groups and stone columns strips produce much less heave than larger ones.

An important study to investigate the effect of stone column installation by applying the cavity expansion theory in finite element program was performed by Shien, (2011). He started with initial cylindrical cavity of initial radius, r_0 of 0.5m to start with, then it was expanded in an undrained condition to a radius, a of 2 m by internal pressure of P enforced in PLAXIS finite element program by using the prescribed displacement loading

function. Using an axisymmetric analysis the results of the numerical study on the effects of the cavity expansion of a stone column in soft clay compared well with the analytical solution and field studies.

Figure 2.71 illustrates the changes of effective horizontal stress with the distance from the cavity wall after the consolidation at different depths, it is clear that the highest value is at the cavity wall and it decreases with the increase in radii from the column centre (Shien, 2011).
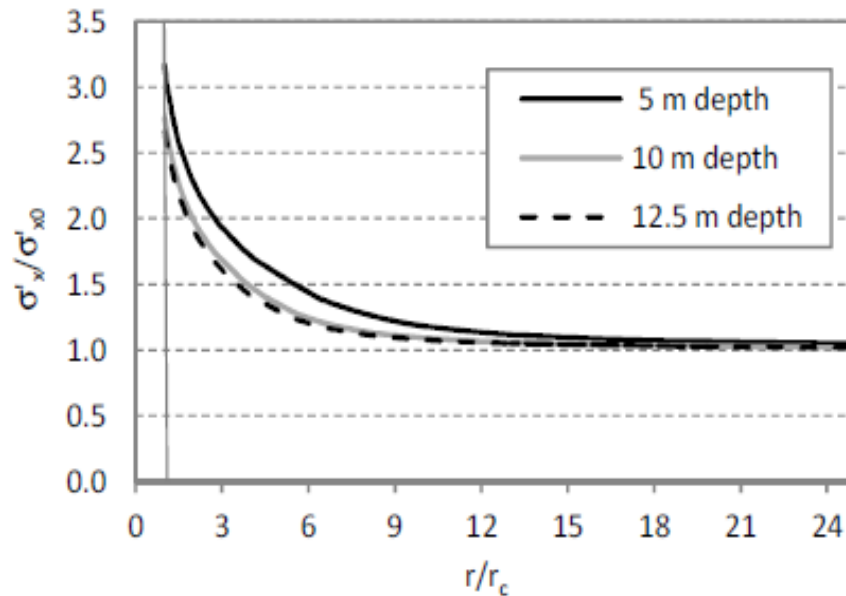
Figure 2.71 Effective horizontal stress after consolidation (Shien, 2011).

Shien et al. (2011) defined the influence zone caused by column installation by plotting the changes of the coefficient of horizontal earth pressure as demonstrated in Figure 2.72 The curve plateaus after about 12 column radius. Field measurement by (Kirsch, 2006) also indicated that the installation influence zone falls between 8 to 16 column radiuses.
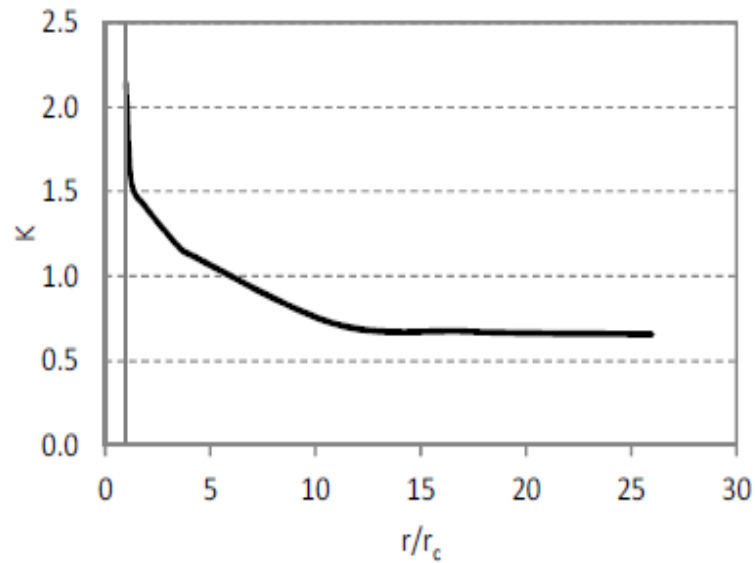
Figure 2.72 Installation effect to coefficient of horizontal earth pressure (Shien et al,2011).

Immediate pore water pressure increases was illustrated in Shien's (2011) during poker penetration and column installation followed by dissipation which occurs afterwards with the time, as is shown in Figure 2.73.
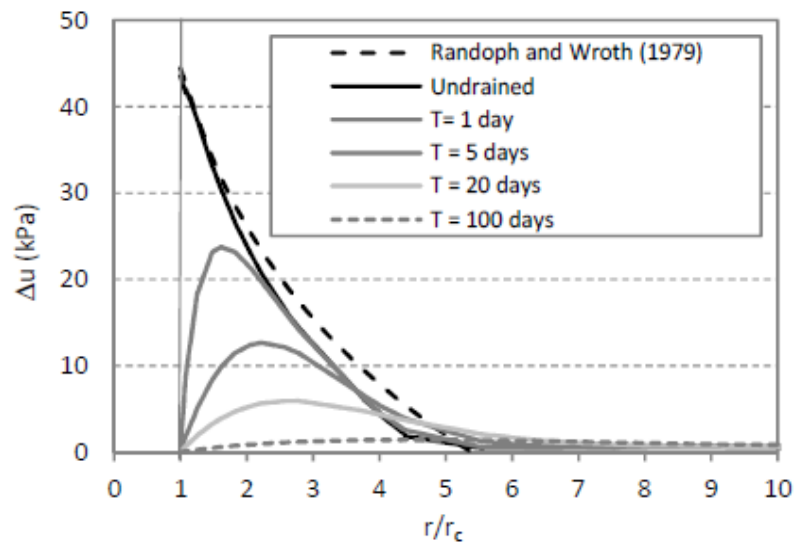
Figure 2.73 Isochrones of pore water pressure dissipations at 10 m depth (Shien et al,2011).

In 2014 Killeen used PLAXIS 3D Foundation to study the settlement performance of a group of different stone column configurations under

square pad footing. He stated that the most appropriate method to simulate column installation effects is to increase the coefficient of lateral pressure (K_0) in the surrounding soil and he neglected any change in the stiffness in this clay. in PLAXIS 3D Foundation is to increase the coefficient of lateral pressure (K_0) in the surrounding soil. Based on a review of numerical analyses which adopted this for Bothkennar test site, he suggested that K_0 increased in the range 0.75–1.50, with an average of 1.00.

2.12.3 Installation Effects Simulation in Numerical Models

After reviewing most of the previous research studies, the simulation of the installation effect of stone columns can be summarized as the following:

- **Increased coefficient of lateral earth pressure**

The increase in the lateral earth pressure coefficient (K_0) in the soil that surround columns could possibly account for the effects linked to stone column installation. As Table 2.1 shows, many authors implemented this technique. Axisymmetric FEA was employed by Elshazly et al. (2007) in the aim of calculating the rise in K_0. This was performed through the back-calculation of the field load tests that were performed on stone columns and were delineated in Mitchell and Huber (1985). Loading is done by a circular footing for a column positioned in the centre of a large group of columns. In a layered estuarine deposit, the 'wet technique' was employed in the installation of stone columns to a 10.8 m depth. Soil samples that were obtained after installation were used to determine the soil features used here. Hence, this helped with the incorporation of any alteration of the features of the soil as a result of the installation of the columns. Observed differences in the curve of load-settlement were held by the authors to be due to an alteration in the state of the stress of the soils that surround the columns. And then K_0 was modified for the curves of load-settlement to match. Given that the assumed soil parameters are correct, an axisymmetric FEA suggests that $K_0 = 1.5$ gives a perfect match between the real and forecasted curves of load-settlement.

The previous analysis was elaborated by Elshazly et al. (2008b) to study the impact of column spacing on the soil stress state after installation. An analysis of a group of column spacings was performed. The spacings corresponded to A/A_C ranging between 2.5 and 4.8. K_0 values, which were back-calculated, extended from 0.7 to 2.0, based on how trustworthy the parameters of soils can be. K_0 can be conservatively estimated as follows: 1.7 for $A/A_C = 2.5$, 1.2 for $A/A_C = 3.7$ and 0.85 for $A/A_C = 4.8$. This shows that a decrease in the installation stresses occurs at high A/A_C (columns that are spaced widely).

Table 2.3 Accounting for the installation of stone columns by increasing K_0 in many studies (after Killeen 2014).

Reference	A/A_C	Coefficient of lateral earth pressure, K
Balaam & Booker (1977)	4 – 10.0	1.00
Barksdale & Bachus (1983)	4 – 10	0.75
Mitchell & Huber (1985)	2.0 – 4.9	1.00
Elshazly *et al.* (2007)	3.4	1.50
Domingues *et al.* (2007a)	3.3 –10.0	0.70
Elshazly *et al.* (2008b)	2.0 – 4.9	0.85-1.70
Killeen (2014)	3.5 – 14.1	1.00

- **Cylindrical cavity expansion**

Axisymmetric FEA was also employed by Debats et al. (2003) and Guetif et al. (2007) for the simulation of impacts of stone columns installation. An undrained cylindrical expansion was applied to a 'dummy material', which was then modified to a stone column after expansion. Cavity expansion is essential for the replication of the actual process of installation to be successful. This needs to extend from the initial diameter (0) to the final column diameter. Nevertheless, performing this in a numerical model would not be possible in theoretical terms because there would be a generation of

infinite strain. Randolph et al. (1979a) performed a numerical analysis for the installation of a pile, and it was found that radius doubling was adequate for a stimulation of the expansion of a cavity from a (0) diameter. The expansion of the 'dummy material' from 500 mm initial diameter (similar to the diameter of a typical poker) to 1100 mm final diameter of the column was conducted. To minimize high stresses in the column when it is expanded, a 'dummy material' with a nominal stiffness was used.

A numerical investigation was performed by both authors to understand the impact of this technique on increasing the strength of the soil that surrounded the columns as well as the area of the impact for the columns that were being expanded. They found that large excess pore water pressures in the soil were induced by the undrained cavity expansion and these increased significantly at low A/A_C. An increase occurred in the stiffness of the soil and the mean effective stress after soil consolidation. The proportion of increase in the stiffness of soil ranged between 30% and 40% as reported by Debats et al. (2003); this occurred within the radius 2D of the cylindrical zone for (6 – 10) m spacing of the columns . Nevertheless, these results are based on Mohr-Coulomb model. Indeed, greater increases in the stiffness of the soils were found in wider areas of influence when more developed model was used (i.e., Hardening Soil model). It was observed by Guetif et al. (2007) that the earth pressure lateral coefficient rose above unity in the surrounding soil.

- **Cylindrical cavity expansion and increased soil stiffness**

In a field study conducted on two sets of 25 columns, Kirsch (2006) simulated the effects of installation. On each column, an individual cylindrical expansion was applied and the stiffness in the enhancement area around the footing was increased. As suggested by Kirsch (2006), the most appropriate match between the actual and forecasted curves of 'load-settlement' was reached through the application of a moderate cylindrical expansion on the stone column (lateral strain, ε_r = 4%) and increasing the stiffness in the enhancement area existing at a point surrounding the central

line of outer row columns between 2d and 5d. Employing the FEM (incorporating the installation effects), a back-calculation of the performance of the load settlement for the two footings was performed. The FEM was observed to be consistent with analytical design methods and field data (Goughnour and Bayuk, 1979; Priebe, 1995).

In a study by Kirsch (2006), the impact of installation effects of global and individual columns was studied on the factor of settlement improvement for a square footing of 7.2 m; the number of columns used to support this was 25. It was found that an 8% increase in the radial expansion of the individual column diameter led the settlement improvement factor to increase by 45%. Investigating the impacts of the global installation indicated that a triple increase in the stiffness of this area would lead the settlement improvement factor to increase by 25%. Nevertheless, this increase was found to depend on the loading stage as the increase was lost with higher loads and the domination of plastic deformation was noticeable. Overall, the ultimate behaviour of stone column is not influenced by the effects of installation, but a positive role is played by these effects to improve the settlement behaviour

2.13 Summary of Column Installation Effects

The formation of stone columns happens with the help of a vibrating poker which conveys horizontal vibrations and displace soils. The resulting forces from horizontal vibration are taken by soils of fine grains. And change its *situ* stress state. According to the findings of some laboratory experiments based on cylindrical cavity expansion theory, it was possible to forecast the displacement of soil because of the installation of a driven pile. The researchers applied this method for modelling stone column installation in two-dimensional axisymmetric FEA.

Information from the field shows that soil stiffness and horizontal stress rise in a zone ranging from 4d–8d from the columns centre-line. The impacts of remoulding and dynamic excitation within 4d offset the rise in soil stiffness and horizontal stress. There was also a favourable agreement between the

analytical formula proposed by Randolph et al. (1979b) and the rise in excess pore water pressure because of the initial poker penetration. The impacts of column installation seems to have a positive effect on the development of the settlement behaviour of stone columns.

For the simulation of column installation effects, there are a number of methods which are listed below:

1. Increase the coefficient of lateral earth pressure (K_0) in soil

    - Increases in K_0 ranges from 0.75 to 1.50 (K_0, average = 1.0)

2. Apply cylindrical cavity expansion to stone column

    - Expand a dummy material (with a nominal stiffness)

    - Convert properties to stone backfill after expansion

3. Apply cylindrical cavity expansion to stone column and increase soil stiffness

    - Apply cavity expansion to stone columns

    - Increase the stiffness in an enhancement zone (2d–5d from centreline of outer columns).

2.14 Knowledge Gaps

The literature review illustrated the findings and results of an extensive work carried out over the last 40 years which led to improvements in understanding the behaviour of vibro stone column reinforced foundations as a promising ground improvement technique to construct on weak and soft deposits. Nevertheless, few of these studies have tried to quantify some of the key design parameters, namely the changes in the stiffness and stress state of the treated soil, or have considered these parameters in the design and the calculation process. Consequently, semi empirical and conservative design methods are still being used by ground improvement companies with a significant variety of results in engineering practice (Ambily and Gandhi, 2007).

After reviewing and comparing most of the existing approaches and theories for the design of vibro stone column reinforced foundations, the following conclusions can be drawn:

1. In reality all installation methods of stone columns involve in partial to full radial displacement to the cylindrical hole in the soft clay. So the effect of this degree of lateral expansion on the response of the surrounding clay should be taken into consideration in the design process of the reinforced ground.

2. Adoption of a unit cell concept in the analysis and design of stone column reinforced foundations will lead to a conservative estimation of the performance of these systems. This is because stone column foundations normally consist of a number of columns that work together with the surrounding clay to create one system. The unit cell approach neglects the columns/soil stiffness and column/column interactions by considering that the deformations in the clay are restrained within the unit cell. This restraint prevents the columns and clay from moving laterally, thus the effect of adjacent columns on increasing the confinement of the columns and accumulating more stiffness to the clay between these columns is ignored.

3. The stress concentration ratio is an important parameter in interpreting and tracking the behaviour of the stone column foundations (Aboshi et al., 1979, Bachus and Barksdale, 1984, Balaam and Booker, 1985, Saadi, 1995, Hu, 1995, McKelvey et al., 2004, Killeen and McCabe, 2014). This ratio expresses physically the changes of stresses and stiffness within the column/soil system. These changes happen within the clay immediately after the column installation process (applying radial displacement), and after radial consolidation to the vertical drains (stone columns) before and after applying construction loading. It is clear that the stress ratio is dependent on the progressive consolidation process and it changes with time. Greenwood (1991b) stated that different values of stress concentration ratio have been reported and some of them consider it as a constant in the design process. Saadi (1995) found that the

general trend of the stress concentration ratio is that it decreases with time as consolidation proceeds. This uncertainty and wide range of stress concentration ratio values reflects that researchers have been more concerned about the behaviour of columns rather than the changes in the clay around the columns. It is worth noting here that the stress ratio is critical in designing for the stability of reinforced foundations so that they can bear any immediate applied loading before the clay gains enough strength due to the pore water pressure dissipation. This means that clay may carry a load that exceeds its undrained shear strength in the early stage of loading, consequently failure occurs. Saadi (1995) stated that, for stability purposes, the stress concentration ratio should not be lower than 2 before construction starts.

4. Ground reinforcement with vibrated stone columns is a composite system in which the soil provides lateral support to the column and the column acts as soft piles and drain to consolidate the soil. However, Homogeneous analysis in both theory and numerical simulation is believed to have many shortcomings that reduce the use of such analysis to just the preliminary prediction of composite system. In the case of analytical homogenization theory, homogenized analysis assumes that the improved soil is a homogeneous material block with equivalent properties. This block system imposes a predetermined deformation and failure mode, namely a single brittle shear failure, ignoring any local failure of individual columns (no bulging). Both field observations and laboratory test results have proved that the suggested shear failure in this analysis is unlikely to happened (Vautrain, 1977). This approach does not take into consideration the effect of low stiffness of the clay, which usually leads to punching, bulging or general shear failure of the reinforced system.

    Although the homogenization methods used in numerical analysis give a good approximation to use 2D finite element codes in simulating the 3D problems of stone column reinforced foundations, it

is clear that redistributing the stone column materials to meet the requirements of 2D simulation alters the main mechanism of the composite system. This geometrical conversion keeps the same area of the bearing stone columns; however, it neglects the effects of the new geometry on the clay and the changes in stresses and stiffness due to installation and progressive consolidation processes. These changes play an important role in providing confinement to the columns and supporting loads. In other words, the new geometry will totally alter the strain response of the clay and shorten both the drainage paths and consolidation time. This argument is supported by the results of Mitchell and Huber (1985a), who found that numerical analysis using the homogenization method overestimates settlement compared to that recorded in the field. This highlights the importance of using 3D finite element code that incorporates the changes in stresses and stiffnesses in all directions.

5. Methods of analytical design which were discussed before in section 2.10 have many simplifying assumptions. Guetif et al. (2007), who noticed significant improvement in the Young modulus of soft clay due to the installation, stated that it should be considered in the design procedure. McCabe et al (2009) also highlighted the lack of high quality data in the literature research about the long term lateral effective stress and permanent increase of undrained shear strength imposed by stone column construction. Therefore, this should be taken into account in the settlement performance of stone column foundations.

6. In many of the numerical analyses reported in literature review, the stone columns were simulated as full replacement columns without any consideration of the applied radial displacement to the clay caused by the installation process. So, it is believed that the effect of stone column installation must not be ignored. Another important issue that has also been neglected by many of the previous numerical analyses is the selection of a representative soil model. A model should take into account the plastic behaviour of the clay due to large

displacements and the resultant hardening due to the consolidation process.

7. The clay stiffness gained during long-term consolidation after column installation decreases with distance from the compacted column, as illustrated in Figure 2.70 by kirsch (2006). Therefore, assuming a uniform stiffness is not valid. The variation in stiffness is a function of the installation techniques of the soft piles that disturb the ground when they are improving it. However, most common design methods (Priebe for example) do not take into account this stiffness variation.

8. Although there has been good knowledge of the deformation behaviour of single and stone columns groups by many researchers (Aboshi et al., 1979, Bachus and Barksdale, 1984, Balaam and Booker, 1985, Saadi, 1995, Hu, 1995, McKelvey et al., 2004, Killeen and McCabe, 2014), there is lack of details about the effect of stone column installation on the deformation behaviour of these foundation. In this regard, it was noticed throughout the literature review that the majority of the recent researchers who took the installation effect in their studies and designs were interested to change the stress state of the soft soil that surrounded the stone column and increase the value of coefficient of lateral earth pressure without any certain rule. The more important changes in soil stiffness after consolidation. Killeen and McCabe (2014) have one of the most recent advanced 3D studies for the settlement performance of pad footings on soft clay supported by stone column. They stated that the dynamic excitation and remoulding of the soft soil during stone column installation negates any increase in horizontal stress and stiffness of the soil. This uncertainty in this issue make it very important to restudy it again

9. One of the rare studies that took the stiffness changes into account in design, was Kirsch's (2006). His statement about the role of the adjacent 4d cylindrical remoulded soil around the stone column was very controversial and needs more investigations for the following reasons;

- The radius of the remoulded distance around the stone column was subjected to many factors like; the installation method, vibration energy, displacement degree and soft soil properties.

- The reconsolidation of this area under the high radial stress (compared to the original *in-situ* one) created by the installation will results in high value of stiffness after sufficient long term consolidation.

- The inter-particle area which is very close to the column will have significant effect in increasing the stiffness of this area.

- taking into account the effects the column/soil stiffness interactions, and then use that variation in stiffness in design calculations of the foundation system.

- In most practical projects for stone column reinforcing foundation, the column spacing are less than 4d (Elshazly et al., 2008a), including many of the mentioned field cases in the literature review. The researchers stated the positive role of the surrounding soil in enhancing the settlement performance of the stone column group Mitchell and Huber, 1985b; Elshazly et al., 2008a; Castro and Sagaseta 2009 and Zahmatkesh & Choobbasti, 2010).

Construction techniques effectiveness was examined by McCabe et al. (2009). For this purpose (settlement improvement database).

Figure 2.74 Predicted versus measured settlement improvement factors for all widespread loadings and footings (McCabe et al., 2009).

 presents a comparison between predicted and measured factors of settlement improvement. The construction technique appears to have a great impact on stone columns settlement performance. Moreover, it appears that in soft soils, the installation of vibro stone columns is preferred to be performed using the bottom feed method. In Figure 2.74, some of the data points indicate that the behaviour of the vibro stone columns is not up to what is suggested in the prediction. This could be attributed mainly to the installation of stone columns. In addition to the lack of certainty in the measured data and workmanship (McCabe et al., 2009). So, the main

difference between the stone column construction methods is how to create the body of the stone relatively with the surrounding soft soil (Full replacement to full displacement). Base in this point, the scatter in Figure 2.74 between the predicted and measured factor of settlement improvement might be backed to the ignorance of the stone column installation effect on the soft soil in the calculation methods, especially in wet and dry top feed methods, while the bottom feed system has less difference in performance.
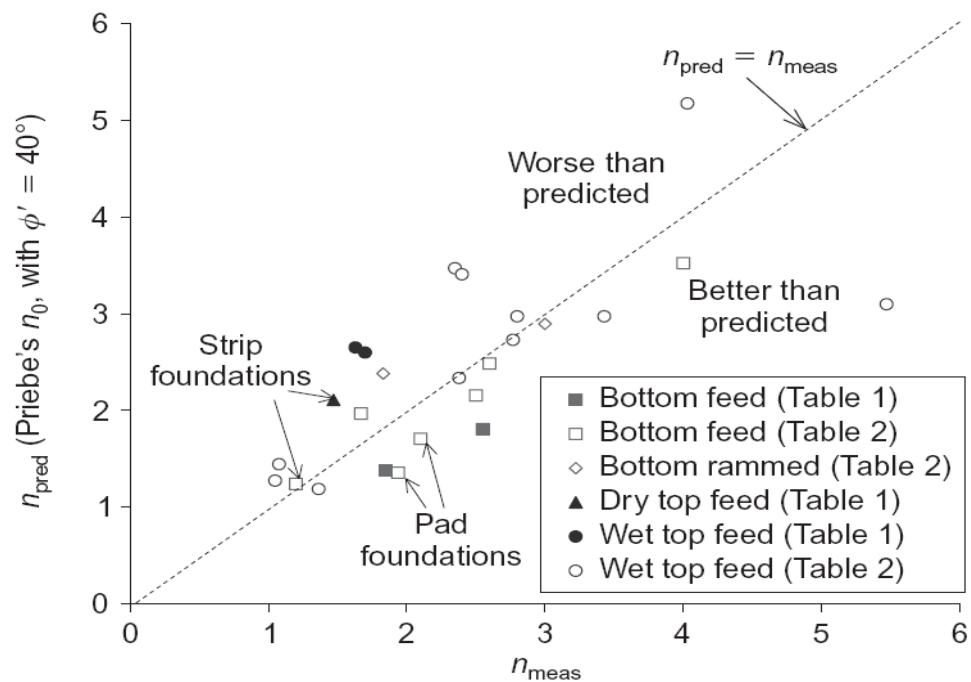
Figure 2.74 Predicted versus measured settlement improvement factors for all widespread loadings and footings (McCabe et al., 2009).

To sum up, the aim of this study is to carry out a FEA with the use of PLAXIS 2D and 3D Foundation building upon previous studies to investigate and clarify the effect of different factors affecting the amount of improvement due to the stone column installation and develop some basic framework to account for its effect in the engineering design.

3 Chapter 3: Background of Finite Element Analysis and Model Building Using Plaxis

3.1 Introduction

Burland (1987) states that, there are three interlinked parts for the practice of geotechnical engineering: the first part is the ground profile, which is developed from the investigation and the second part is the soil behaviour which is based on soil tests. Modelling, which is the third part, applies the knowledge acquired from the first two parts in order to help the engineer in the process of decision-making. The modelling of engineering events can be done through equations, increasing the accuracy in modelling will increase in complexity of these equations. Consequently, more time and labour are required. However, Ford (1999) states that, although solving complex equations usually requires calculation processes and the solutions are approximate, numerical methods of analysis still provide solutions to complicated equations. If such numerical methods of analysis are correctly applied, they are expected to give a reasonable prediction of the ground behaviour. This chapter describes how these solutions can be achieved for the case of composite foundation and the underlying principles.

3.2 Numerical Method Approach

The requirements of compatibility, material behaviour, equilibrium and boundary conditions of displacement and forces should be satisfied in order to have an accurate solution to a geotechnical engineering problem (Potts and Zdravkovic, 1999). Importantly, Potts and Zdravkovic (1999) argued that these requirements are satisfied by numerical methods of analysis. When problems are encountered in geotechnical engineering, numerical methods of analysis are found to be a very flexible tool in finding a solution to the

problems of complicated equations (Cundall and Strack, 1979; Ford, 1999; Potts and Zdravkovic, 1999).

3.2.1 Numerical Method Options

Advanced numerical methods, which are usually used in engineering analysis, have developed because of the spread of new technology and software that are capable of performing very complex calculations in a relatively short period of time. Some of the common numerical methods are the finite difference method, the finite element method, the discrete element method and the boundary element method. Cundall and Strack (1979) initiated the discrete element method which can simulate the interaction and motion of individual particles (Kalala and Moys, 2004, Magnier and Donze, 1998). This method relies on particle interaction modelling which is defined as conditions of particle contact where finite motions, such as rotation and displacement, are taken into consideration (Reddy, 1993). At the point of contact, elements rebound and collide; the calculation of its trajectory can be done by integrating the velocity and direction of the adjacent elements, the geometry, the forces and conditions at collision with Newton Law (Richards et al., 2004). Mohammadi (2003) says this is suitable if a problem has strong interruption in the continuity of geometric features and material. Munjiza (2004) adds it is suitable for problems that involve transient dynamics which reach equilibrium. Discrete element numerical analysis method is applied to solve problems in geotechnical engineering analysis, but it is currently limited because of the time and computing capacity needed to analyse all but the simplest problems (Chen et al., 2011; Richards et al., 2004; Villard et al., 2009a).

The boundary integral method or boundary element method (BEM) is used to solve problems which are formulated as similar to boundary integral equations, which are considered as an obvious answer to the dominant partial differential equation. Generally, this can be achieved in linear partial differential equation. Hence, when the BEM is compared with other numerical methods, it cannot provide an accurate solution to non-linear

problems (Katsikadelis and Nerantzaki, 1999). Nevertheless, it is still an effective choice to find a solution to linear problems.

The Finite Difference Method, which utilizes a topological square network of lines to build the discretisation of partial differential equations, can be very difficult if applied to complicated geometries in multiple dimensions (Peiro and Sherwin, 2005). Consequently, Peiro and Sherwin, (2005) argue that the integral forms of partial differential equations are preferred because of the difficulties encountered when applying such an approach. So, other methods of numerical analysis, such as the Finite Element Method (FEM), have developed.

The FDM is known for ease of implementation over rectangular forms or regular shapes of geometry. The FEM provides a partial solution to differential equations with nodes. The main principle is to discretise a domain into finite elements (discrete number of elements) and provide a solution for the uncertain values which are at the nodes (Zienkiewicz et al., 1977). A mesh is formed when connection is established between the finite elements inside the domain via the nodes. Importantly, the FEM can provide a solution to the majority of well-defined continuum problems.

3.2.2 Numerical Method Summary

Numerical methods which are appropriate to provide solutions to certain kind of problems generally give minimum variation in the results (Fang et al., 2002; Marfurt, 1984; Katsikadelis and Nerantzaki, 1999). However, there has been a debate about the preference of one method over the other, which depends very much on the definition of the referenced process (Zienkiewicz et al., 1977). Various numerical methods can provide different solutions to different problems by using different approaches. Yet, the nature of a problem under study and the advantages/disadvantages of every method decide which is the most suitable method to use in different circumstances (Zienkiewicz et al., 1977).

The FEM and the FDM have generally been found equal in solving similar problems, with sometimes the former being better in output (Marfurt, 1984;

Simpson and Clement, 2003). Fang et al. (2002) conducted a study on a problem of a two-point boundary value, and found that the FEM was slightly better in accuracy than other methods, especially the FDM. The discrete element method was developed for materials exhibiting discontinuities thus limiting its application on cohesive soils. As highlighted above, when the boundary element method is used, solving non-linear problems, which might occur in natural soil loading, becomes very difficult. If the FEM is used, it becomes possible to find solutions for problems of complicated geometries and complicated non-linear equations because the different forms of analytical solution are not required (Zienkiewicz et al., 1977). In solving geotechnical engineering problems, the FEM proves to be effective in dealing with problems of finite-boundary conditions, complex equations and behaviour as a continuum (Potts and Zdravkovic, 1999). Therefore, this method can solve problems of complex loading conditions, restraints and geometries. Because of this advantage and the advantage of the capability of dealing with various complex equations in a continuum, the FEM is preferable to simulate events such as a soil-structure interaction problem with small displacements. Because of the important advantages of FEM discussed above and the computer-supported calculation analysis in successive stages, this method is thought to be appropriate to stimulate the installation of the stone column and the sequence of radial displacement. Also, it can be used to replicate the behaviours of soil material within such sequences. Hence, the FEM was used in this study.

3.3 Finite Element Approach

The finite element method is one of the methods that try to provide solutions to partial integral and differential equations. In a given domain, Desai and Abel (1972) states that the finite element method obtains solutions from problems and gives an approximate value of the variables at a number of points within the domain. The main principle here is that a given domain is divided into finite elements (Reddy, 1993). Figure 3.1 below presents the

discretisation of an irregular shaped object into finite elements. The key in finite element method is to solve a complex problem by finding an approximate rather than an accurate solution to a simpler alternative problem generated from the main complex problem (Rao, 2005). In fact, the finite element method has been a very common approach to solve geotechnical engineering problems. This opinion was supported by Britto and Gunn (1987) and Reddy (2004) who found it as the most popular numerical method to solve geotechnical engineering problems.

Familiar properties of a normal finite element in a given domain are acquired, while functions which approximate the distribution of the actual displacement over each finite element are chosen. Such a process can be done by a mathematical formulation of the physical process. In this case, the derived equation is called the element equation (Reddy, 1993). However, the unknown values of the displacement functions are the displacement at the nodal points (Desai and Abel, 1972). In fact such an equation is distinctive and should be improved for each element inside the domain.

There are two stages to solve time dependant problems in the finite element method. In the first one, the differential equations are approximated to achieve ordinary differential equations. Then, In the second stage, the resultant ordinary differential are solved to derive algebraic equations, which are solved again to obtain the values at the nodes (Reddy, 1993).

Boundary conditions, which introduce a distinctive identity and provide solution to every case, control the element equations. The problem in the given domain can be solved when the properties of the finite elements are assembled in a meaningful way. The assumption behind the assembly here is that the solution is continuous at the inter element boundaries which are controlled by the nodes (Reddy, 1993).

The accuracy of the approximate solution can be developed in the finite element method by increasing the number of finite elements, which are identified in the domain. This is because the approximate solution converges to the actual solution since there is a tendency to infinity in the number of

finite elements. As a result, the global error, which is the total finite element error, converges to zero (Reddy, 1993).

Finite element identified
In different clusters

Continuum properties enabled within a typical finite element meeting adjoining finite element at nodes as identified
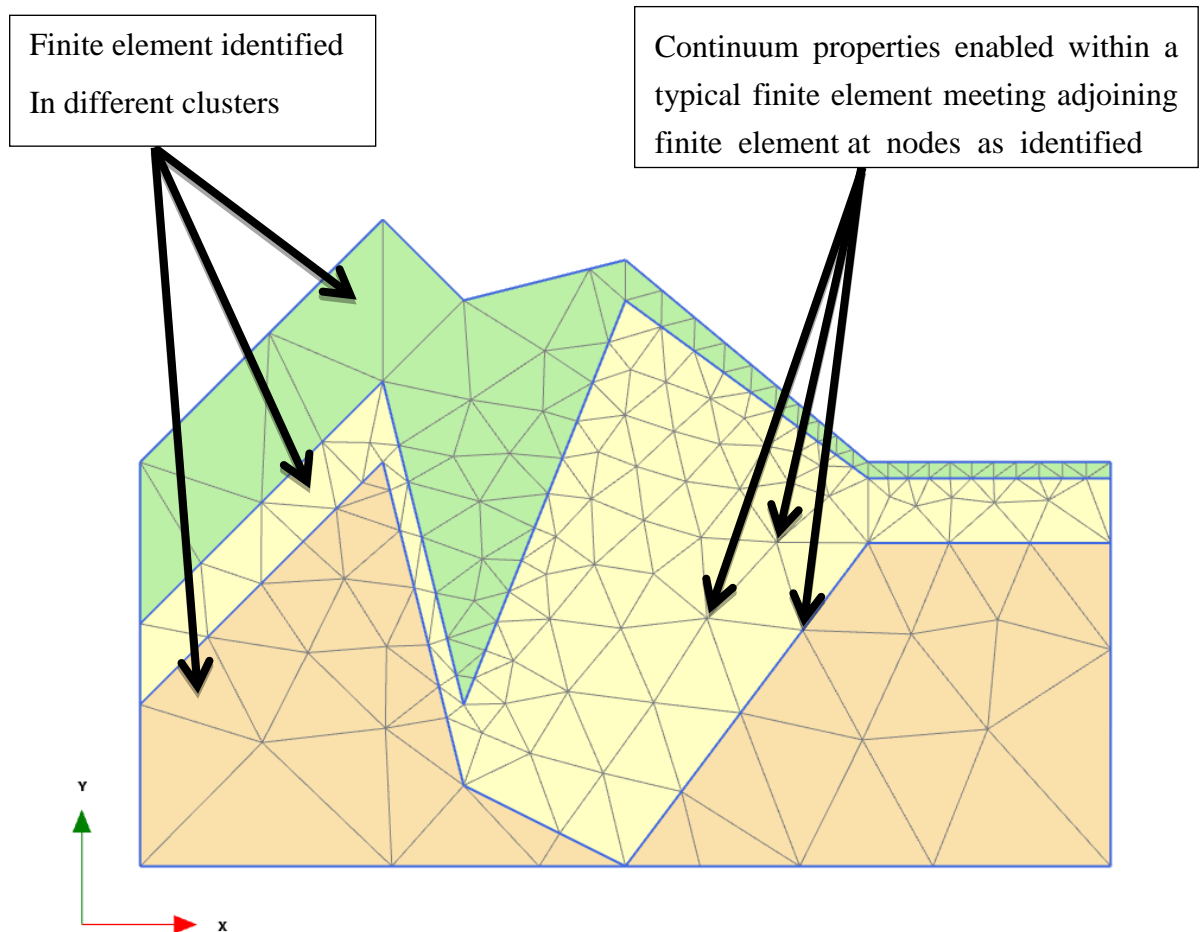
Figure 3.1 Finite element discretisation of an irregular shape modelling a soil mass with cluster representing different soil types.

3.4 The Software of Finite Element

The design of many computer software programs which are used commercially or privately has involved the use of the finite element method principles (ABAQUS, SAP, PLAXIS….). One additional advantage of the commercially available finite element software is that its application is tested in an independent way as academics and professionals use it widely. Both

general and specialized types of finite element software are commercially available. Although software of general application is useful in analysing engineering problems in many fields of engineering, it is not sufficiently powerful when used in specialized applications. The use of such software in specialized applications entails modifying it to suit the purpose of these applications. This also would need effort, time and resources to validate its use. Moreover, its use in some specialized applications in specific engineering fields is not appropriate.

The field of geotechnical engineering has observed the development of several specialized software. Some of such software include Plaxis 2D by Plaxis bv, Netherlands, SVSoild by soil vision systems Ltd, Canada and Frew by Oasys Limited, Arup Group (Smadi, 2012). One of the specialized type of software that is widely used and proved effective in the geotechnical engineering problem analysis is Plaxis. An important advantage of this software is that since it has been used for a long time (since 1987), it has been developed significantly (Brinkgrene et al., 2008).

The wide use of Plaxis finite element software program is attested in the large number of published studies in the field of geotechnical engineering which used Plaxis in the analysis of their results. The geotechnical problems that Plaxis has been used to solve include slope stability, consolidation and soil-structure interaction analysis (Abusharar et al., 2009, Lovisa et al., 2010, Tan, 2008, Howard and Warren, 2009, Cui and Zhou, 2009).

3.5 Plaxis Software

The PLAXIS finite element programme has been developed to study the soil behaviour in geotechnical problems by using either plane strain or axisymmetric models. It is provided with full features that enable a realistic simulation for the generation of element meshes and also has refinement options for global and local meshes. The construction process can be simulated in this program by activating and deactivating clusters of elements (soils, plates, anchors and others), changing water tables and application

117

loads and displacements. Boundary conditions are designed to cover most of the conditions of real soil problems. The analysis procedure allows for a realistic assessment of the stress and strain that results from the construction process. According to the geotechnical problem being studied, drained or undrained conditions can be adopted. For undrained conditions the consolidation analysis is usually simulated as an automatic time stepping procedure allowing the pore water pressures to dissipate with time. PLAXIS includes models of soil and structural behaviour which can be utilized in order to simulate the behaviour of the interaction between soil-structure and soil. The Mohr-Coulomb model is considered a very basic model and an extended package of advanced soil models starting with the hyperbolic soil model to user-defined models (Brinkgreve, 2014). The software has also some special programs which model constitutive relations in simulating non-linear and time-dependent behaviour of soils (PLAXIS, 2010b). Moreover, the software has some distinguished procedures to deal with non-hydrostatic and hydrostatic pore pressures.

Two Plaxis software application were used in this thesis; the first was Plaxis 2D AE, which was adopted to develop a numerical model of the case of axisymmetric single stone column that supports a rigid foundation and analyse the large deformation due to the cavity expansion made by stone column installation. Then, it estimates the changes in both the stress state and improved stiffness within the improved soft soils and quantifies their effects on the settlement performance of the treated ground.

The second Plaxis application was Plaxis 3D, which was adopted to apply the results of the single stone column model for the group of stone columns, incorporating the post-installation improvement of the soft soil between the stone columns by accumulating their effects. Then, it validates the 3D numerical analysis of stone column group with well-documented field case. Including the original ground dimensions and properties. Using Plaxis 3D has overcome one of the most common shortcoming that many researchers could not avoid due to the unavailability of 3D finite element geotechnical software at their times, it is the homogenisation and dimensional changing

processes to create a new distribution of stone columns that can be modelled as axisymmetric or plane strain using 2D finite element codes. Plaxis 3D can efficiently capture the real dimensions of the stone columns foundations.

A question might be asked in this research is why is the Plaxis 3D not used for all the numerical analysis models? The answer is based on two previous experience for McCabe et al (2008) and Killeen (2014) who tried to study the stone column installation effect in soft soils.

McCabe et al (2008) tried to capture the effect of stone column installation on both radial total stresses and excess pore water pressure by model 5m long, 600mm diameter stone column using Plaxis 3D and compared the result with two theoretical curves adopted by Gibson & Anderson (1961) and Randolph et al. (1979), respectively.

$$\sigma_{rl} = \sigma_{r0} + c_u[1 + log_e \frac{E}{2C(1+v)}] \qquad (3\text{-}1)$$

Where σ_{r0}, E, v and c_u are the total lateral stress, the elastic modulus, Poisson's ratio and the undrained shear strength of the soil, respectively.

In 1979 Randolph et al. made a detailed study of the application of cylindrical cavity expansion in modelling the installation of driven piles. Randolph's solution made use of the analysis developed for the interpretation of pressuremeter test in estimating the stress changes within the plastic zone, R after the undrained cavity expansion for pile driving in clay and is given by Randolph et al. (1979).

$$\Delta\sigma_r = c_u \left[1 + ln\left(\frac{G}{c_u}\right) - 2ln\left(\frac{r}{r_0}\right)\right] \qquad (3\text{-}2)$$

$$\Delta u = c_u \left[ln\left(\frac{G}{c_u}\right) - 2ln\left(\frac{r}{r_0}\right)\right] \qquad (3\text{-}3)$$

They applied 3 degrees of lateral expansion (a/a_0= 1.03, 1.10, 1.33). Where; (a_0) is the initial borehole radius and (a) is the radius after expansion. Hardening Soil model (HS) was selected to represent Bothkennar soft clay Stone, while Mohr Coulomb (MC) used to model stone material. Figure 3.2 illustrates the results of McCabe's study, where i, ii and iii indicates to applied lateral expansion.

119
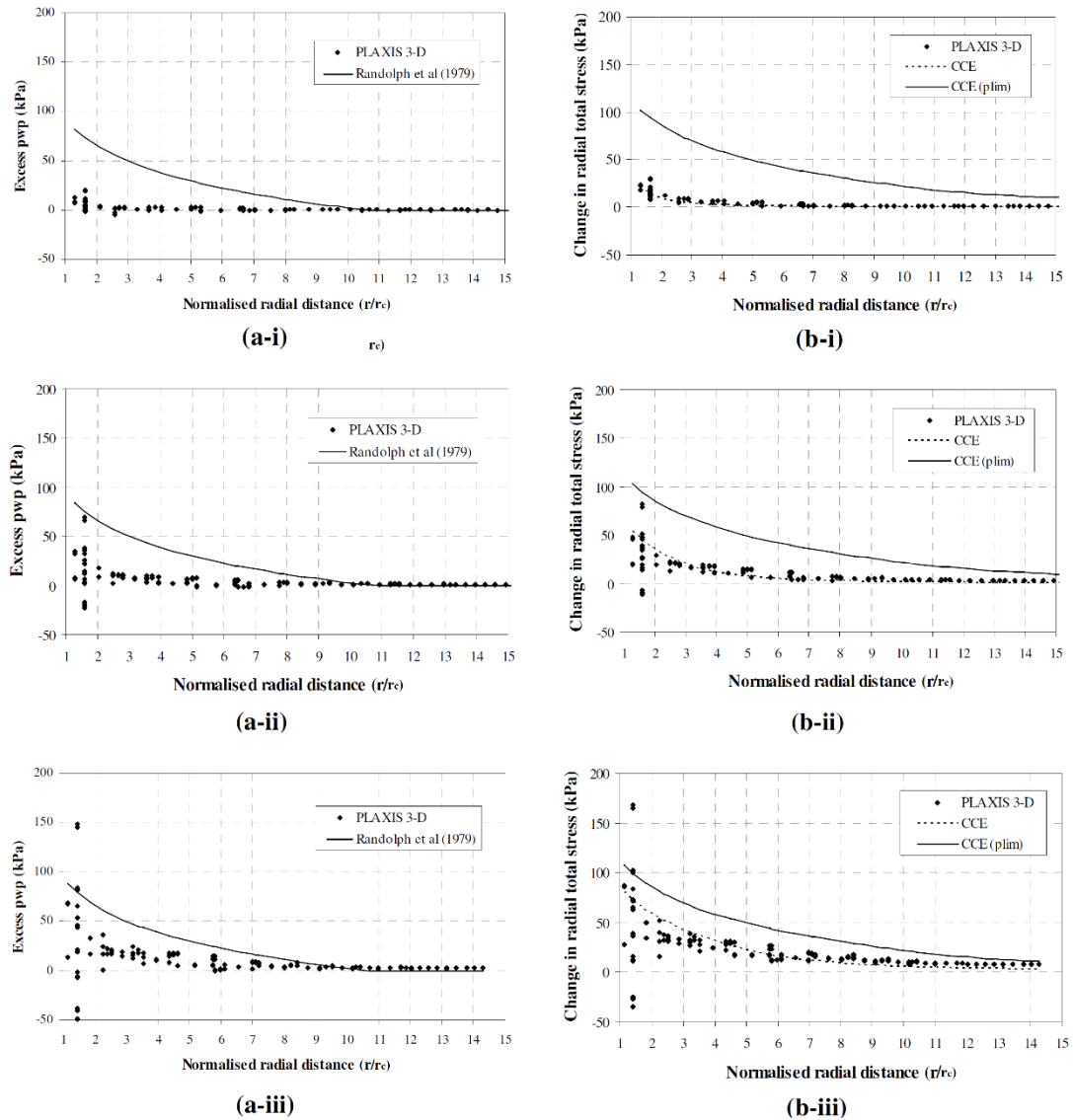
Figure 3.2 Variation of (a) Excess pore pressure (pwp) and (b) total radial stress with normalised radial distance for lateral expansions (r_c/r_0) of (i) 1.03, (ii) 1.1 and (iii) 1.33 (McCabe et al., 2008).

Although the general trend of the finite element results is similar to that theoretical ones, both radial total stress and excess pore pressure changes are not smooth and vary widely in the most important range ($r_c < r < 2r_c$) close to the column. These significant anomalies, even for very small expansion ($r_c/r_0 = 1.03$), raise the concerns about the reliability of this study. MeCabe et al. (2008) stated that this clear scatter at the level of expansion would be unacceptable. MeCabe et al. (2008) return the anomalies to the poor undrained cavity expansion prediction ability of Plaxis 3D. It has many

limitations in terms of modelling large strains. So, it is not beneficial at all to model the installation effect in stone columns group which are at 1.2 – 3.0 m typical field spacing. MeCabe then decided that, in the interim, stone column behaviour due to installation can be realistically captured by only increasing the post-installation K above K_0 to a maximum of K_p=1. Killeen (2014) also suggested that Plaxis 3D is incapable of simulating the column installation. So, he adopted the same conservative approach of increasing the coefficient of lateral horizontal pressure to $K_0 = 1$ in studying the behaviour of a small group of stone columns.

3.6 Numerical Model Development and Specifications

3.6.1 Introduction

The scope of this Chapter is to build and develop a numerical model to simulate the case of axisymmetric single stone column that supports a rigid foundation. Realistic boundary conditions including restraints, ground water table, applied loads, columns installation methods are adopted. Models that represent both stone column material and soft saturated clay are selected too.

In order to build a realistic model for a single stone column that supports a circular foundation on soft clay soil, the modelling process should involve a series of challenges, including the appropriate approach for simulation, dimension of the model, mesh geometry, boundary positions, selection of parameters used in the analysis and the right choices for the constitutive model that represents the studied soil. Some assumptions related to the construction process of the stone column installation are presented in the next chapter. Figure 3.3 illustrates the main stages for the model development.

```
┌──────────────┐  ┌──────────────┐  ┌──────────────┐  ┌──────────────┐
│  Clusters &  │  │    Mesh      │  │Units of finite│  │ Soil/Stone  │
│  Geometry    │  │Specifications│  │   elements   │  │  parameters  │
└──────┬───────┘  └──────┬───────┘  └──────┬───────┘  └──────┬───────┘
       │                 │                 │                 │
       └─────────────────┴────────┬────────┴─────────────────┘
                                  ▼
┌──────────────┐  ┌──────────────┐  ┌──────────────┐
│  Forces &    │  │ Boundaries & │  │ Assumptions &│
│ Displacements│  │ restrictions │  │considerations│
└──────┬───────┘  └──────┬───────┘  └──────┬───────┘
       └─────────────────┴─────────────────┘
                         ▼
              ┌──────────────┐ ┌──────────────┐
              │  Simulation  │─│   Studied    │
              │    phases    │ │    points    │
              └──────┬───────┘ └──────┬───────┘
                     └────────┬───────┘
                              ▼
                     ┌──────────────┐
                     │   Results    │
                     └──────────────┘
```
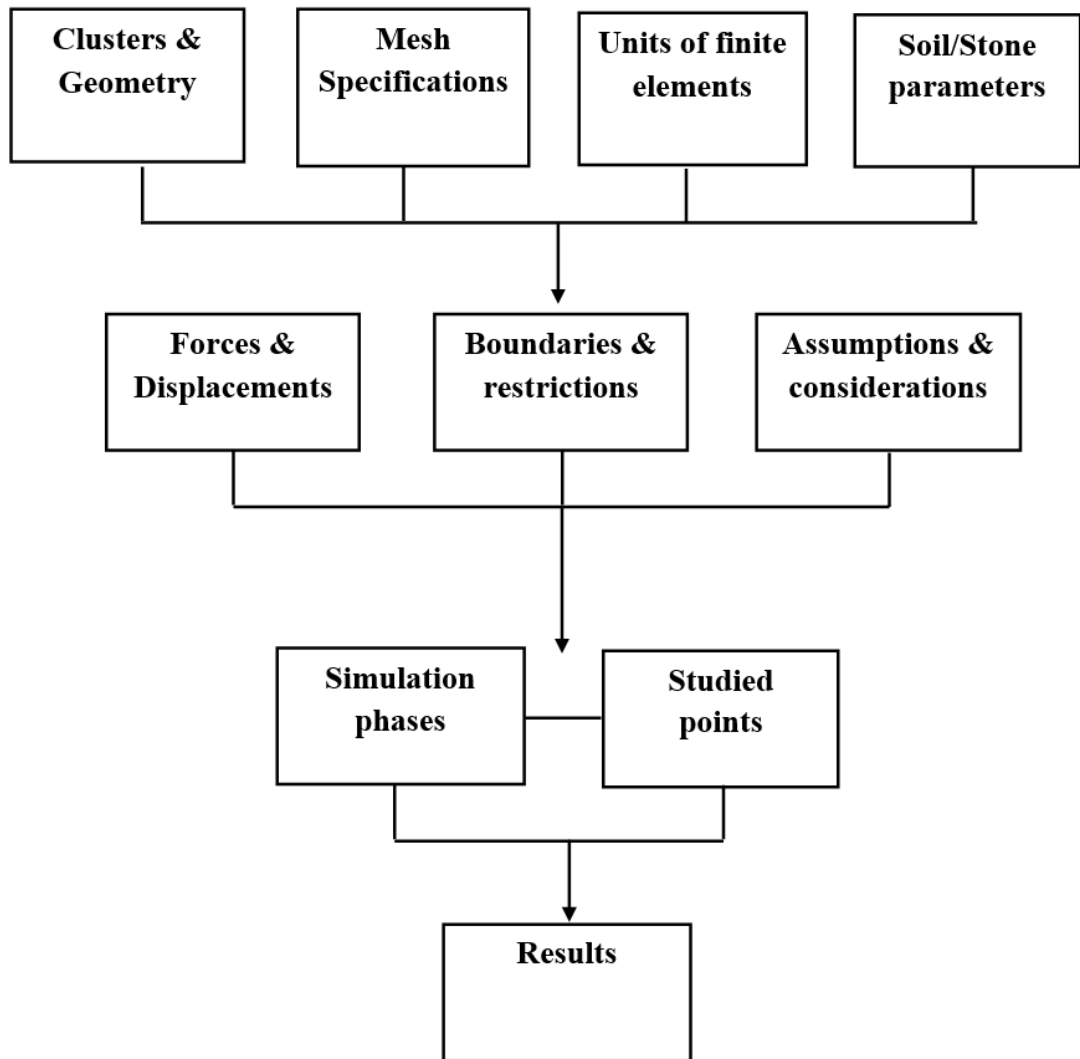
Figure 3.3 Model development flow summary.

Plaxis 2D has two choices for analysis; the first is the plain strain which is used when the problem geometry has a uniform cross section and corresponding loading scheme, and stresses and boundary conditions over a certain length, as shown in figure 3.4a. The second is axisymmetric analysis, which is suitable for circular geometries with uniform radial cross section, loading and stress state around the central axis (figure 3.4b) (Brinkgreve, 2014). It is clear that the axisymmetric analysis is the right one to simulate the case single stone column, where X represent the radial coordinate, Y represents the axial coordinate and Z represents the tangential direction.
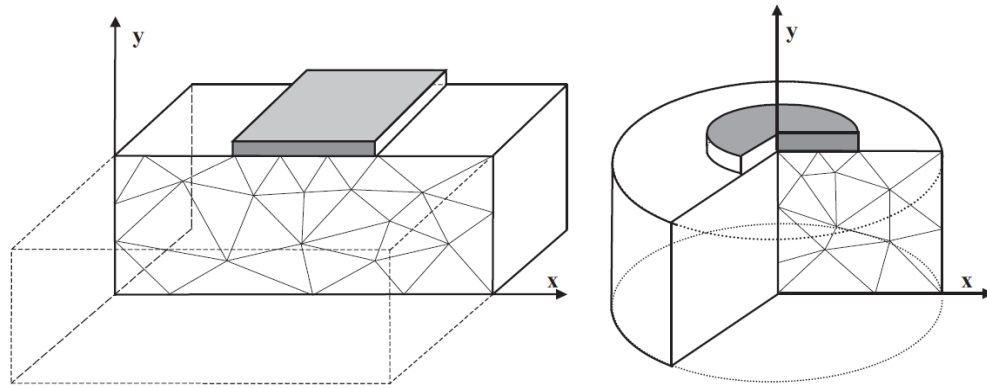
Figure 3.4 Plain strain (a) and axisymmetric problem (b) (Brinkgreve, 2014).

3.6.2 Units and Model Type

Before describing the modelling process, it should be mentioned that the units of the input parameters including the geometry, forces, stresses and time in all this research models were taken as the default units in Plaxis 2D AE (m, N, day). Consequently, all output data and curves are shown using the same units.

3.6.3 Boundary Conditions

Unless a certain structure or loaded body is constrained to be kept in equilibrium, it might experience a boundless and inflexible body motion. Achieving a solution in equilibrium requires boundary conditions, which would set a boundary value problem. There are two types of boundary conditions that can be applied and these are the forced or geometric and the free or natural (Rao, 2005; Anandarajah, 2010). A combination of both boundary condition types are used for the sake of solving problems of finite elements. The loads and displacements that might be experienced by finite elements control these boundary conditions.

The model is controlled with a group of boundary conditions that can be applied differently for each calculation phase to reach an equilibrium state with the internal stresses and strains.

The geometry boundary conditions of the model are shown in Figure 3.5.

1. The default general fixities were automatically applied to the boundaries of the studied model, where all nodes of the model vertical sides are fixed in X-direction ($U_x = 0$) and free in Y- direction, to represent the infinite extension of the soil body mass in x-direction, while the bottom boundary which represent the deep soil is constrained in Y- directions ($U_y = 0$) to allow the application of radial cavity expansion. The ground surface has no fixities in any direction. Boundary conditions are listed below and illustrated in Figure 3.5;

2. The default gravity acceleration, g, of 9.810 m/s², was applied to create the weight of soil. The default unit weight of the water is 10 kN/m³.

3. The ground water level was at 0.6m below the surface of the soft clay. The water was allowed to flow from the clay to the stone column drain during consolidation. No drainage was allowed from the boundary of the model.
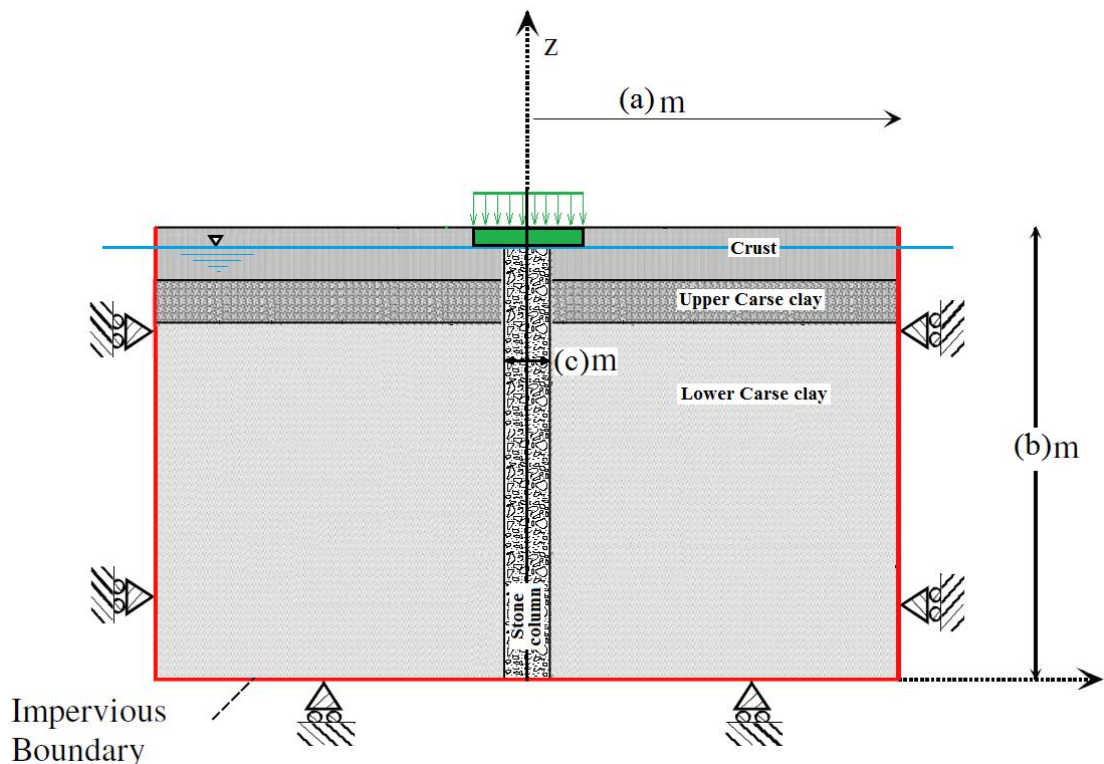
Figure 3.5 The Boundary conditions and geometry of the model.

3.6.4 Discretisation

Quantifying and defining the approximate geometry of a problem is the main point in the finite element approach. The domain under consideration forms the cluster which can be a soil layer within the soil mass, the whole of the soil mass or the structure within the soil mass. The next stage is a process of 'discretisation' which means dividing the domain into a mesh of finite elements. As a result, a cluster of smaller discrete regions, which form the domain, is formed of finite elements (Desai and Christian, 1977; Reddy, 1993).

Reddy (1993) explains that the main advantage of discretisation is that it allows "accurate representation of complex geometries and inclusion of dissimilar materials and accurate representation of the solution within each element to bring out local effect." Importantly, the degree of the accuracy of the representation of the geometry decides the accuracy of the results of the finite elements. Another advantage for discretisation is that it controls the number of the finite elements in the domain. The degree of accuracy in the finite element method is controlled by the number of elements in the domain. The finite elements in Plaxis 2D are usually quadrilateral or triangular in the two dimensional domain. The user may select either 6-node or 15-node triangular element as shown in Figure 3.6 (a) and (b) respectively. The finite element in Plaxis 3D are 15- node wedge elements which contain 6 nodes in each triangular faces and 8 nodes in the vertical surfaces (Figure 3.7).

Nodal lines separate finite elements which intersect in a nodal point (Desai and Christian, 1977). The nodes form the corners in the finite elements with straight sides. The coordinates in the geometry of the domains identify the geometry of the nodes (Potts and Zdravkovic, 1999).
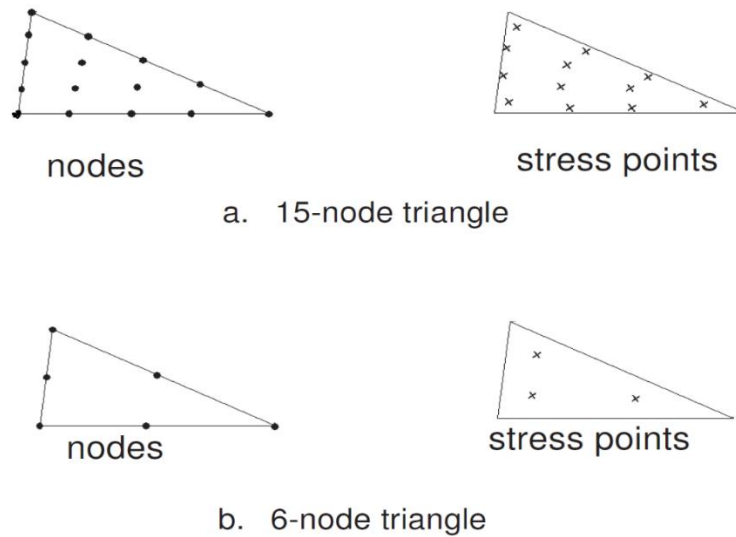
Figure 3.6 Types of Plaxis mesh elements and positions of nodes and stress points in Plaxis 2D (Brinkgreve, 2014).
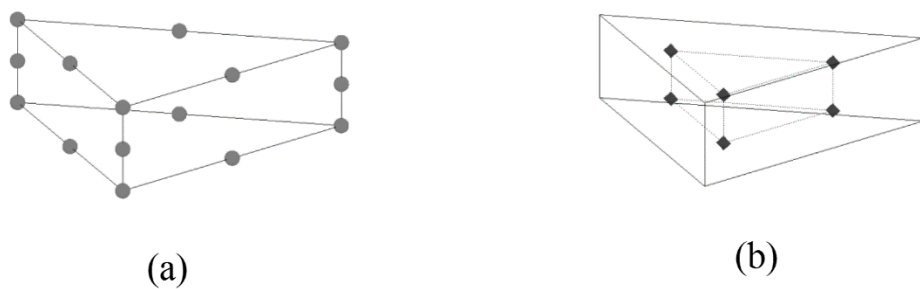
Figure 3.7 Distribuation of (a) nodes and (b) stress points within 15 node wedge elements.

In order to have accurate results for the analysis using Plaxis finite element code and make these results dependant only on soil properties and geotechnical problem conditions, a group of important analysis for the features and conditions like the mesh density and the distance of the boundaries were investigated to avoid any reaction on the model results. The mesh geometry and boundary positions were investigated to assess their effect on the results of the analysis. A sensitivity analysis was carried out on the boundaries to ensure that their location had little effect on the results. Before starting the sensitivity analysis, it is important to give a brief description of the adopted soil profile and the available models in Plaxis that can be adopted to represent this soil.

3.6.5 Soil Profile (Bothkennar Clay)

The case of a single stone column might not be applicable as a real case, but it can be used to create a framework for typical field cases. Never the less, the soft clay soil and stone column material parameters and geometry of stone column and footing were taken to be as realistic as possible. To start a comprehensive study comprising a numerical analysis to study the effect of stone column installation on soft clay soil in the performance of the reinforcement system and carrying out a calibration with the field behaviour, an extensively characterised Bothkennar soft clay soil was selected to study the soil in the 2D Plaxis analysis.

Due to the high demand for a soft clay test bed site in United Kingdom for purpose of study and research the construction on soft clay, and after investigations for few test sites located around United Kingdom, Bothkennar test site was chosen and purchased by the Science and Engineering Research Council (SERC) in 1987 to meet all the requirements selection procedure mentioned in Table 3.1 (Hawkins et al., 1989). This site located in Scotland, on the south side of the River Forth, near Grangemouth. As shown in Figure 3.8.

Table 3.1 Required geotechnical specifications for the research bed site (Nash et al., 1992a).

Geotechnical specification		General specification	
Material	Homogeneous clay (without peat), with firm crust	Area	>5 ha (for purchase/rent)
Clay fabric	Not markedly laminated	Access	Good national and local road access
OCR	Normally/lightly over consolidated	Flooding	The site should not flood regularly
Thickness	>10 m	Mining	No plans for undermining
Shear strength	S_u <40 kPa, sensitivity not specified	Security	Risk of vandalism should be low
Plasticity	>20%		
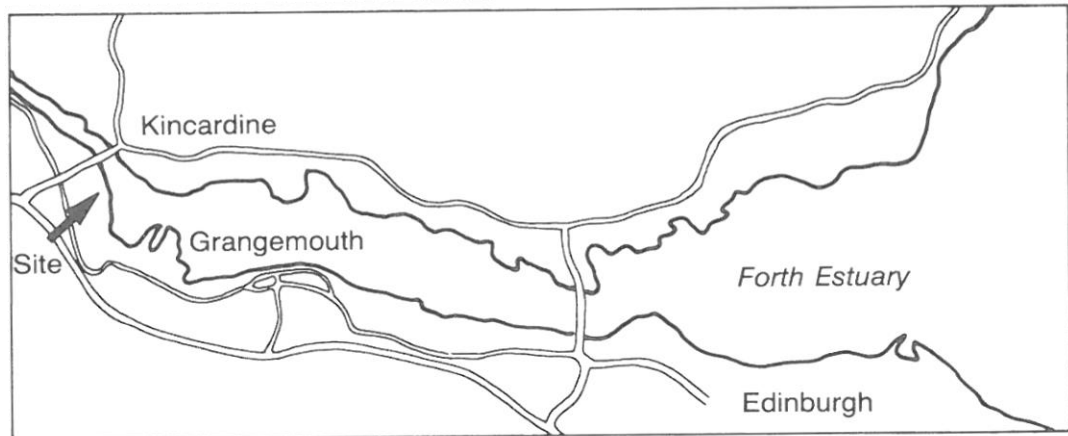
Figure 3.8 Bothkennar Site location (Nash et al., 1992a).

One of the main reasons for considering Bothkennar clay in this study is the high effective strength parameters and high undrained strength for it (Nash et al., 1992a). Moreover the stratigraphy of the site relatively consists of uniformly soft clay deposits as a result of the post-glacial sediment of the Forth River (Nash et al., 1992a). Post to purchasing, an intensive programme of field and laboratory investigations and researches were carried out to establish a full geotechnical profile for the site, including full characterisation (Hight et al., 1992), Permeability and hydraulic features (Leroueil et al., 1992), yielding and mechanical properties (Smith et al., 1992) and (Allman and Atkinson, 1992) and disturbance and destructuration prior to laboratory testing (Clayton et al., 1992). In the following sections a brief explanation of the important aspects and results of these studies, which related to this research are going to be presented;

3.6.5.1 Stratigraphy

Bothkennar site sediments forming the Bothkennar clay were transported and deposited in shallow inter-tidal water when sea level was rising. It mainly consists of a crust of about 1.5m of stiff dark brown silty clay, underlined by 12-22m of general consistent of soft silty clay layer commonly called as Carse clay, over a deep layer of Bothkennar gravel. The mineralogy of the clays is illite, kaolinite, quartz and feldspar, and the silt is

128

quartz and feldspar. The ground water level is 0.5-1m below the ground level (Hawkins et al., 1989). More detail about the site stratigraphy and basic geotechnical properties are shown in Figure 3.9.
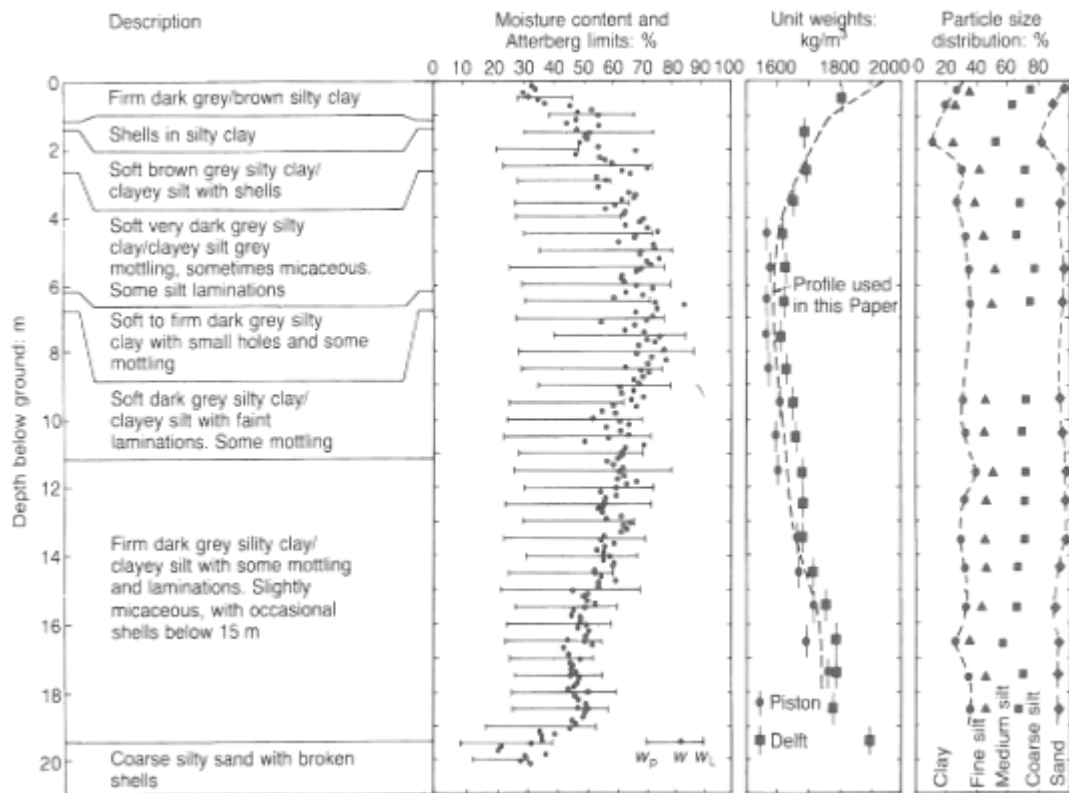
Figure 3.9 Stratigraphy and basic geotechnical properties of the Bothkennar soil layers (Nash et al., 1992a, Richards et al., 2004).

3.6.5.2 Soil State

The soil is classified as clayey silt according to BS5930 with low content of sand less than 10%, and clay of average (35-50) %. The silt particles noted to be very angular giving higher friction angle for Bothkennar clay. As a result of the significant organic content in the main clay layer (3-5) %, which was measured by loss on ignition at 425c⁰ method, the soil classified to be high plasticity (Hight et al., 1992). Atterberg limit test results are presented in Figure 3.9. The moisture content starts in 30% in the surface layer, and then increases dramatically with the depth to reach about 80% at 8m depth. After that, it decreases to 40% at top of Bothkennar gravel. (Hight et al., 1992). Measurements show that the bulk density varies significantly with the depth mirroring the high difference of water content across the soil height. It starts

with about 1800 kg/m3 at the top of the crust then reduces to reach a minimum value of 1570 kg/m3 at about 5m depth. After that it increases slowly to 1800 kg/m3 at the base of the Carse clay, Figure 3.9.

3.6.5.3 In Situ Stresses and Yield Stress Profile

The lateral earth coefficient has been calculated as a ratio between vertical and horizontal effective stress and has been plotted by (Nash et al., 1992b) in Figure 3.10.
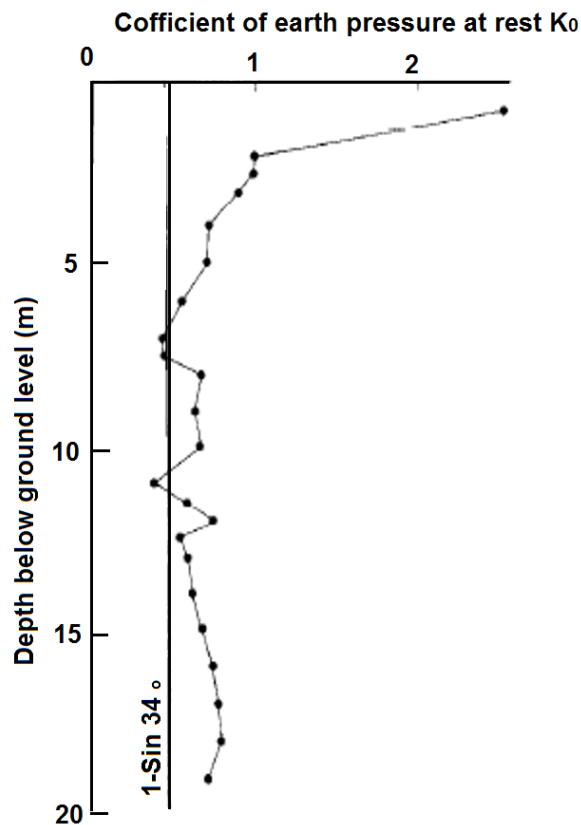
Figure 3.10 Profiles of in situ stresses: (a) total stresses; (b) effective stresses; (c) K_0, (Nash, 1992b).

It is clear that K_0 for the crust clayey layer has a high values compared with the underneath Carse clay, where K_0 become less than 1, then it decreases slowly with the depth. This indicates that the over consolidation ratio (OCR) is high for the top layer and then reduces slowly with the depth, which

means geologically that Bothkennar test site has exposed to an over burden pressure during its geological history. (Nash et al., 1992b) estimated this over burden to reach a maximum of 15 kPa. Nash, Sills and Davison (1992) have performed a full programme of one dimensional odometer test for a set of samples obtained from along the whole depth and they presented the yield stress ratio which equivalent to (OCR) in Figure 3.11.
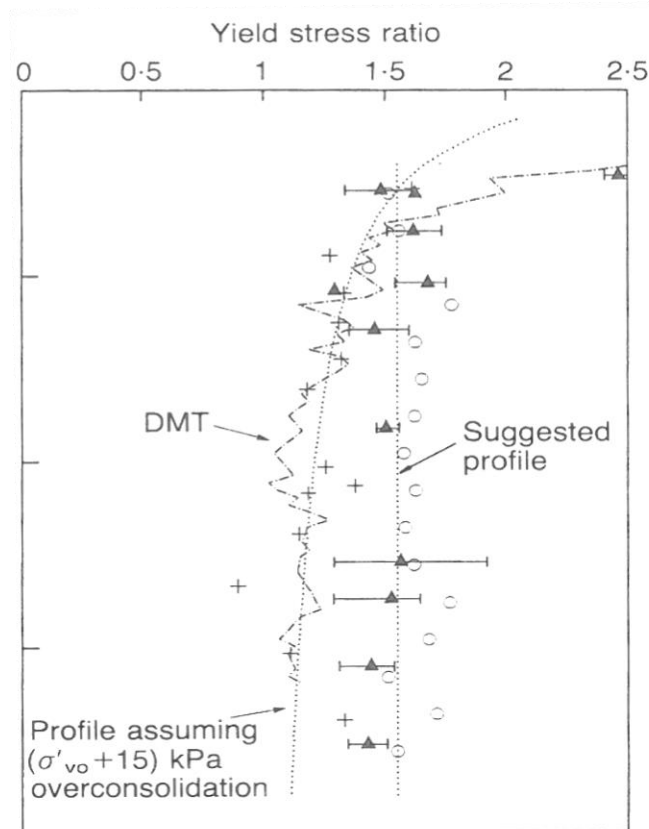
Figure 3.11 Yield stress ratio from one dimensional incremental load consolidation tests (Nash b, 1992).

One important parameter related to yield stress profile and very linked to the behaviour of stone column installation is the void ratio, which was difficult to determine because of the presence of salts in the pore water in Bothkennar clay samples. (Nash et al., 1992b) assumed a constant specific gravity of 2.68 for Carse clay and they covered most of the clay depth to apply a series of load increments up to the in situ vertical stress. Killeen (2012) re-assorted the results of the intact samples collected by Nash et al. (1992)b for

both compression index Cc and e_0 in Figure 3.12a and Figure 3.12b respectively.
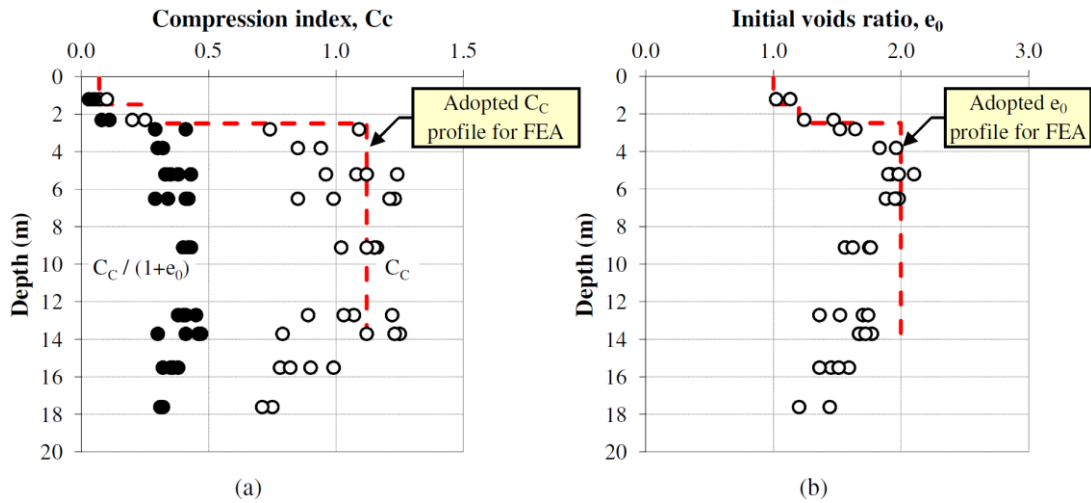
Figure 3.12 Variation of (a) compression index Cc and (b) initial voids ratio e0 with depth (Killeen and McCabe 2014).

Strength and stiffness parameters of Bothkennar Carse clay was investigated by Allman and Atkinson (1992) after three stages of laboratory tests;

- Reconstitute Bothkennar Carse clay and turn it in to slurry with water content at 1.25 of the liquid limit.
- Reconsolidate the slurry by compressing it one dimensionally to return it back to normal consolidated.
- Carry out a series of triaxial test to determine the strength characteristics φ' and c'.

They found high value of internal friction angle (φ' = 34°) for the soft Bothkennar Carse clay which has been attributed to the high proportion of angular silt. Effective cohesion C' was nominated 3kPa and 1kPa for the Crust and Carse clay, respectively. Swelling index (Cs) can be calculated based on the expression $\frac{\lambda}{\kappa} = \frac{C_S}{C_C}$ where Cc values for different depth have been taken from Figure 3.12(a). Slopes of normal compression line (λ) and swelling line (κ) for the reconstituted Carse clay found have been estimated

by Allman and Atkinson (1992), and found to be 0.181and 0.025 respectively (from triaxial tests).

3.6.5.4 Permeability Characteristics and Consolidation Coefficient

Hydraulic characteristics are very important in studying the performance of stone column foundation, because it works as a vertical drain besides improving the performance of the soil. The main related parameters in this study are   the horizontal and vertical hydraulic conductivity, K_h and K_v. (Leroueil et al., 1992) have measured these parameters using many laboratory and field tests. In this study, the self-boring permeameter results were taken as they are most reliable to apply in this study as it is shown in Table 3.2.

3.6.6 Soil Models in Plaxis

Soil models, which use the finite element approach, have a group of mathematical equations that are integrated into the finite element software code (Plaxis) in order to generate output. These outputs would replicate the outputs which might be generated by the behaviour of soil. Mathematical equations in such models consider parameters which, under certain conditions, might have an effect on the special behaviour of soil in order to render anticipated results.

The behaviour of real soil is highly non-linear, with both strength and stiffness depending on the stress and strain level (Potts & Zdravkovic, 1999). Furthermore, soil often shows time-dependent behaviour and anisotropic tendencies. The behaviour of soil may be approximated in order to render anticipated results by varying degrees of accuracy using material models. Nowadays, there are many complex or simple kinds of soil models. Certainly, analysis cost will depend on the degree of simplicity or complexity of the soil model. However, variation in the simplicity or complexity of the soil model does not guarantee highly relevant results. In order to decide the suitability of a soil model, relevancy of the characteristics of soil type and the

controlling parameters and features should be carefully taken into consideration.

Plaxis has a number of sophisticated models of soil behaviour. In this regard, the Plaxis Mohr Coulomb model is seen as the first order model of approximation for soil behaviour and quick assessment in modelling. A detailed review of the Mohr Coulomb model and Hardening Soil model are presented later.

By using the undrained total stress analysis or the undrained effective stress analysis, it will be possible to model the undrained behaviour in Plaxis. The undrained total stress analysis needs undrained parameters in analysis and renders outputs in total stress. The undrained effective stress analysis, on the other hand, takes into consideration pore pressures and the effective stress separately, which makes it possible to execute the undrained analysis with effective stress input parameters (PLAXIS, 2010a).

3.6.6.1 Linear Elastic Model

This model is ideal for linear elastic material. It is based on Hooke's law of elasticity, thus precluding the development of irreversible strains. The material behaviour is defined by two parameters, Young's modulus (E) and Poisson's ratio (v). This model is only adopted to represent structural elements e.g. concrete, steel. It is too crude to accurately capture the sophisticated stress-strain behaviour of soil.

3.6.6.2 Mohr Coulomb Model

The Mohr Coulomb model in Plaxis, which is a material soil model, is designed to stimulate the behaviour of perfect elastic plasticity. A fixed yield boundary identifies plasticity onset. If the values of stress are less than the fixed yield value, there will be reversible strains and a behaviour of perfect elasticity. As is shown in Figure 3.13 below, strains are made up of the elastic and plastic components.
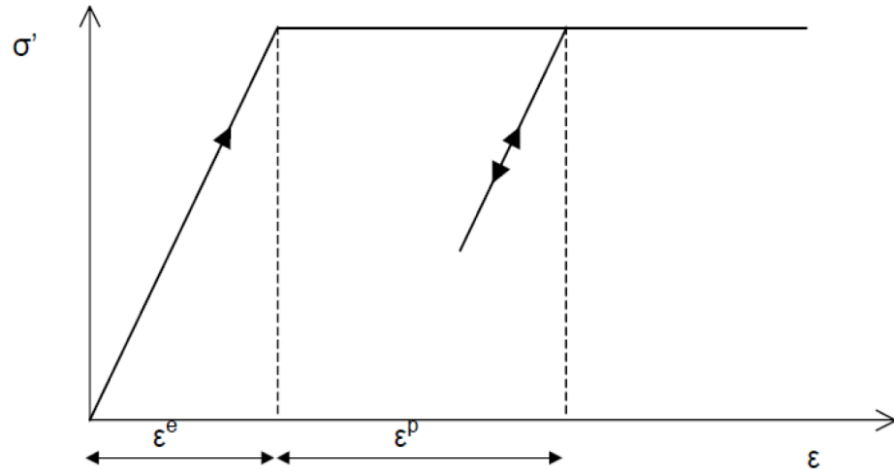
Figure 3.13 Stress strain representation of an elastic perfectly plastic model (PLAXIS, 2010a).

$$\tau = c' + \sigma' tan\emptyset' \qquad (3\text{-}4)$$

$$\frac{1}{2}(\sigma'_2 - \sigma'_3) = \frac{1}{2}(\sigma'_2 - \sigma'_3)sin\emptyset' + c'cos\emptyset' \qquad (3\text{-}5)$$

Plasticity in this model is presented by the Mohr Coulomb failure criteria, which is defined in Equations 3-4 and 3-5 above, by two parameters, angle of internal friction (ϕ) and cohesion (c). This failure criterion is an extension of Coulomb's friction theory. This failure criteria can be represented by six functions when formulated with regards to the stress principle, as is shown in Equations 3-6 to 3-10. As is shown in Figure 3.14, these six functions formulate a hexagonal cone yield surface in principal stress space when all the functions presented together are zero.
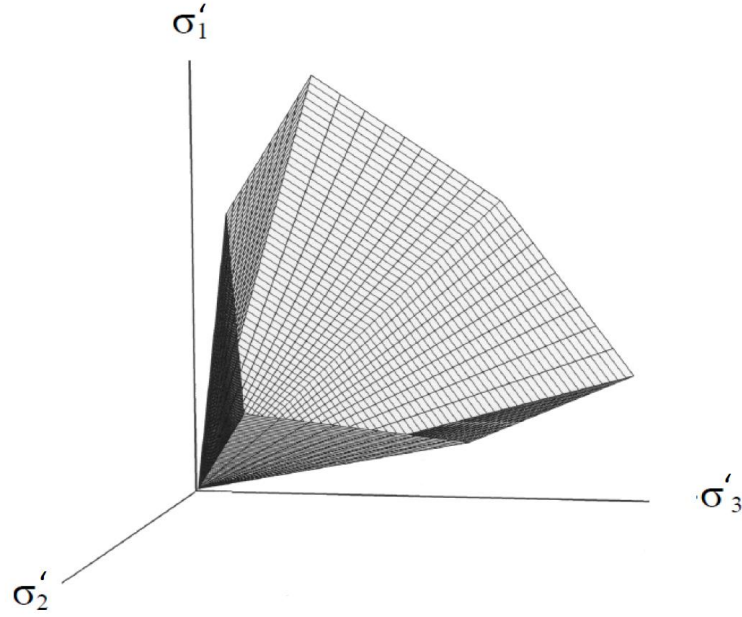
Figure 3.14 Mohr-Coulomb failure surface in principal stress space where c=0. Modified (PLAXIS, 2010a).

$$f_{1a} = \frac{1}{2}(\sigma'_2 - \sigma'_3) + \frac{1}{2}(\sigma'_2 + \sigma'_3)sin\emptyset' - c'cos\emptyset' \leq 0 \qquad (3\text{-}6)$$

$$f_{1b} = \frac{1}{2}(\sigma'_3 - \sigma'_2) + \frac{1}{2}(\sigma'_3 + \sigma'_2)sin\emptyset' - c'cos\emptyset' \leq 0 \qquad (3\text{-}7)$$

$$f_{2a} = \frac{1}{2}(\sigma'_3 - \sigma'_1) + \frac{1}{2}(\sigma'_3 + \sigma'_1)sin\emptyset' - c'cos\emptyset' \leq 0 \qquad (3\text{-}8)$$

$$f_{2b} = \frac{1}{2}(\sigma'_1 - \sigma'_3) + \frac{1}{2}(\sigma'_1 + \sigma'_3)sin\emptyset' - c'cos\emptyset' \leq 0 \qquad (3\text{-}9)$$

$$f_{3a} = \frac{1}{2}(\sigma'_1 - \sigma'_2) + \frac{1}{2}(\sigma'_1 + \sigma'_2)sin\emptyset' - c'cos\emptyset' \leq 0 \qquad (3\text{-}10)$$

$$f_{3b} = \frac{1}{2}(\sigma'_2 - \sigma'_1) + \frac{1}{2}(\sigma'_2 + \sigma'_1)sin\emptyset' - c'cos\emptyset' \leq 0 \qquad (3\text{-}11)$$

The basic parameters of the Mohr Coulomb model in Plaxis include angle of dilatancy, Ψ in degrees, angle of internal friction, $\emptyset'$ in degrees and cohesion, c' in kN/m² . Alternative stiffness parameters within this model include; Oedometer modulus, E_{0ed} and Shear modulus, G (Shear stress / Shear strain). Relationship between the oedometer modulus and Yound modulus is presented in Equation 3-12. Equation 3-13 is the relationship between shear modulus and Young's modulus.

$$E_{oed} = \frac{(1-v\prime)E\prime}{(1-2v\prime)(1+v\prime)}$$
(3-12)

$$G = \frac{E\prime}{2(1+v\prime)}$$
(3-13)

3.6.6.3 Hardening Soil Model

The Hardening Soil model is an advanced constitutive model which can be used to simulate the elasto-plastic behaviour of both soft and stiff soils (Schanz, 1998). The model is an extension of the hyperbolic model developed by Duncan & Chang (1970). Soil shows irreversible strain and decreasing stiffness when it is exposed to loading. Such properties of soil are captured by the Hardening Soil model in Plaxis, which is designed for this purpose. Because of plastic straining in this model, the yield surface is not fixed in the principle stress space, but it is varying.

The main design purpose of Hardening Soil model Plaxis code is to simulate the behaviour of stiff and soft soil (Schanz and Vermeer, 1998). The common hyperbolic material model is superseded by this model because of the introduction of the yield cap and soil dilatancy in this model (Duncan and Chang, 1970; Kondner, 1963; PLAXIS, 2010a). There are many characteristics in this model such as failure in accordance with the Mohr Coulomb model, observed yield cap, elastic reloading and unloading, plastic straining because of compression or primary deviatoric loading, dilatancy, stress-based stiffness in accordance with power law, and the relationship of hyperbolic stress strain.

The Hardening Soil model depends on a hyperbolic relation between deviatoric stress and vertical strain in the primary triaxial loading. The curves, in a standard triaxial test, might be described as is shown in Equation 3-14 in which the deviatoric stress q, is less than that at failure, q_f, and ε_1 is the strain.

$$\varepsilon_1 = \frac{q}{E_i - (E_i q / q_a)}$$
(3-14)

The shear strength asymptotic value is qa and E_i is the initial stiffness. There is a relationship between E_i and E_{50} as is shown in Equation 3-15. E50 is the confining stress dependent stiffness modulus, dependent on stress for primary loading and can be derived with E50ref being a reference stiffness modulus, which corresponds to the reference confining pressure pref from equation 3-16. In this equation, m is the power which defines stress dependency of the modulus on the corresponding effective stress, while pref has a default value which is equal to a hundred stress units. The deviatoric stress at failure and the asymptotic value of the shear strength are defined in Equations 3-17 and 3-18 respectively. qf is derived from the Mohr Coulomb failure criterion in which q is equal to qf,. When the failure criterion is satisfied, the relationship of stress strain turns to be perfectly plastic. As is shown in Figure 3.15, the failure ratio Rf, in Plaxis, gives the ratio between qa and qf where the default value is 0.9.

$$E_i = \frac{2E_{50}}{2-R_f} \tag{3-15}$$

$$E_{50} = E_{50}^{ref} \left(\frac{c'\cos\emptyset' - \sigma'_3 \sin\emptyset'}{c'\cos\emptyset' + p^{ref}\sin\emptyset'} \right)^m \tag{3-16}$$

$$q_f = (c'\cot\emptyset' - \sigma'_3)\frac{2\sin\emptyset'}{1-\sin\emptyset'} \tag{3-17}$$

$$q_a = \frac{q_f}{R_f} \tag{3-18}$$

E_{50}^{ref} in Equation 3-16 is replaced by E_{ur}^{ref} in order to provide a description of the relationship for the stress dependent stiffness modulus, E_{ur} for unloading and reloading, as is illustrated in Equation 3-19. E_{ur}^{ref} is the referenced Young's modulus for reloading and unloading which corresponds to the reference pressure, pref.

$$E_{ur} = E_{ur}^{ref} \left(\frac{c'\cos\emptyset' - \sigma'_3 \sin\emptyset'}{c'\cos\emptyset' + p^{ref}\sin\emptyset'} \right)^m \tag{3-19}$$

$$E_{oed} = E_{oed}^{ref} \left(\frac{c'\cos\emptyset' - \frac{\sigma'_3}{K_0^{NC}}\sin\emptyset'}{c'\cos\emptyset' + p^{ref}\sin\emptyset'} \right)^m \tag{3-20}$$

In Plaxis E_{ur}^{ref} is set to $3E_{50}^{ref}$ by default. The relationship between E_{oed}^{ref} and E_{oed} is defined by Equation 3-20. E_{oed}^{ref} is the referenced tangent stiffness modulus corresponding to the reference pressure, p^{ref}.

The basic parameters for the Plaxis Hardening Soil model include: Cohesion, c' in kN/m², angle of internal friction, $\emptyset'$ in degrees, angle of dilatancy, Ψ in degrees, secant stiffness in standard drained triaxial test, E_{oed}^{ref} in kN/m², tangent stiffness for primary oedometer loading E_{oed}^{ref} in kN/m², unloading and reloading stiffness, E_{ur}^{ref} in kN/m², power of stress level stiffness dependency, m. Alternative stiffness parameters include: Compression index, C_c, swelling index C_s, initial void ratio e_{int}.
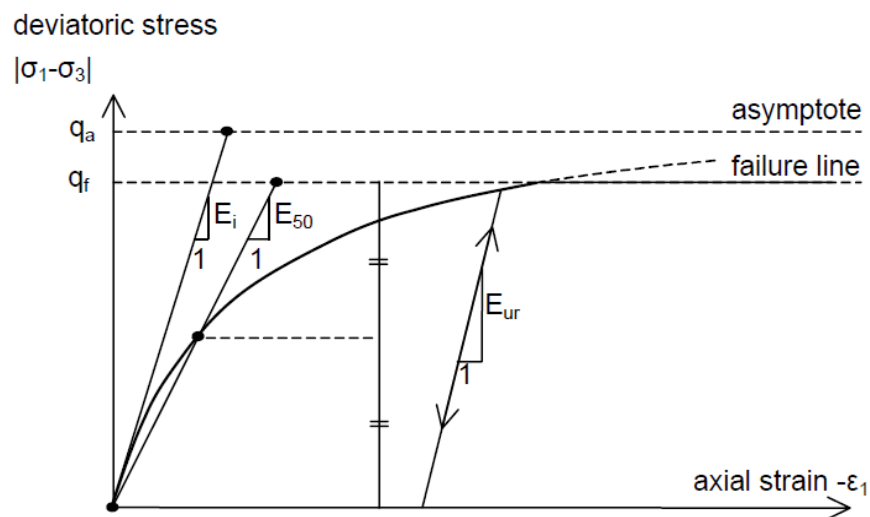
Figure 3.15 Hyperbolic stress strain relationship. Modified (PLAXIS, 2010a).

There are some more soil models available in Plaxis, such as Soft Soil model, Soft Creep model, Modified Cam Clay model and Hardening Soil model with small strain stiffness.

Although, the basic features of the Soft Soil models are designed for soft soils, they have many limitations related to their tendency to over predict the range of elastic soil behaviour. Consequently, over prediction of deformation in problems especially for normally consolidated soils. So, the behaviour of

the soft soil materials in Bothkennar Clay around the installed stone column may not be accurately modelled using the Soft Soil and the Soft Soil Creep model (PLAXIS, 2010a).

A review of the composition of the Modified Cam-Clay soil model highlights its shortcomings in analysing the stone column installation. Beside the limitation of the Soft Soil models, it has the tendency to give a softening behaviour, which might lead to mesh dependency and convergence problem of iterative procedures (PLAXIS, 2010a).

The Mohr Coulomb model is characterized by the simulation of elastic and perfect plastic behaviour of soil. This simulation is with a certain yield value at which the soils show a perfect plastic behaviour, but before this value, the behaviour of soils is expected to be perfectly elastic. Mohr Coulomb model does not take into consideration irrecoverable soil deformation on loading under the yield stress value and the hardening of soft soil during plastic deformation (the stiffness response is considered to be constant for each soil). The model only assumes perfectly plastic straining at the yield stress value. The Mohr Coulomb model is consequently not suitable in accurately modelling the soft soil properties around the stone column.

The Hardening Soil model and the Hardening Soil model with small strain stiffness are models based on the same principles. However, the Hardening Soil model with small strain stiffness is enhanced to capture soil behaviour at infinitesimal strains. The Hardening Soil model with small strain stiffness requires inputs resulting from very small strain values (usually in the order of 0.001%). It cannot be applicable in this case with large deformation caused by the installation of stone column.

The Hardening Soil model as formulated by Plaxis, within this research, is considered the best model for simulating the relevant features of the soil behaviour, originating from a combination of different soil types subjected to large deformations. Its ability of taking into account of stress dependency of stiffness moduli and accounting for the shear and volumetric Hardening

make it the most realistically model to capture the features soft soil combination. The Hardening Soil model is therefore selected to represent the behaviour of both soft clay soil and stone column material.

3.6.7 Development of Soft Soil Parameters

As mentioned in section 3.5.5, for development and validation purposes, the selected soft clay soil used in this model was Bothkennar clay, which was fully profiled previously in this chapter. The parameters of Hardening soil model that represents both soft Bothkennar clay and stone column material can be directly obtained from Table 3.2.

All Bothkennar clay parameters (except the stiffness parameters E_{50}^{ref}, E_{oed}^{ref}, E_{ur}^{ref}) that are shown in Table 3.2 were extracted directly from an intensive programme of field and laboratory investigations that researches carried out to establish a full geotechnical profile for the site, including full characterisation (Hight et al., 1992), strength parameters (Nash et al., 1992a), Permeability and hydraulic features (Leroueil et al., 1992), yielding and mechanical properties (Smith et al., 1992) and (Allman and Atkinson, 1992) and disturbance and destructuration prior to laboratory testing (Clayton et al., 1992). Full detail about the geotechnical profile is explained later in chapter 5.

Stiffness three dimensional parameters for Hardening Soil model (E_{50}^{ref}, E_{oed}^{ref}, E_{ur}^{ref}) have been calculated using the following equations (Brinkgreve and Broere, 2006);

$$E_{oed}^{ref} = \frac{2.3(1+e_0)p^{ref}}{c_c} \tag{3-21}$$

$$E_{ur}^{ref} = \frac{2.3(1+e_0)(1+v)(1-2v)p^{ref}}{c_s(1-v)} \tag{3-22}$$

$$E_{50}^{ref} = E_{oed}^{ref} \tag{3-23}$$

Where; compression index (c_c) and initial void ratio (e_0) values for different depths have been adopted from Killeen (2012).

3.6.8 Development Stone Column Material Parameters

One of the main objectives for developing the single stone column is to use for studying the infinite group of stone columns settlement performance, as it is the most common case of the stone column improvement method. For this purpose, and in order to utilize from some of the most recent field and numerical records of the studied Bothkennar clay and other well documented sites, stone column material properties and load specification were as follows:

- Jardine et al (1995) found that the ultimate capacity of the unreinforced Bothkennar soft clay foundation is about 138kPa (Figure 3.17). This study is designed for typical working load and according to (Atkinson, 2007), the design factor of safety for foundations on soft soils with high settlement tendancy is around 3. So, that gives an allowable load of 46kPa. 50 kPa has been selected as a design loading for Bothkennar soft clay.

- Stone column material physical properties were similar that taken previously by many other researchers; where γ =1900 kg/m^3, γ_{sat} =1900 kg/m^3 Mitchell and Huber (1985), Domingues et al. (2007), Killeen and McCabe (2014)). Vertical and horizontal coefficients of permeability for stone column material $k_h = k_v$ =1.7 m/day (Elshazly et al (2008b), Killeen and McCabe (2014)).

- Main strength parameter for stone material was Φ = 45° based on the MeCabe et al. (2009) field stone column test review; he stated that using bottom feed system in installing the stone column material makes the value Φ = 40° ,which conventionally used to be adopted by Priebe design method, conservative. Cohesion is supposed to be zero, but for some numerical analysis requirement for Plaxis, it was taken c = 1 kPa. Dilatancy angle was calculated based on Bolton (1986) empirical equation (ψ = Φ -30° = 45 – 30 = 15°).

- Different values have been reported for Stiffness parameter (Young's modulus E), which varied from 30 to 70 MPa. The low values were estimated for the columns formed by the top feed methods (Barksdale

142

and Bachus (1983), Elshazly and Elkasabgy (2007), and Zahmatkesh and Choobbasti (2010). While Killeen and McCabe (2014) and Sexton (2013) adopted McCabe's (2009) recommendation of the better performance of stone column in bottom feed installation method. So they took high value of Young's modulus (E_{50} =70 MPa), which has been adopted for this study too.

- An appropriate power of stress level stiffness dependency, m = 0.3 was used for stone column (Gab et al. (2008) and Killeen and McCabe. (2014)).

To sum up, soft clay and stone column material parameters used in this numerical analysis are presented in Table 3.2.

Table 3.2 Soil parameters adopted for finite element analysis.

Soil Parameter	Stone Column	Crust	Upper Carse clay	Lower Carse clay	Unit
Material model	Hardening Soil model	Hardening Soil model	Hardening Soil model	Hardening Soil model	-
Depth	14.5	0.0-1.5	1.5-2.5	2.5-14.5	(m)
Type of material behaviour	Drained	Undrained	Undrained	Undrained	-
Soil unit weight (γ)	19.0	18	16.5	16.5	kN/m^3
Soil saturated unit weight (γ_{sat})	21.0	18.0	18.0	18.0	kN/m^3
Over-consolidation ratio	-	1.5	1.5	1	-
Permeability (K_h)	1.7	1.0×10^{-4}	1.0×10^{-4}	1.0×10^{-4}	m/day
Permeability (K_v)	1.7	6.9×10^{-5}	6.9×10^{-5}	6.9×10^{-5}	m/day
Young's modulus (E_{ref})	70000	-	-	-	kN/m^2
Poisson's ratio (v)	0.2	0.35	0.35	0.35	-
Cohesion (C_{ref})	0	3	1	1	kN/m^2
Friction angle (Φ')	45	34	34	34	^{0}
Dilatancy angle (Ψ)	15	0	0	0	^{0}
Initial voids ratio, (e_0)	0.5	1.0	1.2	2.0	-
Compression index, (C_C)	-	0.07	0.25	1.12	-
Swelling index, (C_S)	-	0.01	0.03	0.16	-
Reference pressure, p^{ref})	100	13	20	30	kN/m^2

Lateral earth coefficient K_0	1.0	1.5	1.0	0.75	
m	0.3	1.0	1.0	1.0	
E_{50}^{ref}	70000	1068	506	231	kN/m²
E_{oed}^{ref}	70000	1068	506	231	kN/m²
E_{ur}^{ref}	21000	5382	3036	1164	kN/m²

3.6.9 Development of Structure Modelling (Footing)

Plaxis has the ability to simulate and analyse the structural behaviour of either one or any combination of plates, tunnels, hinges and rotation springs, fixed end anchor and end to end anchor. It is also possible to control the effect of structural members and their presence in the analysis. For instance, it is possible to gradually eliminate or introduce parts of the structures or the whole structures in successive phases of the analysis for the simulation of construction processes. All of these details can be found in Plaxis reference manual (PLAXIS, 2010b). The features of the effect of the structure on the soil play an important role in the choice of the structure model that will be used in modelling.

 The only structure model applied in this study, which is the last component of the 2D axisymmetric single stone column foundation model, is the concrete footing. Typical parameter values for the reinforced concrete material were assumed for the footing as shown in Table 3.3. Footing thickness was assumed to be 0.6m, which was rigid enough to cause both the stone column and soft clay to settle. A linear elastic model was used to simulate the footing material.

Table 3.3 Material properties of footing.

Parameter	Name	Value	Unit
Material type	Type	Linear Elastic	-
Normal stiffness	EA	$5 \cdot 10^6$	kN/m
Flexural rigidity	EI	$8.5 \cdot 10^3$	kNm^2/m
Unit weight	γ	24	kN/m^3
Poisson's ratio	v	0.15	-
Height	H	0.6	m
Diameter	D	2	m

3.6.10 Soil Profile and Parameters Validation

Before continuing in developing the axisymmetric single stone column case, it is important to validate the ability of Plaxis 2D AE and its Hardening Soil model to capture the behaviour of Bothkennar soft clay using the parameters developed above (Sections 3.6.7and 3.6.8). Plaxis 2D has been used to replicate a historical case that has a high status of importance evidenced by its popularity in the field performance. This is also arguably one of the most convincing tests carried out to investigate the load-displacement behaviour of Bothkennar clay.

3.6.10.1 Field Load Test Description

The field load test performed by Jardine et al. (1995) to investigate the load-displacement behaviour under two rigid footings. It was utilised to validate the use of Plaxis 2D AE with Hardening Soil Model parameters selected for Bothkennar profile in Table 3.2. Two square pad footings A and B were founded at 0.8m below the ground level with 2.2m and 2.4m width, respectively. The first one A was designed to examine the failure load in short term behaviour, while the second Pad B was loaded to about 67% of the ultimate capacity with long term loading for two years. Figure 3.16 Showed the loading rates for both pads A and B with time.
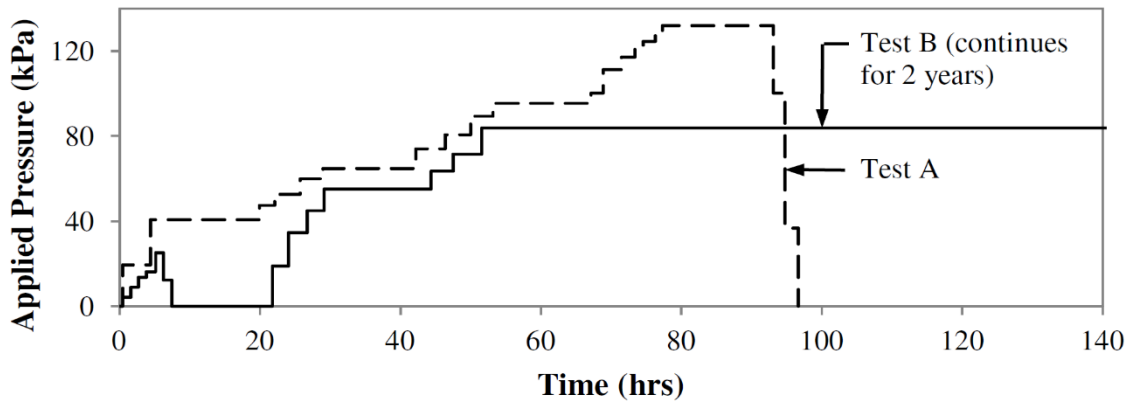
Figure 3.16 Field loading test with time on Bothkennar clay (Jardine et al. 1995).

3.6.10.2 Comparison between Field Records and Plaxis 2D Results

Load test A, to the ultimate bearing capacity, was chosen to be simulated with Plaxis 2D foundation as adequate for validation. Load test B was not taken in simulation to avoid the secondary settlement resultant of unloading – reloading behaviour applied in this test, which the Hardening Soil model may be unable to model. Based on the site stratigraphy and undrained loading because of short load terminal. Test A was simulated using Plaxis 2D and loading up to failure. Figure 3.17 illustrate the comparison between both field and numerical results.
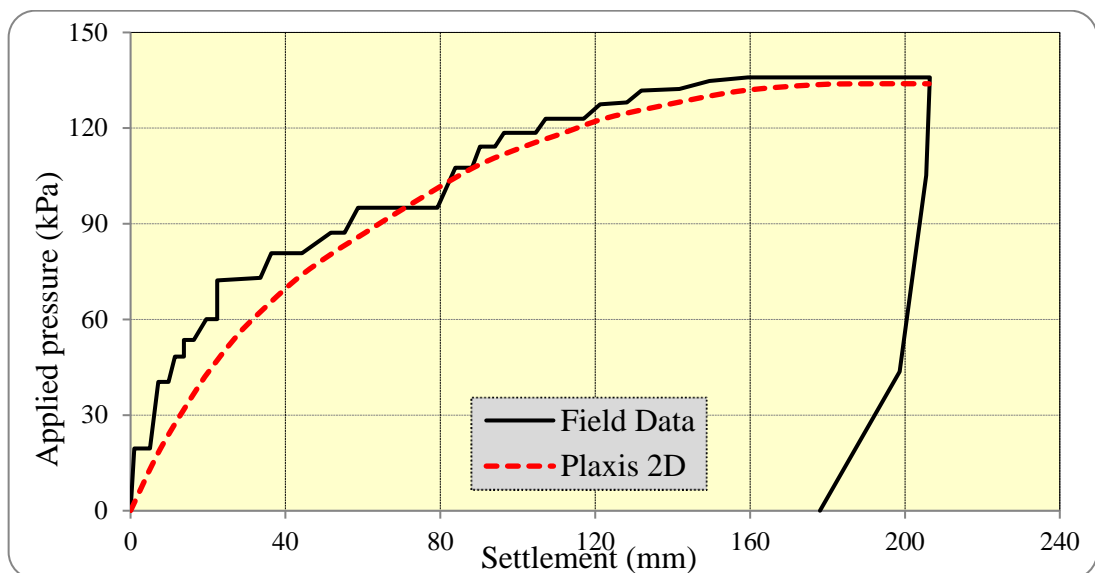
Figure 3.17 Comparison of Plaxis 2D V9 modeling results with real load-displacement behaviour for a field Pad footing done by [Jardine et al (1995)].

146

Figure 3.17 shows that the Hardening Soil model using Plaxis 2D is able to predict the settlement behaviour of Bothkennar Clay. It does appear that the initial stiffness of the field test is under estimated, but it is clear the trend is the same and the ultimate bearing capacity is similar. this validates the use of Plaxis 2D and the choice of selected Hardening Soil Model parameters to be adequate for the next step.

3.6.11   Sensitivity Analysis (Boundaries and Mesh)

1. Influence of boundary distance

External boundaries are an artificial representative of real forces, extensions and conditions that define the situation of a finite element model. It is not possible to include real natural extension of a mass of soil or some events applied on it, so finite element code (Plaxis 2D AE) enables the user to substitute the reaction of these extensions and events as a restraints, displacements and forces at the boundary. Consequently, user can quantify these effects and assign them to the studied model with minimum effect on the accuracy of this model. Positions of boundary restraints can significantly affect finite element simulation results. Since the generated reaction forces and displacement in these boundaries can influence the impact of the applied forces on the zones of interest. So to avoid any restriction, that reflected on the accuracy of the finite element model, a user should select the location of these boundaries to be sufficient distant from any zone of interset, but at same time the user should consider them not to be exceedingly far, costing more time in the analysing process.

Practically, for the model of Bothkennar clay, the sensitivity analysis was carried out on the model for only the side boundary. Bottom boundary is already considered as a natural boundary of the Bothkennar as it was stiff gravel at 14.5m deep. To ensure the neutrality of any influence in analysis of the side boundary, two group of points were considered in sensitivity analysis to compare the settlement, vertical stress and radial stress for different distances of the boundaries. First group of points were taken

147

horizontally at mid of Bothkennar Lower Carse clay, at $2r_c$, $4r_c$, $7r_c$ from the centre of stone column to make sure that the side boundary is not effecting the results after applying the expansion cavity (column installation); where r_c is the radius of stone column and $7r_c$ is the expected distance that the soft clay soil can be affected by the stone column installation, as reported by many researchers, i.g. (Jiun Liao et al, 2006). The second points group are located at 0B, 1B, 2B deep below the footing (B: footing diameter). Figure 3.18 illustrates all the selected points.
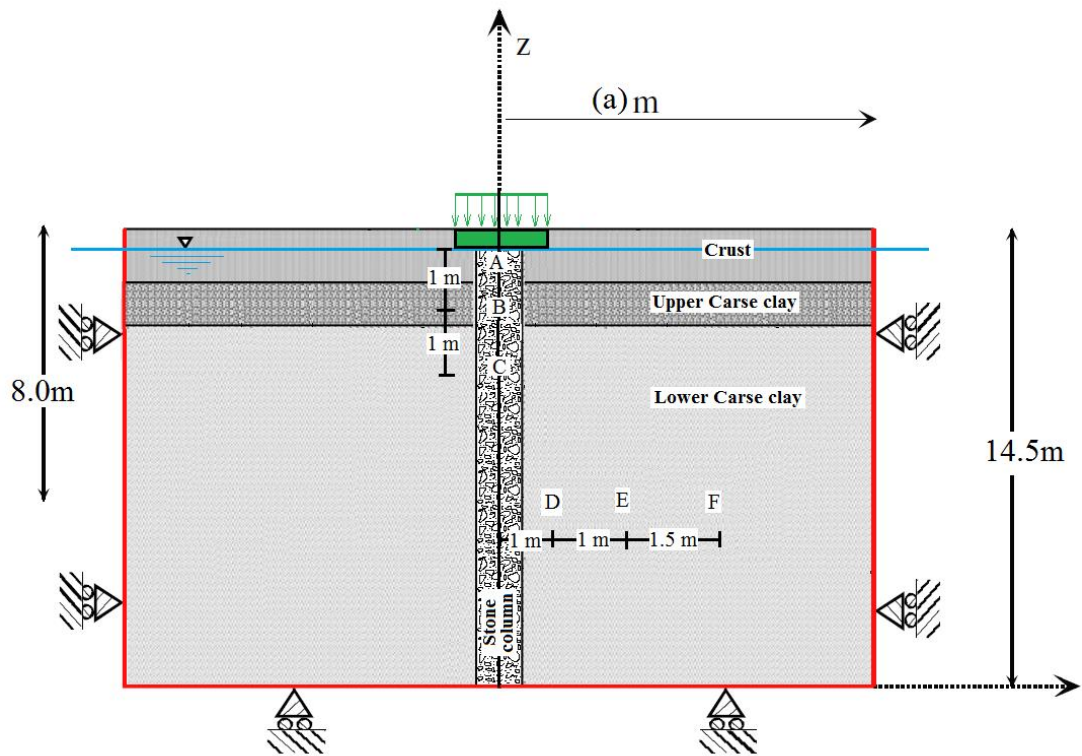
Figure 3.18 Selected points for sensitivity analysis.

The location of the side boundary was varied from (a = 8-20 m). Based on the author experience, 20m distance from the centre line stone column to the side boundary is enough to avoid any influence of it in the numerical analysis results. Normalized differences have been calculated for each side boundary distance case compared to 20m distance as the following for example:

Normalized differences for footing settlement $= \left(\dfrac{u_{y\,(a=x\,m)} \; - \; u_{y\,(a=20\,m)}}{u_{y\,(a=20\,m)}} \right)$

Where: $u_{y(a=20\,m)}$ is settlement at the selected point for the case of side boundary is located at (20) m from the column axis and $u_{y(a=x\,m)}$ is settlement at the selected point for the case of side boundary is located at (x) m from the column axis

Footing loads and radial displacements due to stone column installation were taken at maximum values. Sensitivity analysis outlines for both boundary and mesh effects are illustrated in Figure 3.19.

The results are listed in Table 3.4 and Table 3.5.

It is clear from Table 3.4 compared to Table 3.5 that the result of the lateral displacement and radial stress, which happened mainly due to stone column installation, are more sensitive to the side boundary distance. For the footing settlement and vertical stress, it is enough to make the side boundary about 12 m. While, to avoid any reflection on the accuracy of finite element model of this boundary, it should be at least 14m far from the stone column centre line for the case of lateral displacement and radial stress. Therefore, it has been conservatively chosen at 15m distance, where the effect of the model loading is diminished.
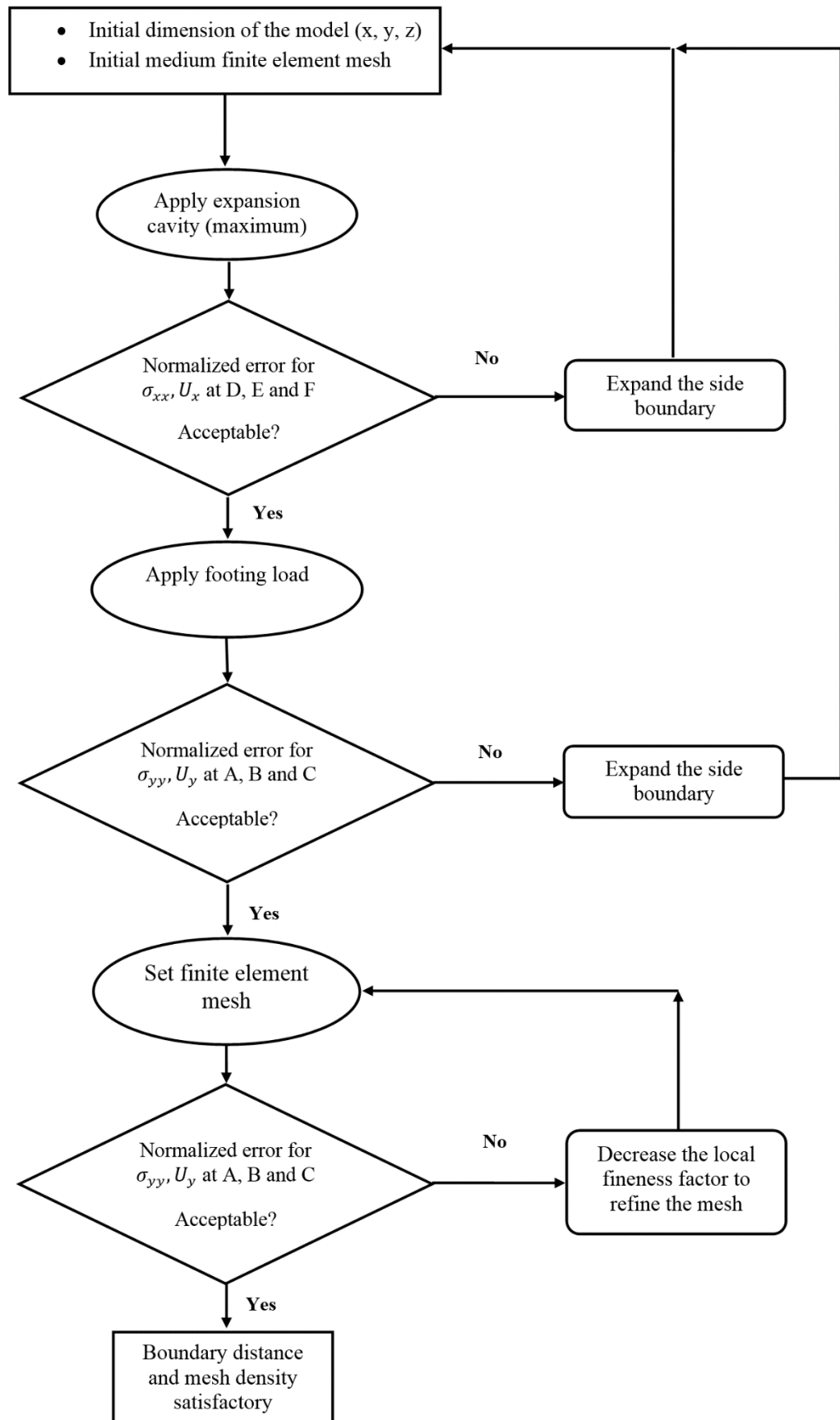
Figure 3.19 Outlines of sensitivity analysis.

Table 3.4 Side boundary distance effect in the lateral displacement and radial stress of numerical model(at mid of Lower Carse layer).

Side boundary distance (m)	Displacement Ux (mm)			Normalized difference (%)			Lateral stress σ_x (kPa)			Normalized difference (%)		
	(D)	(E)	(F)	(D)	(E)	(F)	(D)	(E)	(F)	(D)	(E)	(F)
8.0	14.3	7.9	4.2	11.72	12.22	14.29	151.24	143.72	133.78	0.26	4.95	5.08
10.0	15.8	8.3	4.6	2.47	7.78	6.12	146.60	139.45	131.59	2.82	1.83	3.36
12.0	16.1	8.8	4.8	0.62	2.22	2.04	150.98	137.03	127.97	0.09	0.07	0.52
14.0	16.3	8.9	4.9	0.62	1.11	0	150.89	136.94	127.41	0.03	0	0.79
16.0	16.2	9.0	4.9	0	0	0	150.56	137.01	127.35	0.13	0.05	0
20.0	16.2	9.0	4.9	0	0	0	150.85	136.94	127.31	0	0	0

Table 3.5 Side boundary distance effect in the footing settlement and vertical stress of numerical model.

Side boundary distance (m)	Settlement Uy (mm)			Normalized difference (%)			Vertical stress σ_y (kPa)			Normalized difference (%)		
	(A)	(B)	(C)	(A)	(B)	(C)	(A)	(B)	(C)	(A)	(B)	(C)
8.0	43.9	33.2	22.5	6.81	9.57	10.29	95.12	145.84	190.86	7.03	4.76	4.15
10.0	42.6	31.9	20.9	3.65	5.28	2.45	91.53	142.87	186.98	2.99	2.63	2.04
12.0	41.3	30.4	20.6	0.49	0.33	0.98	88.89	139.79	184.35	0.02	0.42	0.6
14.0	41.2	30.4	20.4	0.24	0.33	0	89.14	139.23	183.25	0	0.01	0
16.0	41.1	30.3	20.4	0	0	0	88.79	139.21	183.25	0.09	0	0
20.0	41.1	30.3	20.4	0	0	0	88.87	139.21	183.25	0	0	0

151

2. The effect of mesh density

Two main aspects should be decided for the mesh in finite element analysis. Firstly, the type of the element into which the soil media in discretised and, secondly, the density of this mesh. As mentioned in Section 3.6.4, there are two triangular mesh elements types in Plaxis code; 6 node elements and 15 node elements Figure 3.6. Although the 15 node element requires higher computed efficiency than the 6 node element, it provides high accuracy output results compared with 6-node triangular element and gives more nodes and stresses points to study soil- structure interaction and local failures in more detail (Brinkgreve et al., 2011). So in the current studied model all the clusters were meshed to 15-node triangular elements.

The mesh density should be sufficiently fine to achieve accurate numerical results. On the contrary, very fine meshes will consume more calculation time. So a balance in mesh fineness is very important in building a successful model. One preferable feature in Plaxis 2D AE is an automatic fine mesh is generated at the interfaces and inter-element boundaries, but it is still important to check any discontinuities that may occur in these regions due to the fast changes of strains and stresses. In this model, the soil under the edge of the footing should be checked after applying the working load and refining the mesh at this area at any discontinuity case.

The mesh can be refined, coarsened locally or globally for the whole model. The global meshing parameter presents five levels calculated from the model outer geometry dimensions; very coarse, coarse, medium, fine and very fine. While local refinement is based on local fineness factor, which gives a relative element size compared with initial global mesh size (if it equals 1; that means no effect for this factor) and by reducing this factor the mesh elements size reduces and get finer mesh. To perform the mesh density sensitivity analysis, the global coarseness was taken to be medium and the varied parameter was the local fineness factor to investigate the effect of mesh density. The same used three points A,B and C used to study the effect of the boundaries were taken to investigate the mesh sensitivity. The results are illustrated in Figure 3.20.

It was found the mesh density has a noticeable influence on model results. Increase the density to local fineness factor to 0.5 led to sufficient accurate analysis
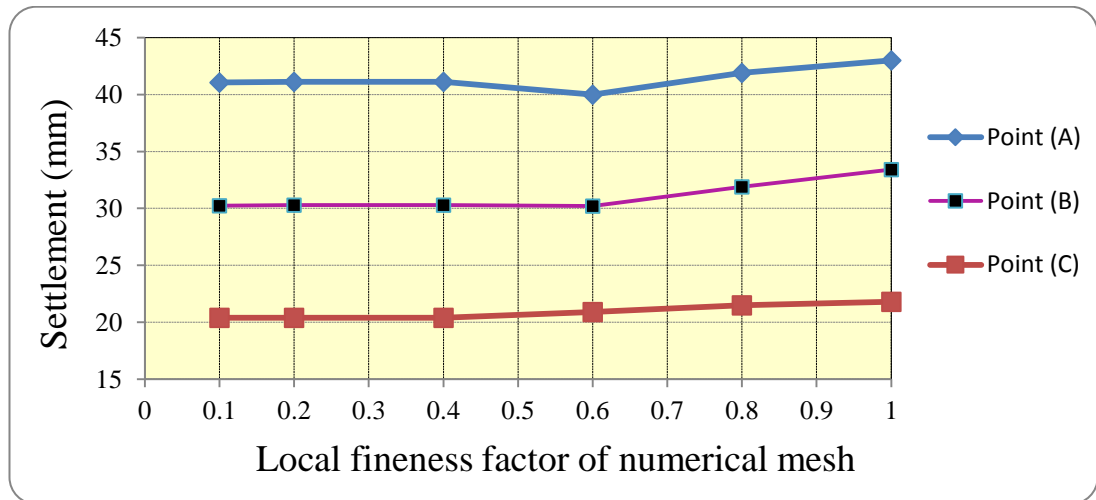
Figure 3.20 Mesh density effect in in the footing settlement of numerical model.

By finishing the sensitivity analysis, the final dimensions have been assigned and the axisymmetric model for the stone column analysis is ready for numerical analysis. It is (30 x 14.5) m cylindrical of solid soft clay. installed vibro stone column diameter ranged between (55-100) cm and the applied footing was 2m diameter of 50 (kPa) distributed load on both stone column and surrounded compacted clay. The model geometry is symmetric so one half of it is enough for simulation. The final model dimensions are illustrated in Figure 3.21.
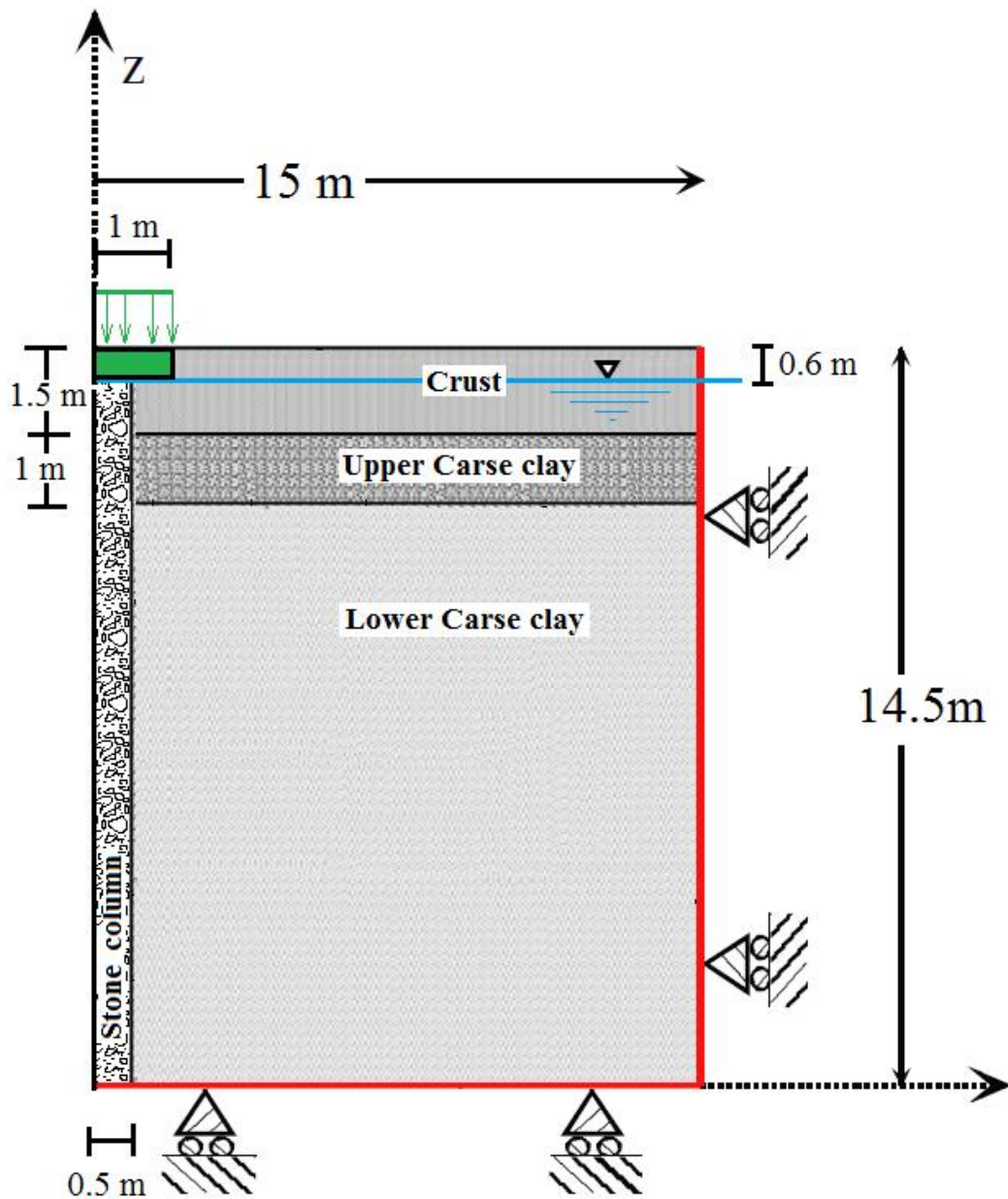
Figure 3.21 Geometric dimensions for the finite element model.

3.7 Summary

This chapter briefly described the numerical method and its application in analysis. A brief description of the more commonly used numerical methods was presented. The finite element method approach adopted in this research was highlighted. An overview of computer software - Plaxis, based on the finite element method, was also presented together with details of the

154

relevant Plaxis software's soil model applications. Implementation of the principles of the finite element method using Plaxis has been applied this chapter in the process of building the axisymmetric model of single stone column installed in well documented Bothkennar soft clay soil. Validation process has been carried out to check the use of Plaxis 2D and the selected Hardening Soil Model parameters to be adequate for representing the soft soil. Finally, primary analysis checks have performed to establish the final geometric dimensions and mesh specification for the finite element model to be ready for studying the stone column installation effect next chapter.

4 Chapter 4: Single Stone Column Installation Effects

4.1 Introduction

Two simulation methods have been used to take into account the effect of stone column installation in improving the settlement performance; the first one is to increase the coefficient of lateral earth pressure (K_0) in the soil around the stone column without applying any radial expansion cavity (Elshazly et al., 2006; Ambily and Gandhi, 2007; Elshazly, 2008b). The second method is using a low stiffness dummy material to expand the stone column, which is then replaced by material with the same properties as those of the stone backfill after expansion (Debats et al., 2003; Guetif et al., 2007; Kirsch, 2008).

In this study, the two methods were combined by applying cavity expansion to stone columns using the Guetif et al.'s (2007) method to take into account the changes in the soil stress state and the improvement in the soil stiffness. The foundation load settlement response of a circular footing was used to assess the performance of the composite foundation.

4.2 Assumption

- The design of foundations on soft soils is usually governed by settlement rather than bearing capacity criteria, due to their high compressibility (Priebe, 1976). Therefore, the settlement performance of stone columns at working load levels is of the upmost importance.
- When the plastic deformation becomes dominant, the stone columns yield and after that the performance of stone columns is not influenced by the impacts of installation. So, this study will concentrate on the working load of the stone column reinforced foundations and not at the ultimate capacity

- There are two main methods to construct the stone column: top feeding and bottom feeding. In the top-feed method the stone material is tipped from the ground surface to the hole created by the poker in controlled amounts, then compacted in layers repeatedly by poker, while in the bottom-feed method, stone is fed from the bottom through a delivery tube that is attached to a hopper. In this study, bottom feed system was chosen to simulate the stone column construction, as is the most commonly used method for vibro stone column installation. It involves supplying granular material gradually from the base upward using vibratory poker is not an instaneous action. Cavity expansion theory was used to simulate the lateral expansion made by column installation process. The predominant displacement of the soft soil, due to the stone column installation, is in a radial direction except at the top zone where the ground heaves, and at the stone column tip where ground displacement is spherical (Section 2.13, and figure 2.68).

- Typical range for the diameter of stone column using bottom feed method is 430-1100mm (McCabe et al, 2008). Diameter was selected 1000 mm in this study.

- The development of stiffness and stress state of the soft soil around the stone column after installation and loading was investigated in mid-depth of the different soil layers.

- Stone column installation starts from an initial diameter of zero to the final designed diameter of stone column; consequently, the lateral strain is effectively infinite. But realistically, and in order to simulate stone column installation effect correctly, Egan et al. (2008) suggested that cavity expansion pressure should reach to its limit value σ_{rl} during the installation. McCabe et al. (2008) applied different degrees of cavity expansion to examine the development of cavity pressure during installation using Carse clay at Bothkennar, Scotland. They found that considerable lateral expansion is required to the limit cavity expansion pressure. The result is showed in Figure 4.1 after

normalising both cavity pressure and expansion with the limit
pressure and initial cavity radius a_0, respectively.
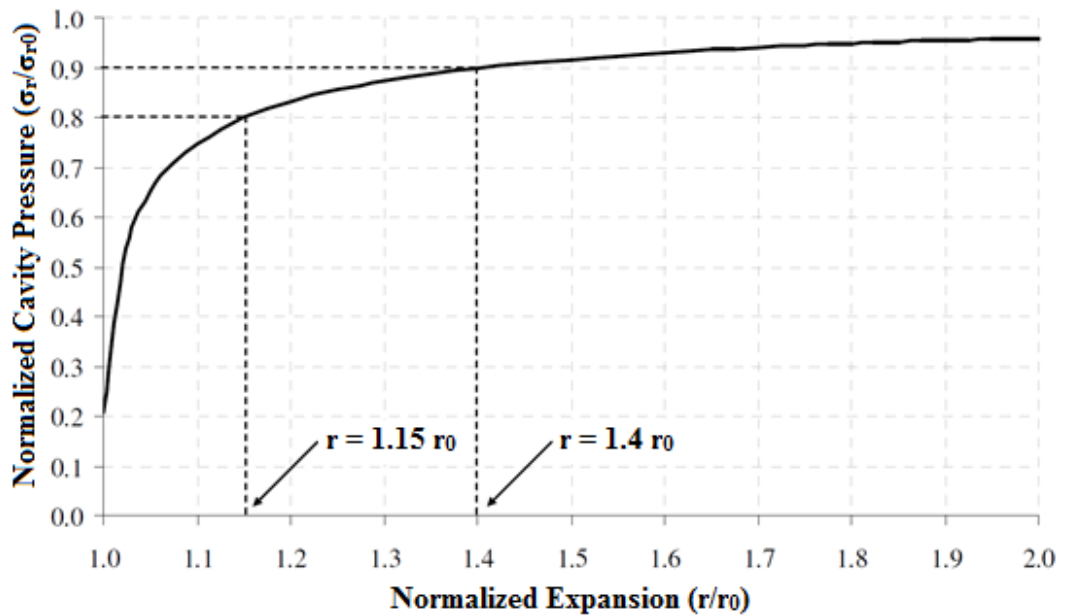
Figure 4.1 Variation of cavity pressure with radius (undrained CCE)
(McCabe et al., 2008).

In chapter 3, an in-depth study to build a model of axisymmetric single stone
column was performed using Plaxis 2D with the input parameters of the
physical and mechanical properties of both stone column material and soft
saturated clay, based on a well-documented realistic field case. Final
geometric dimensions and finite element mesh for this model are shown in
Figure 4.2.
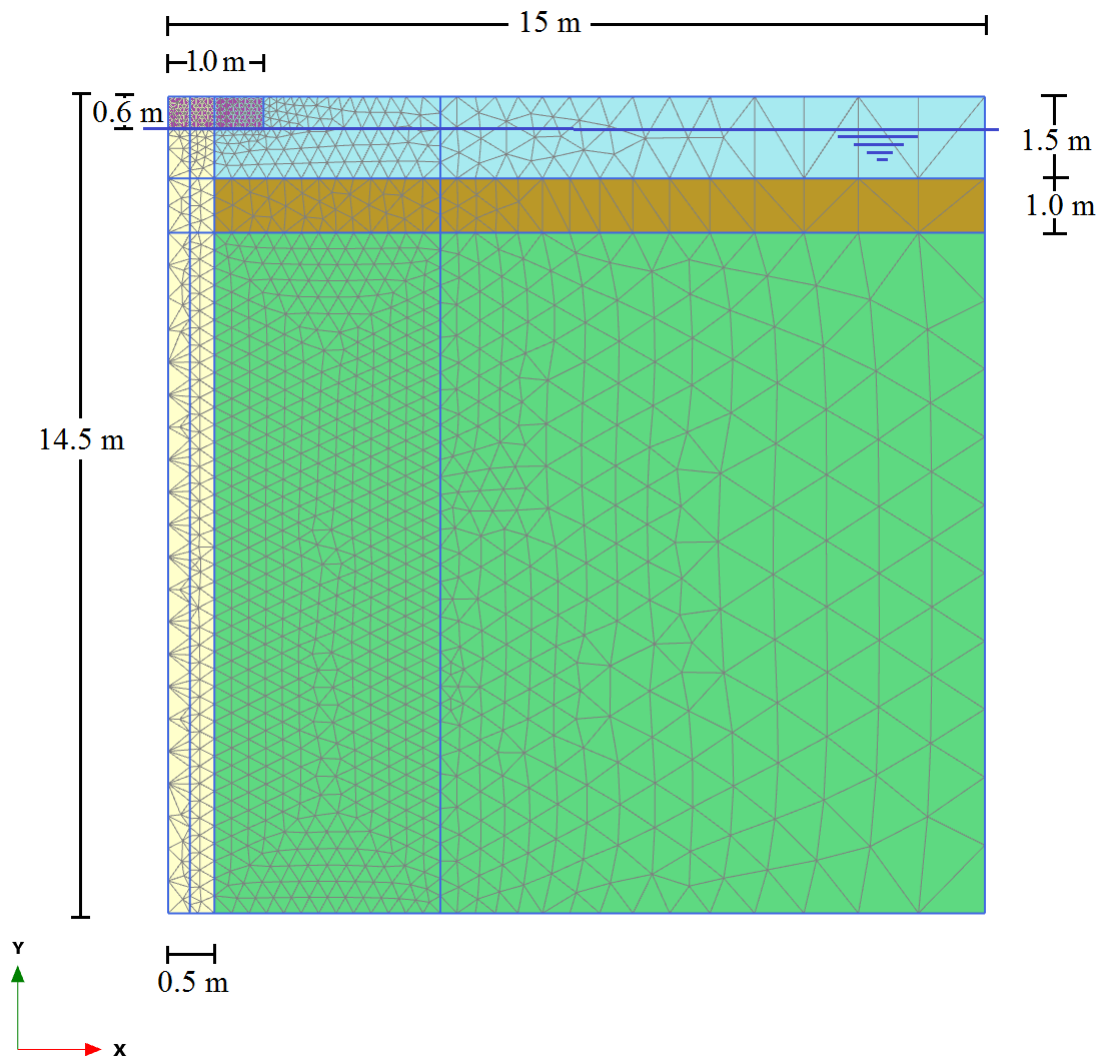
Figure 4.2 Model geometry and finite element mesh.

4.3 Chapter Scope

The scope of this chapter is to use cavity expansion theory to predict the variation of stiffness and stress state in the soft soils due to the installation of stone columns in the short and long term. The chapter also presents the method of quantifying these changes with the different cavity expansion degrees to study the installation effect of the single stone column on the performance of the treated ground under circular footing.

4.4 The Interaction between Soft Soil and Stone Column

Soil-structure interactions is involved in most geotechnical engineering problems. Typically, the properties and characteristics of soil and structural materials are not the same and thus their constitutive behaviour is different. This applies to stone columns which interact with the surrounding soil. So, it is necessary to consider this interaction between the soil and the stone column materials surfaces in the studied model.

The continuity of the finite elements and compatibility of applied load and displacement are very important to prevent any relative displacement of the common node elements between the column and soil. This constraint can be accommodated through modelling the boundary between soil and column by using interface elements (Boulon and Nova, 1990; Viladkar et al., 1994). As Potts and Zdravkovic (1999) state, the interface element is designed to provide the ability of differential movement of two different constitutive behaviours of adjacent elements. Various methods have been advanced to develop the use of interface properties, such as using special joint elements with zero or finite thickness, linkage elements, thin continuum elements and even hybrid methods.

For the case of the studied installed single stone column in Bothkennar clay using Plaxis, interaction between the soil and the stone column materials surfaces (smooth and rough), including any gap or slip displacement that might happen, are the features which interface elements should capture. In this regards, there are two different opinions; Han and Ye (2001), Weber et al. (2009), Killeen and McCabe (2010), Indraratna et al. (2013) and Killeen and McCabe (2010) considered the smear zone created between the stone column and the soft clay after installation as a low permeability region which affects the drainage capacity of stone columns and reduces the rate of consolidation. So they use column-soil interface in their models. Others, e.g. Kirsch, (2006), Guetif et al. (2007a) Gab et al. (2009) and Shahu and Reddy (2012), suggested that the installation of the stone column creates an interface between the soft clay and column material which is fully adhesive; thus the stone columns becomes interlocked with the surrounding soil. In

this model, no column–soil interface was considered for the following reasons:

1. Both the soft clay and stone column material are treated as particulate materials with different geotechnical properties with no discontinuities forming between the materials after installation.
2. The focus of the current model was to study the changes in both the stress state and the mechanical properties of the clay adjacent to the column due to the installation and consolidation. Hence, any assigned properties for this zone may affect the results.
3. The low permeability smear zone created by the poker has no effect on the long term performance of the stone column system.

4.5 Column Installation Modelling

Based on the short period of stone column installation, undrained conditions were assumed for the soft clay soil. So, undrained expansion of a cylindrical cavity was used to perform the installation process of stone column in the finite element simulation (Guetif, 2007;Sexton, 2013). The procedure of analysing the axisymmetric single stone column is based on five stages, which are illustrated in Figure 4.3;
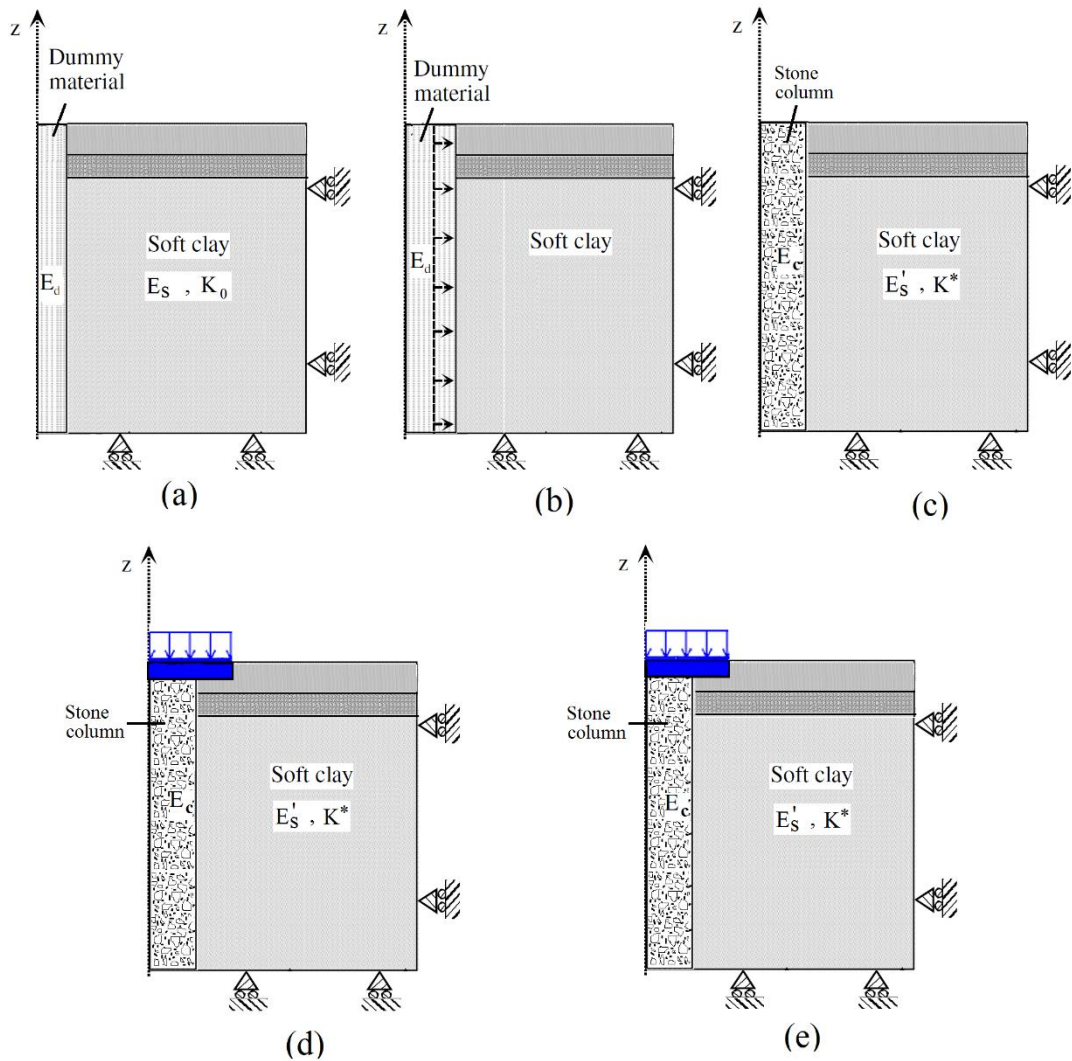
Figure 4.3 Principle of stone column expansion using the dummy material and modelling phases.

- In the field, fully displaced stone column installation involves starting a stone column from zero initial radius and then expanding it with vibratory poker to final stone column radius. Practically, numerical simulation of the actual stone column installation process using Plaxis cannot be performed; that is to avoid any discontinuity in simulating the radial expansion process or any development of infinite circumferential strain. So, finite radius was used (r_0) to start with as an initial one that expressed the cylindrical hole made by the poker. A dummy material was used in defining this initial stage as a first phase, as is shown in Figure 4.3 (a). It was considered a purely elastic

material with a low stiffness in order to deform when it is subjected to radial displacement (vibro compaction of stone column material) until the radial expansion reaches the stone column radius (r_c) (Guetif et al., 2007b).

- Apply the radial expansion (Δr) caused by the stone column material installation using the option ''Prescribed Displacement'' in Plaxis 2D starting from initial radius(r_0), as is illustrated in Figure 4.3 (b). Nine different lateral expansion values have been considered (Δr = 0.05, 0.10, 0.15, 0.20, 0.25, 0.30, 0.35, 0.40, 0.45 m). Due to the large deformation caused by the displacement of Lateral expansion of the stone column applied to the surrounding soft clay, the "updated mesh" option was used in the analysis of the effect of column installation. Since stone columns are usually installed in a short period of time, the applied radial expansion to the surrounding clay was modelled as a prescribed displacement under undrained conditions.

- The dummy material was then replaced by stone column material in the third Phase, which is shown in Figure 4.3 (c). Consolidation analysis was used in this phase giving enough time for the excess pore water pressure to dissipate and to study the long term behaviour of the stone column consequences. This stage is very important because by the end of it, post- installation properties of the soft clay soil can be captured. The soil is allowed to consolidate with the stone column acting as a drain. Based on this, open consolidation time has been given to this stage till the pore water pressure returned close to its original value.

The numerical analysis was conducted assuming infinite permeability between the clay and the stone column and allowing enough time for the excess pore water pressure to dissipate after stone column installation, and the soft clay soil to reconsolidate to a new stress state and gain some more stiffness.

According to Egan et al., (2008), who studied the settlement-time behaviour of same adopted Bothkennar caly for a trial strip foundation rested on a line of stone columns, the immediate elastic settlement

163

takes place within the first 24 hours during construction, while the primary consolidation settlement completed in about 8 weeks of construction. Figure 4.4 illustrates a typical settlement – time curve for a strip footing. For more accurate results, 100 days Consolidation time of 100 days was given after installation.
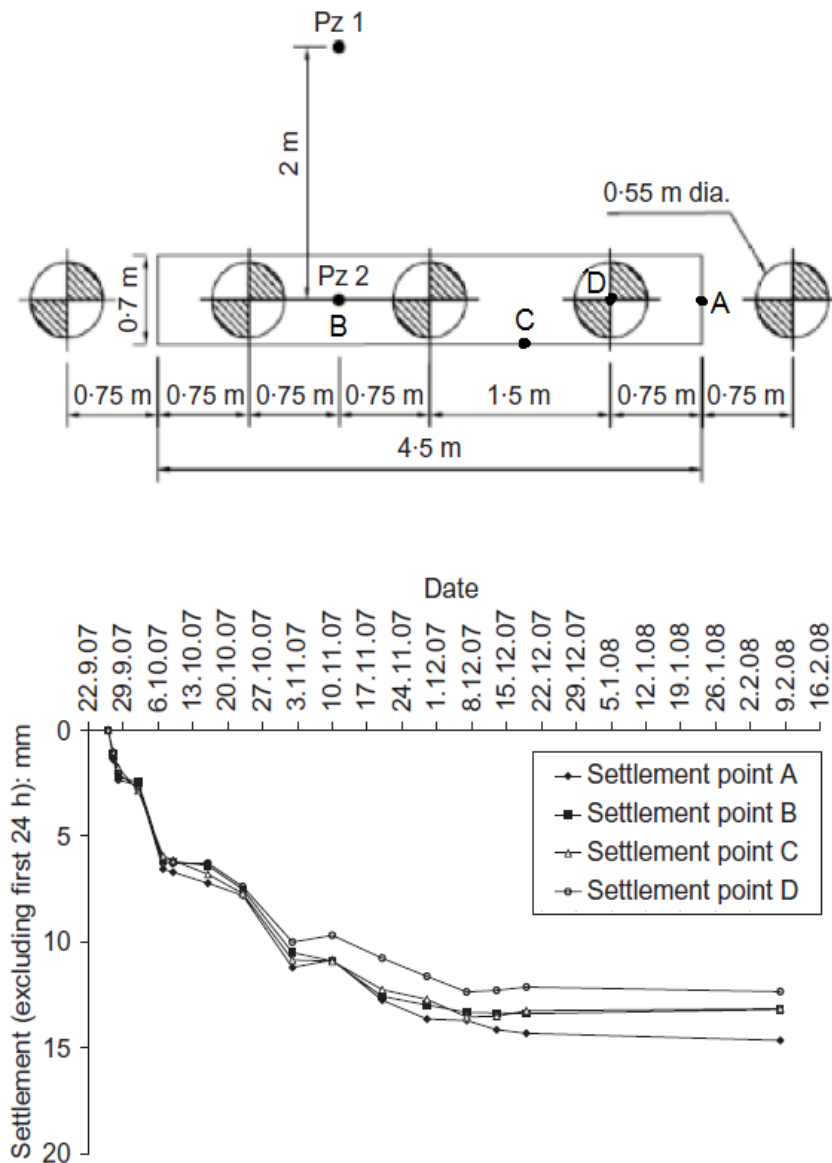
Figure 4.4 Settlement–time behaviour of trial strip footing (Keller Foundations Contract) Egan et al., (2008).

- In order to quantify the settlement performance and the bearing capacity improvement of the treated clay and then compare the response of the soft clay before and after treatment to get the improvement factor, typical working load of 50 kPa on a 2m diameter foundation of 0.6m depth have been selected as a design loading for Bothkennar soft clay, which has been selected based on Atkinson's (2007) design factor of safety for the foundations on soft soils and ultimate bearing capacity test results performed by Jardine et al (1995). Figure 4.3 (d) illustrates this stage.
- Allow Bothkennar soft soil to consolidate after applying the footing load to calculate the final settlement performance (Figure 4.3 (e)).

For the right comparison of the settlement and bearing capacity performance, the final stone column diameter in this study is fixed at ($d_0 + 2\Delta r = Dc = 1.0$ m). So, in order to meet 9 different degrees of applied expansion, the initial stone column diameter r_0 was changed according to the applied cavity expansions.

4.6 Nodes & Stress Points

The finite element method generates results at the specific locations of the nodes and the stress points. These locations should be identified in the Plaxis model before calculation. Therefore, a group of nodes and stress points located under the footing and at mid depth of each different soft soil layer have been selected on the finite element mesh. In Plaxis, it is not possible to select more than 10 points in each run. So for that reason, the numerical analysis runs have been repeated to cover the required location of the studied soft soil behaviour due to the stone column installation.

4.7 Results

Although, the results of this numerical analysis focused on the changes happening to the surrounding soft soil more than the changes on the stone

column material, the presence of the stone column was very necessary to represent the actual permeability of this material during consolidation and, more importantly, to give the real behaviour of interaction between the soft soil and the stone column in all stages of construction and loading.

To quantify the final changes after the full consolidation that happens within the soft soil caused by applying different degrees of cavity expansion during installation, and then estimate the effect of these changes on the performance of both bearing capacity and settlement under the single foundation load, results of changes within the soft soil immediately after installation and their development with time, depth and distance from stone column were presented next.

Most graphs have been drawn at the mid of the lower Bothkennar Carse clay at depth of 8.50m from the soil surface, and to show the general trend of soil changes, cavity expansion degree of Δr = 0.25 m was selected as a reference.

4.8 Short Term Changes after Installation

Short term changes are the alterations that encounter the saturated soft soil immediately after applying the expansion cavity caused by stone column installation. They are not permanent, but their development determines the final alteration of the reinforced soil system.

4.8.1 Lateral Displacement within the Clay due to Installation

The vibrating poker penetrates the soft ground applying horizontal vibratory forces while pushing the stone column material towards the walls of column hole. Radial prescribed displacement was applied along the stone column to simulate the expansion due to the vibratory forces. The fine particles around the stone column absorb these forces and they get displaced horizontally far from the column. They attenuate displacement effect through the soft soil and vanish with the distance from the column after about 7-8 from the final stone column diameter D_c for the Bothkennar clay case. Figure 4.5 presents

166

the contours of total resulted horizontal displacement with the distance from the stone column.
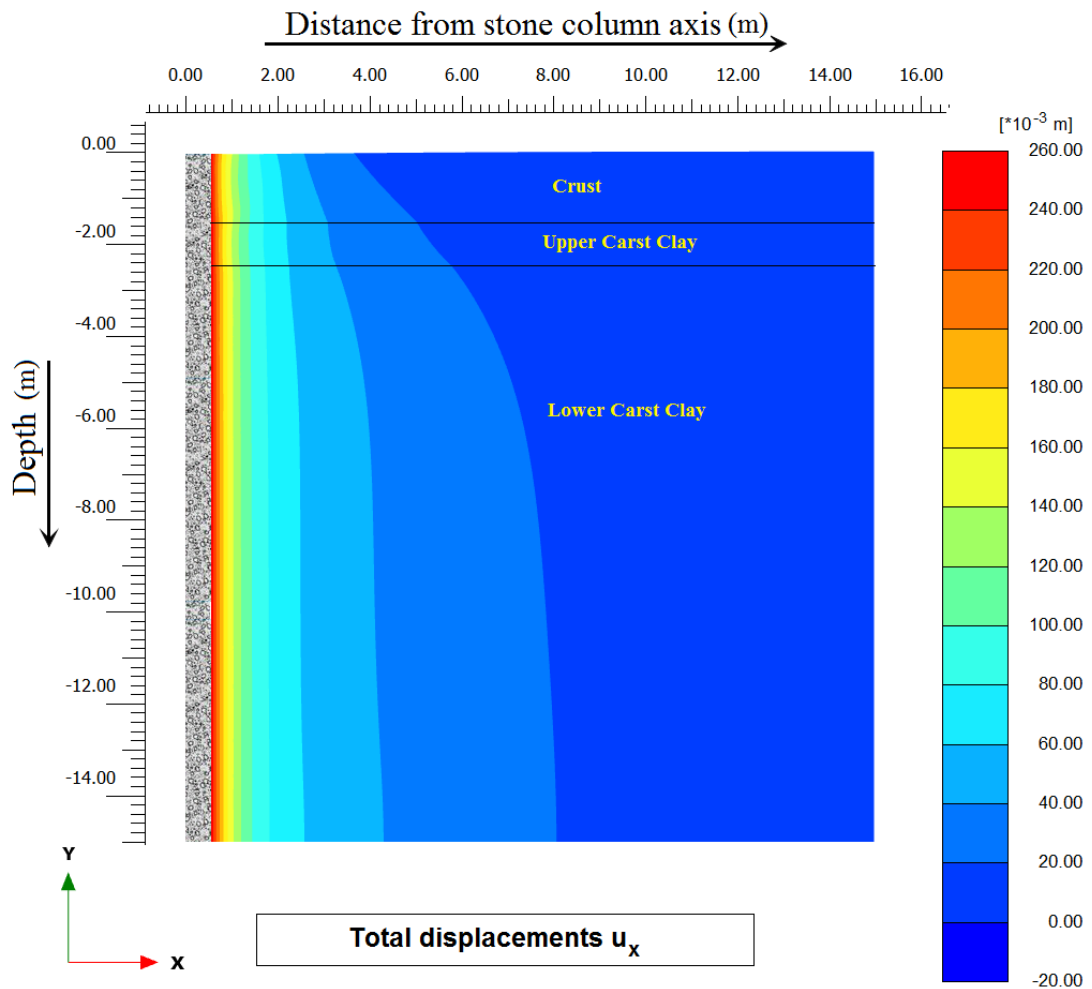
Figure 4.5 Contours of total lateral displacement caused by the stone column installation with 0.25m applied cavity expansion.

Figure 4.6 shows the normalized relative displacement, (u_x/D_c) with distance from the stone column for a range of stone column radii. It is obvious that increasing the cavity expansion degree to 0.45m generates horizontal displacement up to 0.38 from the stone column diameter at 1 m distance from the column axis. It also extends the horizontal distance that is affected by this cavity up to 8 times of the column dimeter, while these values are reduced significantly at low cavity expansion degrees. The curves in Figure 4.6 proves that the vibro installation effect of the stone column is not only absorbed by the disturbed adjacent soft soil, but it has important role in

consolidating the soft soil up to about 8 times of the column dimeter in this case. Figure 4.7 shows the direct influence of increasing the applied expansion degree in increasing the resultant internal displacement within the clay at 0.5 m from the stone column surface after normalizing both terms with the column diameter. It is almost a linear relationship.
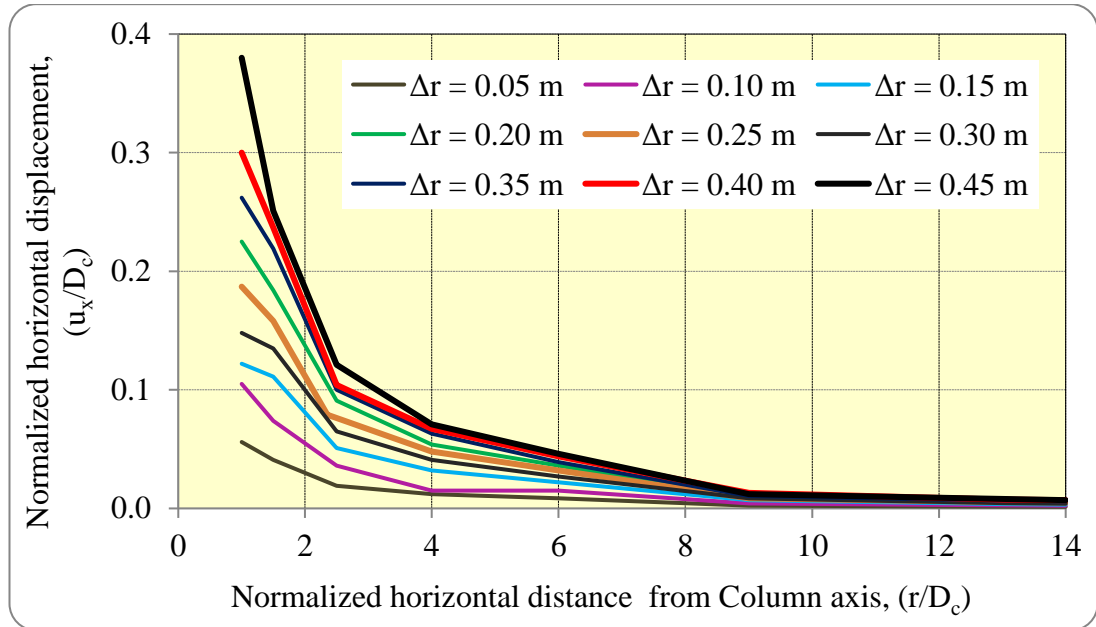
Figure 4.6 Variation of horizontal displacement within the clay with distance from the column axis for the adopted cavity expansion degrees at mid of lower Bothkennar carse caly.

168
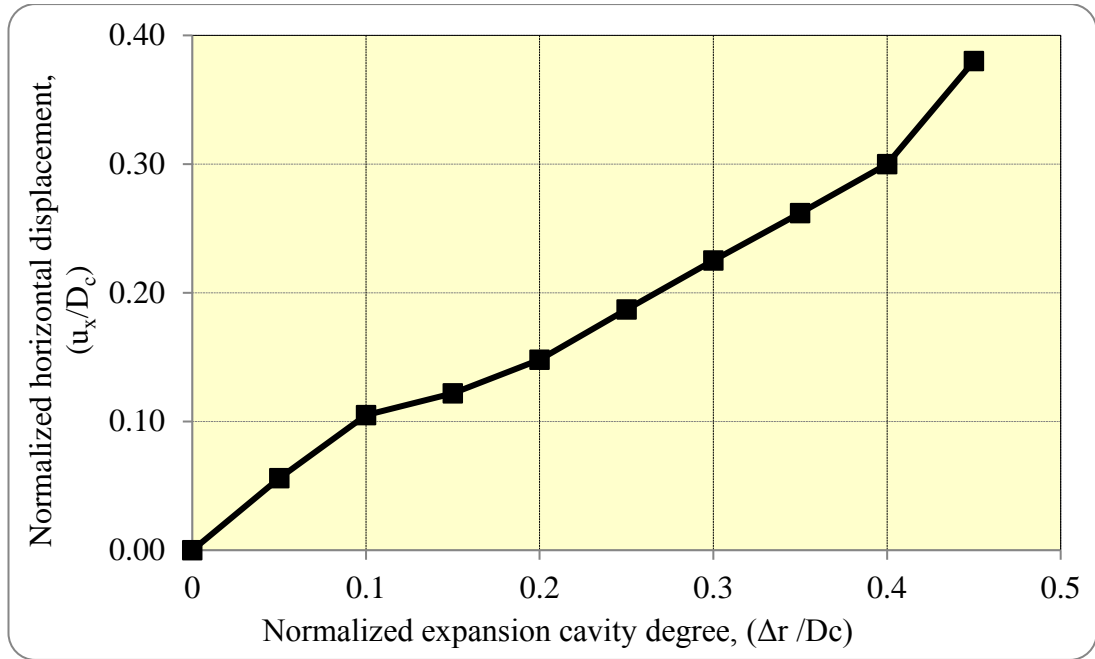
Figure 4.7 Effect of expansion cavity degree on the horizontal displacement within the clay at 1 m distance from stone column centre.

4.8.2 Excess Pore Water Pressure

Immediate increase in both pore water pressure and total horizontal stress happens during vibro penetration in undrained saturated Bothkennar clay. These stresses decrease with distance from the stone column axis. Figure 4.8 illustrates the development of excess pore pressure around the stone column with depth.
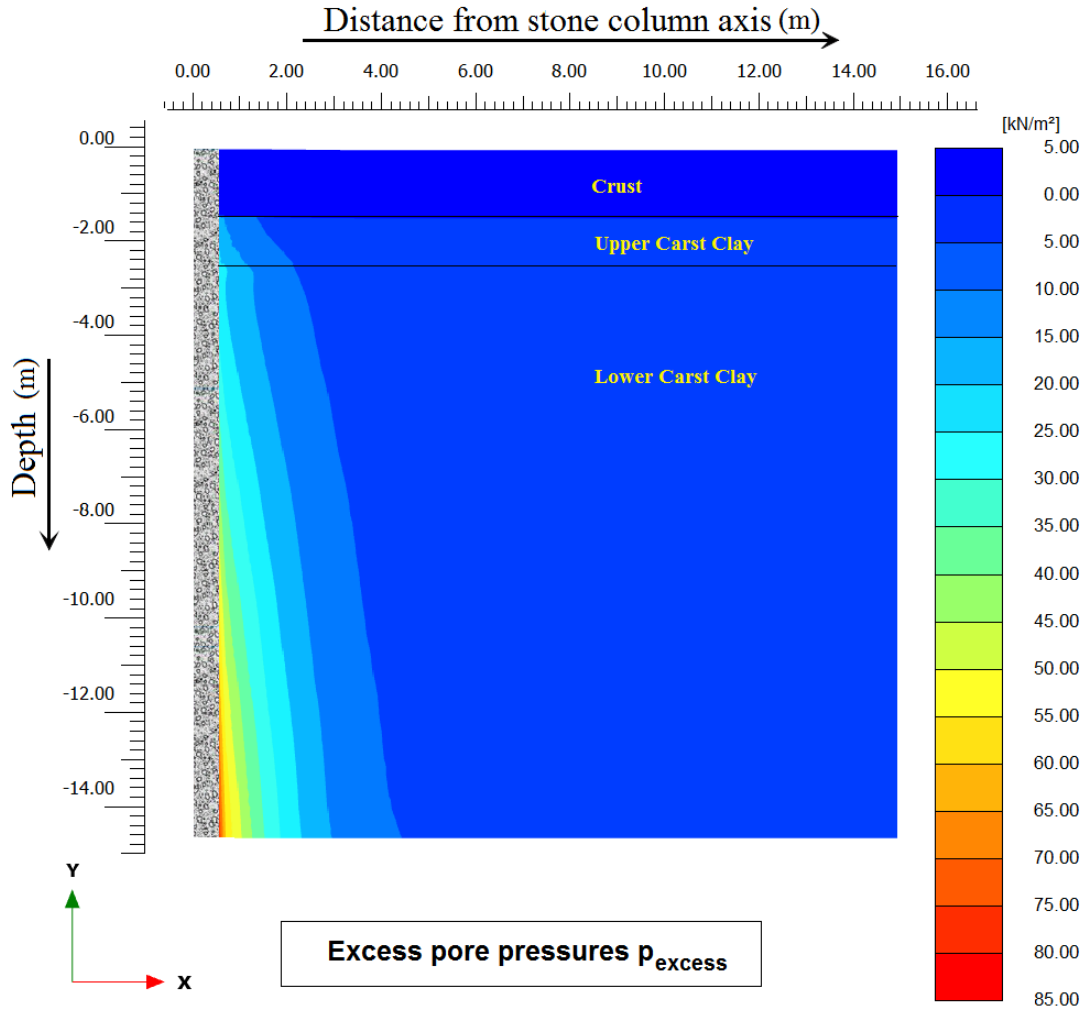
Figure 4.8 Contours of excess pore pressure changes after stone column installation with 0.25m applied cavity expansion.

The dissipation rate of the excess pore pressure is governed by the permeability characteristics of Bothkennar clay. This dissipation rate at mid of the Lower Carse clay, which represents about 80% of soft saturated clay along the stone column, is illustrated in Figure 4.9. Excess pore pressure was generated adjacent to the column at (r/Dc = 1) immediately after applying the cavity expansion, this was followed by dissipation which occurs afterwards with the time. As is shown in Figure 4.9, the soil cylinder close to the stone column, (the points far $1.0D_c$ and $1.5D_c$ from the stone column axis) had a faster dissipation rate and it took about 60 days to reduce close to its original value before the stone column installation, because of the short path to stone column drains, while consolidation time increases for the

further points from the stone column axis. Figure 4.9 shows that 100 days in this studied case is sufficient enough to dissipate more than 90% of the generated pore water pressure.
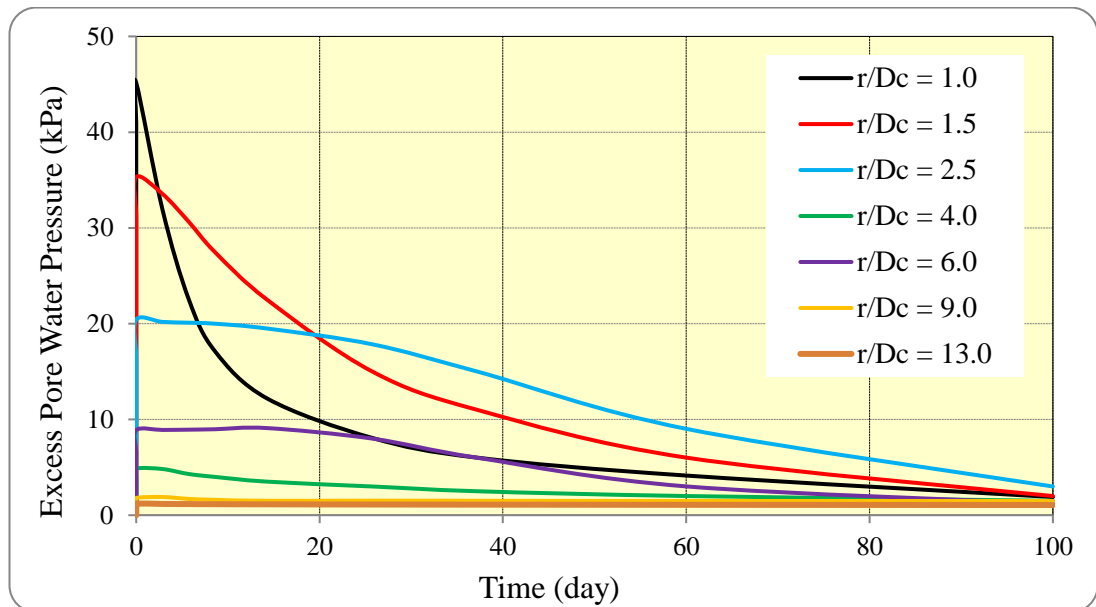
Figure 4.9 Isochrones of pore water pressure dissipation at mid of lower Bothkenner clay after stone column installation with 0.25m applied cavity expansion.

Figure 4.8 shows that the consolidation takes place mainly due to the radial dissipation of excess pore pressure toward the stone column drain, except in the top layer which is very close to the free surface where there is some dissipation to the ground surface. To study the effect of stone column installation on the excess pore water pressure with the depth, three different levels at (-3.0, -8.5 and -14.5m) have been selected and the variation of the excess pore water pressure with the distance from the stone column plotted in Figure 4.10. As can be seen, excess pore water pressure increases with depth to a maximum level at the base of the column (-14.5m).
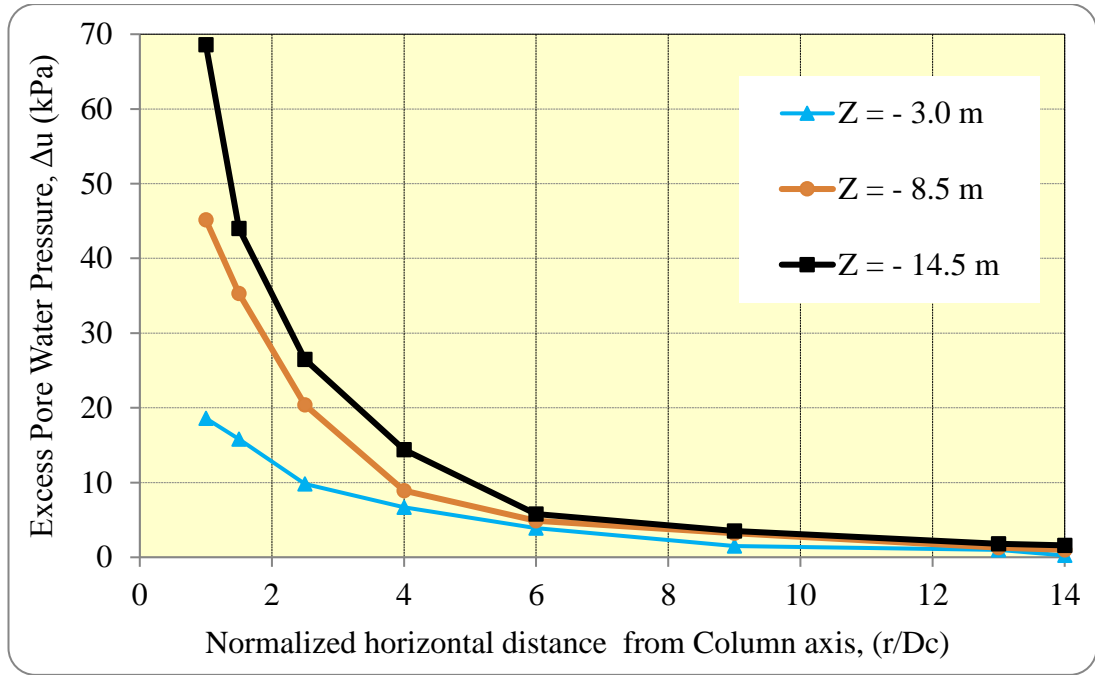
Figure 4.10 Variation of excess pore pressure within the clay with the depth (displacement degree = 0.25 m) after installation

Figure 4.11 illustrates the excess pore water pressure increases around the stone column within a distance up to $14D_c$, for 9 different degrees of expansion applied during stone column installation, where D_c is the final diameter of the stone column. This shows that the peak excess pore pressure depends on the diameter of the stone column, but the significant effect of the installation of the stone column extends to about 8 times the diameter.
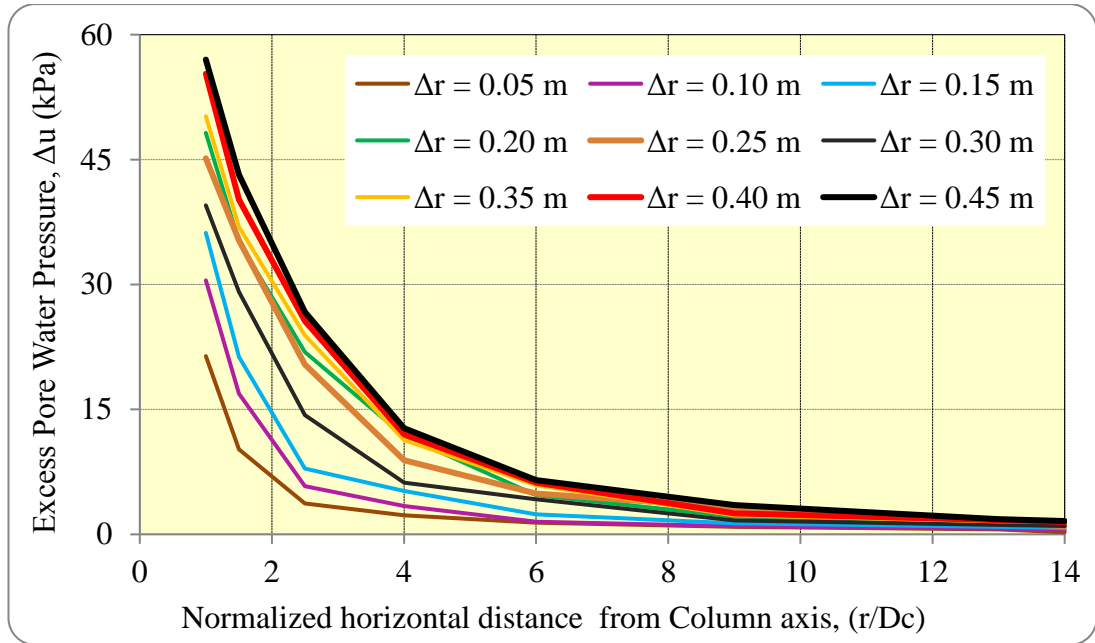
Figure 4.11 Variation of excess pore pressure within the clay with distance from the column axis (displacement degree = 0.25 m) after installation

Figure 4.12 shows the effect of increasing the cavity expansion when installing the stone column by plotting the excess pore water pressure for distances 1, 2.5, 4 and 6 m from the stone column at the mid of lower Bothkennar clay, against the normalized expansion cavity degree, ($\Delta r / Dc$). It shows that the excess pore pressure reduces, as expected, with distance from the stone column. As the pore pressure dissipates, the effective stress, and therefore the undrained strength and stiffness of the soil will increase. Therefore, the stone column/soil composite foundation should have a greater stiffness that the stone column alone.

It can be seen that there is a kind of direct proportion between the adopted cavity expansion during stone column installation and the resultant generated excess pore water pressure in the area close to the column, while as the distance increases from this column excess pore pressure, it seems to increase very slightly after the expansion degree of 0.3m for this study case. This behaviour gives good indication that for the response of any soft soil to be improved, using stone column technique should be studied before to estimate the optimum degree of expansion cavity to achieve the required performance.
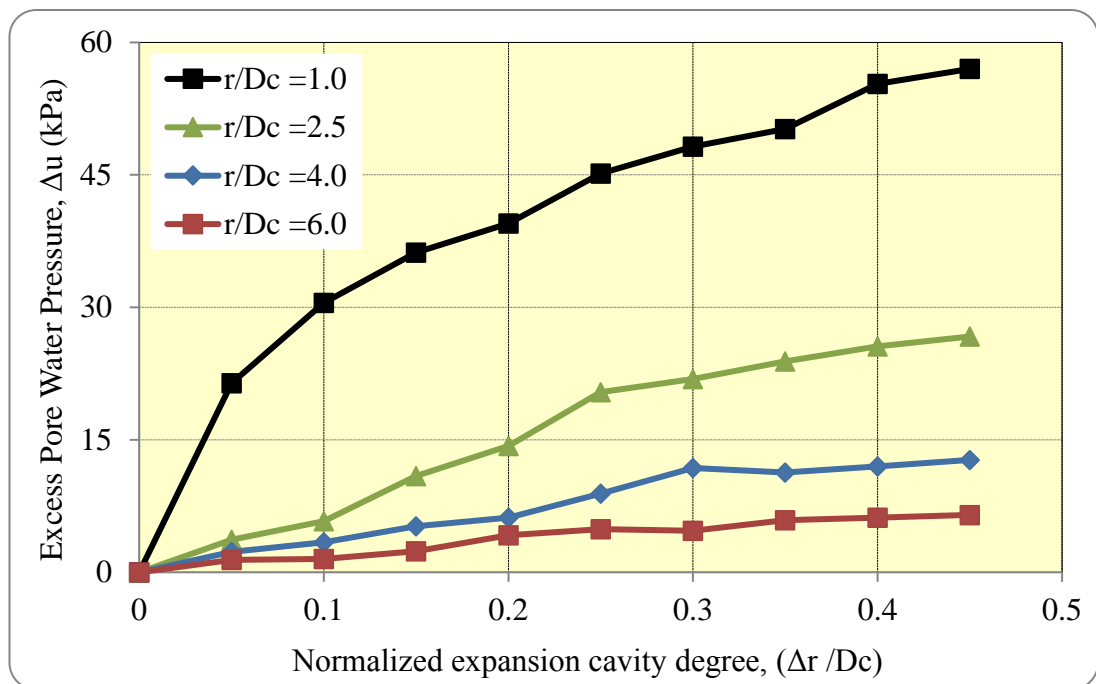
Figure 4.12 Cavity expansion degree effect on the generated excess pore water pressure at 1Dc from the stone column axis immediately after installation.

4.8.3 Total Horizontal Stress

Similar to the excess pore water pressure, an immediate increase in total horizontal stress happens during vibro penetration in the undrained saturated Bothkennar clay. These stresses decrease with distance from the stone column axis. Figure 4.13 illustrates the development of the total horizontal stress around the stone column with the depth and the distance from the stone column of the studied soil.
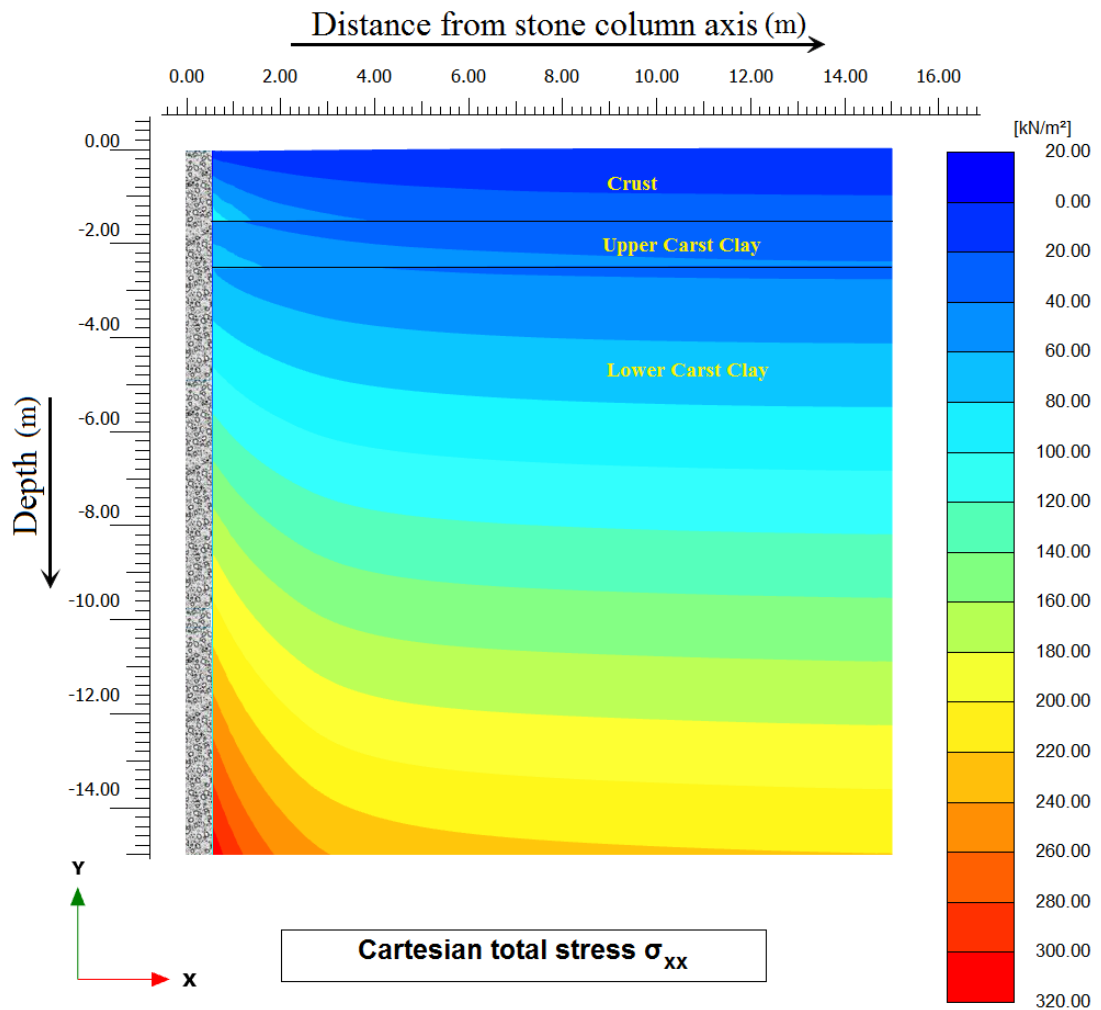
Figure 4.13 Contours of radial stress changes after stone column installation with 0.25m applied cavity expansion.

Figure 4.14 represents the development of total horizontal stresses far 1.0, 1.5, 2.5, 4.0, 6.0, 9.0 and 13.0 m from the stone column axis during installation and consolidation. The sharp increase in the excess pore pressure during the installation of the stone column causes high increase in horizontal stresses, especially close to stone column, up to 50% more than the original value for the case of Δr =0.45 m, as Figure 4.14 shows in the first part of each curve. The second part of the curves represents horizontal stress relaxation during excess pore water pressure dissipation till reaching the balance between pore water pressure and effective horizontal stresses.
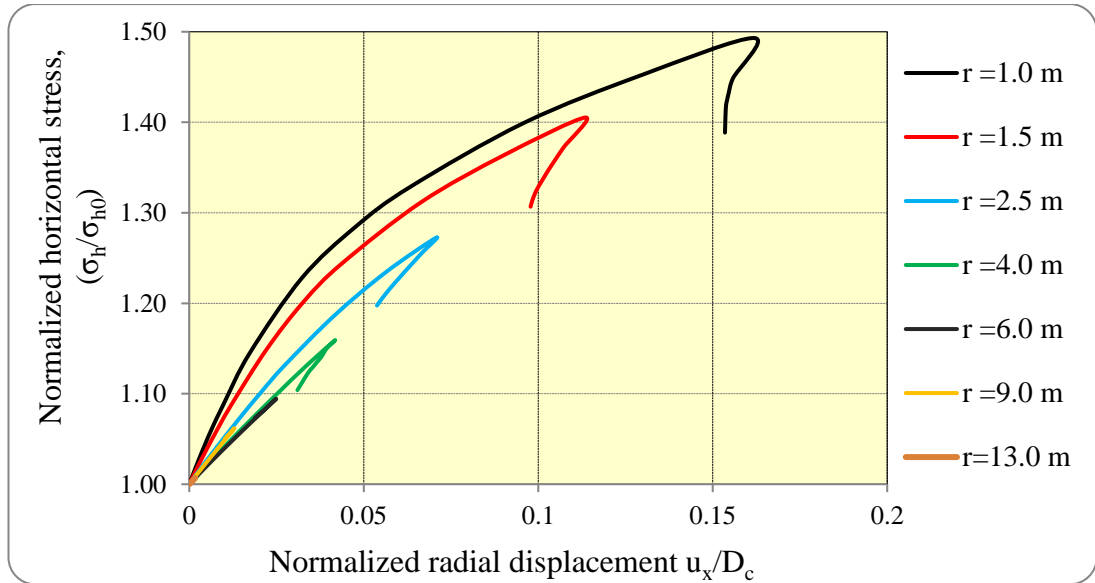
Figure 4.14 Development of total horizontal stresses during installation and consolidation distance from the column axis (cavity expansion degree = 0.25 m).

Figure 4.15 illustrates the increase of total horizontal stresses around the stone column within a distance up to $15D_c$ for cavity expansion degree of 0.25 m. The sharp increase in the excess pore pressure during the installation of the stone column caused increase in horizontal stresses, especially close to the stone column. Increasing the expansion of the stone column had also noticeable effect in generating higher horizontal stresses especially within the distance 4 times the stone column diameter, while the effect of this increased after this distance to finish at about 6 -8 of the stone column diameter D_c.

Horizontal stress values also increases with depth taking the same trend of the excess pore pressure to get maximum value at the bottom level of the stone column.
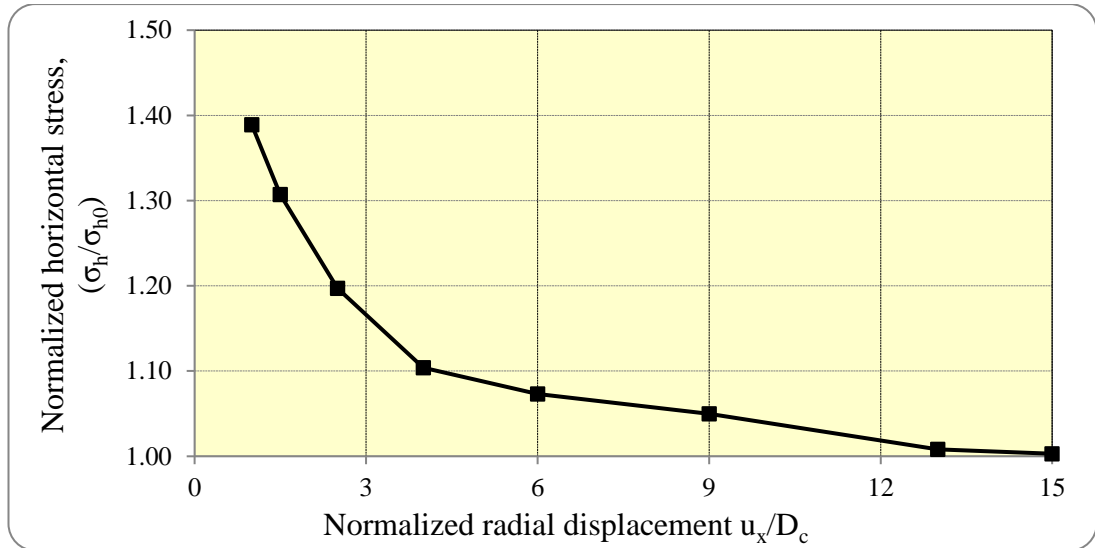
Figure 4.15 Variation of total horizontal stress in reinforced ground before consolidation with distance from the column axis (cavity expansion degree = 0.25 m).

4.8.4 Stress State of the Finite Element Points after Installation

During the consolidation of the saturated clay adjacent to the vibro stone column, which is subject to disturbance because of the installation, soft soil continue to relax with consolidation and hardening under the increase of effective mean stress and unloading of shear stresses caused by large displacement. The soil at greater distance from the stone column volumetrically hardens with the increase of effective mean stress after excess pore water dissipation as .

The results presented show the changes in total horizontal and pore pressure that took place during installation. These excess pore pressure will dissipate with time and leads to more strength and stiffness of the soil.

The Hardening Soil Model was used to estimate the stresses and the stiffness of the soft clay at any stage of soil consolidation. Moreover, Hardening Soil Model makes it possible to determine the stress state of the finite element points, including those that are in plastic state and others that are still within elastic deformations. Figure 4.16 illustrates four kinds of stress points in a plastic state (Brinkgreve et al., 2011);

177

- Tension points: These are the white points at the top of the model adjacent to the installed stone column. These points fail in tension caused by the lateral displacement at the beginning of stone column installation. In practice, they represent the surface heave of the soft soil around the stone column.

- Failure points: These are the red points at the upper part of the soft soil adjacent to the column. In this area, soil fails in shear caused by high lateral stress compared to the vertical one. So, its stiffness approaches to zero.

- Cap + Hardening points: These are the brown coloured points around the stone column along its length. These points represent points that are on the shear and cap hardening at the same time.

- Hardening points: These are the green wide cylindrical area around the stone column. They represent points where volumetric hardening is mainly dominant of the plastic strain.
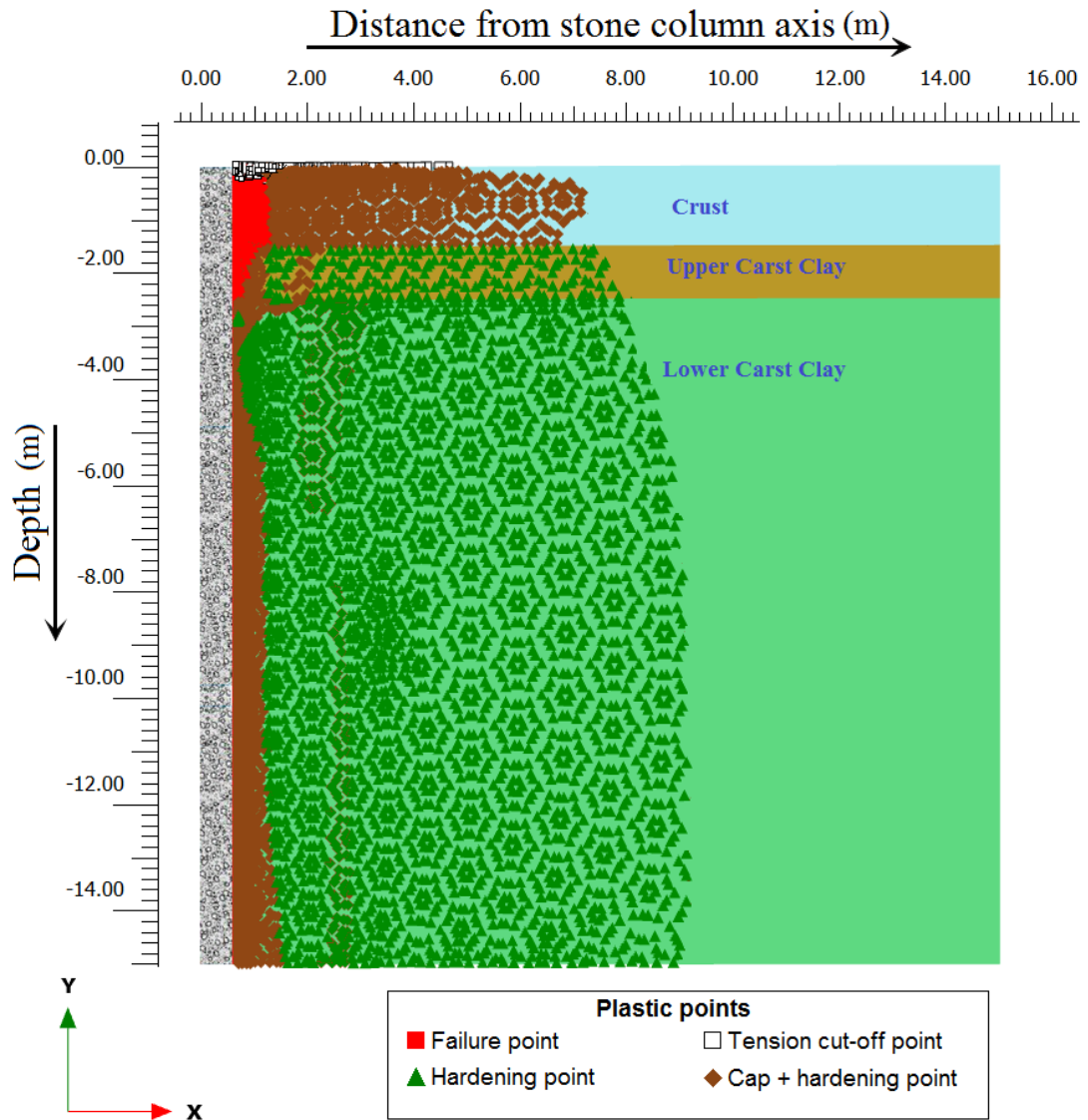
Figure 4.16 Distribution of plastic stress points around the stone column after installation ($\Delta_r = 0.25$m).

It can be noted that displacement of particles of soil in the upper part occurs in outwards and upwards manner to about 5-6 of the applied cavity expansion Δr, but as soon as the vibrator surpasses this distance, a radial displacement takes place and remains relatively static allowing the particles after this range to be ultimately compacted.

4.9 Long Term Changes after Full Consolidation

An equilibrium state is reached within the influence zone of the stone column installation after the dissipation of the excess pore pressure is complete, resulting in a new distribution of stresses within the soft saturated soil. The main feature of this new stress distribution is the increase in the effective stresses across this zone of influence. Consequently, soil stiffness and lateral confinement around the stone column increase. One task of this research is to exactly quantify the permanent improvement in both stress state and stiffness within the soft soil around the stone column with the distance from it due to its installation, and compare the results for different degrees of cavity expansion applied during the installation of this stone column.

4.9.1 Evaluating the New Stress State Changes due to Stone Column Installation

Lateral earth pressure coefficient, which is defined as the ratio between effective horizontal (radial) and vertical effective stresses (σ_h'/σ_z'), can express the new final distribution of the stresses after full consolidation. It is a parameter that indicates the amount of new lateral support for the installed stone column; that is, it expresses the improvement in the capacity of the stone column.

By taking the normalized effective radial stress to effective vertical stress after consolidation, it is possible to estimate the changes in the coefficient of the lateral earth pressure (K). Figure 4.17 shows variation of the coefficient of lateral earth pressure with distance from the column axis for 9 different degrees of cavity expansion. It is clear that increasing the degree of expansion cavity during stone column installation has a positive effect on increasing the coefficient of horizontal earth pressure. The maximum value for K at 1m from the stone column axis in this case is 1.98 correspondence to 0.45m cavity displacement and it decreases with the increase in radii from

the column centre. The figure demonstrates that the installation influence zone falls between 6 and 8 of the column diameter since the increase in K reduces to zero after that distance.
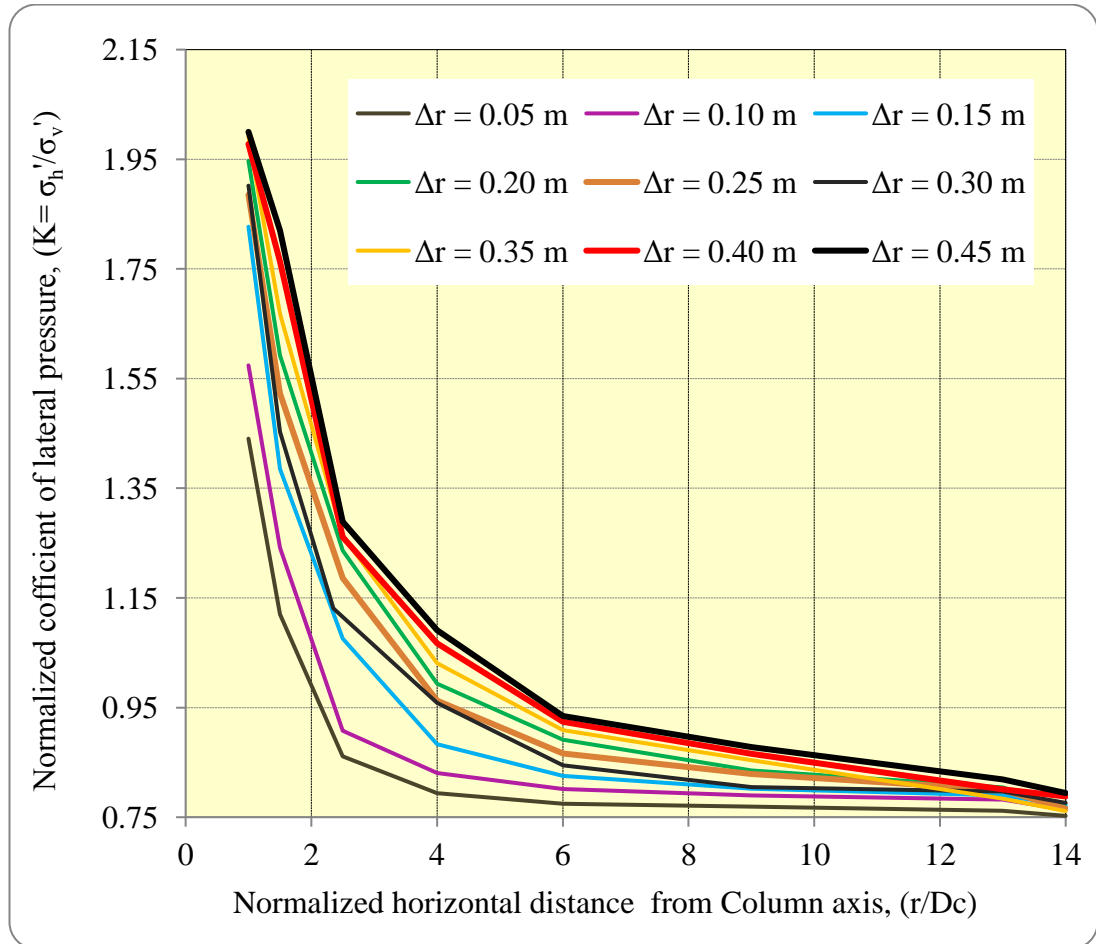
Figure 4.17 Variation of coefficient of lateral earth pressure of Bothkennar clay with distance from the column axis for different degrees of cavity expansion.

Figure 4.18 shows variation of the coefficient of lateral earth pressure expressed in terms of the at rest coefficient (K_0) with distance from the column axis. It shows that K value adjacent to the stone column increases to about 2.7 for the case of (Δ_r 0.45m) expansion cavity when it is compared with the case of full replacement stone column. Figure 4.18 demonstrates that more than 40% development in the confinement around the stone column (K) is achieved when the expansion degree increased from (Δ_r 0.05m) to (Δ_r 0.45m). This indicates the importance of taking the stone

column installation method and the applied expansion cavity in the development of the settlement behaviour of these kinds of foundation.
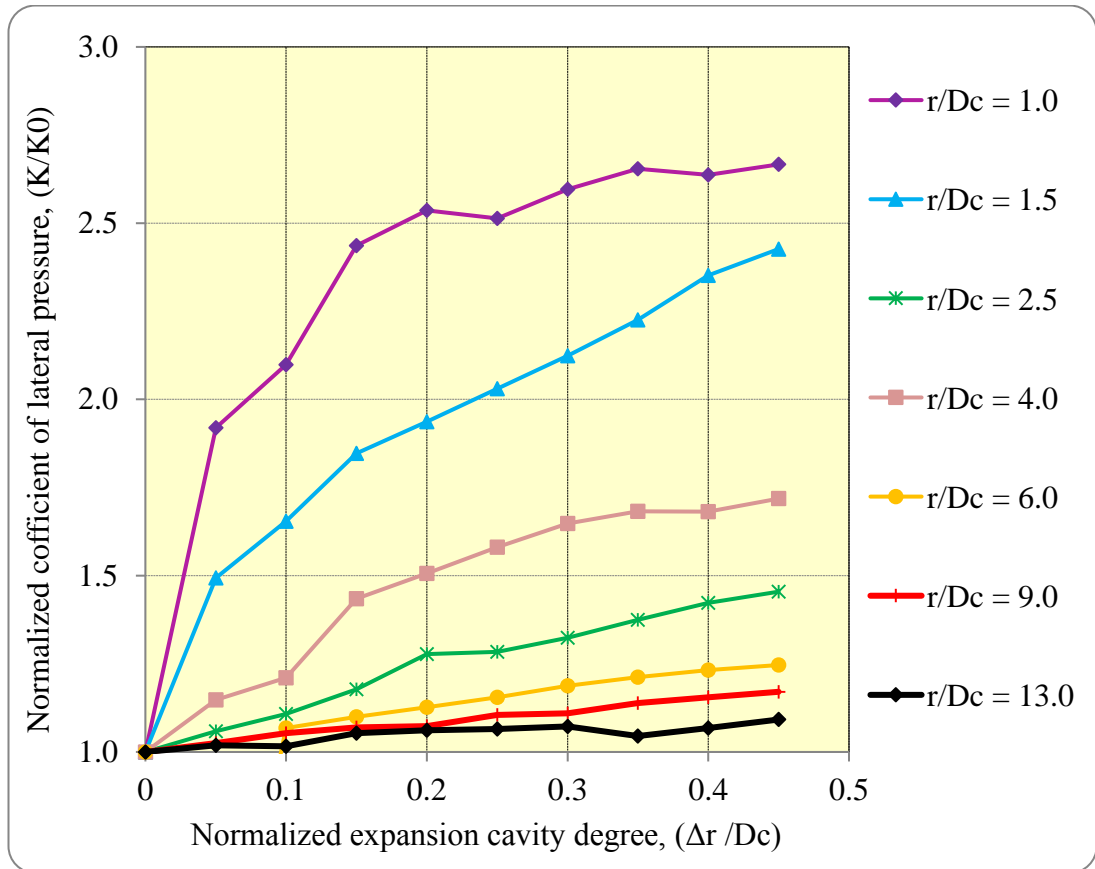
Figure 4.18 Variation of coefficient of lateral earth pressure of Bothkennar clay with distance from the column axis for different degrees of cavity expansion.

4.9.2 Evaluating the Stiffness Changes due to Stone Column Installation

Most of experimental work, field observations and numerical studies that have been carried out to predict the improvement of the characteristics due to vibro stone column installation were limited to estimate the changes in the stress state, namely the increase in the coefficient of lateral earth pressure and the attempt to take it into account in the design by considering one average value and ignoring the decrease of this coefficient with the distance from stone column (Elshazly et al.., 2007; Elshazly et al., 2008a; Castro and Sagaseta, 2009; Zahmatkesh & Choobbasti, 2010; Killeen, 2014). Although many researchers' contributions proved the increase of the soft soil stiffness

around the stone column and tried to assess this increase (Kirsh, 2006; Guetif et al., 2007), most of them neglected its changes in the design methods and calculations.

The development in knowledge and tools in how to estimate the effective stresses acting around the stone column enhances the ability to calculate the exact new stress state and stiffness development for the soft soil around the stone column due to its installation. In this axisymmetric single stone model, numerical investigation was performed to estimate the impact of stone column installation on increasing the stiffness of the soil that surrounded the columns as well as the area of the impact for the columns that were being expanded.

In this study, the adopted methodology in quantifying the soft soil stiffness increase due to stone column installation was based on Biarez et al. (1998), who suggested a power law in equation 4-1, which uses the alteration of mean effective stress to estimating the soft soil stiffness modulus increase. Biarez et al., (1998) is based on elastic perfectly plastic theory to calculate the increase of the soil stiffness with the increase of the mean normal stress level. All these were as apart of using pressuremeter to derive parameters of the tested soil. Brinkgreve and Broere (2006) also proposed that there is a direct proportional relationship between the stiffness of the soil and the mean effective stress for soft soils.

$$\frac{E}{E_0} = \left(\frac{P'}{P'_0}\right)^m \tag{4-1}$$

$$P' = \frac{(\sigma'_a + 2\sigma'_r)}{3} \tag{4-2}$$

where E and P' are Young modulus and effective mean stress respectively, the supscript " $_0$" indicates to the initial state. Exponent m expresses the dependency of the normalized modulus on the corresponding effective mean stress and represents the relationship between confining pressure and stiffness of the soil. Brinkgreve and Broere (2006) suggested a value of (m =1.0) for soft soils.

In The Hardening soil model in Plaxis 2D, which has been used to model the soft clay soil, two soil stiffness parameters are required. The first is the

secant Young's modulus E_{50} to capture the stress stiffness dependency for the case of primary loading, while the second is E_{ur} for unloading – reloading case. According to Brinkgreve and Vermeer (1998), it is recommended for normally consolidated clay to use E_{50} as a reference value of Young's modulus. In Plaxis, E_{ur} is set to 3 E_{50} by default (Brinkgreve and Broere, 2006).

As a principle, the confining pressure (mean effective stress) was developed in both soft soil and stone column material due to the expansion cavity installation of the stone column. But in this study, the concentration was mainly on the stiffness improvement in the soft soil.

Based on equation 4-1, Young modulus, which expresses the stiffness of the soil, has been predicted after calculating the new distribution of the effective mean stresses after column installation and full primary consolidation with the distance from the cavity wall of the stone column for 9 different degrees of cavity expansion. Then, they were normalized with the original value to extract the final development of the soft soil stiffness.

Figure 4.19 illustrates the stiffness modulus normalized to its initial value of the studied Bothkennar soft clay for each expansion cavity degree after 100 days of consolidation.

As can be seen in Figure 4.19, the changes of effective mean stress within the soft clay after consolidation with distance from the stone column axis. It demonstrates that the installation influence zone falls between 2.5 to 4 of the final column diameter. A dramatic increase in the soil stiffness after consolidation can be achieved when applying cavity expansion installation. Moreover, increasing the expansion degree during stone column installation has a significant effect on enhancing the stiffness of the surrounding soft soil, which reaches a peak of 1.29 times the initial soil stiffness for (Δ_r = 0.45m). These effects extend up to distance of 4 times the final diameter of the stone column D_c. However, the stiffness of the soil very close to the cavity wall is not regular and has scattered values caused by high disturbance effect adjacent to the column.
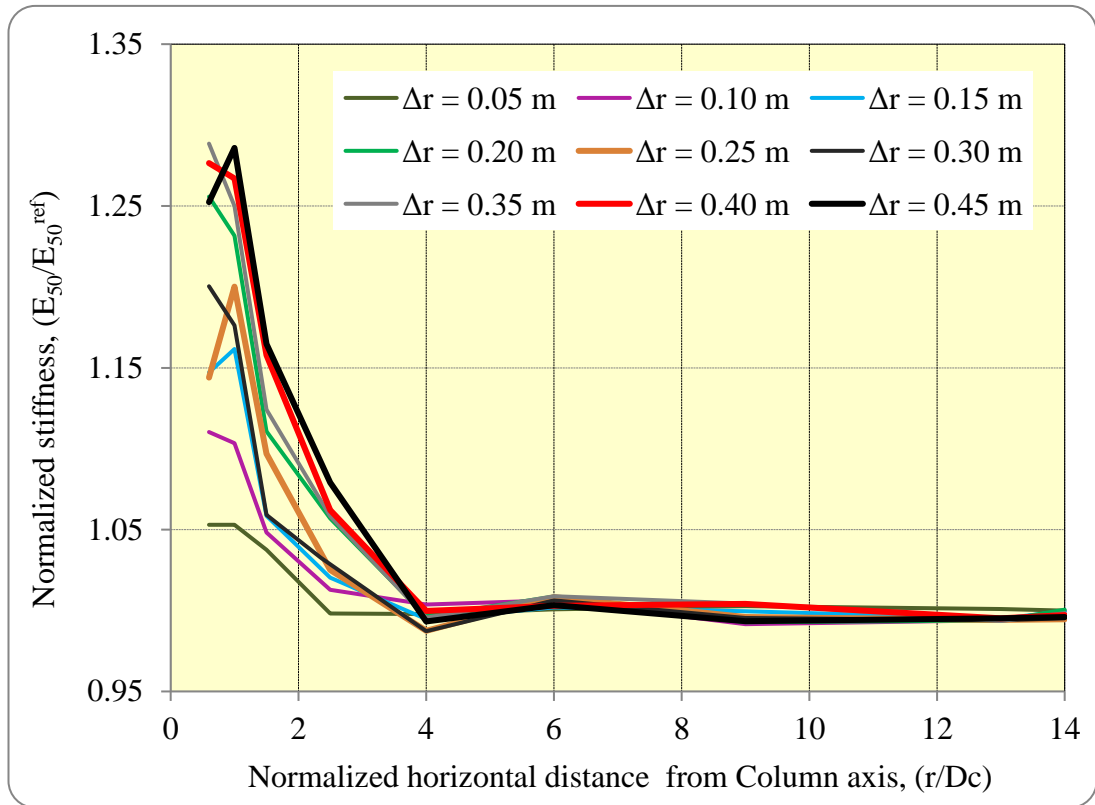
Figure 4.19 Variation of normalized stiffness of Bothkennar lower carse clay with distance from the column axis for different degrees of cavity expansions.

For clearer presentation of the effect of increasing the expansion displacement installation of the stone column, normalized enhanced stiffness modulus of soft soil for different distances from the installed stone column at the mid of lower Bothkennar clay, together with Normalized expansion cavity degree, (Δr /Dc) have been plotted in Figure 4.20. The maximum proportion of increase in the stiffness of soil is about 30%; this occurred within the radius 1of the stone column diameter, while no rise in soil stiffness after the radius of $4D_c$ has been noticed disregarding the cavity displacement degree.
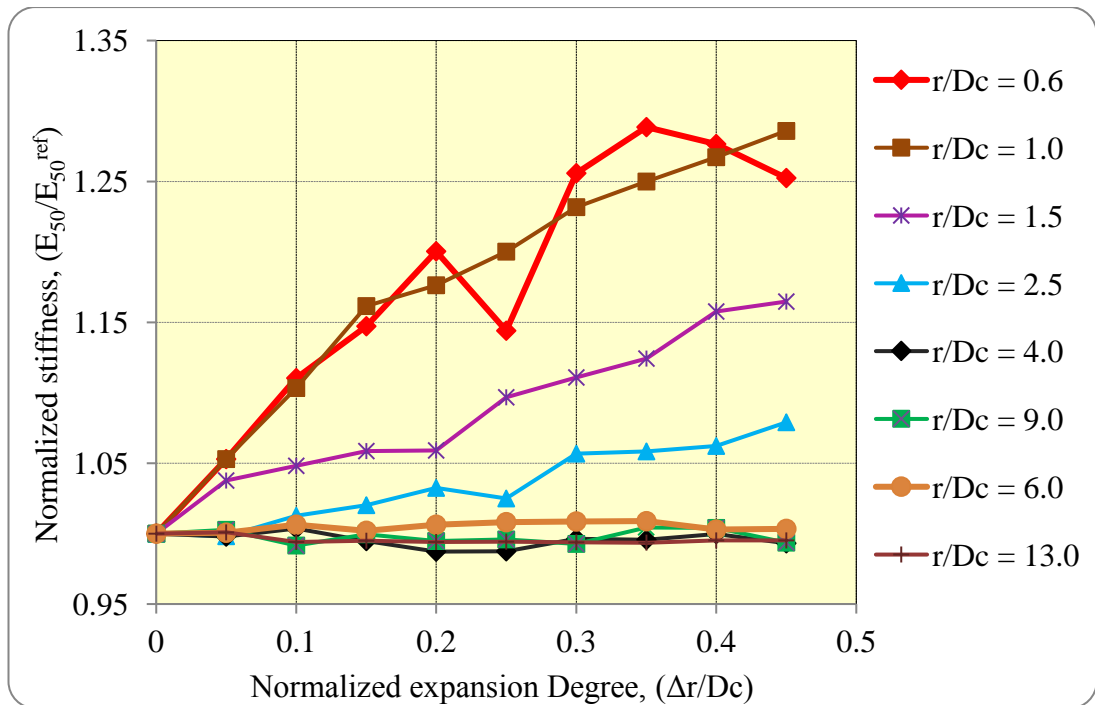
Figure 4.20 Cavity expansion degree effect on the enhanced stiffness modulus of soft soil around the stone column after primary consolidation at mid of lower Bothkennar clay.

4.10 Performance of Single Stone Column Reinforced Footing

The results above show that stiffness of the soft soil around the stone column increased, which means the stiffness of the foundation system increases. Therefore, possible to consider the increased stiffness of the soil as well as the coefficient of lateral earth pressure in the design calculations of these foundations. To meet this goal, a third stage of numerical analysis involving applying the footing load and then allowing Bothkennar soft clay to consolidate for sufficient time to get the final performance of this composite system. Two main aspects of the system performance were assessed at this stage;

- Bearing capacity improvement: A prescribed displacement was applied to get both the ultimate and the allowable bearing pressures that the reinforced soft soil can carry. This process has been repeated for a range of stone column diameters including a full replacement

stone column to compare the results with published data and predict a pressure improvement factors.

- Settlement performance: Settlement is the dominant criterion for the performance of such soft soils. The footing in this case was modelled as a thick plate that was loaded with the typical working pressure of 50 kPa, which has been selected as a design loading for Bothkennar soft clay. The same process was also repeated for all cavity installation degrees including the one of full replacement stone column to be compared later with the others' results and find the final settlement improvement factor.

4.10.1   Stress Concentration Ratio

One important criterion of the improving in stress state of the soft Bothkennar clay around the installed stone column is the stress concentration ratio between the stone column and soft soil. This ratio expresses physically the changes of stresses and stiffness within the column/soil system. These changes happen within the clay immediately after the column installation process (applying radial displacement), and after radial consolidation to the vertical drains (stone columns). It is assessed based on maintaining an equilibrium condition between the stone/clay interface during one-dimensional consolidation caused by loading.

It is clear that the stress ratio is dependent on the consolidation process and it changes with time. But in this study, more concern is directed to the effect of increasing the cavity expansion during stone column installation on this stress ratio. So, the relationship between these two terms was plotted immediately after applying the footing load and after finishing the primary consolidation. The results are illustrated in Figure 4.21. As for the first case, stress concentration ratio increases slightly when applying more expansion during stone column installation till it reaches a small peak at expansion degree of 0.25 m. Then for the higher degrees, more loading start to be carried by the soft soil around the column. An important result that supports

the previous findings about the improvement in both lateral earth pressure and the stiffness of soft soil with the increase in expansion degree, is the trend of the curve after consolidation. It shows significant improvement in the role of the soft soil to carry up to 200% load more that the case of full replacement stone column. Figure 4.21 shows significant effect of increasing cavity expansion degree of installation in enhancing the role of the soft soli around the stone column and reduce the stress concentration ratio from about 7 to less than 3. This means that soft soil stiffness has increased sufficiently to take that big share of loading from the stone column.
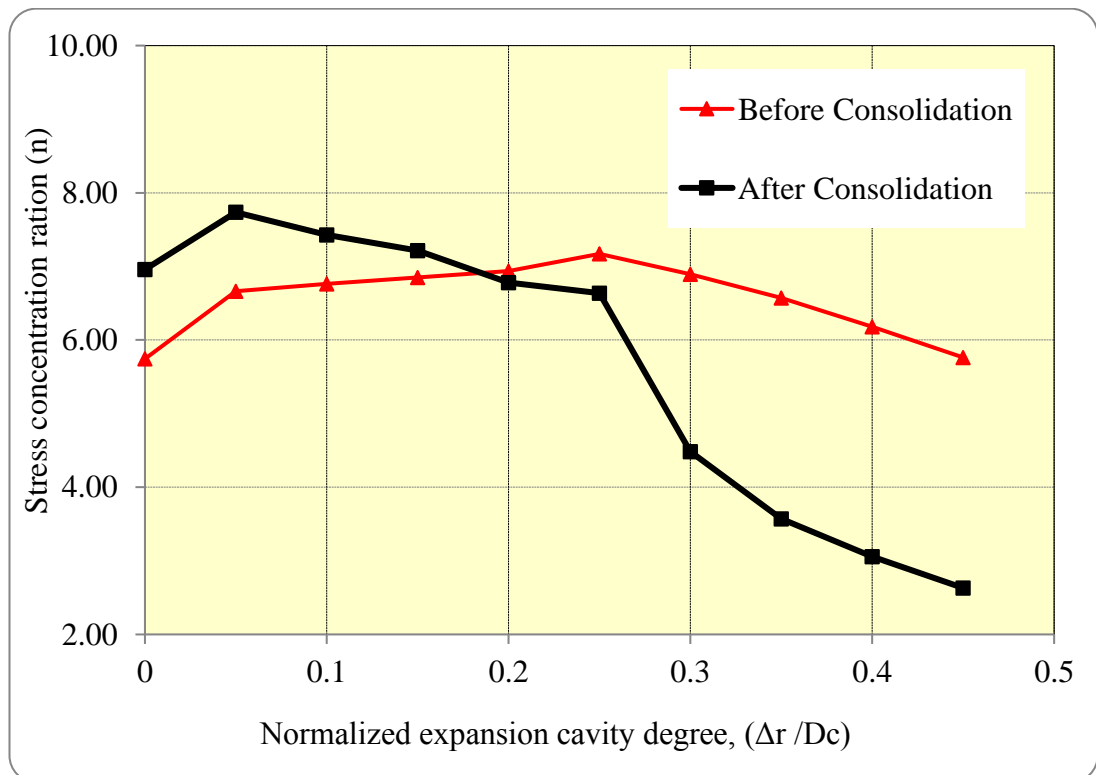
Figure 4.21 Effect of expansion degree of the installed stone column on stress concentration ratio (n).

4.10.2 Effect of Expansion Degree on Ultimate Bearing Capacity Performance

The ultimate pressure – settlement curves under the centre of the footing was generated for 6 different degrees of stone column with lateral expansions beside the non-reinforced soil ; as it is shown Figure 4.22. The

results showed that increasing the expansion during column installation has a noticeable effect on improving the bearing capacity of reinforced ground.
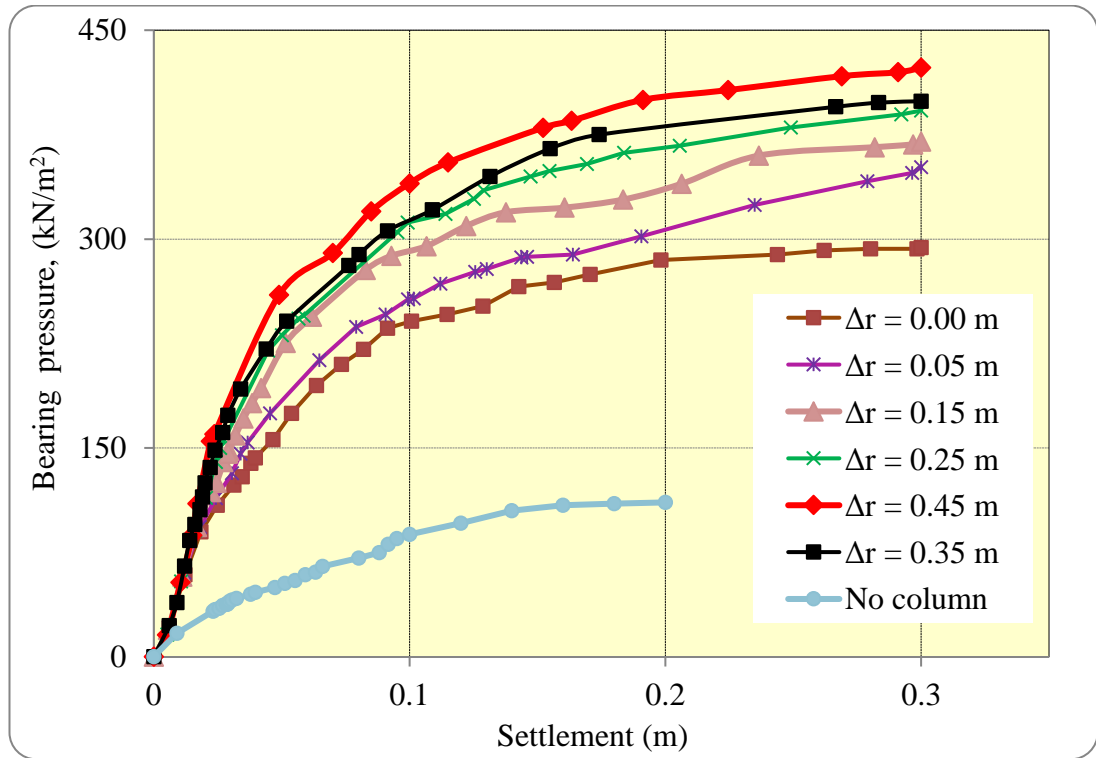
Figure 4.22 Variations of ultimate bearing pressure of a circular footing supported by single stone column for different degrees of cavity expansions.

To calculate the Bearing Pressure improvement factor (m), the ratio of the ultimate bearing pressure of the footing supported by different degrees of stone column with lateral expansions to the ultimate bearing pressure of non-reinforced Bothkennar clay, has been taken and plotted with the Normalized expansion cavity degree, (Δr /Dc) in Figure 4.23. Although, using the full replacement stone column installation increased the ultimate bearing pressure to about 3 folds, it clear that increasing the degree of cavity expansion during stone column installation, added about 1.5 folds more to the previous improvement. This demonstrates the importance of taking the changes of stiffness stress state of the reinforced soft clay into account in these kinds of composite foundations.
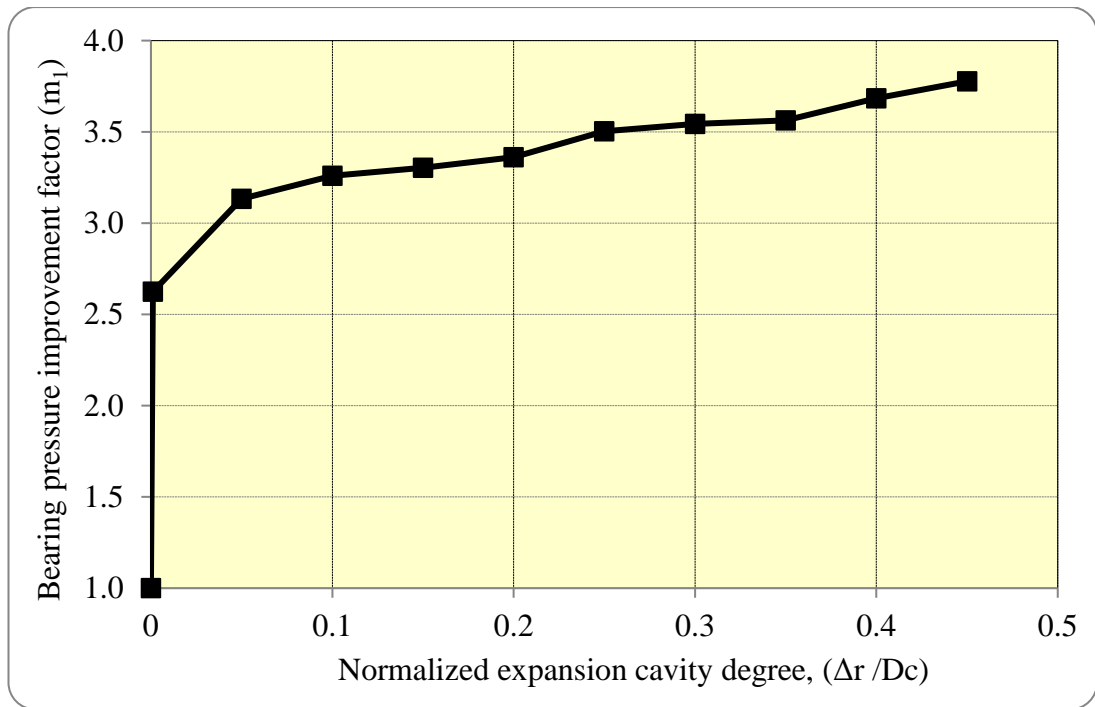
Figure 4.23 Predicted ultimate bearing capacity improvement factor (m_1) for a single reinforced footing for different degrees of expansion cavity.

For more focus on the effect of expansion cavity on ultimate bearing pressure compared with full replacement installation of stone column, Figure 4.23 shows the increase in ultimate bearing pressure for a given expansion expressed in terms of the ultimate bearing capacity of a stone column that replaces rather than displaces the soil is up to 45%. This increase is a direct resultant of stiffness and *K* development around the column due to the installation.

4.10.3 Effect of Expansion Degree on Allowable Bearing Capacity Performance

The footing in this case was modelled as a prescribed displacement and 25mm settlement was applied to get the allowable pressure that the reinforced soft soil can carry. The allowable pressure – settlement curves under the centre of the footing were also generated for 6 different degrees of stone column with lateral expansions beside the non-reinforced soil; as it is shown Figure 4.24. Similar to the ultimate bearing pressure, the results

showed that increasing the expansion during column installation has a noticeable effect on improving the bearing capacity of reinforced ground.
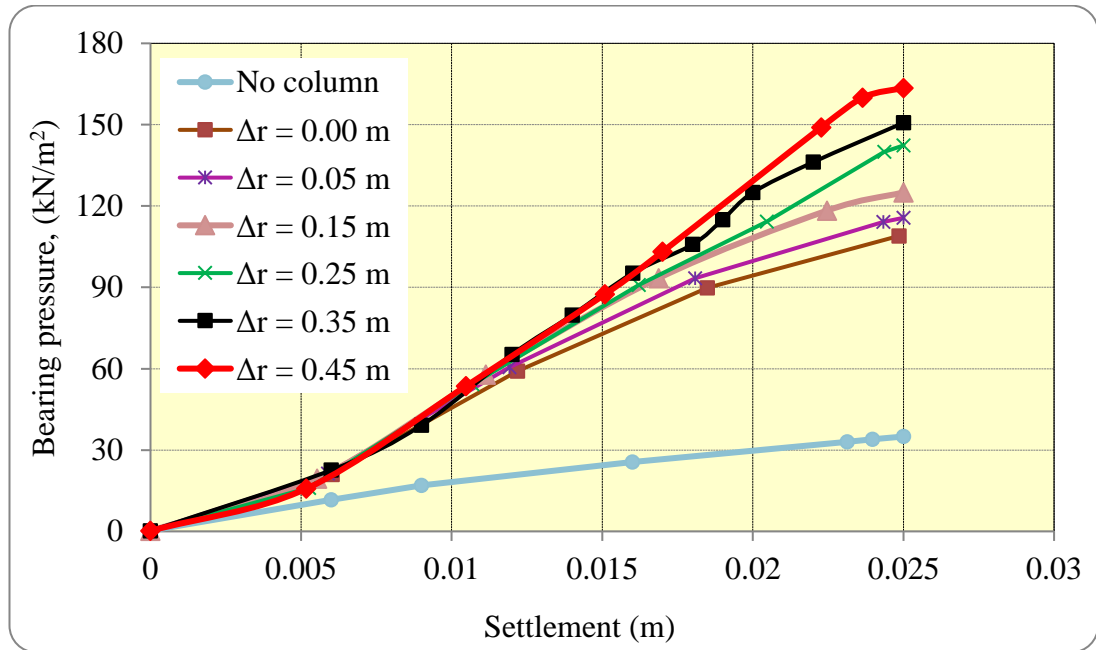
Figure 4.24 Variations of allowable bearing pressure of a circular footing supported by single stone column for different degrees of cavity expansions.

The allowable bearing pressure improvement factor (m_2), which is the ratio of the bearing pressure of the footing supported by different installation degrees of stone column to the bearing pressure of non-reinforced Bothkennar clay, was calculated and plotted with the Normalized expansion cavity degree, ($\Delta r /Dc$) in Figure 4.25. It was found that the allowable bearing pressure has a better improvement factor than the ultimate Bearing Pressure when the degree of cavity expansion increased during stone column installation. It was also found that increasing the degree of cavity expansion during stone column installation, added about 1.5 folds more to the previous improvement.
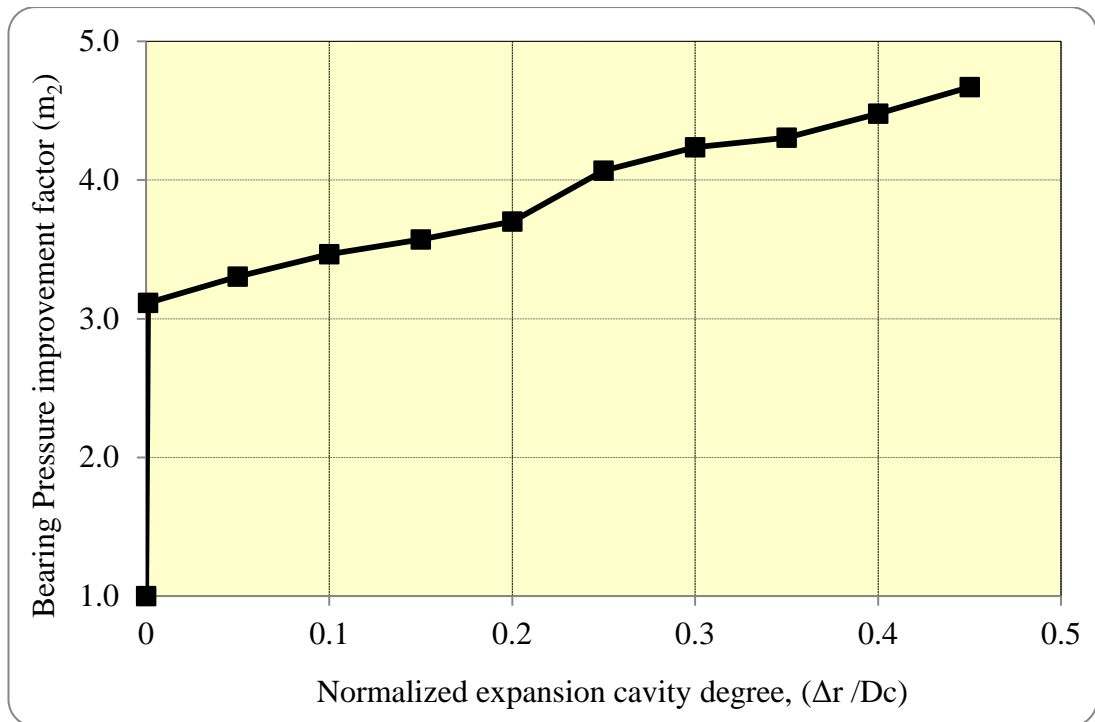
Figure 4.25 Predicted allowable bearing capacity improvement factor (m_2) for a single reinforced footing for different degrees of expansion cavity.

4.10.4 Effect of Expansion Degree on Settlement Performance

Finding the effect of expansion degree on settlement performance is very essential goal for this research as a base to start with in taking this important factor in the design procedure of stone column reinforced foundation. More concern about settlement is taken because of the high compressibility nature of the soft soils that used to treated with stone column improvement method. Consequently, the behaviour of foundations in these soils are usually governed by settlement rather than bearing capacity criteria (Priebe, 1976).

To predict the effect of increasing the cavity expansion in constructing stone column in reducing the settlement of the single 2m diameter footing resting on this column, the stress settlement relationships under the centre of the footing have been plotted in Figure 4.26. The results proved that the improvement in the stiffness and confinement of the soft soil around the

stone column due to increasing the expansion during column installation has a significant effect on reducing the settlement of reinforced ground.
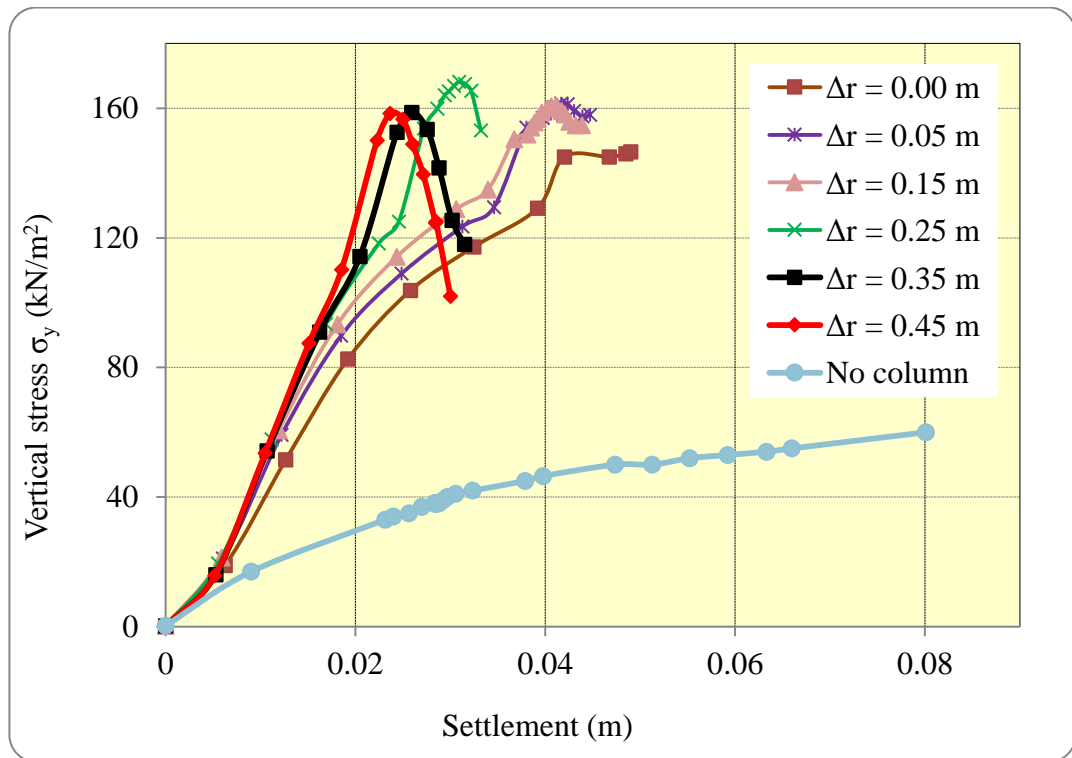
Figure 4.26 Variations of settlement behaviour of a circular footing supported by single stone column under a design loading of 50 kPa for different degrees of cavity expansions.

Another important note can be extract form Figure 4.26. As can be seen, a decrease in the vertical stress under the footing centre after installation is developing with the increase of the applied cavity during installing the stone column. which means the soft soil around the stone column has enhanced its stiffness to carry more loads and increase its share from the stress and the vertical stresses transfer gradually from stone column to the surrounding clay. This also supports that the fact about the decreasing of the stress concentration ratio, between the stone column and surrounding clay with increasing the horizontal displacement during column installation, is a direct consequence of increasing the cavity expansion used in stone column construction.

The reduction in footing settlement due to the displacement installation of the stone was evaluated with 9 different degrees of expansion. Then the

results were compared with settlement of the full replacement stone column case (Δr = 0.0m). The results showed that increasing the expansion during column installation has a very important effect on reducing the settlement of the composite foundation. Figure 4.27 Shows, increasing the applied cavity expensing degree during stone column construction to 0.45m in Bothkennar case has reduced the settlement under the footing 3 times of the non-reinforced soil settlement, with this reduction in settlement was less than 2 for the full replacement stone column.
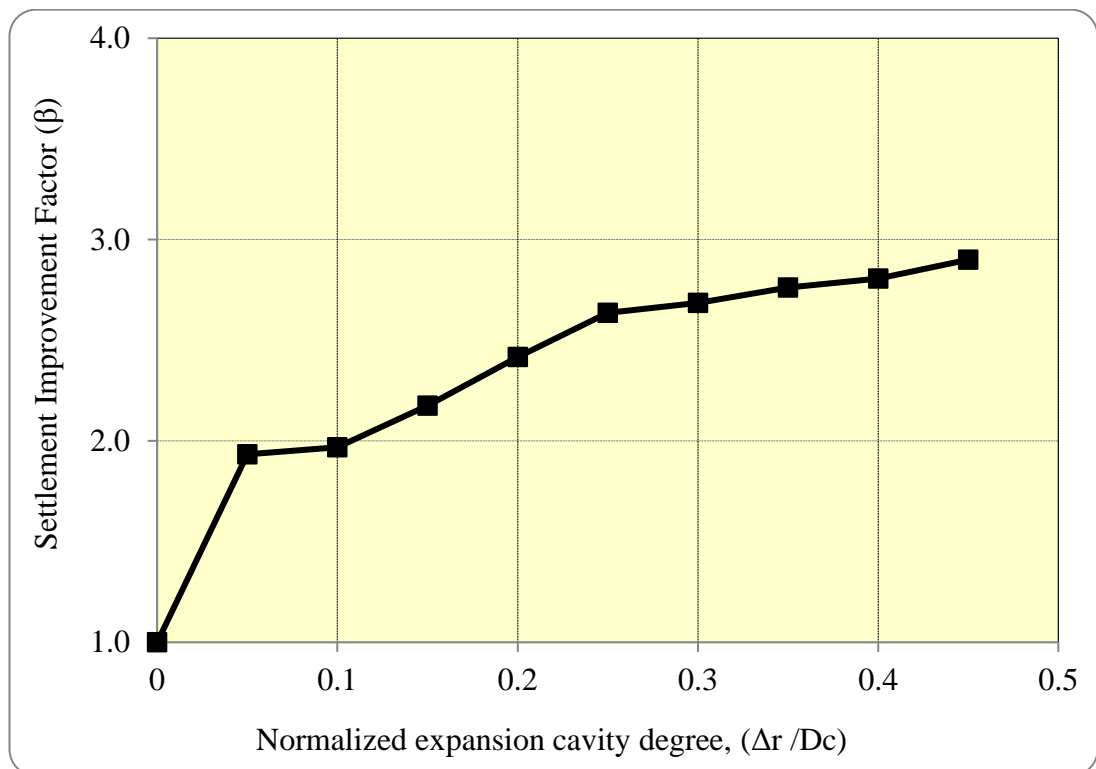
Figure 4.27 Predicted settlement improvement factor for a single reinforced footing for different degrees of expansion cavity.

By taking the comparison between the case of full replacement stone column with others involve installing stone column with gradual higher degrees of expansion cavity, Figure 4.28 shows the reduction in settlement for a given expansion expressed in terms of the settlement of a stone column that replaces rather than displaces the soil is up to 60%.
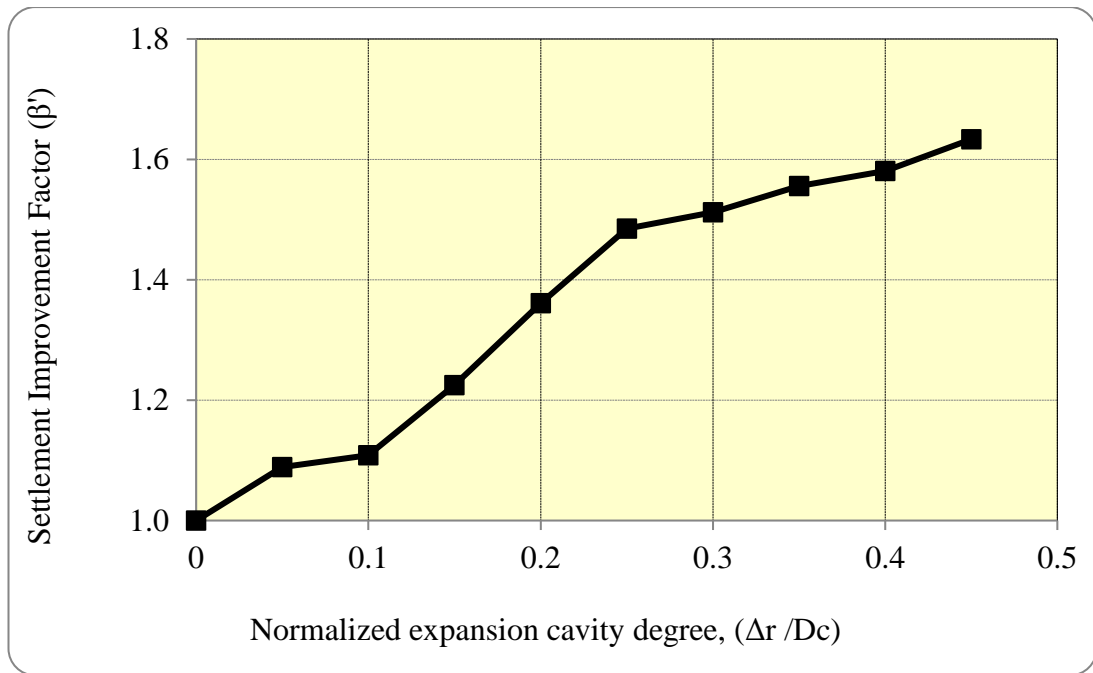
Figure 4.28 Effect of expansion degree of the installed stone column on settlement of single reinforced footing.

A series of axisymmetric numerical analysis has been carried out to study the installation effect of a single stone column in the performance single foundation. Different degrees of stone column lateral expansions were studied, and then the changes in the stress state and stiffness have been calculated. It was proved that stone column installation has a significant effect in increasing not only the coefficient of lateral earth pressure but more importantly the stiffness of the soft soil around the column. Moreover, in order to control and achieve a certain level of settlement reduction performance or bearing capacity requirement, an optimum degree of expansion cavity during stone column construction should be calculated to meet these requirements.

The case of single stone column was taken the effect of cavity expansion caused by stone column installation from only on side, while in the field the improvement comes from more than one column. It is dependent on accumulating the effect of adjacent columns base on the distance between them.

4.11 Development of Design Framework

Stone column foundation is one of the Geotechnical problems that have been extensively investigated since 1970s till now to study its behaviour and predict the performance. Many techniques (i.e; laboratory test results, field recording, unit cell concept , cavity expansion theory, homogenisation and numerical analysis methods) have been utilized for this purpose based on the available theories and tools in each stage and sometimes mixed them to get semi empirical charts. Although these different background theories, techniques and methods give a large scatter of the resulted design parameters, many previous researchers try to compare their results and validate their frameworks based on them, even for different cases and conditions. It is believed that in order to bestow the outcome of a study adequate reliability and generality, it should be applicable in different sorts of soft soils and foundation geometries. Nevertheless, there is no point of compare or try to apply some methods that prove to capture the field performance on other cases with different soil conditions or system specifications, nor to back analysis to construct a reliable mathematical or semi empirical methods, especially if it not possible to produce a real field settlement every time.

The findings of this study can be utilized to develop full understanding of the changes that encounter the soft clay soils during the installation of stone column, including the new stress distribution and excess pore water pressure in short term, and then the resultant long term stiffness and coefficient of lateral pressure parameters. Significant improvement of the soft clay soil behaviour is related to the changes of these parameters.

This research provides a comprehensive method in developing assessment of the settlement improvement factor to include a very important aspect in designing the stone column reinforced foundation beside the soft soil properties and the spacings between the stone columns. It is the effect of installation method. The research highlighted the importance of using an installation method that displaced the soft soil to construct the stone column, like the dry bottom feeding method and make sure about the reliability of the

traditional analytical and semi empirical approach that do not account for the improvement of the soil between the stone column due to the installation effect involve applying.

The results of the research revealed also the important of the stone construction quality, especially with the development of the automated rig instrumentation, that have been provided with sufficient facilities to track and monitor the consumed energy during stone column installation to make most of the positive installation effect and avoid any poor constructed or irregular diameter stone columns

The right selection of the construction method based on the soft soil properties and the energy capacity of the rig that used in the installation process can achieve an optimum, economic and successful design for these method can be selected.

Figure 4.29 illustrates a simplified numerical design framework that designed for infinite group of stone columns (which is the most common). It is based on the development in knowledge and 3D numerical tools in how to estimate the effective stresses acting around the stone column enhances the ability to calculate the exact new stress state and stiffness development for the soft soil around the stone column due to its installation.

Structure requirement

Max static settlement

Max differentiate settlement

Site characterization

Soft soil profile

$\emptyset, C, E, K, e_0, OCR$

Initial Design

- Stone column geometry and Area ratio (column diameter D_c = x m & column spacing S = y m), (column length H=z m)
- Construction method (Displacement degree $\Delta r = \delta$ m)

Calculate the improving response of soil due to single column installation.

Calculate the accumulated improving response of soil due to multi columns installation.

Find the improvement of the soil stiffness after consolidation

$E_n = E_0 * f(\delta)$

Find the new stress state of the soil after consolidation

$K_n = K_0 * f(\delta)$

New soft soil profile

E_n, K_n

Analyse → 3D numerical analysis of infinite group of stone columns using the improved soil properties

Settlement improvement factor (n) meets the structural

Yes

Proceed

No

Correct the initial design

Figure 4.29 Numerical framework that designed for infinite group of stone columns.

198

5 Chapter 6: Model Validation

5.1 Introduction

As explained by Greenberger et al. (1976, cited in Ford, 1999), model validation is a process that illustrates how much confidence exists in the behaviour of a model for a specific application and under certain conditions. The use of computers in model validation and output verification for reliability has made the process more difficult. There are many tests used for model validation; some of these are identified as more prominent than others (Ford, 1999).

- Verification test : a complete independent run of the original test is performed;
- Face validity test: this is a simple evaluation of the sensible and realistic nature of the results;
- Historical behaviour test: previously recorded results are compared to generated results by a recorded case study;
- Extreme behaviour test: the plausibility of the results of a model is checked through testing extreme conditions;
- Detailed model check test: the results components are verified through the use of more detailed models.

Using a model to replicate the historical behaviour has a high status of importance evidenced by its popularity in the field. This is also arguably one of the most convincing tests to prove that the suggested modal can represent the real behaviour in the field.

5.2 Chapter Scope

The scope of this chapter is to validate the results of the model explained in Chapter 3 and Chapter 4, which accounts for improvements of the soft soils due to different degrees of stone column with lateral expansions, using historical behaviour test by replicating a well-documented field case using

Plaxis 2D and Plaxis 3D. The results are compared with the recorded ones in the field.

5.3 Selection of the History Field Case

The field case which was selected to validate the results of the previous model was waste water treatment plant in Santa Barbara, U .S, where over 6500 stone columns were constructed using the top wet installation method. Before presenting the reasons for selecting the current history field case for validation, it is worth, mentioning that many researchers (Aboshi, 1979; (McCabe et al., 2009) tried to validate their work by comparing their experimental or numerical results with other researchers work, disregarding the studied soft soil used by the others, if it is same or different. Although they might found the same trend of settlement behaviour, it is believed that this comparison is not accurate enough to be taken for the following reasons

- The uncertainty in the construction method of stone column has a significant influence in the settlement performance, as it was found in this research. Moreover, the response of a soft soil to be enhanced in stiffness and confinement is different from one to another.
- Their many methods to predict the settlement improvement factor but each one was derived for a certain case taking many assumptions into consideration.
- The geometric specification of both the stone columns and the treated soil are totally different in most cases.
- The time at which the loading/settlement response was estimated (which is usually taken after finishing the primary consolidation), is usually related to the rate of consolidation of the soft soil. Uncertainty in estimating that time will end with measuring different settlement response.

Based on this explanation, the first reason for selecting the Santa Barbara site to validate the results of this research - about the effect of stone column installation in improving the both the confinement and stiffness of the

surrounding soft soil - is that a number of recent works have been done to study the behaviour of the stone column at this site and the settlement performance under the reinforced foundations (Mitchell and Huber, 1985b; Elsazly et al.,2006; Elsazly et al., 2007; Elsazly et al., 2008; Killeen, 2012). These researchers used numerical analysis techniques. the variation in the input soil parameters that relates to the improvement in the soft soil properties due to the stone column installation can be studied using numerical techniques.

The second reason is the nature of the site which consists of a group of soft soil layers that have different characteristics. This enables the special verity results to be analysed respecting the real soil behaviour. Thirdly, the case has been studied for three different stone column spacings used in the project , which makes it good to study the effect of this important factor on the performance of the composite system.

5.4 Field Case: Waste Water Treatment Plant in Santa Barbara, U.S.

5.4.1 Background

Santa Barbara Wastewater Treatment Plant was the first major project which involves using the stone column technique in a soft estuarine deposits in West America in 1976. Field and laboratory tests before and after stone column installation were carried out to provide the soft soil properties and plan replacement ratio that meets the requirements of the project. The design requirements for these stone column foundations were based on the requirement of site plan illustrated in Figure 5.1, where, on the building location, the bearing capacity is up to 145 kPa and settlement less than 6 mm, and less for the open areas between the buildings. The stone column technique was chosen for many reasons; firstly, the site preparation time and cost were limited to 6 months. Secondly, it was very important to avoid any damages that might be caused to the adjacent light industrial structures if the ground water table was lowered using conventional pile foundation method. Finally, the stone column technique introduced a preferable solution

for the potential liquefaction that might happen according to the seismically active records of the Santa Barbara site (Mitchell and Huber, 1985b).

5.4.2 Site Conditions

The Santa Barbara Wastewater Treatment Plant site in California, U.S., is located adjacent to the Pacific Ocean at about 2.5m above the sea level. The site stratigraphy (from top to bottom) is as the following (Mitchell and Huber, 1985b):

- 1- 3 m of Recent fill of clayey sand containing mixture of human industrial wastes like (asphalt, masonry, wood, glass, and metals)
- 5-16 m weak layered soils of estuarine deposits that increase in thickness from northeast to southwest across the site. They consists of silty and sandy to clayey and silty sand, with some local lenses of sand or gravel that may occasionally existed
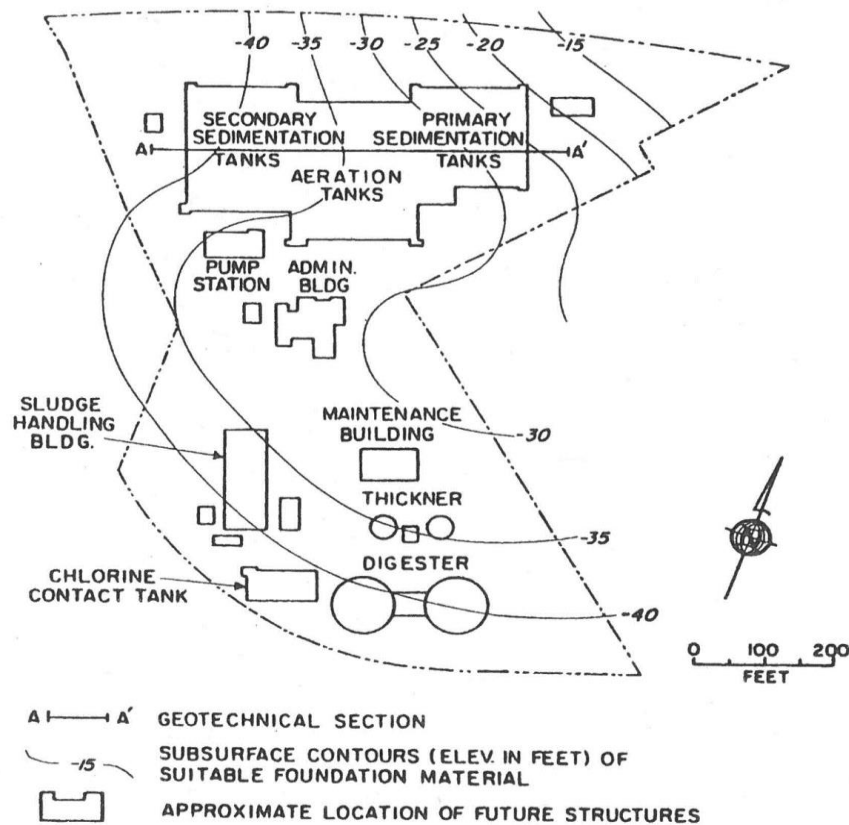

Figure 5.1 Site plan of Santa Barbara Wastewater Treatment Plant (Mitchell and Huber, 1985b).

- An old marine deposits that extended up to 600 m beneath the ground surface. They also compromise a successive of altering cohesive and cohesionless layers of clayey sand, silty sand and lesser amount of sandy clay and sandy silt.
- Ground water level is at 1.5 m below the ground surface.

Figure 5.2 shows the typical Santa Barbara Wastewater Treatment Plant site soil profile of the top 15m deposits, where the stone column method was used and tested to evaluate its performance.

Soil type	Depth (m)		Deposit	Classification
Clayey sand	1·2			Fill
Sandy silt	0·9	GW		Cohesionless
Clayey silt	0·9			Cohesive
Sandy silt	1·2			Cohesionless
Silty clay	1·2			Cohesive
Silty sand	1·2		Estuarine deposit	Cohesionless
Sandy silt	1·2			Cohesive
Silty sand & Clayey sand	2·4			Cohesionless
Sandy clay	1·8			Cohesive
Silty sand	0·9			Cohesionless
Sandy clay	1·2			Cohesive
Silty sand & Clayey sand	1·8		Marine deposit	Cohesionless
Clayey silt	0·9			Cohesive
Clayey sand	2·4			Cohesionless

Figure 5.2 Soil stratigraphy and engineering classification for Santa Barbara waste water treatment plant (after Mitchell and Huber, 1985b).

5.4.3 Stone Column Design and Construction

Over 6500 stone columns were constructed using the top wet installation method. This method is usually used for soft and cohesive soils with a high ground water table. A current of water is jetted from the nose of the vibrator to aid the penetration to the soft soil making (0.50-0.75 m) diameter holes and this water current keeps the side walls of the borehole stable. When the

vibrator reaches the desired depth, well graded backfill of (12-100 mm) gravel was introduced into the hole through the annulus between the borehole and the vibrator and the poker is moved up and down in the borehole to compact the stone column material and push it against the walls of the borehole. The final diameter of the stone columns varied between (0.81- 1.22 m) (Mitchell and Huber, 1985b). Based on the building location, loading and site plan, three main different stone column spacings were adopted for in construction with square and rectangle patterns. The densest pattern consisted of (1.2m X 1.5m) designed for heaviest load of (145 kPa), then a (1.75 X 1.75 m) pattern was used for the medium loads and (2.10 X 2.10 m) for the open areas between the buildings which were designed to carry a load of about (60 kPa).

The stone columns length ranged between (9 – 15 m) supporting the whole length of the soft estuarine deposits, and they had at least 0.3 m penetration in the firm older marine deposits (Mitchell and Huber, 1985b).

5.4.4 Development of Soft Soil Parameters

According to Mitchell and Huber (1985b) the soft soil properties were obtained by taking undisturbed samples of the soft soils between the stone columns after installation. The samples were taken from different depths to cover all various layers using exploratory borings. Despite the variation in properties of both the estuarine and marine deposits, Mitchell and Huber (1985) classified them into four types of soils estuarine cohesive, estuarine cohesionless, marine cohesive and marine cohesionless. The cohesive or cohesionless discription was based on the predominant content of the soil clay or sand respectively. As a result of this classification, cohesionless soils were assumed to be free draining soil and drained triaxial tests were used to obtain their short term properties. Conversely the cohesive soils were considered not to be completely free drained and undrained traxial test was used to establish long term behaviour.

As was found after discussing the features of the available soil models in Plaxis in section 3.6.6, that the Hardening Soil model as formulated by Plaxis is considered the most appropriate model for simulating the relevant features of the soft soil behaviour, originating from a combination of different soil types subjected to large deformations. Its ability to take into account the stress dependency of stiffness moduli and accounting for the shear and volumetric hardening makes it the most realistic model to capture the features soft soil combination. So, the Hardening Soil model was selected to represent the behaviour of both estuarine and marine soils in this study.

Most of the properties and parameters that were used in the Hardening Soil model to represent all the four classes of soft soils can be obtained directly by averaging the results of the triaxial tests for each layer, as is presented in Table 5.1. Some other parameters like K_0 lateral earth pressure at rest, was estimated by Mitchell and Huber (1985b) to be 0.5 for all soil types. The permeability parameters were considered important by Elshazly et al. (2006) in simulation stone column to analyse the consolidation and settlement rates. They stated that due to using the wet top installation method in constructing the stone columns, an infiltration of the fine particles of soil (silt and clay) into the granular material of the stone column, and also the high percentage of fine particles in the cohesion less soil layers does reduce the permeability significantly. Consequently, adopting high permeability coefficients will overestimate the consolidation and settlement rate. Elshazly et al. (2006) assumed the horizontal permeability coefficient to be double the vertical one based on a suggestion by Lambe and Whitman, (1979). Three dimensional stiffness parameters for Hardening Soil model (E_{50}^{ref}, E_{oed}^{ref}, E_{ur}^{ref}) were estimated by Elshazly et al. (2008a), where E_{50}^{ref} was taken equal to the reference stiffness modulus extracted from experimental tests, while E_{oed}^{ref}, E_{ur}^{ref} were believed not to affect the settlement of the field load tests because of the monotonic nature of the loading problem. Therefore, Elshazly et al. (2008a) adopted $E_{ur}^{ref} = 5E_{50}^{ref}$ and $E_{oed}^{ref} = E_{50}^{ref}$ as a reasonable value for Hardening Soil model.

A summary of the adopted material parameters for both cohesive and cohesionless soils are presented in Table 5.1.

Table 5.1 Soil parameters adopted for finite element analysis.

Soil Parameter	Stone Column	Estuarine cohesive	Estuarine cohesionless	Marine cohesive	Marine cohesionless
Material model	Hardening Soil model	Hardening Soil model	Hardening Soil model	Hardening Soil model	Hardening Soil model
Type of material behaviour	Drained	Undrained	Drained	Undrained	Drained
Dry unit weight (γ) (kN/m³)	18.6	15	15	17	17
Saturated unit weight (γ_{sat}) (kN/m³)	21.6	19	19	20	20
Permeability (K_h) m/day	2×10^{-5}	2×10^{-8}	2×10^{-6}	2×10^{-8}	2×10^{-6}
Permeability (K_v) m/day	1×10^{-5}	1×10^{-8}	1×10^{-6}	1×10^{-8}	1×10^{-6}
Failure ratio R_f	0.86	0.87	0.69	0.84	0.67
Poisson's ratio (v)	0.2	0.2	0.2	0.2	0.2
Cohesion (C') (kN/m²)	0	0	0	0	0
Friction angle (Φ) (º)	41	34	38	34	37
Dilatancy angle (Ψ) (º)	0	0	0	0	-
Initial voids ratio, (e_0)	0.5	0.5	0.5	0.5	0.5
Reference pressure, p^{ref} (kN/m²)	100	100	100	100	100
Lateral earth coefficient K_0	0.5	0.5	0.5	0.5	0.5
m	0.65	0.69	0.65	0.90	0.59
E_{50}^{ref} (kN/m²)	29200	8500	17000	8700	12600
E_{oed}^{ref} (kN/m²)	29200	8500	17000	8700	12600
E_{ur}^{ref} (kN/m²)	146000	42500	85000	43500	63000

An angular to rounded gravel, which was brought from the alluvial valley of Santa Ynez and Ventura Rivers and consisted of about 85% gravel and 15% sand, was used for stone column material (Mitchell and Huber, 1985). Based

on the available field data, the average stone column diameter was 1.06m. The adopted physical and mechanical properties of this material was obtained from results of a group of consolidated drained triaxial compression tests carried out on reconstituted gravel samples. Mitchell and Huber (1985) averaged these results and derived the required parameters for the Hardening Soil model. A summary of these parameters is presented in Table 5.1.

5.4.5 Field Load Test Description and Footing Modelling

28 field loading tests were performed to investigate the load-displacement behaviour under a group of different sizes of circular rigid footings which can be rounded to three different diameters 1.0m, 2.0m and 2.2m, that corresponded to the three studied cases of stone column inter spacing; (1.2×1.5m), (1.75×1.75m) and (2.1×2.1m). The load tests were performed according to the requirements of ASTM D1194-66, except for the steel loading plate, which was replaced with a circular concrete footing of 1.2m deep. The loading procedure was based on applying 45kN increments until the settlement rate was less than 0.25mm/h. Mitchell and Huber (1985) returned this selection of incremental to shorten the required time for each stage of the test. The test continued till reaching the maximum load of 350-400 kN. After that, the load was maintained 6 hours after reaching the settlement rate of 0.25mm/h to finish.

In order to calibrate the effect on stone column installation and then accumulate this effect from adjacent columns, an important factor in this study, which was not taken into account effectively in previous research (Mitchell and Huber, 1985; Elshazly et al., 2006; Elshazly et al., 2008a; Killeen, 2012), was the time between stone construction and the loading test. This time varies from one test to another, but in the current numerical analysis an average value of 18 days was suggested based on the available load tests data (Mitchell and Huber,1985b).

Figure 5.3 illustrates the load – settlement curves that obtained of loading tests after stone columns installation for the three columns patterns densities mentioned above.
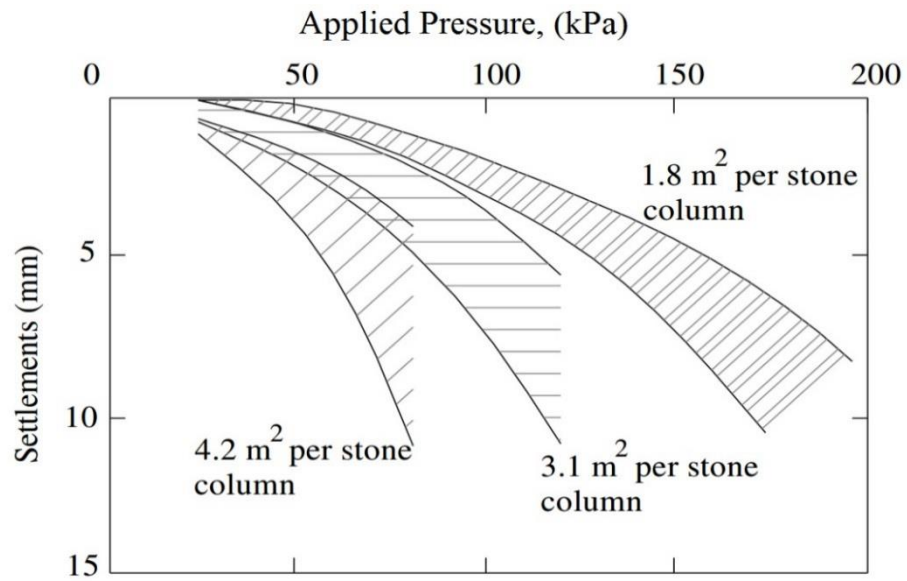
Figure 5.3 Ranges of load-settlement curves for different stone column patterns. (Elshazly et al., 2008a).

The footing and the top surface fill were modelled as elastic- -perfectly plastic material. Typical parameters values for both materials are shown in Table 5.2. Footing thickness was taken to be 1.2m, which was rigid enough to cause both the stone column and soft clay to settle (Mitchell and Huber,1985; Elshazly et al., 2008a).

Table 5.2 Material properties of footing.

Material	Footing (concrete)	Fill
Material type	Elastic-perfectly plastic	Elastic-perfectly plastic
Behaviour	Non porous	kN/m
Dry unit weight (γ) (kN/m³)	25	16
Saturated unit weight (γ_{sat}) (kN/m³)	-	19
Cohesion (C') (kN/m²)	4000	0
Friction angle (Φ') (º)	40	30
Poisson's ratio (v)	0.15	0.33
E (kN/m²)	2×10^{7}	10000
Permeability (K_h) m/day	0	2×10^{-6}
Permeability (K_v) m/day	0	1×10^{-6}

To fulfil the scope of this chapter in validating the results of the previous model, three analyses had to be carried out;

- **First step:** To model the installation of single stone column within the estuarine soft soil, then study the alteration in both stress state and stiffness after installation and consolidation within each of the different cohesive and cohesionless layers and quantify the improvements of these soils due to different degrees of stone column lateral expansions.

- **Second step:** To simulate the installation of another stone column adjacent to the first one, then assess the accumulative improvement effect of stiffness and confinement from two sides. As was the real field case.

- **Third step:** To use Plaxis 3D finite element code to incorporate the resulted changes in stresses and stiffness that proved in first step and accumulated in the second step (between two stone columns). Then, simulate the case of Santa Barbara stone column group and compare the results with field records. Using Plaxis 3D helped to avoid using the homogenization methods and geometrical conversion of the stone column reinforced system.

5.5 Single Stone Column Installation Effect

As was agreed in section 3.5 and proved by MeCabe et al. (2008), Plaxis 3D is unable to predict the undrained cavity expansion and it has many limitations in terms of modelling large strains imposed by installation of the stone columns. Plaxis 2D were used in this step of validation to estimate the improvement in both coefficient of lateral earth pressure and stiffness modulus for the different estuarine soil layers due to the installation of the stone column (axisymmetric case).

5.5.1 Numerical Model Development and Specifications

To build and develop a numerical model for the case of installing single stone column, an axisymmetric model with realistic boundary conditions including restraints, ground water table, applied loads, columns installation methods were adopted. Then a sensitivity study was carried out to decide the final dimensions and appropriate finite elements mesh coarseness of model. All these steps and some assumptions related to the construction process of the stone column installation can be summarized as the following;

1. The default general fixities were automatically applied to the boundaries of the studied model, where all nodes of the model vertical sides were fixed in X-direction ($U_x = 0$) and free in Y-direction, to represent the infinite extension of the soil body mass in x-direction, while the bottom boundary which represented the deep soil was constrained in Y- directions ($U_y = 0$) to allow the application of radial cavity expansion. The ground surface has no fixities in any direction.

2. The ground water level was at (-1.5m) under the soil surface. The water was allowed to flow from the clay to the stone column drain during consolidation. No drainage was allowed from the boundary of the model.

3. As the aim of this first step of validation was to quantify the improvement in stiffness and lateral pressure of the enhanced area around the stone column, and no vertical loading at this stage was applied. So, in this model, only the estuarine cohesive and cohesionless layers were simulated as the stone columns ended at top of the marine layers and there was no installation effect beyond the estuarine deposits.

4. In order to have accurate results for the analysis using Plaxis 2D code and make these results dependant only on soil properties and geotechnical problem conditions, a group of important analysis for the features and conditions like the mesh density and the distance of the boundaries were investigated to avoid any reaction on the model

210

results. The mesh geometry and boundary positions were investigated to assess their effect on the results of the analysis. A sensitivity analysis was carried out by adopting the same methodology in section 3.6.11on the boundaries to ensure that their location had little effect on the results. It was found, based on the result of the lateral displacement and radial stress after applying the maximum cavity expansion, that it is enough to make the side boundary about 13 m. to avoid any reflection on the accuracy of finite element model of this boundary. Therefore, it was conservatively chosen at 15m distance. The finite element mesh was based on 6-node or 15-node triangular elements, global coarseness was taken to be fine and the local fineness factor should be at least 0.5 to have sufficient accurate analysis. Final geometric dimensions and finite element mesh for this model are shown in Figure 5.4.
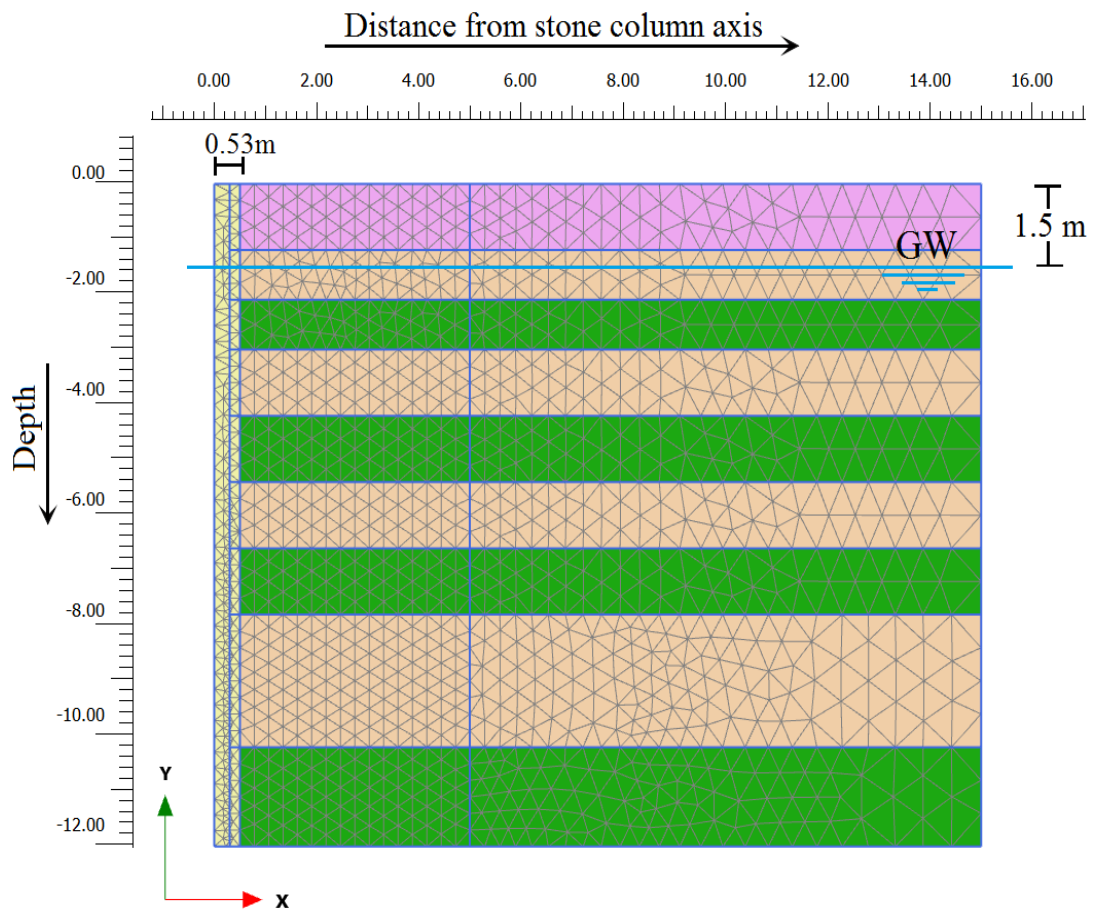
Figure 5.4 Model geometry and finite element mesh.

5. The development of stiffness and stress state of the soft soil around the stone column after installation was investigated in mid-depth of each cohesionless and cohesive estuarine layers.

6. Based on the discussion in section 4.4, no column–soil interface was considered between the soft soil and the stone column material.

7. As mentioned in Section 5.4.2 about the site stratigraphy, the top layer of the Santa Barbara site is a mixture fill of clayey sand human industrial wastes like (asphalt, masonry, wood, glass, and metals) (Mitchell and Huber, 1985b). In addition to that, foundations level was at the bottom of this layer. So, the changes within this layer, due to stone column installation, was not taken into account in this studying.

5.5.2 Stone Column Installation Modelling

The simulation method that was adopted in modelling the case in stone column installation in Santa Barbara site is the same as that used in Chapter 4, Section 4.5 by applying cavity expansion based on the short period of stone column installation to take into account the changes in the soil stress state and the improvement in the soil stiffness, as is shown in Figure 5.5.
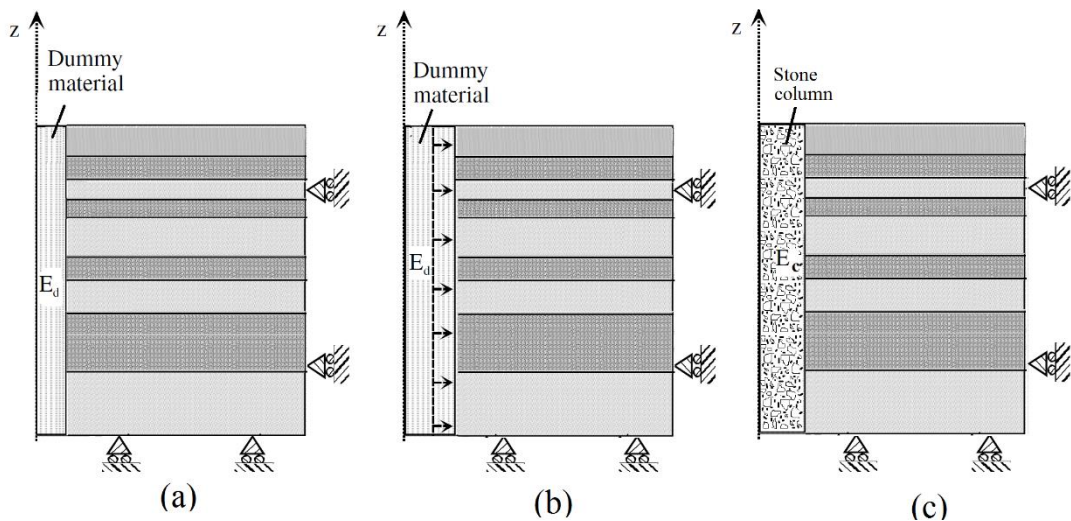
Figure 5.5 Principle of stone column expansion using the dummy material and modelling phases.

The construction method used to for the stone columns in this history case was the top wet installation, where the vibrator penetrates the soft soil

making (0.50-0.75 m) diameter holes in the soft soil. This finite radius (r_0) was used to start with as an initial one that expressed the cylindrical hole made by the poker. When the vibrator reaches the desired depth, gravel was introduced into the hole and it was compacted to form the stone columns of final diameters that vary from (0.81- 1.22 m) (Mitchell and Huber, 1985b). Based on the difference between the initial vibrator holes and final stone column diameters, the average maximum cavity expansion was applied due to the vibration process and compaction accompanied to the construction of the stone column was about 0.25m.

For the right comparison of the settlement performance in the third step, the final stone column diameter in this study is fixed at (d_0 + 2Δr = Dc =1.06 m). So, in order to meet 5 different degrees of applied expansion, the initial stone column diameter r_0 was changed according to the applied cavity expansions.

A dummy material was adopted in defining this initial stage as a first phase, as is shown in Figure 5.5 (a). It was considered a purely elastic material with a low stiffness in order to deform when it is subjected to radial displacement (vibro compaction of stone column material) until the radial expansion reaches the stone column radius (r_c). Then, a prescribed displacement was applied to express the radial expansion (Δr) starting from initial radius(r_0), as is illustrated in Figure 5.5 (b). Five different lateral expansion values were applied (Δr = 0.05, 0.10, 0.15, 0.20 and 0.25m). The "updated mesh" option was used in the analysis of the effect of column installation to account for the required update of soil stiffness matrix. Figure 5.6 illustrate the terms (r_0, r_c, r and Δr) in this case.

The dummy material was then replaced by stone column material in the third Phase, which is shown in Figure 5.5 (c). That is to give the real behaviour of interaction between the soft soil and the stone column in all stages of construction and loading and to represent the actual permeability of this material during consolidation.
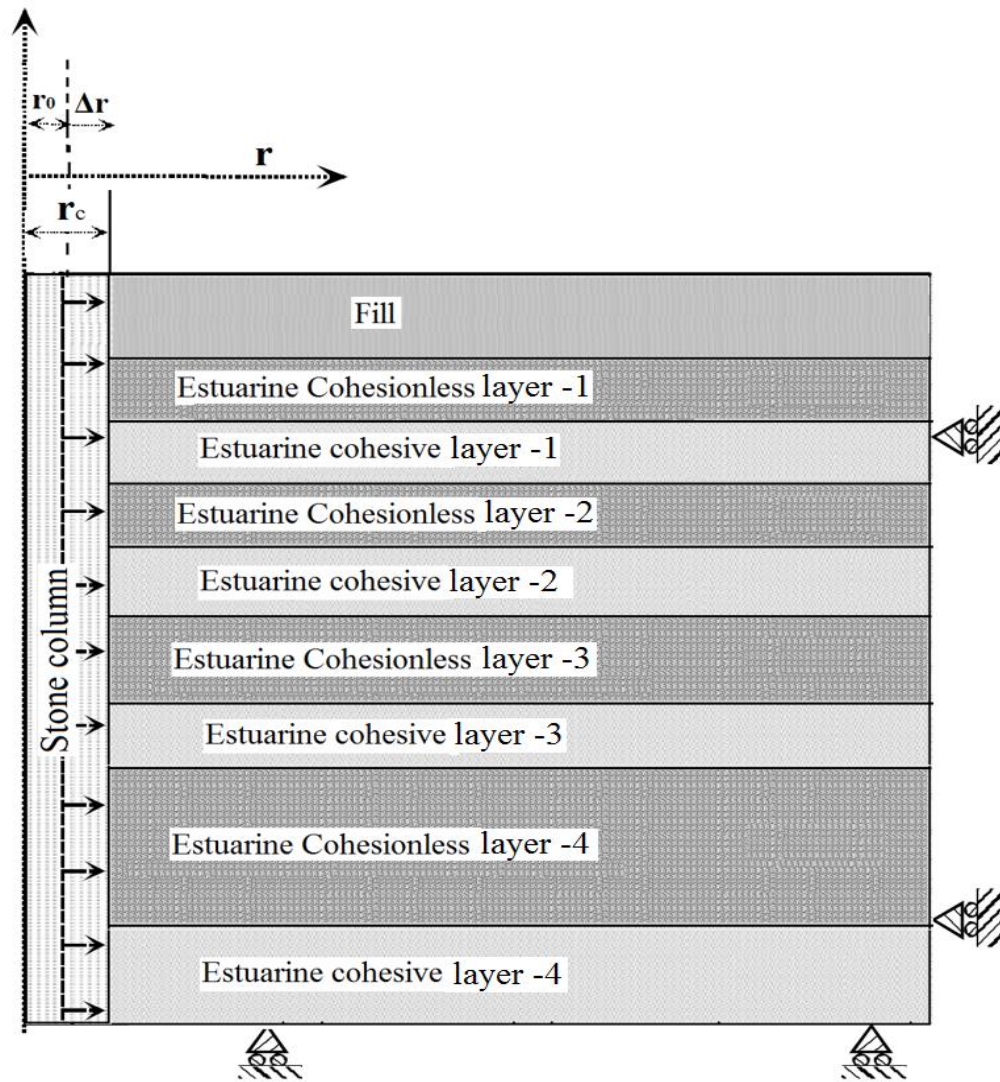
Figure 5.6 illustration of the terms (r_0, r_c, r and Δr).

Consolidation analysis was adopted in this phase allowing the excess pore water pressure to dissipate. This stage is very important because by the end of it, post- installation properties of the soft clay soil could be captured. It was mainly based on permeability specifications for both estuarine soil deposits and the allowable time for consolidation to the new stone columns drains. Based on Mitchell and Huber (1985b) classification the estuarine cohesive soil was assumed undrained, while estuarine cohesionless soil was assumed to be free draining soil.

Time between installation and loading was not taken into account effectively in previous research (Mitchell and Huber,1985; Elshazly et al., 2006;

Elshazly et al., 2008a; Killeen, 2012). This time varied from one test to another, but in the current numerical analysis an average value of 18 days was suggested based on the available load test data in order to compare the results of the installation process.

5.5.3 Nodes & Stress Points

The finite element method generates results at the specific locations of the nodes and the stress points. Due to the existence of 8 different deposits of estuarine soft soil, a group of nodes and stress points were selected at mid depth of each different estuarine deposits on the finite element mesh. In Plaxis, it is not possible to select more than 10 points in each run. So, for this reason, the numerical analysis runs were repeated to obtain the effect of the installation in the soil layers.

5.5.4 Results due to Single Stone Column Installation Effects

Changes that encounter the saturated soft soil after applying the expansion cavity caused by stone column installation are different from one layer to another based on the physical and mechanical properties of the soil, i.e., drainage conditions (cohesionless or cohesive) and the depth of the layer. To quantify these changes in both of the cohesionless and cohesive estuarine deposits, soil profiles have been numbered from top to bottom as illustrated in Figure 5.6.

The main concentration in this part of analysis was to estimate the improvement in the soil properties just before applying the loading, and then to use them in the comparison of the results of analysing 3D infinite stone column group in Santa Barbara soft soil with the loading-settlement field records.

Short term changes that encountered the estuarine soft soil immediately after stone column installation are similar to those presented in Chapter 4,

Section 4.8. Those changes are not permanent and are summarized as follows:

- The applied prescribed displacement along the stone column to express its installation process was directly absorbed by the soil particles around the stone column. The displacement effect reduced through the soft soil with the distance from the column. There was a direct influence of increasing the applied expansion degree in increasing the resultant internal displacement within the clay and the affected distance by this displacement. It was noted that estuarine cohesionless deposits tended to respond to the degree of expansion more than cohesive deposits.

- Immediate increase in both pore water pressure and total horizontal stress happens as a response to stone column installation, especially in the estuarine cohesive deposits which were simulated as an undrained material. Then, dissipation occurred afterwards with a faster rate due to the existence of the estuarine cohesionless deposits as a drained material, that alternate with cohesive deposits with the depth. Although increasing expansion during the installation of stone column has a significant influence in generating higher excess pore pressure and increasing the horizontal stress, it has very limited effect on the required dissipation time, which was found to be less than one day to reduce the excess pore pressure close to its original value before the stone column installation.

- Another clear immediate response is the high increase in horizontal stresses especially close to stone column proportional to the cavity installation degree of the stone column. Then, it relaxed with the dissipation of the excess pore pressure to develop effective horizontal stress as a permanent alteration within the soil.

An equilibrium state is reached within the zone of influence caused by the stone column installation after finishing the dissipation of the excess pore pressure, resulting in a new distribution of stresses within the soft saturated soil. The main feature of this new stress distribution is the increase in the

216

effective stresses of the enhanced zone. Consequently, soil stiffness and lateral confinement around the stone column increase.

The main task of this stage of validation was to quantify the permanent improvement in both stress state and stiffness within the soft soil around the stone column with the distance from it due to the column installation, and then to compare the results for different degrees of cavity expansion applied during this stone column installation.

5.5.4.1 Evaluating the Coefficient of Lateral Pressure due to Single Stone Column Installation

The lateral earth pressure coefficient (K) expresses the new final distribution of the effective horizontal stresses after consolidation. It is the parameter that indicates the increase in lateral support for the installed stone column; It also represents the increase in stiffness since that is dependent on the effective stress

By taking the normalized effective radial stress to effective vertical stress at mid-point of each soil layer and with the distance from the column axis, the changes in the coefficient of the lateral earth pressure (K) in both vertical and radial directions have been estimated. Figure 5.7 shows variation of the coefficient of lateral earth pressure (K) with distance from the column axis for 5 different degrees of cavity expansion. Each of these figures represents one of the estuarine deposits. For all of these layers, it is clear that increasing the degree of expansion cavity during stone column installation has a significant effect on increasing the coefficient of horizontal earth pressure (K). Some irregular random values of (K) were encountered very close to the stone column wall and after that, the trend of (K) curve is the same as the distance from the column for all deposits till they plateau close to the initial value at rest (K_0). The zone of influence after installation falls between 6 and 7 of the final column diameter (D_c), as can be seen in all of the eight figures. The maximum value for (K) was about (4.0) at 0.75m from the stone column axis in estruarine cohesionless layer-4 correspondence to 0.25m cavity displacement. A noticeable difference between the response of

the estuarine cohesionless deposits and cohesive ones when compare their (K) curves in Figure 5.7. Cohesionless deposits developed higher lateral pressure coefficient at average (K=3.3) compared to average (K=2.95) for the cohesive deposits. This demonstrates that soil has a different response to the expansion displacement of the stone column, based on its composition and properties.

(Estruarine cohesionless layer-1)
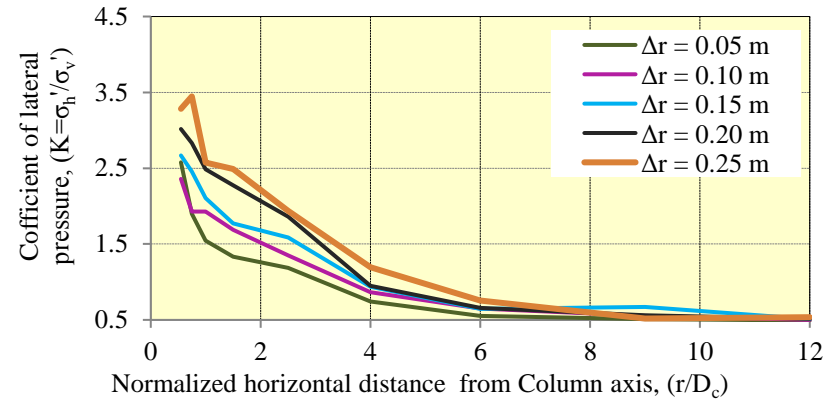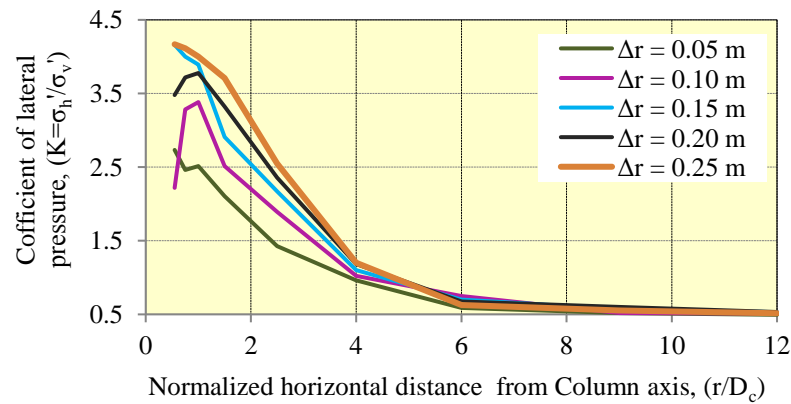
(Estuarine cohesive layer-1)

(Estruarine cohesionless layer-2)

(Estuarine cohesive layer-2)

219
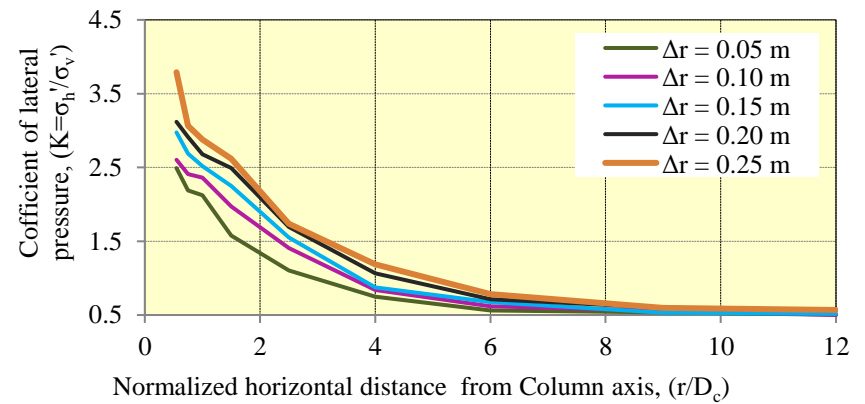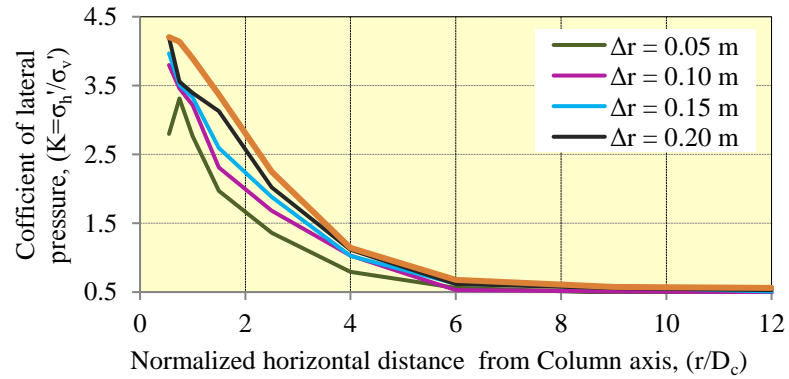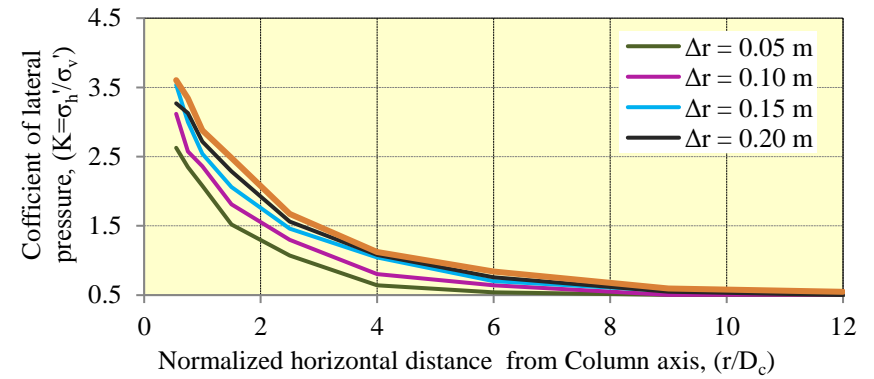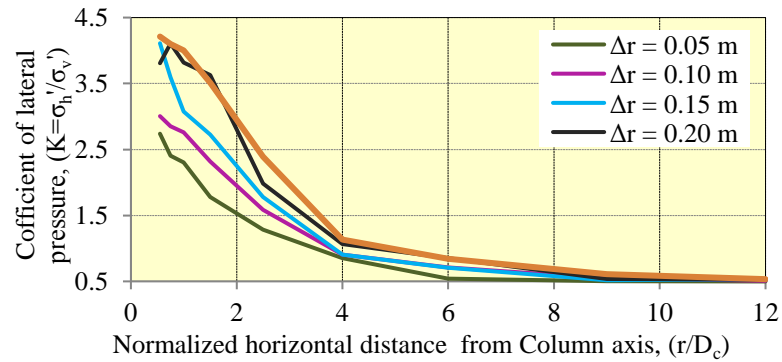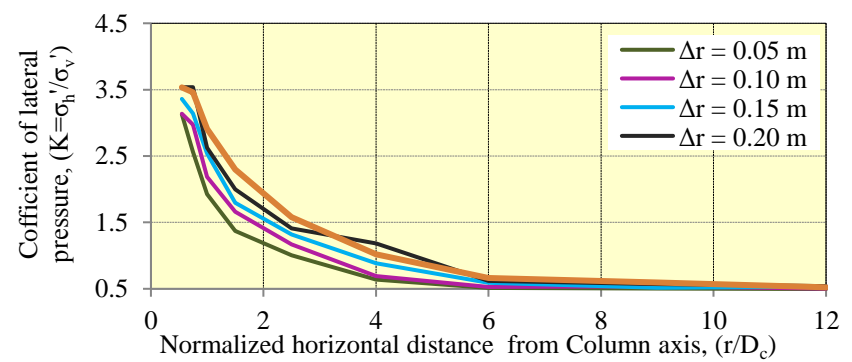
Figure 5.7 Variation of coefficient of lateral earth pressure of estuarine deposits of Santa Barbara treatment plant with distance from the stone column axis for different degrees of cavity expansion.

The area of interest in this stage is the ring of the estuarine soil with a thickness ranged between (1.0 – 1.5) m, which correspondence to stone column tributary area of soil within the stone column group area of infinite reinforced system. To show the effect of the stone column installation in this area, the variation of the coefficient of lateral earth pressure with the normalized degree of stone column expansion to the final stone column diameter (D_c), was plotted at distance (r =1.0m) from the column axis. Figure 5.8 shows that (K) values adjacent to the stone column increases between 5 to 7 times of the initial value of (K_0) at rest for the case of (Δ_r=0.25m) expansion cavity.

Figure 5.8 also demonstrates that (20-40)% development in the confinement around the stone column (K) is achieved when the expansion degree increased from (Δ_r 0.05m) to (Δ_r 0.25m) for the estuarine cohesive deposits as an average, while this improvement increased to about (40-65)% for the case of estuarine cohesionless deposits.
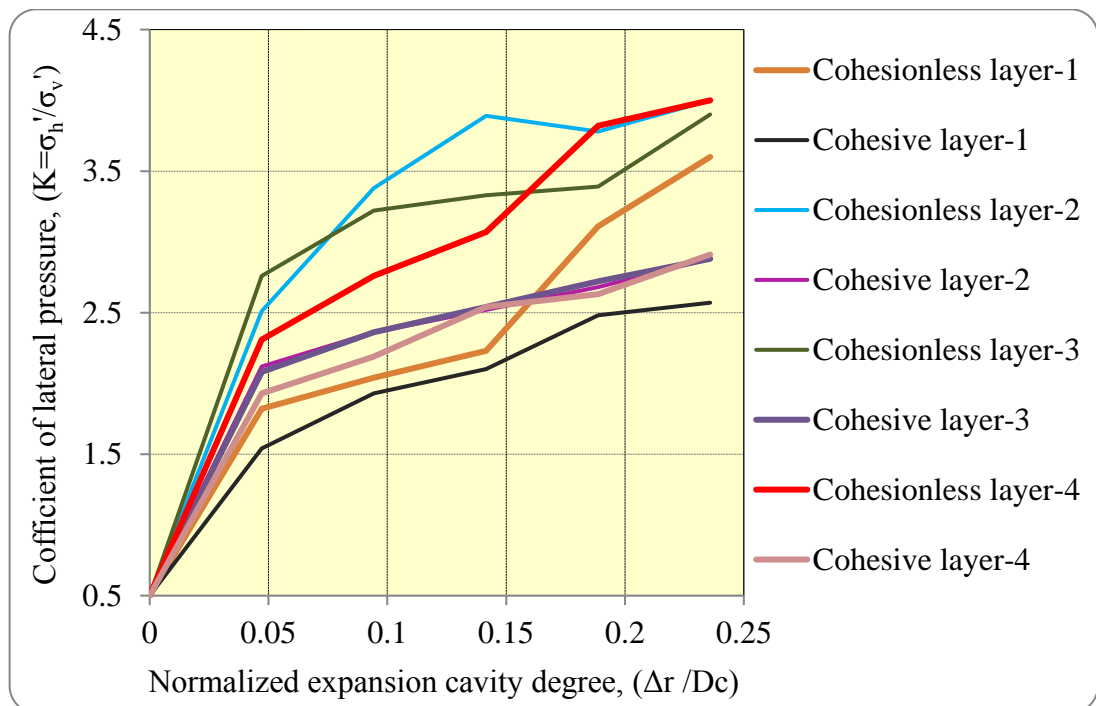

Figure 5.8 Variation of coefficient of lateral earth pressure of estuarine deposits in Santa Barbara treatment plant with different degrees of cavity expansion at 1m distance from the stone column axis.

5.5.4.2 Evaluating the Stiffness Changes due to Single Stone Column Installation

Soil stiffness modulus increase was based on the direct proportional relationship between the stiffness of the soil and the effective mean stress that was suggested by Biarez et al., (1998). This method was explained in detail in the last chapter in Section 4.9.2. According to Brinkgreve and Vermeer (1998), and because the secant Young's modulus (E_{50}) is designed to capture the stress stiffness dependency for the case of primary loading, it is recommended for normally consolidated clay to use (E_{50}) as a reference value of Young's modulus.

The development of mean effective stress was estimated first within the estuarine soil deposits after 18 days consolidation with distance from the stone column axis. Then, based on equation 4-1, Young modulus has been predicted within both of cohesionless and cohesive estuarine deposits for 5 different degrees of cavity expansion. The results were normalized with the original value of stiffness secant modulus (E_{50}^{ref}) to extract the final development of the soft soil stiffness due to single stone column installation from one side, as is shown in Figure 5.9.

A dramatic increase in the soil stiffness after consolidation can be achieved when applying cavity expansion installation. Moreover, increasing the amount of expansion during stone column installation has a significant effect on enhancing the stiffness of the surrounding estuarine soil, which reaches a peak up to 3 times to initial soil stiffness adjacent to the stone column for (Δ_r = 0.25m) in the estruarine cohesionless layer-1. These effects extend up to distance of about 5 times the final diameter of the stone column (D_c). However, the stiffness of the estuarine soil very close to the cavity wall is not regular and has some scattered values caused by high disturbance effect adjacent to the column especially in the estuarine cohesive deposits.

By comparing the development of the soil stiffness and the degree of expansion cavity of stone column installation, it was noticed that estruarine cohesionless depositss tend to gain more stiffness with increasing (Δr) than do estruarine cohesive deposits.

(Estruarine cohesionless layer-1)


(Estuarine cohesive layer-1)

(Estruarine cohesionless layer-2)

(Estuarine cohesive layer-2)

223
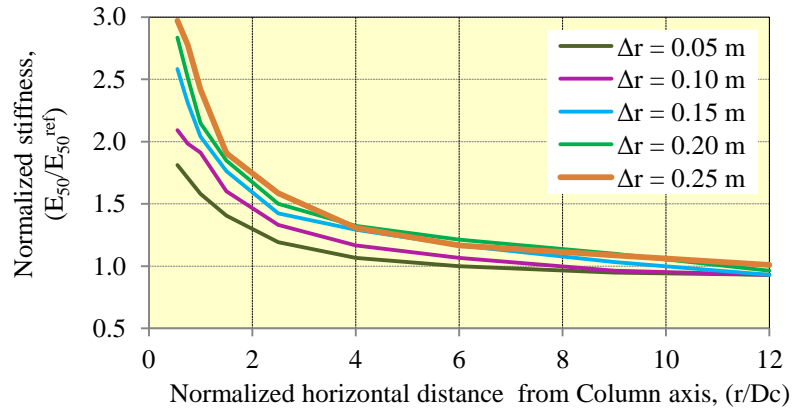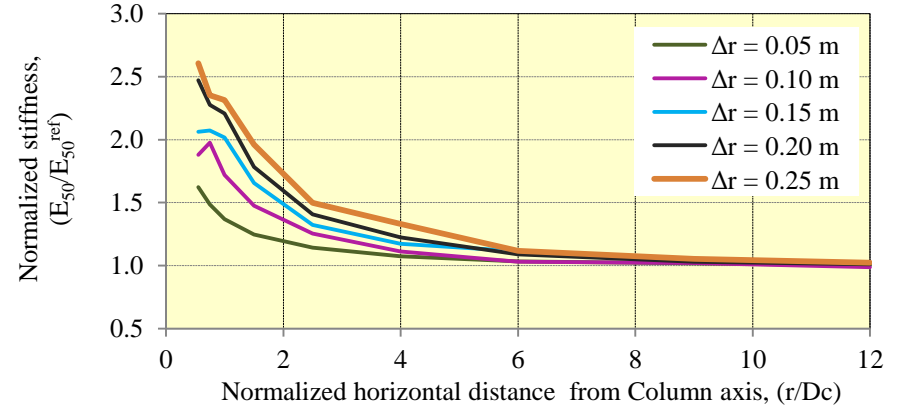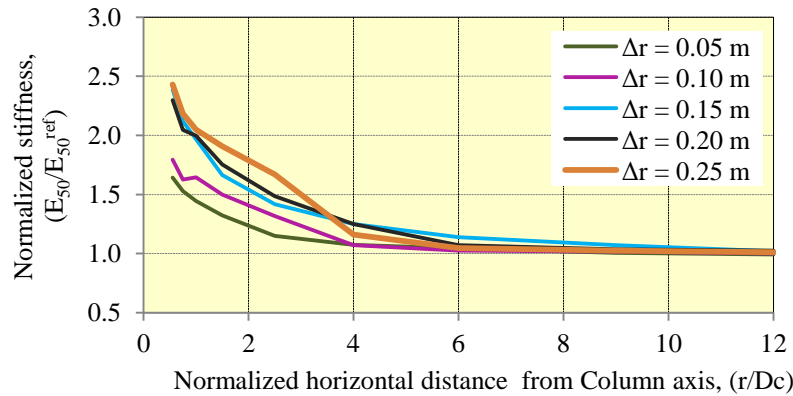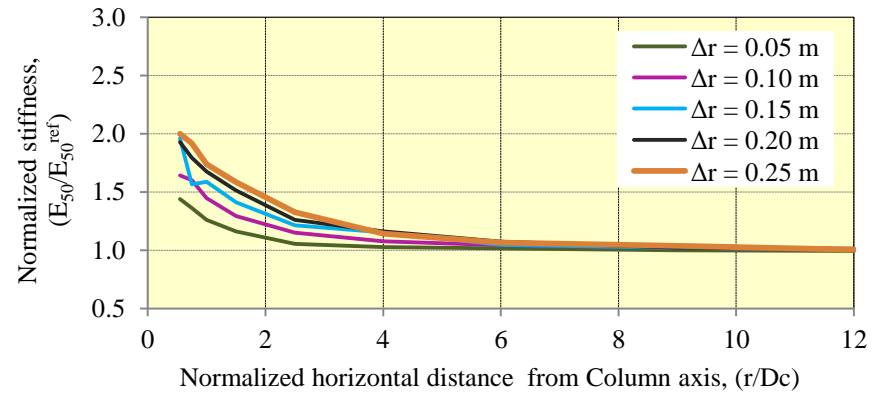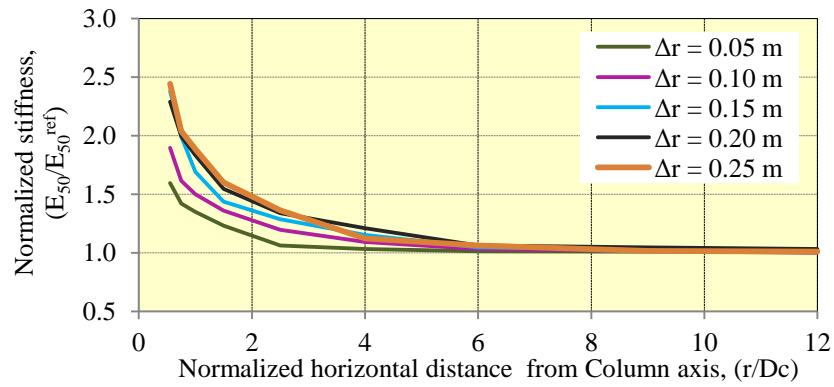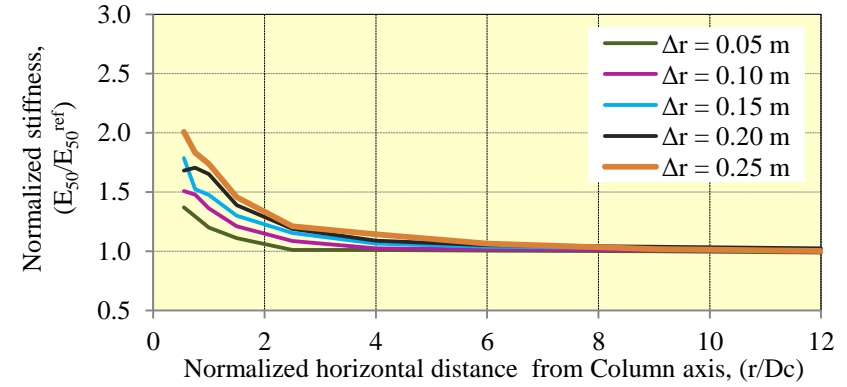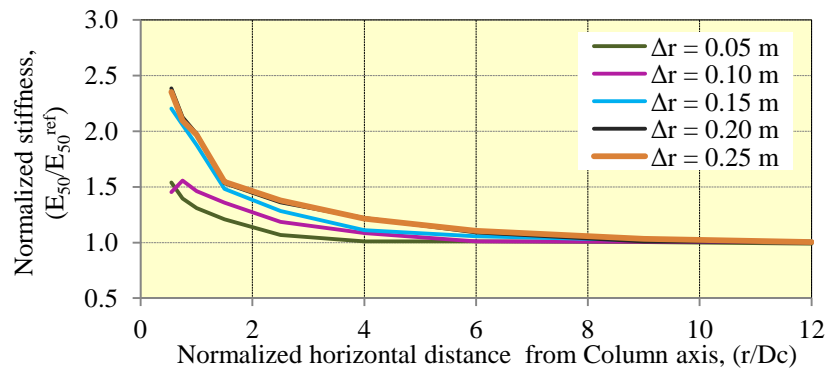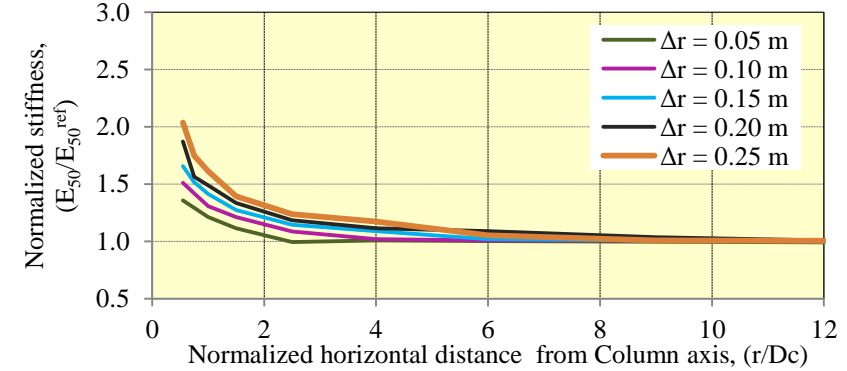
Figure 5.9 Variation of normalized stiffness modulus of estuarine deposits with distance from the column axis for different degrees of cavity expansion.

For clearer presentation of the effect of increasing the expansion cavity installation of the stone column, normalized enhanced stiffness modulus of each of the estuarine deposits, at 1m distance from the installed stone column, together with normalized expansion cavity degree, (Δr /D_c) have been plotted in Figure 5.10. This figure shows that (E_{50}) values at 1m distance from the stone column axis increased between 1.5 to 2.5 times of the initial stiffness modulus value of (E_{50}^{ref}) for the case of (Δ_r = 0.25m) expansion cavity.

The curves show significant increase in the soil stiffness within the enhanced zone. The maximum proportion of average increase in the stiffness of estruarine cohesionless layers when the expansion degree increased from (Δ_r = 0.05m) to (Δ_r = 0.25m) is about 120%; this occurred at a radius (1.0 m) of the stone column diameter, compared to about 70% average increase on the estuarine cohesive depositss stiffness. Figure 5.10 also shows thet the stiffness modulus of both cohesionless and cohesive deposits increased with depth allowing more efficincy for the expansion cavity installation of the stone column for the deep layers.
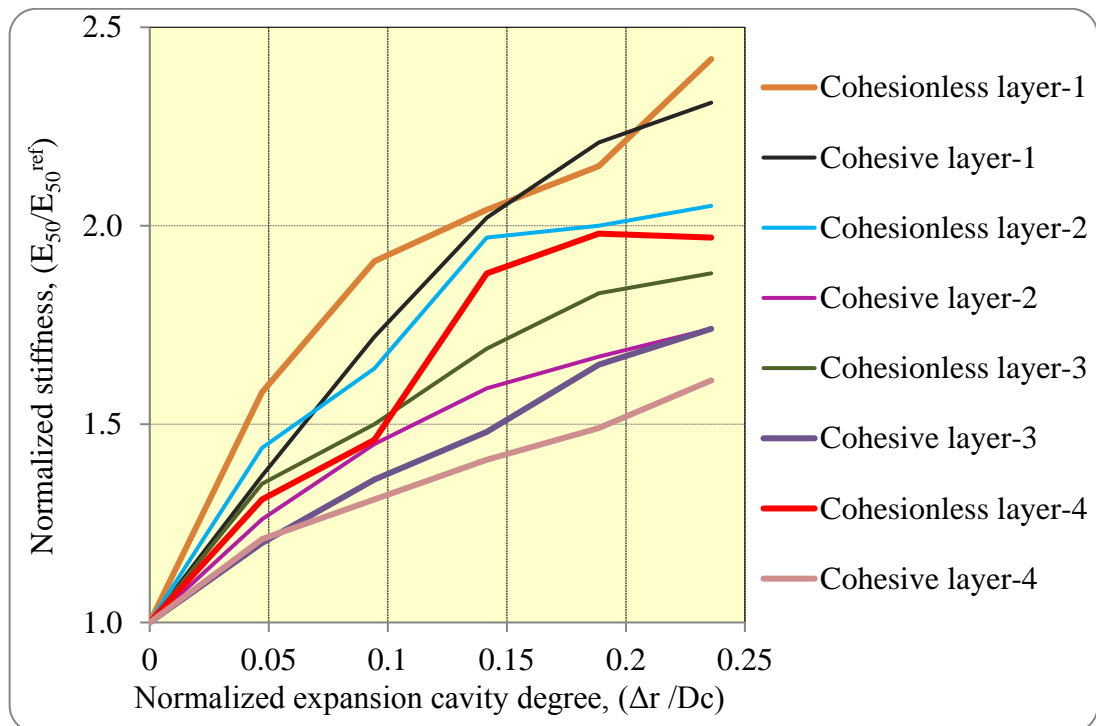

Figure 5.10 Cavity expansion degree effect on the stiffness secant modulus of estuarine deposits around the stone column after primary consolidation at 1m distance from the stone column axis.

5.6 Results due to Installation of Another Stone Column Installation Adjacent to the First One.

Adoption of the improvement of the soft soil due to the installation of only single stone column in the design of stone column reinforced foundations will lead to a conservative estimation of the performance of these systems. This is because stone column foundations normally consist of a number of columns that work together with the surrounding clay to create one system. Thus the effect of adjacent columns in increasing the confinement of the columns and accumulating more stiffness to the soil between these columns, as Figure 5.11 shows, was taken into account in this step to complete the validation of the built model in Chapter 4.
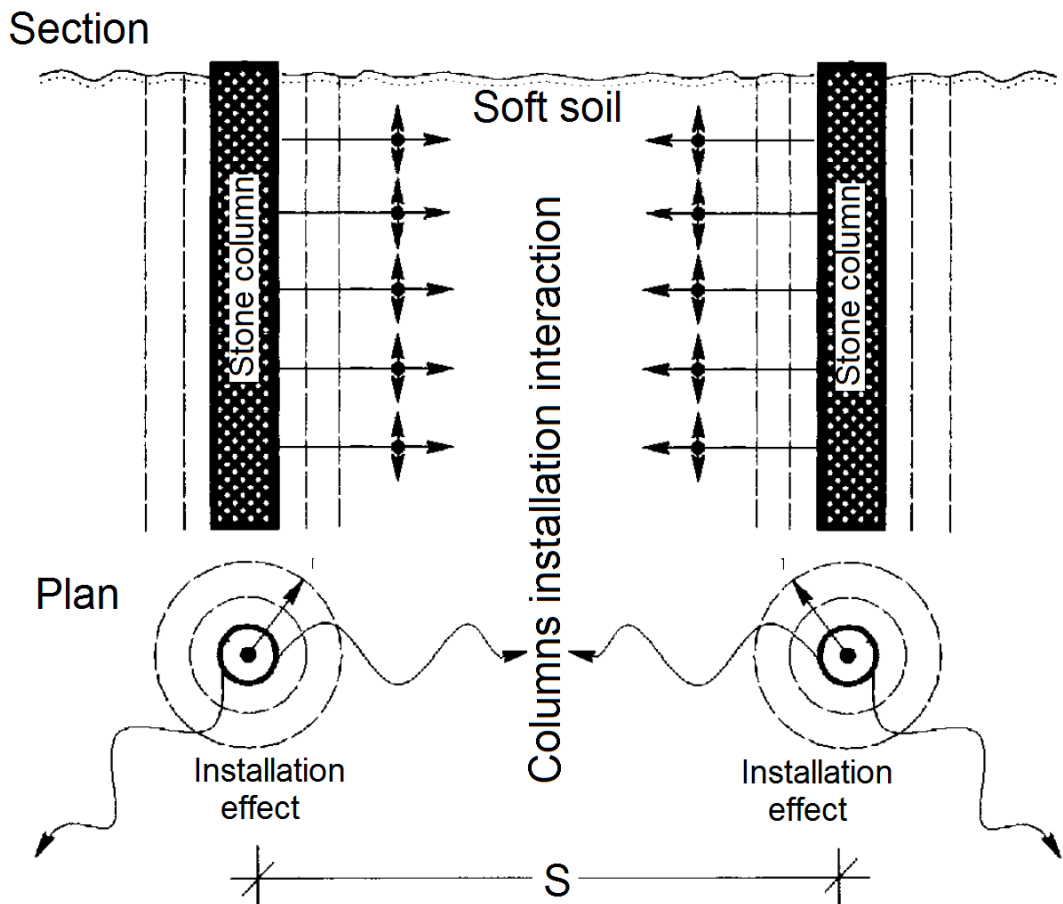

Figure 5.11 Schematic illustration of the accumulative effect of cavity expansion due to the vibro interaction of two adjacent installed stone columns.

Calculation of the changes happen to the soft soil caused by single stone column installation with different degrees of cavity expansion has been done in Section 5.5.4, which means these changes are from one side and reduce with distance from the stone column; whereas the soil between stone columns will be affected by adjacent stone columns. In this section, and to meet the actual conditions of stone column group for the case of Santa Barbara treatment plant, the soft soil was compressed from both sides to represent the existence of another stone column installed adjacent to the first one in the same method proposed by Guetif et al., (2007) and the same degree of expansion at three different distances (S = 1.50, 1.75, 2.10m) that have been recorded in this field case. Consequently, the magnitude of these changes increased in the soil and were accumulated based on the increase in the confinement pressure within the soil.

5.6.1 Problem Simulation (Conceptual Model)

In order to take into account the effect of installing a second stone column at a distance (S) from the axis of the first column in the soft soil properties between them, the following methodology was used to estimate the changes in stress state and stiffness after installing another stone column adjacent to the first one, which has been studied in detail in the first step of this validation.

- Based on the first step, both new stress state and stiffness at mid-point of each layer of estuarine deposits were calculated at different distances from the stone column axis and for the five degrees of stone column expansion. The area of interest in this stage is ring the estuarine soil with a thickness ranged between (1.0 – 1.5m), which correspond to stone column tributary area of soil within the stone column group area of infinite reinforced system. Although this area is the most affected by the installation of the stone column and its improvement changes within its thickness, it is relatively thin compared to the stone column diameter and the new values of both lateral pressure coefficient and stiffness modulus were

227

approximately averaged based on the area calculation under the curves that represent the changing of (E_{50}) and (K) for all the 8 different estuarine deposits and for all cases of the degrees of expansion cavities. Figure 5.12 (a) illustrates the principle of this stage.

- Based on the last stage a new soil profile has been created for the effect of the single stone column installation from one side, a data base of the values of both (E_{50}) and (K) for each of estuarine cohesionless and cohesive layers and for all installation expansion degrees have been saved to be input data for the second stage where the effect of installing second stone column calculated. These data were also plotted for each case of the stone column spacing later in this chapter and can be seen in the black colour curves in Figure 5.15 and Figure 5.16 for the columns spacing (S = 1.50m), Figure 5.17 and Figure 5.18 for the columns spacing (S = 1.75m) and Figure 5.19 and Figure 5.20 for the columns spacing (S = 2.10m).

- The second stage is illustrated in Figure 5.12 (b), where the installation effects on another stone column at a distance of (S = 1.5, 1.75 and 2.1m) were estimated. In this stage, the input soil profile was updated base on the results of the improvement in soil stiffness and confinement of last stage, which were presented in figures 5.16, 5.18 and 5.20 for the coefficient of lateral pressure and figures 5.17, 5.19 and 5.21 for the stiffness modulus. It is clear from these figures that each layer of the estuarine cohesionless and cohesive has a new (E_{50}) and (K) different from the others (as a result of difference in depth and properties) .
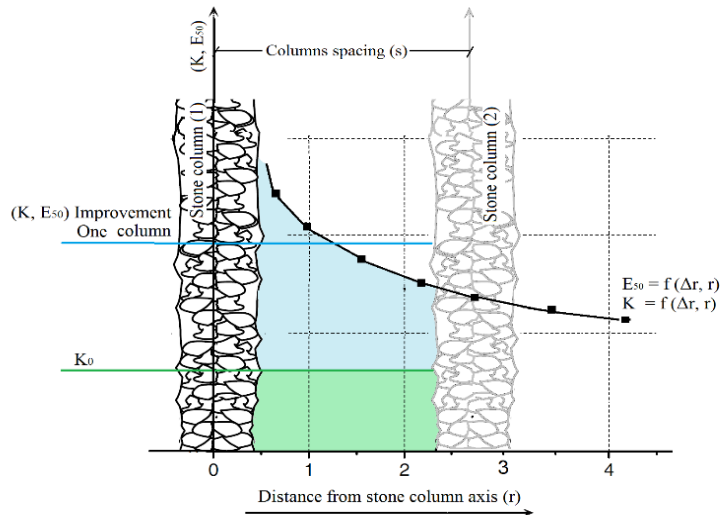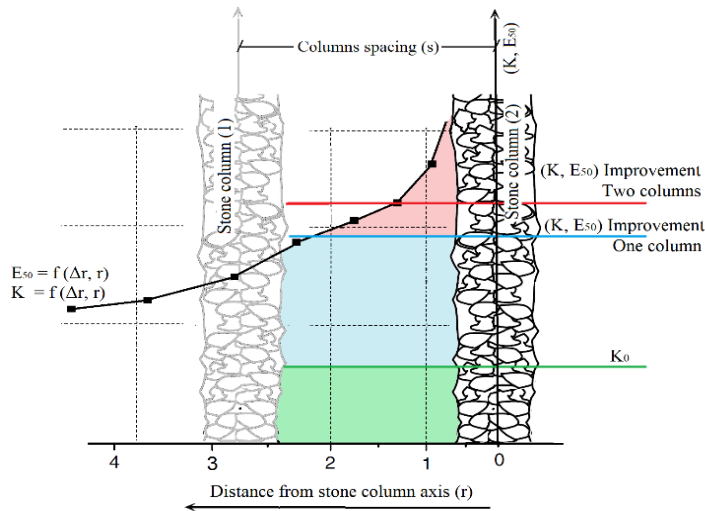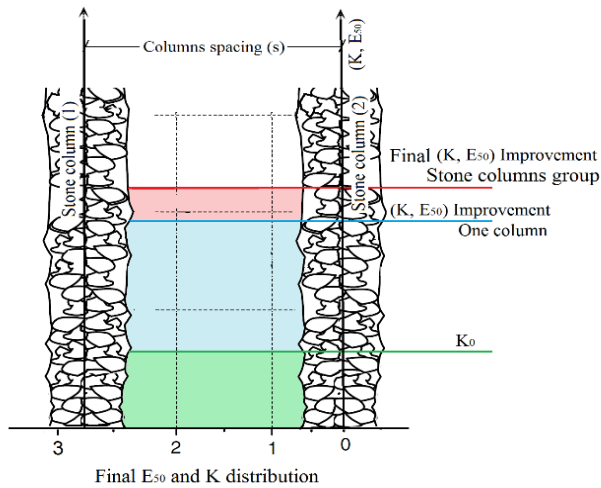
Figure 5.12 Conceptual method used in accumulating the effect on installing a second stone column at a distance (*S*) from the axis of the first column in the soft soil properties between them.

229

In order to take into account the effect of installing a second stone column at a distance (*S*) from the axis of the first column in the soft soil properties between them, two main conditions should be available; the first is the presence of the stone column, which is very necessary to represent the consolidation from the surrounding soft soil to the stone column material and give the real behaviour of interaction between the soft soil and the stone column. The second is the 3D simulation of the problem to be similar to the actual field case. The axisymmetric homogenization method was used in numerical analysis in Plaxis 2D to account for the effect of the second column installation in improving the estuarine soil with the presence of the other columns achieving as much similarity as the actual case.

5.6.2 Adopted Homogenization Method for Santa Barbara Treatment Plant Field Cases

Axisymmetric homogenization methods are dimensional changing processes to create a three-dimensional distribution of stone columns within the treated soil in a way that considers these stone columns modelled as axisymmetric. The new dimensions of the stone column distribution are calculated to keep the replacement ratio of the area, the distance between the columns and total surface area as in the 3D actual situation. Figure 5.13 illustrates the idealization of concentric rings of stone column grid to use the axisymmetric homogenization methods in Plaxis 2D for the three stone column spacings (*S* = 1.5×1.2m, *S* = 1.75×1.75m and *S* = 2.10×2.10m).

Although the axisymmetric homogenization methods, which are used in this numerical analysis redistributed the stone column materials to meet the requirements of 2D simulation, it alters the main mechanism of the composite system and ignores the drainage properties and changes the consolidation process. It keeps the replacement ratio of the area and the distance between them as in the original situation. However, the main target of this step was not to study the final settlement response of the reinforced system and no footing load was applied at this stage, but only to estimate the improvement in stiffness modulus (E_{50}) and coefficient of lateral earth

pressure (K) added to the soil after installing stone columns from two sides (similar to the actual field case). Moreover, it was found at the end of the consolidation time of 18 days, both two parameters (E_{50}) and (K) had achieved equilibrium.


(a)

(b)

(c)
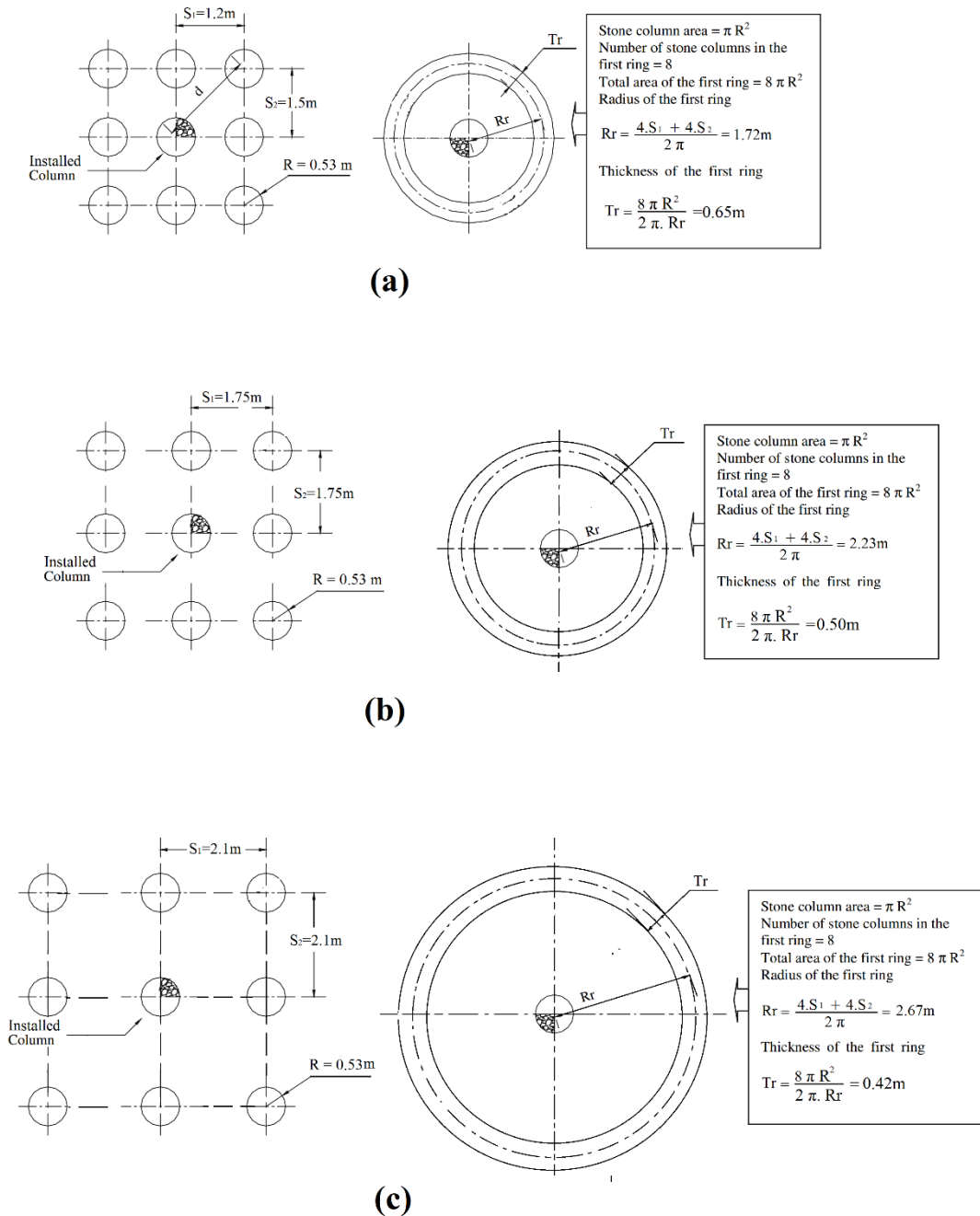
Figure 5.13 Adopted geometric modelling of stone column grid to accumulate the effect of stone column installation from two sides for Santa Barbara treatment plant field case, stone column spacing (a) S = 1.5×1.2m, (b) S = 1.75×1.75m, (c) S = 2.10×2.10m. (after Elshazly et al., 2008a).

5.6.3 Numerical Model Development and Specifications

The numerical model in this case is similar to that built for the last step when the effect of the single stone column was studied, except of the existence of the stone column rings that represent the new distribution of the stone column group to meet the requirement for 2D axisymmetric simulation. Figure 5.13 (a), (b) and (c) illustrate the exact dimensions for the concentric rings of stone column grid that was used for the stone column spacings cases (S = 1.5×1.2m, S = 1.75×1.75m and S = 2.10×2.10m) respectively.

Another important input (different from the previous model) which has been changed due to the improvement gained after the single stone column installation, is the new values of stiffness secant modulus (E_{50}) and coefficient of lateral pressure (K). Each of these two parameters was calculated for eight different estuarine deposits when applying five degrees of stone column expanding installation and for three columns spacings to get 120 different values of each of them. All these values were plotted with the applied expansion cavity in Figure 5.15 and Figure 5.16 for the columns spacing (S = 1.50m), Figure 5.17 and Figure 5.18 for the columns spacing (S = 1.75m) and Figure 5.19 and Figure 5.20 for the columns spacing (S = 2.10m).

Rest specifications of the development process of this model are similar to that explained in the single stone column case, including the boundary conditions, restraints and ground water table.

Column installation methods were also similar to the single stone column model, which is illustrated in Figure 5.5. where the average maximum cavity expansion applied due to the installation of the stone column was 0.25m. Modelling started with a finite radius was used (r_0) (dummy material). Then, a prescribed displacement (Δr) was applied to express the radial expansion of five different lateral expansion values (Δr = 0.05, 0.10, 0.15, 0.20 and 0.25m). The final stone column diameter in this study is fixed at (d_0 + 2Δr = Dc =1.06 m). So, in order to meet 5 different degrees of applied expansion, the initial stone column diameter r_0 was changed according to the applied cavity expansions.

232

Again Figure 5.6 illustrates the terms (r_0, r_c, r and Δr) and defines the names of each estuarine deposits used later in this case.

Sensitivity investigations of the final dimensions and appropriate finite elements mesh coarseness of this model revealed that it is enough to set the side boundary about 13 m. to avoid any reflection on the accuracy of finite element model of this boundary. Therefore, it was conservatively chosen at 15m distance. And for the finite element mesh which was 15-node triangular element, global coarseness was taken to be fine and the local fineness factor should be at least 0.5 to have sufficient accurate analysis. Final geometric dimensions and finite element mesh for the three cases of stone columns spacings of this model are shown in Figure 5.14 (a), (b) and (c).

5.6.4 Results of Second Stone Column Installation Effects

The development of stiffness modulus and coefficient of lateral pressure of the soft soil around the stone column after installation was investigated in mid-depth of each cohesionless and cohesive estuarine layers.

After installing another stone column adjacent to the first one, it limited an area of the estuarine soil with a thickness that ranged approximately between (1.0 – 1.5m) based on the studied columns spacings case. For each of estuarine layers and with the five different degree of expansion cavity installation, the improvement of both stiffness modulus (E_{50}) and coefficient of earth pressure (K), has been estimated with the distance of the new installed column. This calculation process was repeated for the three cases of field recorded columns spacings. Finally, an averaging calculation of each of (E_{50}) and (K) within the affected thickness of the estuarine soil was performed to find the added effect of installing the second stone column in improving (E_{50}) and (K), and then its effect was accumulated to that caused by installing the first single stone column to get the final new estuarine soil profile for all the studied cases. This final profile was used later in the third step of the model validation. Figure 5.12(b) illustrates the conceptual method of this calculations.
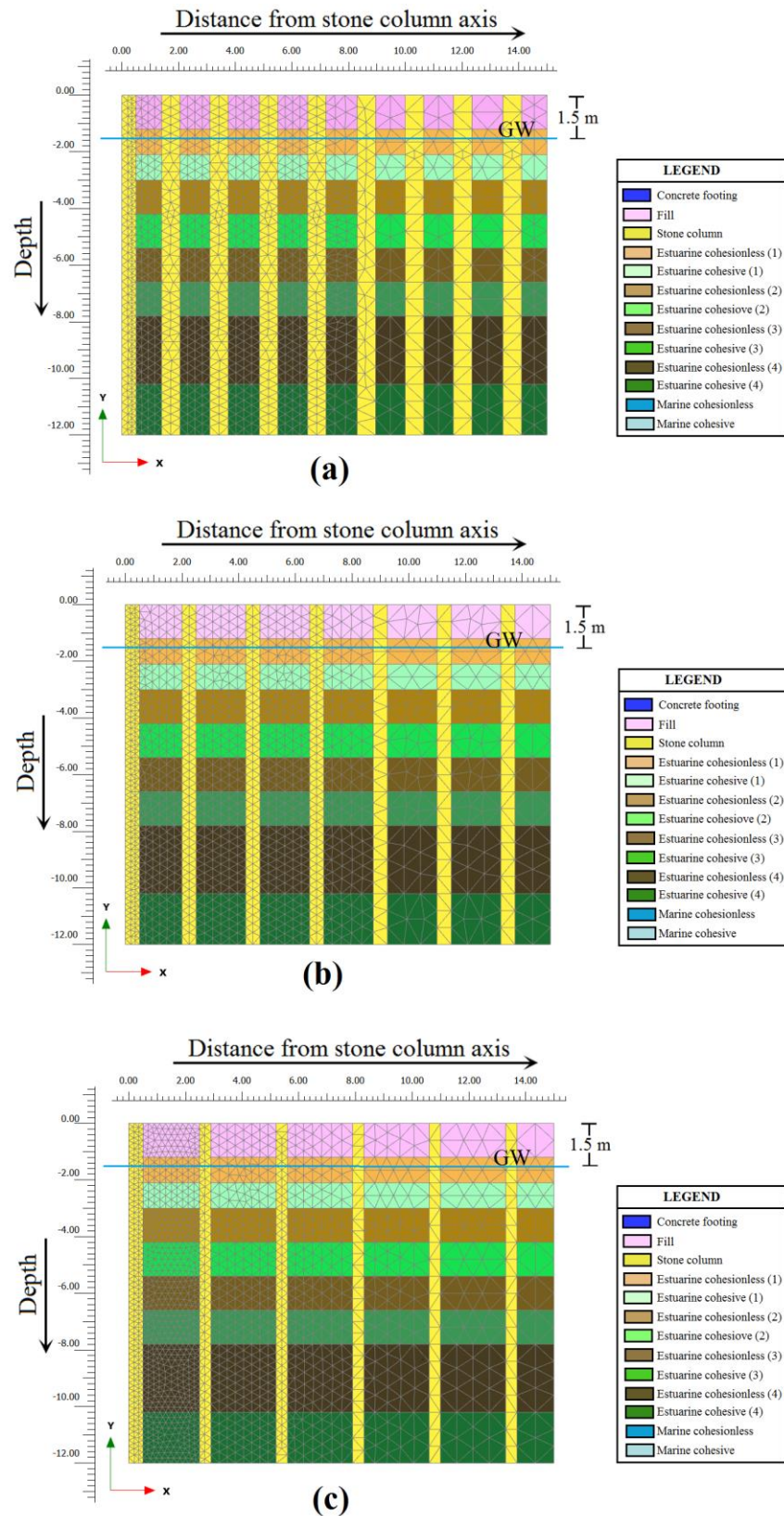
Figure 5.14 Model geometry and finite element mesh (For homogenization model) to study the accumulative effect of installing more than one stone column on the improvement of soil stiffness and lateral pressure for the spacing (a) S=1.5×1.2m, (b) S=1.75×1.75m, (c) S=2.10×2.10m.

The final values of (E_{50}) and (K), after accumulating the effect of the second stone column installation, for each of cohesionless and cohesive estuarine deposits and for the five applied degrees on stone column expansion were plotted next to those results from the case of single stone column and presented in Figure 5.15 Figure 5.16 for the columns spacing ($S = 1.50$m), Figure 5.17 and Figure 5.18 for the columns spacing ($S = 1.75$m) and Figure 5.19 and Figure 5.20 for the columns spacing ($S = 2.10$m).

5.6.4.1 Evaluating the Coefficient of Lateral Pressure

Based on the figures 5.16, 5.18 and 5.20, which are related to the coefficient of lateral pressure, the following findings can be extracted;

- In general, it is clear that installing another stone column at a distance (S) from the previous one has an effect on applying more confinement for the estuarine soil between them and consequently, increasing the coefficient of horizontal earth pressure (K), which reaches more the 8 times its initial value at rest (K_0) .

- Figures 5.16, 5.18 and 5.20 demonstrate that an average (10-15)% development in the confinement around the stone column (K) was achieved when the expansion degree increased from ($\Delta_r = 0.05$m) to ($\Delta_r = 0.25$m) for both of the estuarine cohesive and cohesionless deposits, except for the top three deposits, which behave different from the others.

- The increase in confinement due to the installation of the adjacent stone column does not apply to all the estuarine soil layers. The curves that represent the top three layers, for all the three columns spacings cases, applying high expansion cavities ($\Delta_r = 0.20$ and 0.25m) show a reduction in (K) for the second stone column effect compared to its value related of single stone column. This negative effect can be traced to the level of vertical overburden pressure situated in the top layers compared to the bottom ones, therefore, the ground heaves as well as undergoing some radial expansion. This is the reason the surface of the ground experienced the heave. These

findings agreed with Egan et al. (2008) who states that the heave is a function of the method of construction of the stone column.

- This negative effect increased when the columns spacing decrease, as can be seen when comparing the curves in the top three deposits for the three different spacings. Moreover, this effect is also apparent more in the estuarine cohesive deposits compared to the cohesionless ones

- By comparing the difference between the improved coefficient of lateral pressure for single stone column with that related to the second column for different estuarine deposits, it can be seen that the cohesionless deposits had a better response to increase its (K) compared with the cohesive deposits.

5.6.4.2 Evaluating the Stiffness Secant Modulus

The curves that present the response of the soil stiffness to installing another stone column adjacent to the first one are illustrated in figures 5.17, 5.19 and 5.21. The findings can be summarized as follows;

- Installing another stone column at a distance (S) from the previous one has a positive effect on improving the stiffness of the estuarine soil deposits between them. Moreover, increasing the expansion degree during the installation of this column had a significant effect on enhancing the stiffness of the soil. Figures 5.17, 5.19 and 5.21 demonstrate that an average (15% and 25%) development in the stiffness of the cohesionless and cohesive deposits were achieved from installing the second stone column compared to that gained by single column, at a distance (S = 2.1m) respectively. While these percentages become about (25% and 40%) for the case (S = 1.75m) and about (30% and 55%) for the case (S = 1.50m).

- The increase of the expansion cavity during the installation of the adjacent stone column seemed also to cause a reduction in the stiffness secant modulus of the top estuarine layers, but this reduction has less influence in (E_{50}) compared to (K) results and it included only

the top two deposits, as it is seen in cohesionless layer-1 curves in figures 5.17, 5.19 and 5.21.

- By comparing the difference between the improved stiffness secant modulus for the single stone column with that related to the second column for different estuarine deposits, it can be seen that on opposite to (K), stiffness modulus (E_{50}) had a better response in the cohesionless deposits compared with the cohesive deposits.
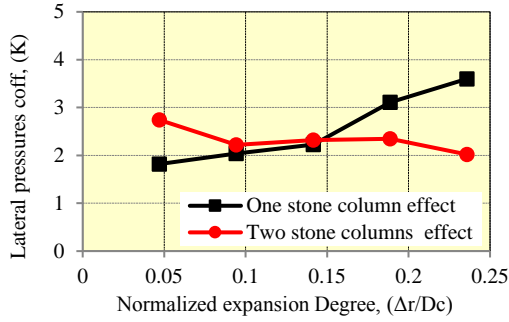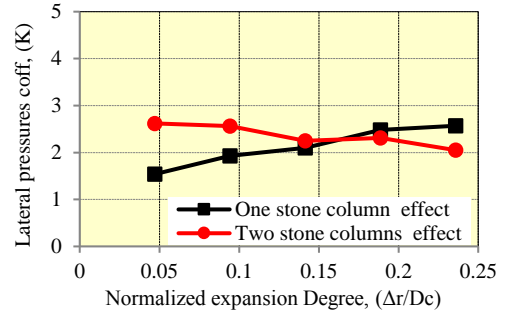
(Estruarine cohesionless layer-1)

(Estuarine cohesive layer-1)
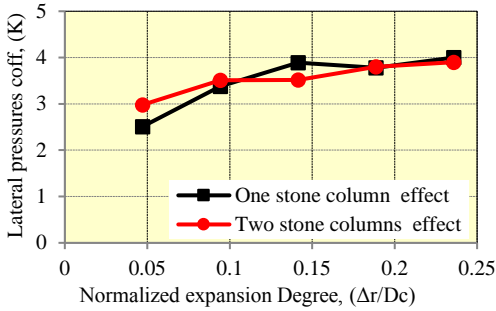
(Estruarine cohesionless layer-2)
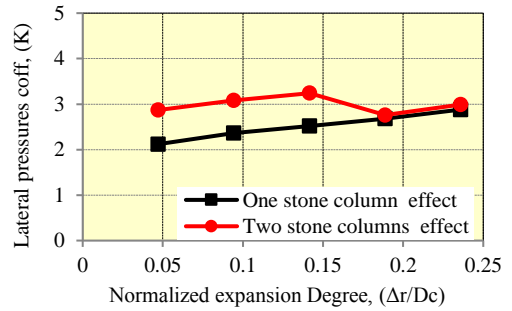
(Estuarine cohesive layer-2)
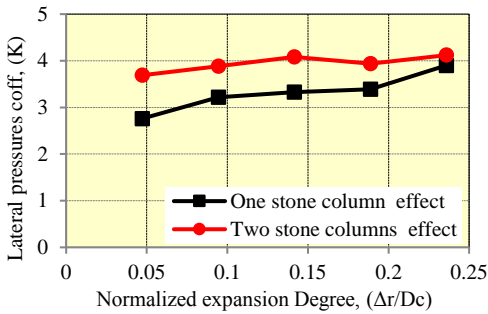
(Estruarine cohesionless layer-3)
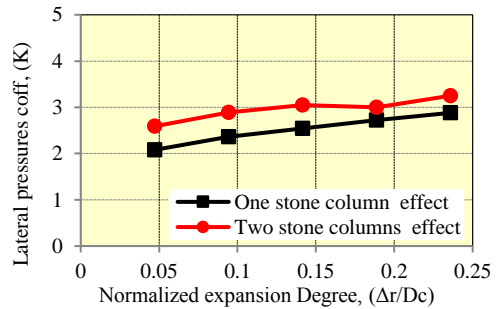
(Estuarine cohesive layer-3)
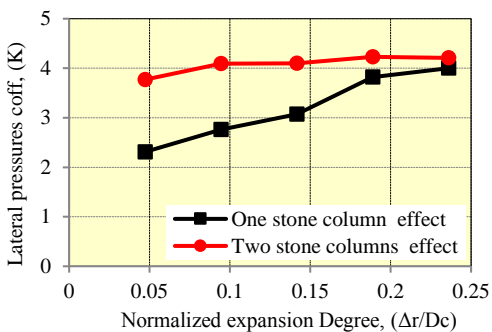
(Estruarine cohesionless layer-4)
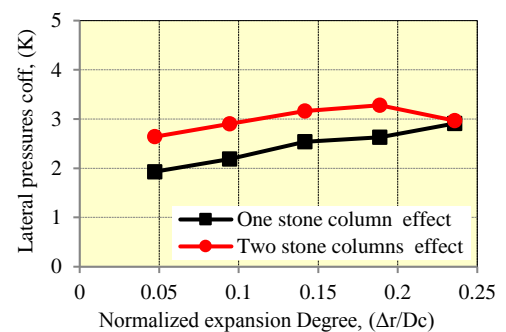
(Estuarine cohesive layer-4)

Figure 5.15 Improvement in lateral pressure coefficient due to second column installation with different expansion degrees of stone column installation and for the columns spacing (S=1.50m).

238
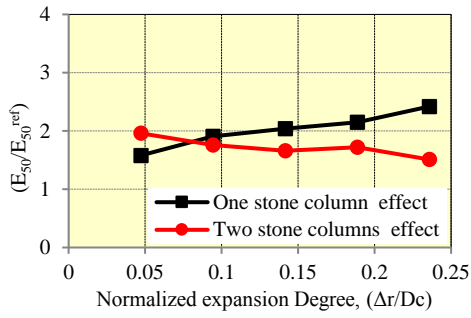
(Estruarine cohesionless layer-1)
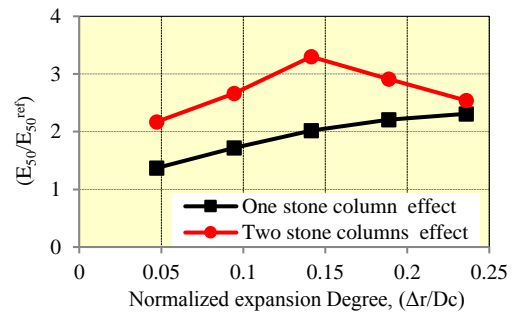
(Estuarine cohesive layer-1)
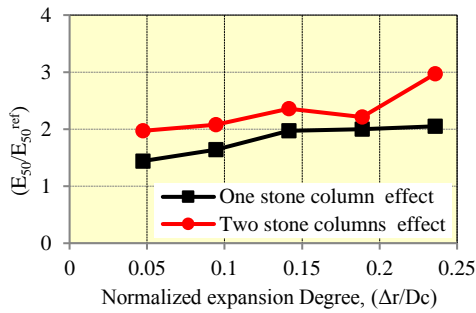
(Estruarine cohesionless layer-2)
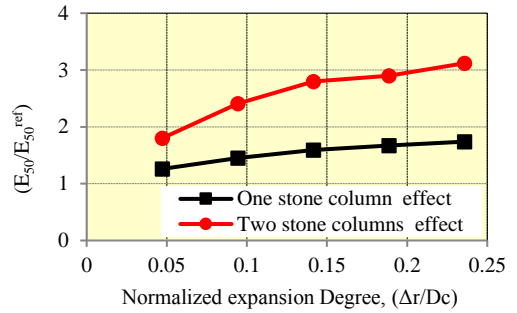
(Estuarine cohesive layer-2)
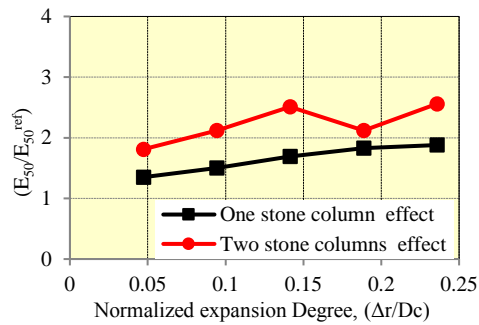
(Estruarine cohesionless layer-3)
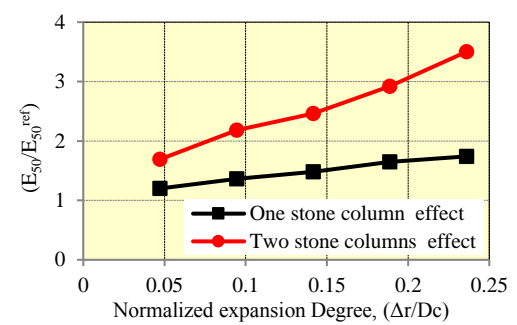
(Estuarine cohesive layer-3)
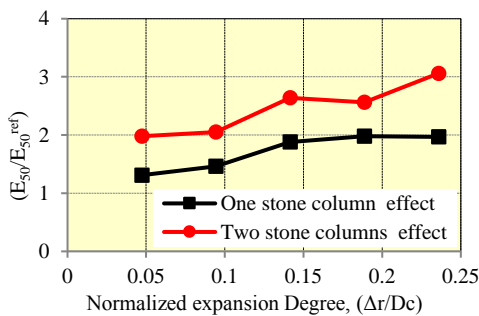
(Estruarine cohesionless layer-4)
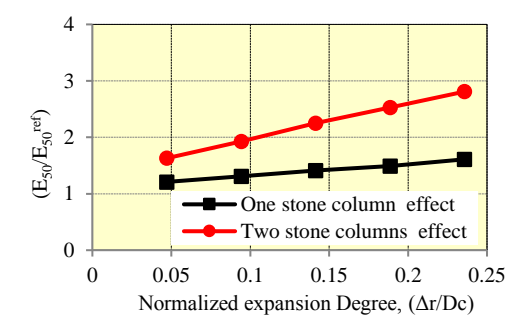
(Estuarine cohesive layer-4)

Figure 5.16 Improvement in normalized secant stiffness modulus due to second column installation with different expansion degrees of stone column installation and for the columns spacing (S=1.50m).

239
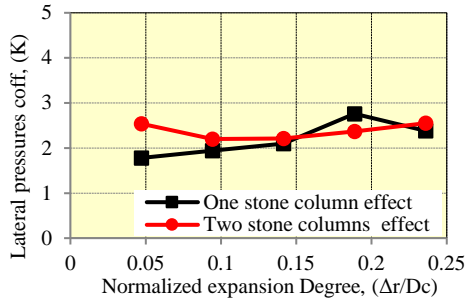
(Estruarine cohesionless layer-1)
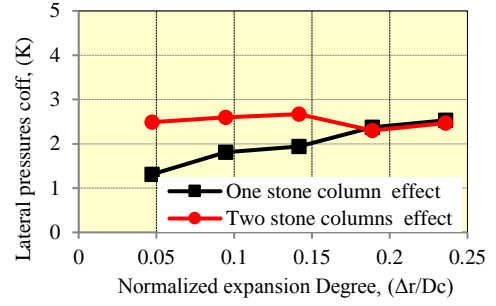
(Estuarine cohesive layer-1)
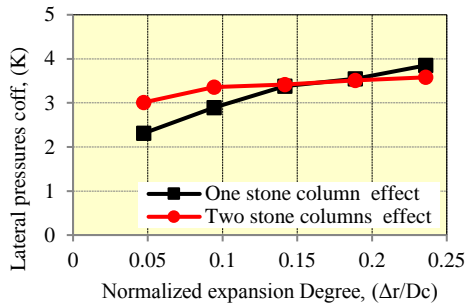
(Estruarine cohesionless layer-2)
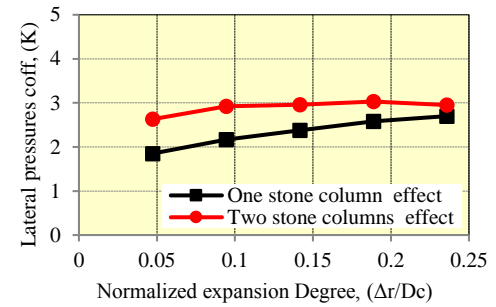
(Estuarine cohesive layer-2)
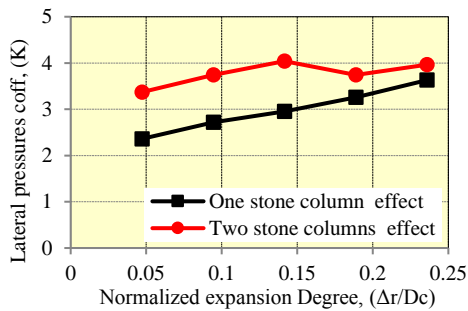
(Estruarine cohesionless layer-3)
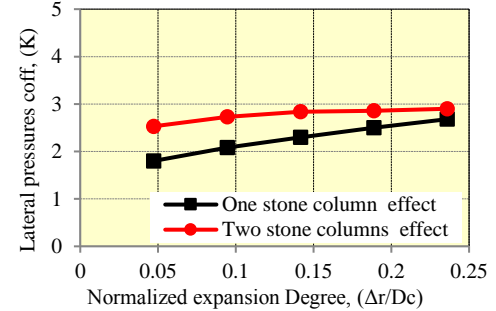
(Estuarine cohesive layer-3)
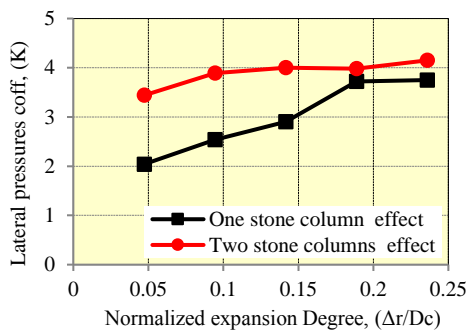
(Estruarine cohesionless layer-4)
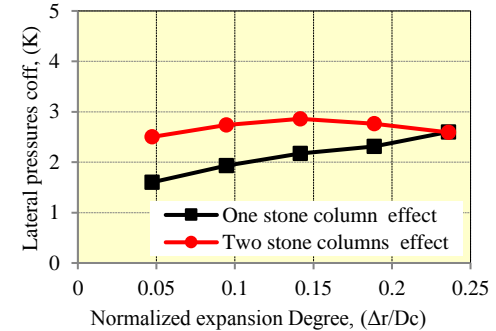
(Estuarine cohesive layer-4)

Figure 5.17 Improvement in lateral pressure coefficient due to second column installation with different expansion degrees of stone column installation and for the columns spacing (*S*=1.75m).
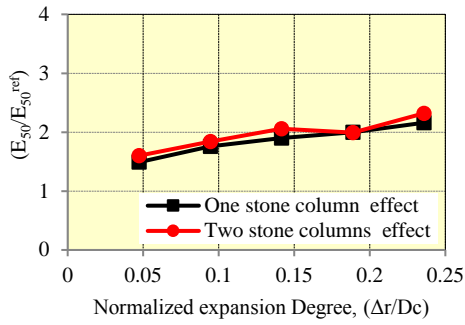
(Estruarine cohesionless layer-1)
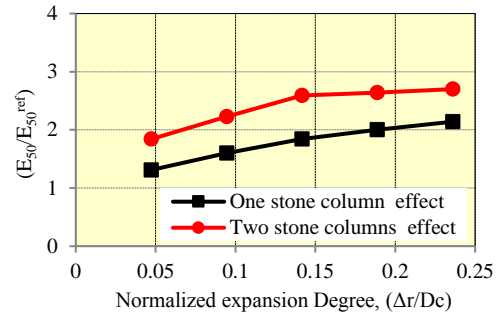
(Estuarine cohesive layer-1)
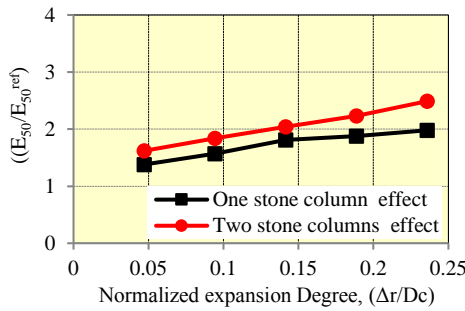
(Estruarine cohesionless layer-2)
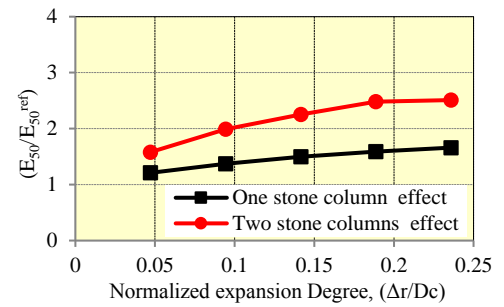
(Estuarine cohesive layer-2)
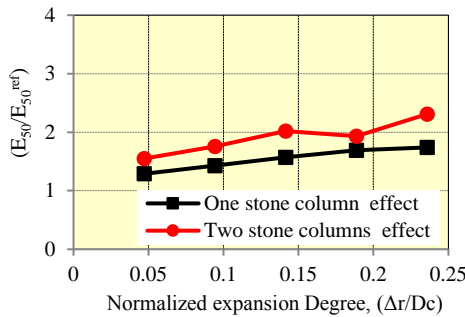
(Estruarine cohesionless layer-3)
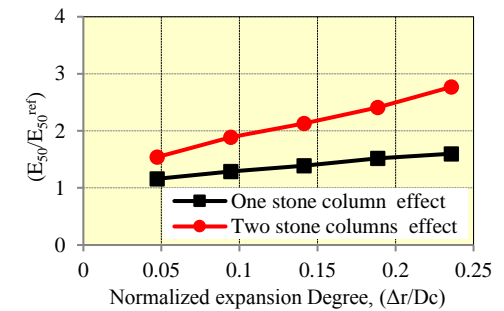
(Estuarine cohesive layer-3)
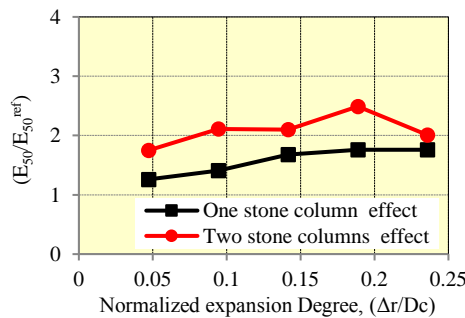
(Estruarine cohesionless layer-4)
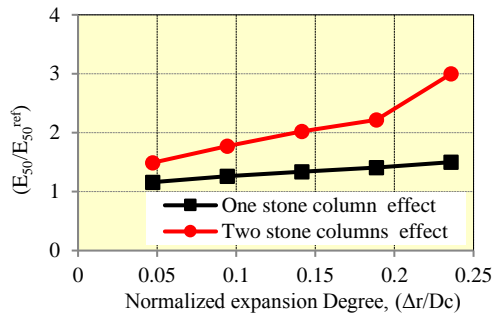
(Estuarine cohesive layer-4)

Figure 5.18 Improvement in normalized secant stiffness modulus due to second column installation with different expansion degrees of stone column installation and for the columns spacing (S=1.75m).
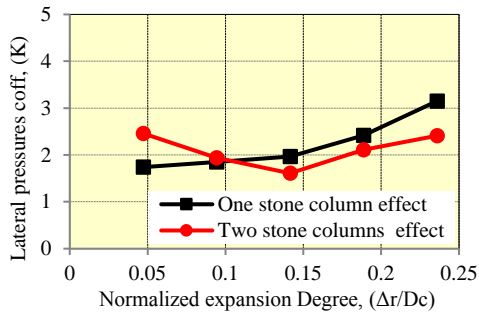
(Estruarine cohesionless layer-1)
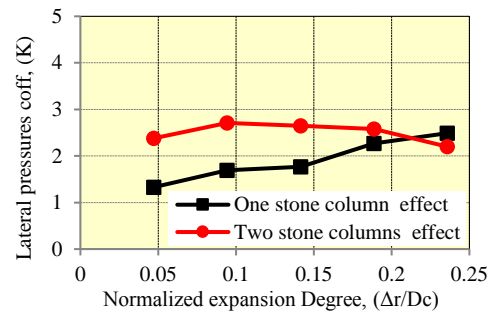
(Estuarine cohesive layer-1)
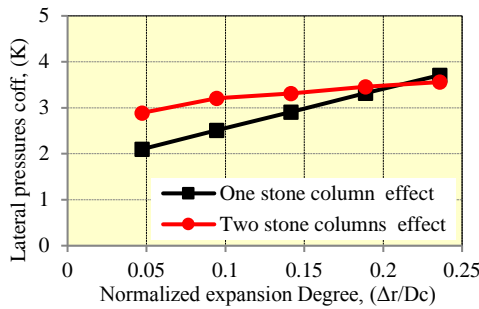
(Estruarine cohesionless layer-2)
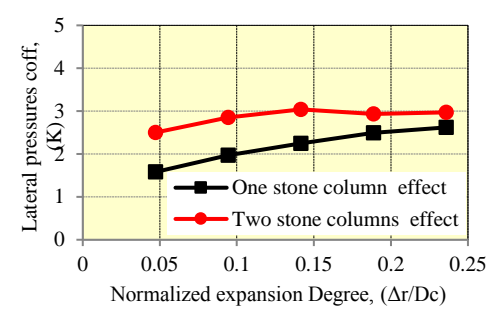
(Estuarine cohesive layer-2)
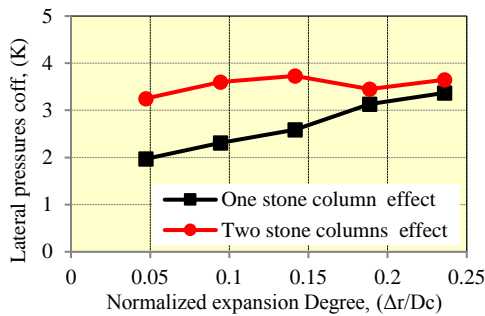
(Estruarine cohesionless layer-3)
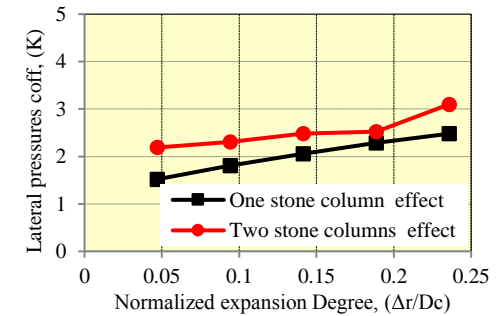
(Estuarine cohesive layer-3)
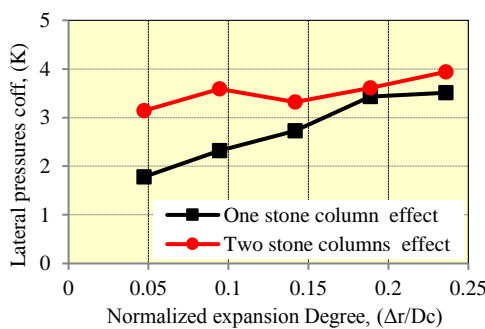
(Estruarine cohesionless layer-4)
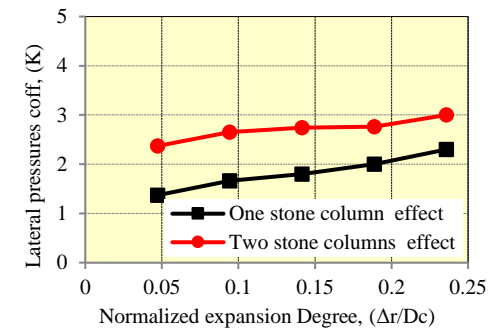
(Estuarine cohesive layer-4)

Figure 5.19 Improvement in lateral pressure coefficient due to second column installation with different expansion degrees of stone column installation and for the columns spacing (*S*=2.10m).

242
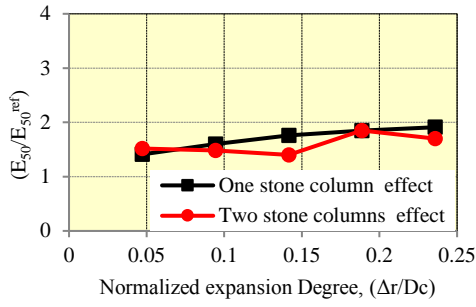
(Estruarine cohesionless layer-1)
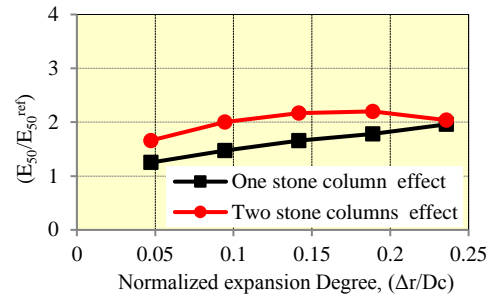
(Estuarine cohesive layer-1)
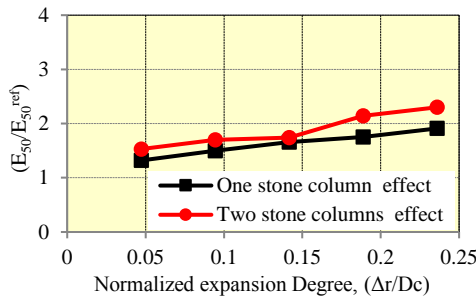
(Estruarine cohesionless layer-2)
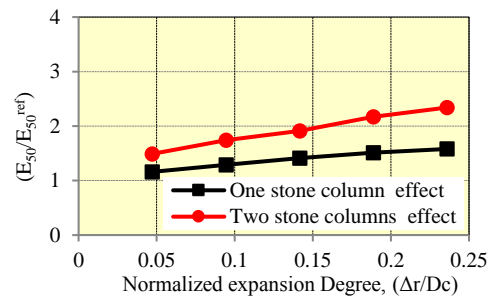
(Estuarine cohesive layer-2)
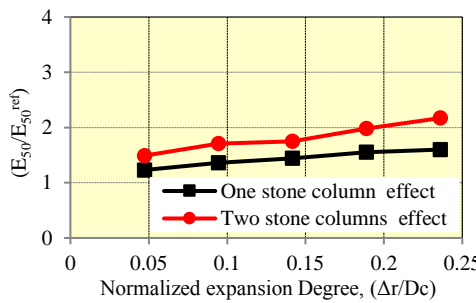
(Estruarine cohesionless layer-3)
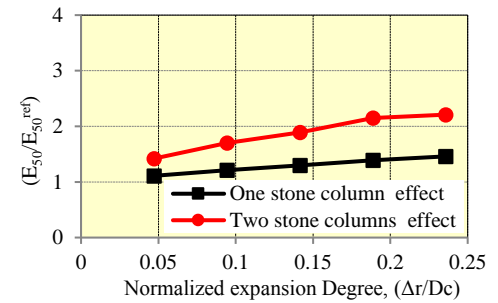
(Estuarine cohesive layer-3)
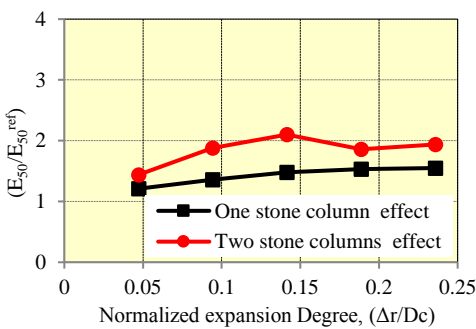
(Estruarine cohesionless layer-4)
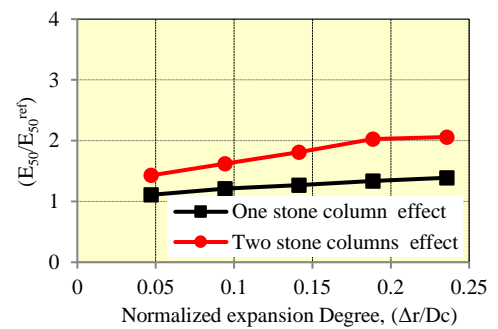
(Estuarine cohesive layer-4)

Figure 5.20 Improvement in normalized secant stiffness modulus due to second column installation with different expansion degrees of stone column installation and for the columns spacing (S=2.10m).

5.6.4.3 Effect of Stone Column Interspacing

For clearer presentation of the effect stone column inter spacings in improving the coefficient of lateral pressure (K) and stiffness secant modulus (E_{50}), the curves that represent the development of both of them with the increasing of cavity expansion installation degree, for each different deposit, have been plotted for the three column spacings in the same graphs; Figure 5.21 for (K) and Figure 5.22 for (E_{50}).

Figure 5.21 and Figure 5.22 demonstrate a noticeable improvement in both (K) and (E_{50}) with the reduction of the stone columns inter spacing. This improvement does not apply for the top two deposits (estruarine cohesionless layer-1 and estuarine cohesive layer-1), which react to the increase in excavity by pushing up toward the ground surface and form the heave around the top of the stone column.

Estruarine cohesionless deposits showed regular respone in developing (K) with the reduction of the stone column spacings more than estruarine cohesive ones. While, for (E_{50}) the opposite is true.

The finding in Figure 5.21 and Figure 5.22 demonstrate the importance of the stone columns inter spacing as an important factor that can be utilized not only to increase the replacement area ratio, but to achieve a certain degree of improvement for both (K) and (E_{50}) of the soft soil between the stone columns, especially when it coupled with applied degree of expansion cavity to create an optimum design requirement for the reinforced system.
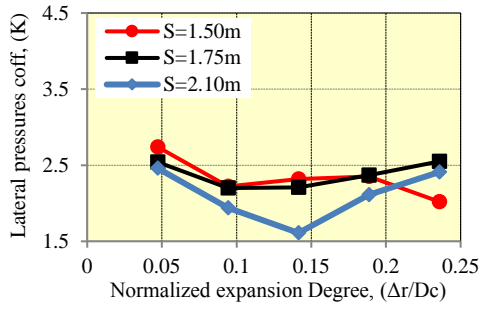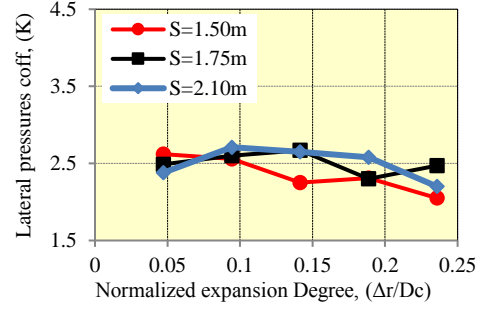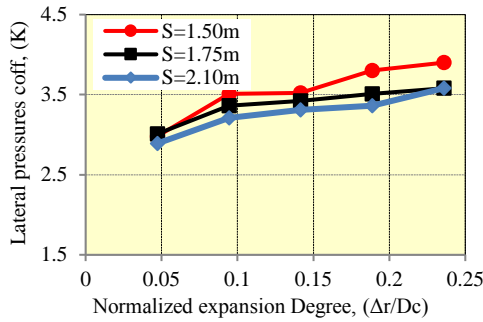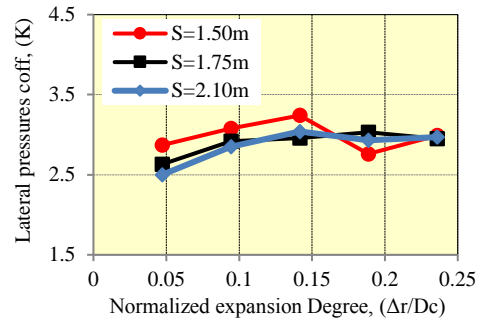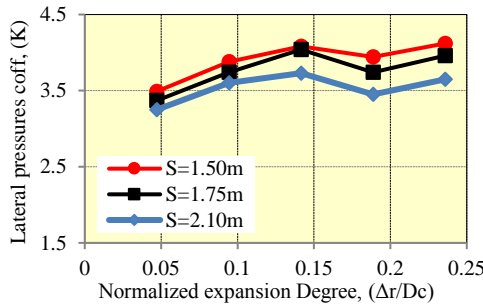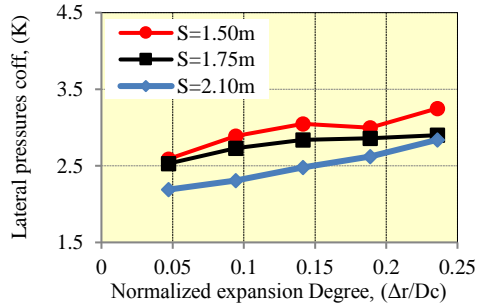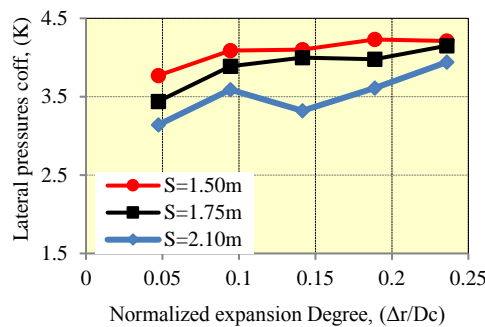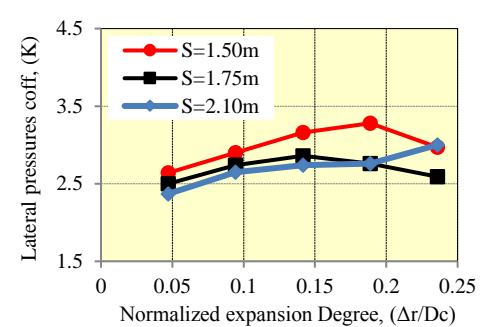
Figure 5.21 Effect of stone column inter spacing in improving the lateral pressure coefficient due to different expansion degrees of stone column installation.
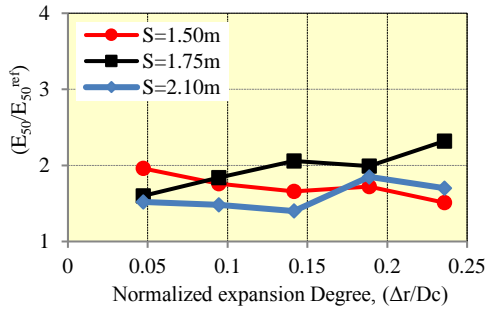
(Estruarine cohesionless layer-1)
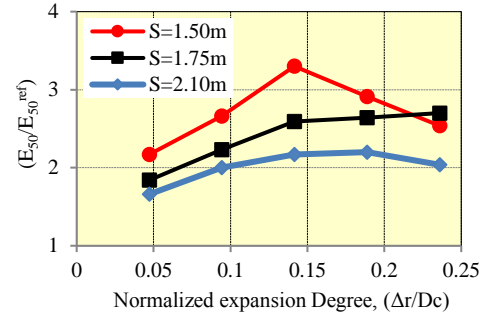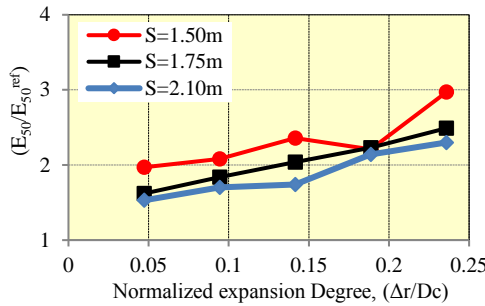
(Estuarine cohesive layer-1)

(Estruarine cohesionless layer-2)
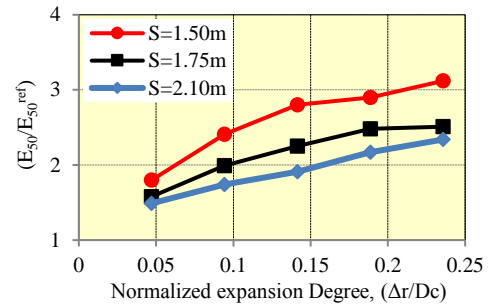
(Estuarine cohesive layer-2)
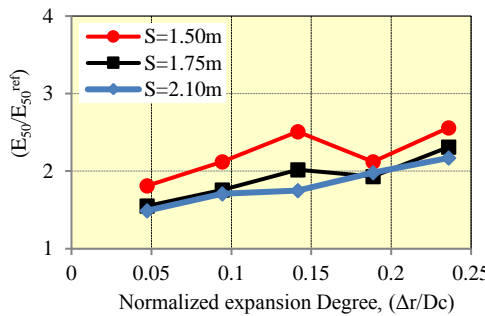
(Estruarine cohesionless layer-3)
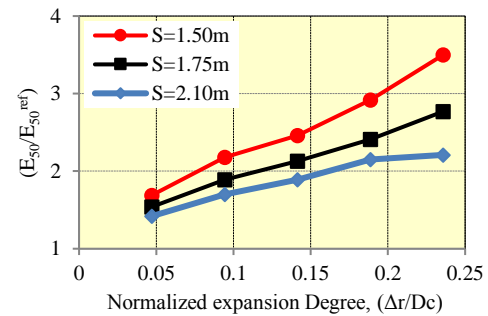
(Estuarine cohesive layer-3)
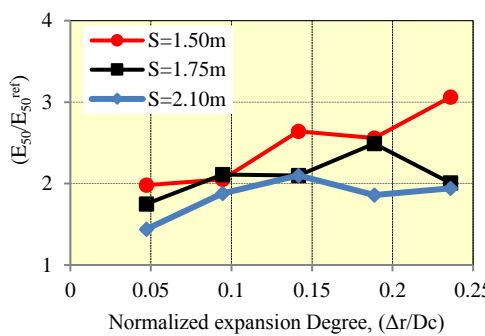
(Estruarine cohesionless layer-4)
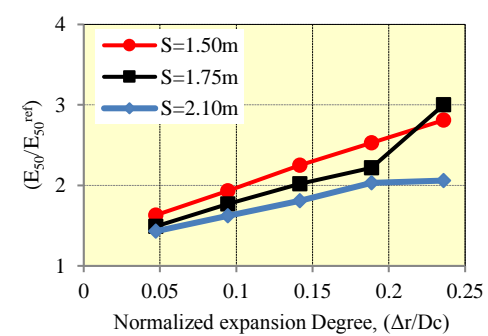
(Estuarine cohesive layer-4)

Figure 5.22 Effect of stone column inter spacing in improving the secant stiffness modulus due to different expansion degrees of stone column installation.

246

5.7 Infinite Stone Column Group in Santa Barbara Soft Soil

Plaxis 3D AE Version 01 has been used to simulate the actual geometry of the infinite installed stone columns in Santa Barbara water platform field case, after applying the results of the last two steps in estimating the improvement in both of the lateral pressure coefficient (K) and the stiffness secant modulus (E_{50}) due to the single stone column installation and incorporating the post-installation improvement of the soft soil between the stone columns by accumulating their effects.

The 3D analysis using Plaxis 3D can accurately simulate the real dimensions of the infinite group of stone columns and capture the actual behaviour and settlement performance of the reinforced system for the three columns spacings field cases.   In this case, there is no need for any homogenisation methods like the one was used by Mitchell and Huber (1985) and Elshazly et al. (2008) for this same field case.

5.7.1 Numerical Model Development and Specifications

To build the 3D numerical model for the three stone columns spacings cases of Santa Barbara Waste water treatment plant, realistic boundary conditions including restraints, ground water table, applied loads, stone columns were adopted. Then a sensitivity study was carried out to decide the final dimensions and appropriate finite elements mesh coarseness of model. All these steps and some assumptions related to the construction process of the stone column installation can be summarized as the following;

1. The default general fixities were automatically applied to the boundaries of the studied model, where all nodes of the model vertical sides were fixed in both X-direction and Y- direction ($U_x = U_y = 0$), while the bottom boundary which represented the deep soil was constrained in all directions (($U_x = U_y = U_z = 0$). The ground surface has no fixities in any direction.

2. The ground water level was at (-1.5m) under the soil surface. The water was allowed to flow from the clay to the stone column drains during consolidation. No drainage was allowed from the boundary of the model.

3. 15- node wedge elements which contain 6 nodes in each triangular faces and 8 nodes in the vertical surfaces were used in finite element in Plaxis 3D, (Figure 3.7).

4. The selected nodes and stress points in this stage were located under the footing to estimate the settlement response to the vertical pressure and then compare it with the field records of the loading tests.

5. The Hardening Soil model was selected to represent the behaviour of both estuarine and marine soils in this study. The properties and parameters that were used in the Hardening Soil model are presented in Table 5.1, except for the improved parameters; lateral earth pressure and the stiffness modulus at rest, they were taken ready for all the different estuarine deposits from the previous stage.

6. The footing and the top surface fill were modelled as elastic- -perfectly plastic material. Typical parameters values for both materials were assumed as shown in Table 5.2. Footing thickness was taken to be 1.2m, which was rigid enough to cause both the stone column and soft clay to settle (Mitchell and Huber,1985; Elshazly et al., 2008a).

7. In order to have accurate results for the analysis using Plaxis 3D code and make these results dependant only on soil properties and geotechnical problem conditions, a group of important analysis for the features and conditions like the mesh density and the distance of the boundaries were investigated to avoid any reaction on the model results. The mesh geometry and boundary positions were investigated to assess their effect on the results of the analysis. A sensitivity analysis was carried out by adopting the same methodology in section 3.6.11on the boundaries to ensure that their

location had little effect on the results. It was found, based the result of the settlement under the footing for the case of stone columns spacings of (S = 2.10×2.10m), that it is enough to make the side boundary about 11m from the footing axis. to avoid any reflection on the accuracy of the 3D finite element model of this boundary. Therefore, it was conservatively chosen at 13m distance. Bottom boundary in this model includes 5 deposits of the old marine soil till the depth of (-19.2m) which is considered as a natural boundary of this 3D model. The global coarseness of the finite element mesh was taken to be fine and the local fineness factor should be at least 0.5 to have sufficient accurate analysis. Final geometric dimensions and finite element mesh for the three cases of stone columns spacings of this model are shown in Figure 5.23 (a), (b) and (c).
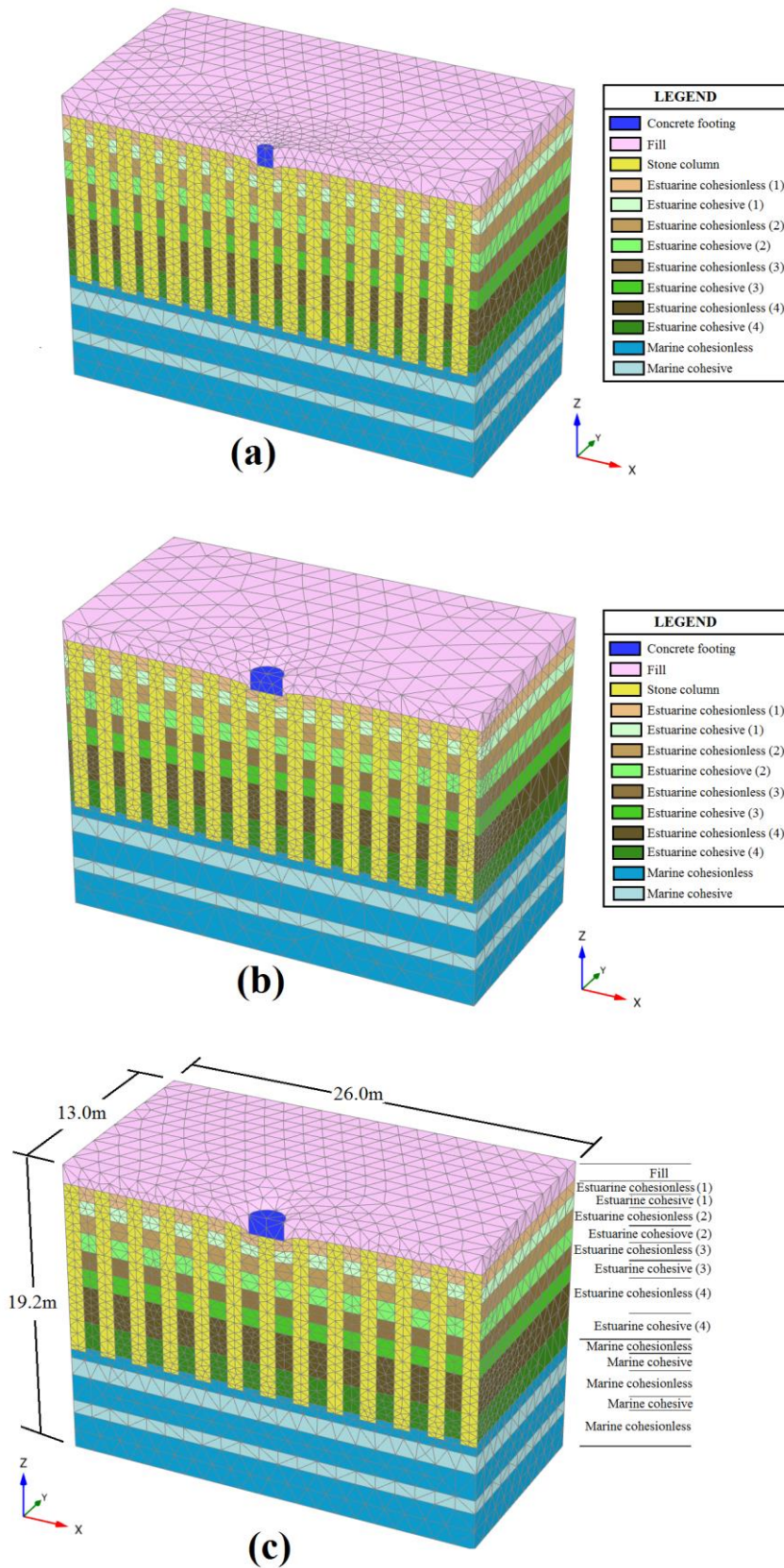
Figure 5.23 3D model geometry and finite element mesh of the of estuarine and marine deposits of Santa Barbara treatment plant case for the spacing (a) $S = 1.5 \times 1.2$m, (b) $S = 1.75 \times 1.75$m, (c) $S = 2.10 \times 2.10$m.

5.7.2 Validation Results

The final stage of validation is to compare the load-settlement results of the 3D numerical analysis for the stone columns group with the field data. To perform this comparison, the load-settlement for all degrees of applied expansion installation of the stone columns were plotted together with field records to produce Figure 5.24, Figure 5.25 and Figure 5.26 for the stone columns spacings of (S= 1.5m×1.2m), (S= 1.75m×1.75m) and (S= 2.10m×2.10m) respectively. Two additional curves were added to each of these three cases; the first is the load-settlement curve for the case of full replacement stone columns and the second for the non-reinforced soil. The three figures show that the 3D numerical load-settlement curves seem to capture the field data very well not just as a general trend, but also they appear to predict both of the upper and lower limits of most of field records based on the applied expansion cavity of the stone columns.

For the columns spacing case of (S= 2.10m×2.10m) and based on this model results, the field load-settlement data showed that the stone columns were installed with an expansion degree ranged between (0.05m – 0.20m), and for the case of (S= 1.75m×1.75m), higher expansion degree was required in installing the stone columns. This 3D model was not able to capture exactly the upper limit of the field load-settlement response for the third case of stone column spacings (S= 1.5m×1.2m), but it is not far from the load-settlement curve that correspondence to (Δ_r = 0.25m), while the bottom limit was approximately captured when (Δ_r = 0.15m). The author believe that the reason behind the shortage of the 3D results in the third case is the very close distance between the stone columns (S= 1.5m×1.2m) which caused regression in the development of both (E_{50}) and (K) to become less than their values for the case of single stone column in the top deposits.
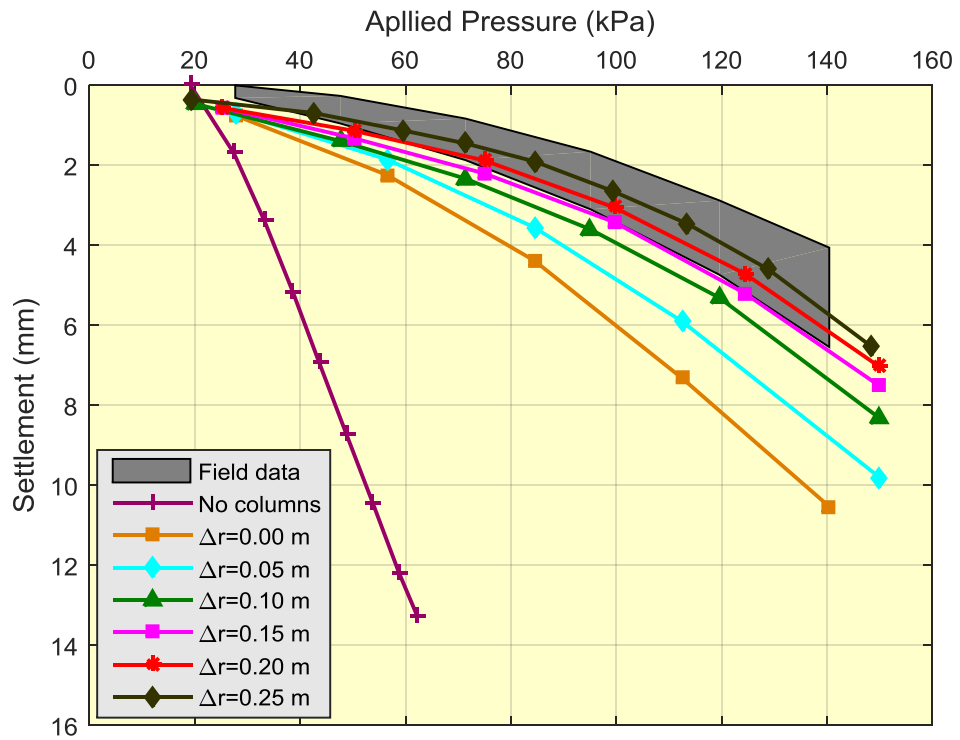
Figure 5.24 Comparison of the field load-settlement data with 3D numerical analysis results for the stone columns spacing (S= 1.5m×1.2m).
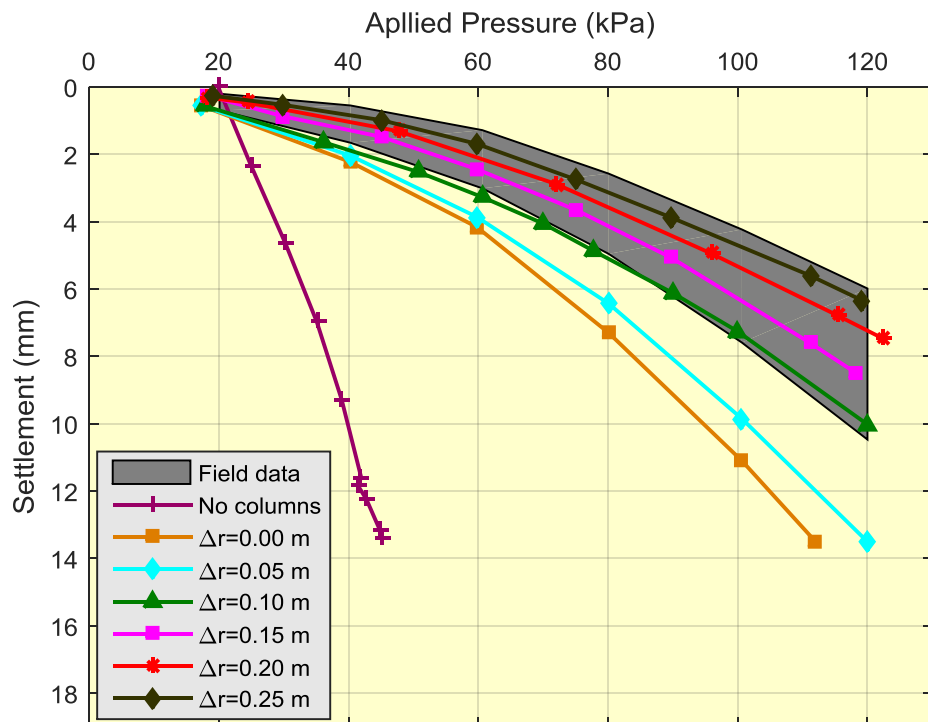
Figure 5.25 Comparison of the field load-settlement data with 3D numerical analysis results for the stone columns spacing (S= 1.75m×1.75m).
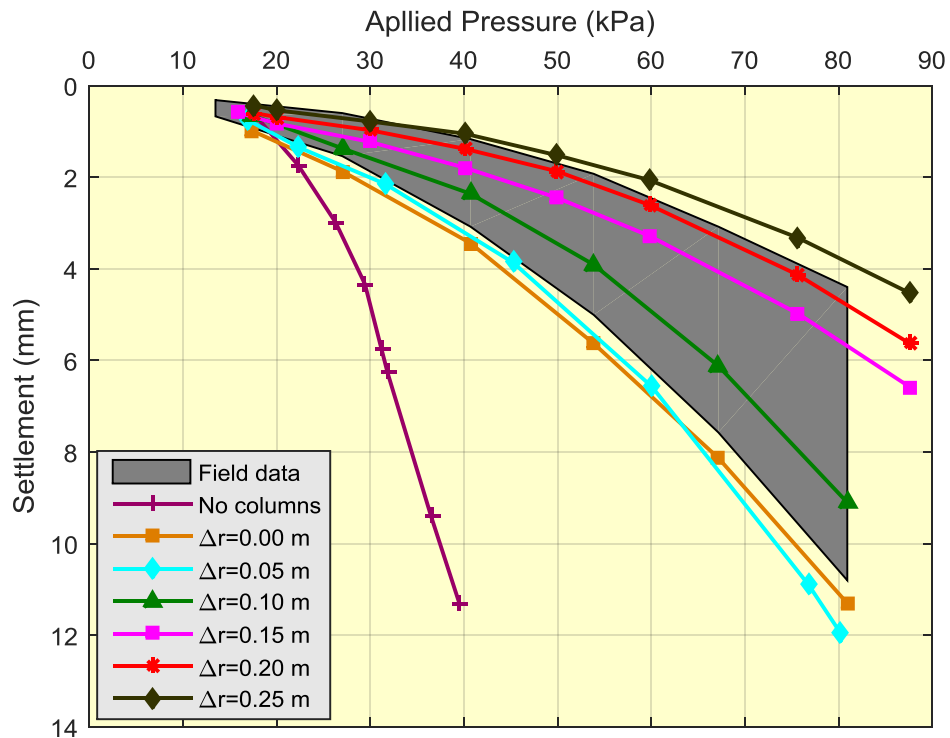
Figure 5.26 Comparison of the field load-settlement data with 3D numerical analysis results for the stone columns spacing (S= 2.10m×2.10m).

5.7.3 Comparison of 3D Numerical Analysis with Field Records and Previous Works

For accurate comparison of this study results, three different studies (Mitchell and Huber, 1985b; Elsazly et al., 2008; Killeen, 2012) performed to study the settlement performance under the reinforced foundations at Santa Barbara water platform site have been selected. All these studies used numerical analysis techniques. Moreover, all of them suggested an improvement to the coefficient of the lateral pressure (*K*) due to the stone column installation.

Mitchell and Huber (1985b) were the first to adopt the axisymmetric homogenization technique, using finite element model developed by Duncan and Chang (1970) at the University of California. They compared the field load-settlement relationship with the predictions resulting from an axisymmetric finite element model. The results of the comparison showed that the predicted settlement is greater than observed real settlement, which

means an over estimation for the settlement of the reinforced soil as is shown in Figure 5.27, Figure 5.28 and Figure 5.29. There are two main shortcomings that might make the results of Mitchell and Huber (1985b) unable to predict the actual field behaviour; the first is the new geometry of the stone columns under the footing after the redistribution using the axisymmetric homogenization methods. The author believed that the second reason is neglecting the effect of stone columns installation in improving the estuarine soil properties. He just adopted an estimation for the lateral pressure coefficient ($K=1$) for all the different spacings cases.

Although Elshazly et al. (2008) applied the same axisymmetric homogenization method used by Mitchell and Huber (1985) to restudy the field loading tests, they were more aware about the changing in the stress state of the estuarine soil between the stone columns. They calibrated this parameter utilizing the back-analysis method and found that the coefficient of lateral pressure (K) of the estuarine soil surrounding the stone columns increases from the original value of untreated clay to (1.70, 1.2 and 0.85) for the columns spacings of (S= 1.5m×1.2m), (S= 1.75m×1.75m) and (S= 2.10m×2.10m) respectively. Elshazly et al. (2008) also underestimated the settlement performance of the reinforced soil more than Mitchell and Huber (1985b), but their load-settlement curves have a better trend, which might be because of the using of advanced Hardening Soil model.

The most recent study was by Killeen (2012) who used 3D numerical analysis in his study with the Hardening Soil model, which was very positive to avoid any geometric idealizations for the stone columns distribution. As can be seen in Figure 5.27, Figure 5.28 and Figure 5.29, his load-settlement curves have a good trend and are relatively close to the lower limit of the field data, especially for columns spacing (S= 2.10m×2.10m). But, again he adopted the same value of the coefficient of lateral pressure(K= 1) used by Mitchell and Huber (1985b). Moreover, he neglected any improvement in the stiffness of the estuarine soil between the stone columns due to their installation.

The only difference between the current study results, which captured the field data very well and that Killeen's (2012), is the consideration of the improvement of the soil stiffness and lateral pressure coefficient due to the installation of the stone columns. This demonstrates the important role of improvements that occurred in the soil due to the installation of the stone columns and take the applied degree of expansion installation as an important factor to achieve an optimum design requirement for the reinforced system.
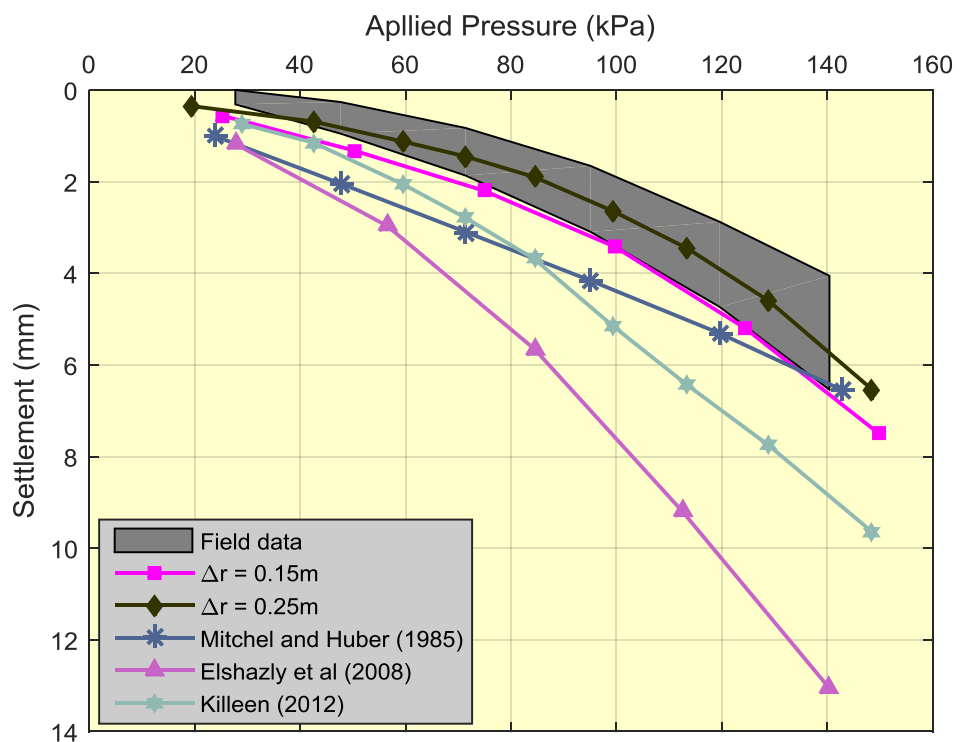
Figure 5.27 Comparison of the 3D numerical analysis results with previous research works for the stone columns spacing (S= 1.5m×1.2m).
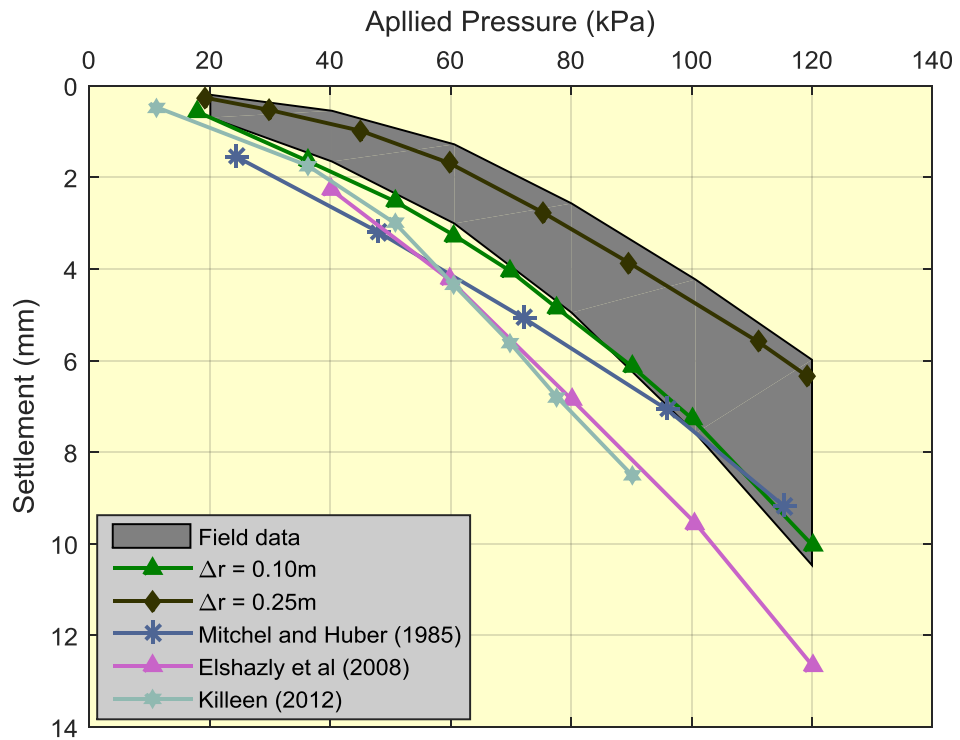
Figure 5.28 Comparison of the 3D numerical analysis results with previous research works for the stone columns spacing (S= 1.75m×1.75m).
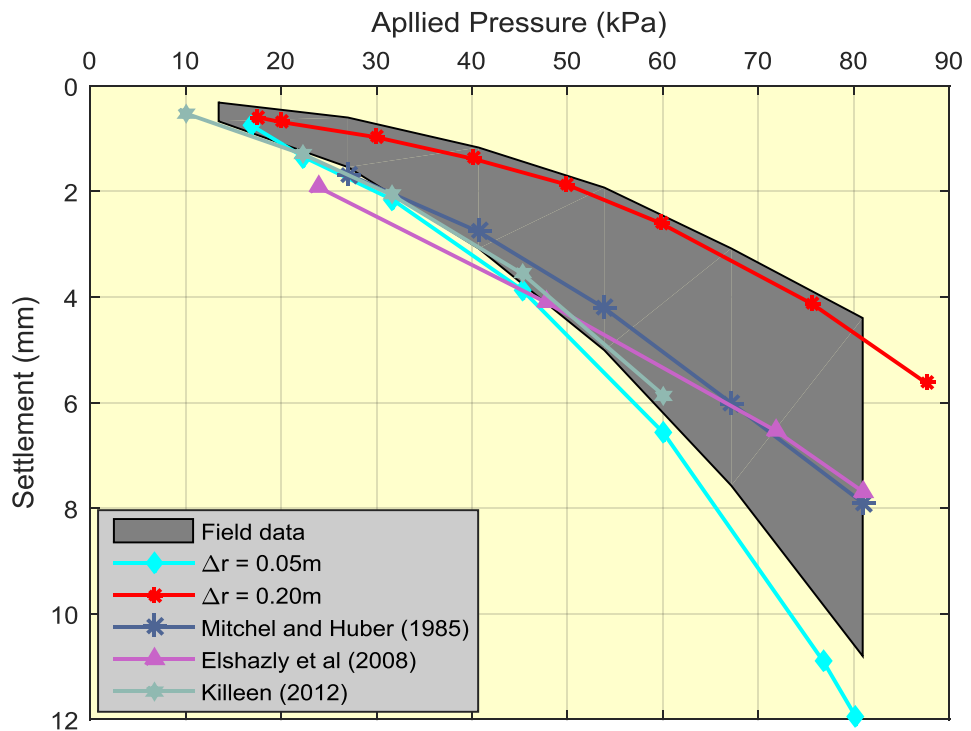
Figure 5.29 Comparison of the 3D numerical analysis results with previous research works for the stone columns spacing (S= 2.10m×2.10m).

6 Chapter 6 Conclusion and Recommendations for Future Research

6.1 Introduction

Vibro stone columns, one of the most commonly used soil improvement techniques, have been utilized worldwide to increase bearing capacity and improve the settlement performance of structures constructed on soft and weak soils. It has become of great importance after the development of its technology giving more applications for the geotechnical practice in low effective cost construction techniques, and provide effective solutions for environmental issues including recycled industrial waste, reduction of CO_2 emissions and construction energy.

The current design of stone column reinforced foundations is generally based either on theories or semi empirical methods that were developed for single stone columns or considering the composite system of the stone column reinforced ground as a homogeneous medium, ignoring the effect of the column/soil interaction, which is caused by changes in the stiffness and stress state that occur after column installation and consolidation, on the performance of this reinforced system. Although, accounting for the effect of the stone column-soil interaction problem due to the vibro installation presents challenges to engineers and academics alike, generally ignoring it in design has ended with under-estimating the performance of the reinforced system.

This thesis reports the findings of a series of 2D and 3D finite element numerical analysis which has been carried out using Plaxis 2D and Plaxis 3D Codes to study the installation effect of stone columns in soft soils on the settlement performance of the reinforced system, and then to establish design guidelines based on its findings, towards a more efficient stone column foundation design, construction and use.

257

Detailed explanation of the concept and advantages of stone column improvement technique was presented in this thesis. The comprehensive literature review in this thesis highlighted the increasing use of the stone column technique and its construction methods. Previous research efforts to study the performance of stone column reinforced system as well as proposed design methods were presented. Literature review was carried out to gain an insight into soil behaviour and characteristics that arise from the soil-structure interaction caused by the stone column installation. The literature review was also carried out to appreciate the principles and application of the finite element numerical modelling method and Plaxis software features to be applied to model stone column construction.

Cavity Expansion Theory was used to estimate the tendency of the soft soil to be improved by increasing the cavity expansion during stone column installation.

An Advanced Hardening Soil model was adopted to represent the soft soil. Soft soil profile was obtained from two different well documented field cases; the first was Bothkennar soil in Scotland because it was extensively characterised soft clay soil. It was used to create the model of single axisymmetric stone column to assess both improvement of stiffness and stress state of the soft surrounding clay due to column installation. The second was the soil of waste water treatment plant site in Santa Barbara, U.S, which was used to validate the results of the previous model for the case of stone column group, starting with accumulating the stress interaction effect of two adjacent stone columns. Then, Plaxis 3D was used to validate the finding by comparing them with the results of three load –settlement records.

This study also conducted stages and methodology for developing realistic models of single stone column and group of stone columns that led to a greater understanding of the stress interactions between the installed stone column and the surrounding soft soils. Data generated from the single and group of stone columns models were analysed for a greater insight into the performance and optimal design of stone column reinforced foundation. The

created models, methodology and findings of these studies are presented below;

6.2 Numerical Modelling

Plaxis 2D and Plaxis 3D were used to perform a series of numerical analysis to obtain the installation effect of stone column in soft soils on the settlement performance. The main stages and milestones for the Plaxis use can be summarized as follows;

- Developing a comprehensive axisymmetric model of a single stone column using Plaxis 2D AE to study the effect of installing this column in well-tested Bothkennar soil using an advanced Hardening Soil model for both of the soft soil and stone column materials.

- Validating the ability of Plaxis 2D AE and its Hardening Soil model to capture the behaviour of Bothkennar soft clay by replicating the load-displacement behaviour of this historical case.

- Using cavity expansion theory to simulate the installation of stone column to predict the variation of the excess pore water pressure and total radial stress as a short temporary changes that lead to the permanent alteration in stiffness and stress state in the soft soils. These changes were quantified with the different degrees of cavity expansion to study the installation effect of the single stone column on the performance of the treated ground under a circular footing.

- Rebuilding an axisymmetric model for single stone column installation of the well-documented Santa Barbara site which consisted of several soil layers.

- Simulating the installation of another stone column adjacent to the first one to study stress interactions between them and assess the accumulative improvement effect on stiffness modulus and lateral pressure coefficient. The axisymmetric homogenization method was used to develop a three-dimensional model for two adjacent columns to study stress interactions between these two columns. The new

259

three-dimensional distribution of stone columns within the treated clay materials has been conducted to meet the requirements of 2D simulation and keep the replacement ratio of the area, the distance between the columns and the total surface area as in the original situation.

- Developing 3D numerical model for infinite group of stone column using Plaxis 3D finite element code to incorporate the resulted changes in stresses and stiffness proved in single stone column case and accumulated in the second step (between two stone columns). The case of Santa Barbara infinite stone column group was simulated and the results were compared with the records from the field. The results shed new light on the mechanisms of group of stone column behaviour and demonstrated the value of research using 3D numerical analysis for the stone columns improvement technique.

For all the above performed stages, realistic boundary conditions including restraints, ground water table, applied loads and stone columns were adopted. Consolidation time was selected to meet the required conditions of the problem. Based on the short period of stone column installation, undrained expansion of a cylindrical cavity was used to model the installation process of a stone columns, which was applied as prescribed displacement in the finite element simulation. "Updated mesh" option was used in the analysis to account for the large deformation caused by the different degree of expansion column installation.

Due to the significant limitations in the ability of the Plaxis 3D to account and capture the installation effect of the stone column in terms of modelling large strains in soft soils, stone column installations in all of the previous stages were simulated using Plaxis 2D.

For accurate results of the analysis using Plaxis 2D and 3D code, that depends only on soil properties and geotechnical problem conditions, a sensitivity study was carried out to decide the final dimensions and appropriate finite elements mesh coarseness of model. Group of nodes and stress points located under the footing and at mid-depth of each different

260

soft soil layer were selected on the finite element mesh to generate the required results at these points.

In this thesis, the results of numerical analysis were extracted after three main phases, namely;

- Immediately after vibro installation of stone columns, quantifying the temporary changes of stress regime and pore water pressure within the zone of influence for the stone column.

- After finishing dissipation of the excess pore pressure to the stone columns drains, where an equilibrium state is reached within the zone of influence caused by the stone column installation, the result was in a new distribution of stresses within the soft saturated soil. The main feature of this new stress distribution is the increase in the effective stresses of the enhanced zone. Consequently, soil stiffness and lateral confinement around the stone column increase.

- Construction loading was applied in order to predict the effect of improved stiffness and stress variation on the settlement performance of the reinforced foundations.

6.3 Effect of Single Stone Column Installation

All the numerical analyses were performed with the presence of the stone columns to represent the actual permeability of this material during consolidation and, more importantly, to give the real behaviour of interaction between the soft soil and the stone column in all stages of construction and loading.

6.3.1 Short-Term Effect

The short-term changes that take place in the saturated soft soil immediately after stone column installation and before they develop to determine the final alteration of the reinforced soil system, are the following;

Radial displacement: The vibrating poker penetrates the soft ground applying horizontal vibratory forces while pushing the stone column material

towards the walls of column hole. Radial prescribed displacement was applied along the stone column to simulate the expansion due to the vibratory forces. The soil around the stone column absorb these forces and they undergo radial displacement. These displacement effect attenuated through the soft soil and vanished with the zone of influence distance from the column after about 7-8 from the final stone column diameter D_c for the Bothkennar clay case. This proves that the vibro installation effect of the stone column was not only absorbed by the disturbed adjacent soft soil, but it had important role in consolidating the further soft soil till it vanishes after about 6-8 times of the column dimeter in this Bothkennar case.

An approximate linear relationship was found between the increasing cavity expansion and the generated horizontal displacement within the treated soil adjacent to the stone column. Increasing the cavity expansion degree also slightly extends the horizontal zone of influence affected by this cavity up to 8 times of the column dimeter.

It was also noted that displacement of particles of soil in the upper part occurred in outwards and upwards manner to about 5-6 of the applied cavity expansion Δr, but as soon as the vibrator surpassed this distance, a radial displacement took place and remained relatively static allowing the particles after this range to be ultimately compacted.

Stresses distribution: Immediate increase in both excess pore water pressure and total horizontal stress happened during the vibro stone column installation in the undrained saturated Bothkennar clay. They started with high values adjacent to the stone column and gradually decreased to reach close to zero at a distance that ranges between 6 to 8 of final stone column diameter D_c.

To show the effect of increasing the cavity expansion when installing the stone column, 9 different degrees of expansion were applied during stone column installation, in addition to the full replacement one. Excess pore water pressure of the soil for different distances from the installed stone column at the mid of lower Bothkennar clay were compared with the

normalized expansion cavity degree, ($\Delta r /D_c$). where D_c is the final diameter of the stone column.

Increasing expansion degree during the installation of stone column had a significant influence in generating higher excess pore pressure around the stone column and within an influence area reaching about 6 - 8 D_c, and after that it had very limited effect. The pattern of excess pore pressure variation was very similar for all degrees of cavity expansion and the increase of the excess pore pressure started with a high value adjacent to the stone column and gradually decreased close to zero after the end of influence zone. Moreover, there was a kind of direct proportion between the cavity expansion during stone column installation and the resultant generated excess pore water pressure in the area close to the column. As the distance increased from this column, excess pore pressure seemed to increase very slightly after the expansion degree of 0.3m for this study case.

The sharp increase in the excess pore pressure during the installation of the stone column caused increase in horizontal stresses, especially close to the stone column. Increasing the expansion of the stone column had also noticeable effect in generating higher horizontal stresses especially within the distance 4 times the stone column diameter, while the effect of this increased after this distance to finish at about 6 -8 of the stone column diameter D_c.

6.3.2 Consolidation Stage

The excess pore pressure, that was generated adjacent to the stone column during installation started immediately to dissipate with time. In general, the soil cylinder close to the stone column, had a faster dissipation rate reducing the excess pore pressure close to its original value before the stone column installation, because of the short path to stone column drains, while consolidation time increased for the further points from the stone column axis. The consolidation time depends on the permeability characteristics (It was found that the cases of Bothkennar clay took about 60 days to dissipate

more than 90% of the generated pore water pressure, while Estuarine cohesive deposits in Santa Barbara site needed less than one day for the dissipation).

The consolidation in both cases took place mainly due to the radial dissipation of excess pore pressure toward the stone column drain, except in the top layer which was very close to the free surface, where there was no clear dissipation path.

The dissipation of the excess pore water pressure was accompanied by a reduction of horizontal stress to value in excess of the in-situ conditions. Obvious remaining increase in the total horizontal stresses after full dissipation indicates the development of effective horizontal stress, which is more important for determining the new stress state of the soft soil around the stone column and an increase in its stiffness

6.3.3 Improvement in the Coefficient of Lateral Earth Pressure

By the end of consolidation, an equilibrium state was reached within the zone of influence caused by the stone column installation, resulting in a permanent new distribution of effective stresses within the soft soil. As expected increasing the confinement around the stone column was a reaction of its expansion installation. This new confinement, which is an expression of the increase of the effective stresses, remained after the consolidation of the zone of influence. Consequently, soil stiffness around the stone column increased.

The normalized effective radial stress to effective vertical stress after consolidation was calculated to estimate the changes in the coefficient of the lateral earth pressure (K). It illustrates the new final distribution of the stresses after consolidation, and it indicates the amount of new lateral support for the installed stone column. That is, it expresses the improvement in the capacity of the stone column due to an increase in confinement.

Although some irregular random values of (K) were encountered very close to the stone column wall due to the vibro expansion installation of the stone

column, a significant increase in the coefficient of lateral earth pressure was found in the surrounding soft soil compared to its value at rest (K_0). This value decreases with the increase in radii from the column centre to return back to around (K_0) by end of the zone of influence which falls between 6 and 8 of the column diameter. The improvement in (K) was found to be varied with soil type and depth. For example, Bothekennar lower clay K reached up to 3.5 times (K_0) when applied expansion cavity of ($\Delta r = 0.45m$), while this increase was more in estuarine soil in Santa Barbara site to get up to 5-7 times (K_0) for different cohesion and cohesionless deposits. These values for both cases are higher than the average value used by the researcher who did study these two sites as Table 6.1 illustrated. This underestimation of the lateral pressure coefficient by the previous researchers ended with under estimation of the settlement performance reinforced soil.

Table 6.1 Coefficient of lateral earth pressure, (K) values that found by some previous researchers

Reference	Studied case	Coefficient of lateral earth pressure, (K)
Mitchell & Huber (1985)	Santa Barbara site	1.00
Elshazly *et al.* (2007)	Santa Barbara site	1.50
Elshazly *et al.* (2008b)	Santa Barbara site	0.85-1.70
Killeen (2012)	Santa Barbara site	1.00
Killeen & McCabe (2014)	Bothekennar Site	1.00

Increasing the degree of expansion cavity during stone column installation has a significant effect on increasing the coefficient of horizontal earth pressure. The maximum value for K at 1m from the stone column axis in this case is 1.98 correspondence to 0.45m cavity displacement and it decreases with the increase in radii from the column centre. More than 40% development in the confinement around the stone column (K) was achieved when the expansion degree increased from ($\Delta r = 0.05m$) to ($\Delta r = 0.45m$) for

the case of Bothkennar clay. While Santa Barbara case demonstrates 20-40% development in (K) was achieved when the expansion degree increased from ($\Delta r = 0.05m$) to ($\Delta r = 0.25m$) for the estuarine cohesive deposits as an average, this improvement increased to about 40-65% for the case of estuarine cohesionless deposits. This noticeable difference between the response of the estuarine cohesionless deposits and cohesive ones demonstrates that each soil has a different response to the expansion displacement of the stone column, based on its composition and properties. Another note was found about the top part of the treated soil, where it was found that the ground heaves as well as undergoing some radial expansion.

6.3.4 Improvement of Stiffness Modulus

Most of experimental work, field observations and numerical studies that have been carried out to predict the improvement of the characteristics due to vibro stone column installation were limited to estimate the changes in the stress state, namely the increase in the coefficient of lateral earth pressure and the attempt to take it into account in the design by considering one average value and ignoring the decrease of this coefficient with the distance from stone column (Elshazly et al., 2007; Elshazly et al., 2008a; Castro and Sagaseta, 2009; Zahmatkesh and Choobbasti, 2010; Killeen, 2014). They also consider that the increase in the lateral earth pressure coefficient (K_0) in the soil that surround columns could possibly account for the total effects linked to stone column installation. Some of them like Elshazly et al. (2007) implemented the finite element analysis technique to calculate the rise in K_0 through the back-calculation of the field load tests that were performed on stone columns.

In reality, the soft soil adjacent to the vibro installed stone column continues to relax with consolidation and hardening under the increase of effective mean stress and unloading of shear stresses caused by large displacement.

In this thesis, the methodology in quantifying the soft soil stiffness increase due to stone column installation was based on Biarez et al. (1998), who suggested a power law relationship between the alteration of mean effective stress and the soft soil stiffness modulus based on elastic perfectly plastic theory. Brinkgreve and Broere (2006) consider this relationship as a direct proportion between the stiffness of the soil and the mean effective stress when they suggested a value of (m =1.0) for soft soils.

266

The development of mean effective stress was estimated for both Bothkennar and Santa Barbara field cases after full primary consolidation with distance from the stone column axis. Then, based on Biarez et al. (1998) equation, secant Young Modulus has been predicted within both soils. The results were normalized with the original value of stiffness secant modulus (E_{50}^{ref}) to extract the final development of the soft soil stiffness due to single stone column installation. A dramatic increase in the soil stiffness after consolidation can be achieved when applying cavity expansion installation for both cases.

Increasing the amount of expansion during stone column installation has a significant effect on enhancing the stiffness of the surrounding soil. For the case of Bothkennar soil, 9 different degrees of cavity expansion were applied. Normalized stiffness reaches a peak of 1.29 times the initial soil stiffness at 1.0m distance from column axis for ($\Delta_r = 0.45m$). These effects extend up to distance of 4 times the final diameter of the stone column D_c. While for Santa Barbara case where 5 different degrees of cavity expansion were applied, it reached a peak up to 3 times to initial soil stiffness adjacent to the stone column for ($\Delta_r = 0.25m$) in the estruarine cohesionless deposits. These effects extend up to distance of about 5 times the final diameter of the stone column (D_c) However, the stiffness of the soil close to the cavity wall, in both cases, was not consistent with some variation by high disturbance effect adjacent to the column, especially in predominant clay soils like Bothkennar clay and the estuarine cohesive deposits.

By comparing the development of the soil stiffness and the degree of expansion cavity of stone column installation, it was noticed that each soil has its response to be compacted with increasing the radial displacement, so it was found, for example, estruarine cohesionless deposits tend to gain more stiffness with increasing (Δr) than do estruarine cohesionless deposits. Again, this response is related to the soil characteristics and depth.

Results demonstrate a significant improvement in the performance of this composite foundation when the applied lateral displacement of the installed column increases.

6.3.5 Stress Concentration Ratio

The stress concentration ratio, which expresses physically the changes of stresses and stiffness within the column/soil system, is an important

parameter in interpreting and tracking the behaviour of the stone column foundations. The uncertainty and wide range of stress concentration ratio values were found by different researchers (Aboshi et al., 1979; Bachus and Barksdale, 1984; Balaam and Booker, 1985; Saadi, 1995; Hu, 1995; McKelvey et al., 2004; Killeen and McCabe, 2014) who motivated the author to investigate the reasons for this wide variation.

In order to understand the mechanism of load transfer between the stone and surrounding soil after the vibro installation of the stone column and the effect of increasing expansion installation degree on it, stress concentration ratio was calculated as an important criterion of the improvement in stress state stiffness of the soft Bothkennar clay around the installed stone column. These changes happen within the clay immediately after the column installation process (applying radial displacement), and after radial consolidation to the vertical drains (stone columns). It was assessed assuming an equilibrium condition between the stone/clay interface during one-dimensional consolidation caused by loading.

It was found that the stress ratio is dependent on the progressive consolidation process and it changes over time. However, in this study, more concern is directed to the effect of increasing the cavity expansion during stone column installation on this stress ratio.

So, stress concentration ratio increases slightly when applying more expansion during stone column installation till it reaches a small peak at expansion degree of 0.25 m. Then, for the higher degrees, more loading start to be carried by the soft soil around the column. An important result, which supports the previous findings about the improvement in both lateral earth pressure and the stiffness of soft soil with the increase in expansion degree, is the trend of the curve after consolidation. It shows significant improvement in the role of the soft soil to carry up to 200% load more that the case of full replacement stone column. It was found that increasing cavity expansion degree of installation had a significant effect in enhancing the role of the soft soil around the stone column and reduce the stress concentration ratio from about 7 to less than 3. This means that soft soil

stiffness has increased sufficiently to take that big share of loading from the stone column.

6.3.6 Performance of Single Stone Column Reinforced Footing

The results of the enhanced stiffness modulus and lateral pressure coefficient of the soft soil were considered to assess the effect of the stone column installation on the stone column foundation system performance. To meet this goal, a numerical analysis involving applying a circular footing load and then allowing Bothkennar soft clay to consolidate for sufficient time to get the final performance of this composite system. Three main aspects of the system performance were assessed at this stage:

- **Allowable bearing capacity improvement:** The footing in this case was modelled as a prescribed displacement and 25mm settlement was applied to get the allowable pressure that the reinforced soft soil can carry.
- **Ultimate bearing capacity improvement:** As the first stage, but predetermined high settlement was applied to get the ultimate pressure that the reinforced soft soil can carry.
- **Settlement performance:** Settlement is the dominant criterion for the performance of such soft soils. The footing in this case was modelled as a thick plate that was loaded with the typical working load of 50 kPa, which was selected as a design loading for Bothkennar soft clay.

The three above stages were repeated for all cavity installation degrees including the one of full replacement stone column to be compared later with the others' results and find the final settlement improvement factor.

6.3.7 Allowable Bearing Capacity Performance

The allowable pressure – settlement curves under the centre of the footing were generated for 6 different degrees of stone column with lateral expansions beside the non-reinforced soil. The results showed that

increasing the expansion during column installation has a noticeable effect on improving the bearing capacity of reinforced ground.

To estimate the improvement in the footing bearing pressure, the allowable bearing pressure improvement factor (m_2), which is the ratio of the bearing pressure of the footing supported by different installation degrees of stone column to the bearing pressure of non-reinforced Bothkennar clay, was calculated and plotted with the Normalized expansion cavity degree, (Δr /Dc). It was found that using the full replacement stone column installation increased the ultimate bearing pressure by a factor of three. It was also found that increasing the degree of cavity expansion during stone column installation, added about 1.5 folds more to the previous improvement.

6.3.7.1 Ultimate Bearing Capacity Performance

Similar to the allowable bearing pressure improvement, the ultimate bearing pressure showed significant improvement up to 45% more than the ultimate bearing capacity of a stone column that fully replaced, when the stone column expansion degree increases to ($\Delta r = 0.45m$).

6.3.7.2 Settlement Performance

The reduction in footing settlement due to the displacement installation of the stone was evaluated with 9 different degrees of expansion. The results were compared with settlement of non-reinforced soil case. It was found that increasing the expansion during column installation to ($\Delta r = 0.45m$) reduced the settlement by a factor of three compared to that of the non-reinforced soil settlement. Moreover, by taking the comparison between the cases of full replacement stone column with others involve installing stone column with gradual higher degrees of expansion cavity, the reduction in settlement for a given expansion expressed in terms of the settlement of a stone column that replaces rather than displaces the soil is up to 60%.

It was proved the importance of taking the improvement of stiffness and stress state of the reinforced soft soil due to the stone column installation into account in designing these kinds of composite foundations.

6.4 Effect of Stone Columns Installation within Group

After estimating the changes of the Bothkennar clay due to the installation of single stone column and then quantifying its settlement and bearing pressure under a circular footing for a group of 9 different degrees of expansion cavities, it was successfully proved that the stone column installation has a significant influence on the performance of the settlement and bearing capacity. Although the case of a single stone column might be used to create a framework in taking the improvement of stiffness and stress state into account in designing the composite foundations, but it cannot be applicable as a real case and it will lead to a conservative estimation of the performance of these systems. This is because stone column foundations normally consist of a number of columns that work together with the surrounding clay to create one system. Consequently, an actual history field case of a stone column group that constructed in Santa Barbara waste water treatment plant, U.S was selected to validate the single stone column model and study of the stress interactions between two adjacent stone columns to represent the real behaviour in the field. The case of stone column group was studied in three steps;

First step: Simulate the installation of single stone column within the soft soil using Plaxis 2D, then quantify the alteration in both stress state and stiffness after installation and consolidation within each of the different deposits and for 5 different degrees of stone column lateral expansions. The new coefficient of lateral earth pressure (K) and secant stiffness modulus (E_{50}) at mid-point of each deposit were calculated and averaged within a thickness ranged between (1.0 – 1.5m), which corresponded to area of influence of each stone column within the group area of infinite reinforced system.

Second step: Use an axisymmetric homogenization method to simulate the installation of another stone column adjacent to the first one in Plaxis 2D. Then study stress interactions between the two columns and assess the

accumulative improvement effect of stiffness and confinement. The soft soil input parameters in this case took the results of the first step to account for the improvements in (K) and (E_{50}) caused by the first stone column installation. Same degree of expansion were used to install the neighbouring stone column and at three different distances (S = 1.50, 1.75, 2.10m) that corresponded to the records in Santa Barbara field case. Installing the neighbouring stone column produced more radial and mean effective stresses within the soft soil between the two column. Consequently, it generated a noticeable increase in the coefficient of lateral earth pressure and the stiffness modulus compared to the improvements in these two parameters for the case single stone column. The magnitude of these increases were calculated for 5 different expansion degrees of stone column installation and the findings can be summarized as follows;

- Increasing the expansion degree during the installation of neighbouring column had a significant effect on enhancing the lateral pressure coefficient (K) and increasing the stiffness secant modulus of the soil. For example; increasing the expansion degree from (Δ_r = 0.05m) to (Δ_r = 0.25m) for the case of inter stone column spacing (S = 2.1m) enhanced (K) up to (10%-15%) and increased (E_{50}) at about (15% and 25%). These percentages increased for less columns spacings.

- The increase in soil stiffness modulus and lateral pressure coefficient due to the installation of the adjacent stone column does not apply to all soil layers. A reduction in (E_{50}) and (K) for the top three layers were found from the second stone column effect compared to its value related of single stone column. This negative effect was traced to the level of vertical overburden pressure situated in the top layers compared to the bottom ones, therefore, the ground heaved as well and underwent some radial expansion.

- The response of soil to improve its stiffness modulus and coefficient of lateral pressure due to installing another stone column varies with its properties and depth. For example the cohesionless deposits had a better response to increase its (K) compared with the cohesive deposits, while the opposite was true for stiffness modulus (E_{50}).

272

Third step: Plaxis 3D was used to simulate the actual geometry of the infinite installed stone columns in Santa Barbara water platform field case. The resulted the lateral pressure coefficient (K) and the stiffness secant modulus (E$_{50}$) from the last step, where the effects from two stone columns installation were accumulated, were used for the soft soil among the stone column group. The load-settlement for all degrees of applied expansion installation of the stone columns were plotted together with field records to produce for the stone columns spacings of (S= 1.5m×1.2m), (S= 1.75m×1.75m) and (S= 2.10m×2.10m). Two additional curves were added to each of these three cases; the first is the load-settlement curve for the case of full replacement stone columns and the second for the non-reinforced soil. The three figures show that the 3D numerical load-settlement curves seemed to capture the field data very well not just as a general trend but also they appear to predict both of the upper and lower limits of most of field records based on the applied expansion cavity of the stone columns.

For the columns spacing case of (S= 2.10m×2.10m) and based on this model results, the field load-settlement data showed that the stone columns were installed with an expansion degree ranged between (0.05m – 0.20m), and for the case of (S= 1.75m×1.75m), higher expansion degree was required in installing the stone columns. This 3D model was not able to capture exactly the upper limit of the field load-settlement response for the third case of stone column spacings (S= 1.5m×1.2m), but it is not far from the load-settlement curve that correspondence to (Δ_r = 0.25m), while the bottom limit was approximately captured when (Δ_r = 0.15m).

6.5 Effect of Stone Columns Inter Spacings

Effect of the stone columns inter spacings on the improvement of both (*E$_{50}$*) and (*K*) due to the installation of these stone columns within a group was studied by plotting their values against the applied expansion cavity for the

three different columns spacings. Noticeable improvement in both (K) and (E_{50}) was found with the reduction of the stone columns inter spacing. This improvement does not apply for the top two deposits for the case of Santa Barbara soft soil, which reacted to the increase in expansion cavity by heaving toward the ground surface.

These findings demonstrate the importance of the stone columns inter spacing as an important factor that can be utilized not only to increase the replacement area ratio, but also to achieve a certain degree of improvement for both (K) and (E_{50}) of the soft soil between the stone columns, especially when it is coupled with applied degree of expansion cavity to create an optimum design requirement for the reinforced system.

6.6 Contribution and Relevance Summary

- Modelling the installation of stone column as an expansion cavity with the stone column acting as a vertical drain showed that the confining pressure acting on the stone column increased and the stiffness of the surrounding soil increased.
- The increase in confining pressure and stiffness varied with the soil properties and depth.
- The effect of the increase in confining pressure and stiffness on a single stone column was assessed using a shallow foundation. It showed a reduction in settlement for a given load compared to that for a full replacement column (no modification in the soil properties) and an increase in capacity.
- The capacity of the soft soil reinforced with stone columns at various locations was investigated to compare the predicted behaviour with that observed in field records. It was found that taking into account the increase in confining pressure and soil stiffness gave a better

prediction of behaviour compared to matters that do not take into account the improvement of soil due to stone columns.

6.7 Recommendation for Future Research

- By studying the improvements in both stress state and stiffness of a certain soil, an optimum value for the required cavity expansion can be calculated to achieve the most of vibro installation. the energy of construction technology can be designed for this purpose. Not taking the correct degree of expansion cavity in design may lead either to less functionality of the stone column reinforced foundation by not utilizing from all its capacity, or over estimation of the required stone material and construction time and energy needs in installing. This indicates the importance of studying effectivity of the stone column installation method on the stone column reinforced system, which depends on
  1. The soil type and its properties
  2. Spacings between the stone columns
  3. Installation method of the stone column (degree of displacement).
- Stone column reinforced foundation construction used to involve adding a finishing layer of crashed aggregates and stone called "platform" with 0.5-1.0m thickness, as a final stage to distribute the stresses between the stone columns and surrounded clay under the foundation and minimize the differential settlement. It is believed that adding this platform before installing the stone columns has a positive effect in distribute loads uniformly between columns and surrounding clay, increasing the overburden pressure over the top treated soil and reduce the heaves of the soil surface. Consequently, improve the overall settlement performance of the reinforced system. There is a need to investigate the effect of platform thickness on the performance of this stone column reinforced system.
- The current design methods of stone column foundation (semi empirical, analytical and numerical) are all based on continuum mechanics with many simplification assumptions like neglecting the fractional and lateral forced interacting at the interface between the stone column and soft

soil. It is an important suggestion related to future work is to study the inter-particle boundary between the stone column and soft soil as force-controlled particle interface, which is affected by the shape and size of the stone column particles. This can be applied using discrete element methods.

- It was found that each soil has its response to be compacted with increasing the radial displacement, this radial displacement accompanies with negative effect of ground heave of the soil top part. Egan et al. (2008) stated the presence of relationship between the density of the stone column and the heave size. It was suggested by the authors that heave is a function of the method of construction, spacing and the size of the columns. The arrangement of footing also has an impact on the heave size; smaller groups and stone columns strips produce much less heave than larger ones. There is a need to investigate the negative effect of the ground heave on the effectivity of stone column installation process.

- Although there has been good knowledge of the deformation behaviour of single and stone columns groups by many researchers (Aboshi et al., 1979, Bachus and Barksdale, 1984, Balaam and Booker, 1985, Saadi, 1995, Hu, 1995, McKelvey et al., 2004, Killeen and McCabe, 2014), there is lack of details about the effect of stone column installation on the deformation behaviour of these foundation.

7   7 List of References and Bibliography

ABOSHI, H., MIZUNO, Y., and KUWABORA, M. (1991). 'Present state of sand compaction pile in Japan', Deep Foundation Improvements: Design, Construction, and Testing, ASTM - STP 1089, 132-46.

AMMARI, K. ; CLARKE, B. (2016), 'Predicting the Effect of Vibro Stone Column Installation on Performance of Reinforced Foundations ', World Academy of Science, Engineering and Technology, International Science Index 110, International Journal of Civil, Environmental, Structural, Construction and Architectural Engineering, 10(2), 111 - 117.

ABOSHI, H., ICHIMOTO, E., ENOKI, M. & HARADA, K. The compozer—a method to improve characteristics of soft clays by inclusion of large diameter sand columns. Proc., Int. Conf. on Soil Reinforcement: Reinforced Earth and Other Techniques, 1979. Ecole des Ponts ParisTech/Laboratoire Central des Ponts et Chaussées (ENPC/LCPC), Champs-sur-Marne France, 211-216.

ALLMAN, M. & ATKINSON, J. 1992. Mechanical properties of reconstituted Bothkennar soil. Géotechnique, 42, 289-301.

AMBILY, A. P. & GANDHI, S. R. 2007. Behavior of stone columns based on experimental and FEM analysis. Journal of Geotechnical and Geoenvironmental Engineering, 133, 405-415.

ANANDARAJAH, A. 2010. Computational Methods in Elasticity and Plasticity: Solids and Porous Media, New York, Springer.

AQIL, U., TATSUOKA, F., UCHIMURA, T., LOHANI, T. N., TOMITA, Y. & MATSUSHIMA, K. 2005. Strength and deformation characteristics of recycled concrete aggregate as a backfill material. Soils and foundations, 45, 53-72.

ATKINSON, J. 2007. The mechanics of soils and foundations, CRC Press.

AYADAT, T., HANNA, A. M. & HAMITOUCHE, A. 2008. Soil improvement by internally reinforced stone columns. Proceedings of the ICE-Ground Improvement, 161, 55-63.

BALAAM, N. & BOOKER, J. 1985. Effect of stone column yield on settlement of rigid foundations in stabilized clay. International journal for numerical and analytical methods in geomechanics, 9, 331-351.

BALAAM, N. & BOOKER, J. R. 1981. Analysis of rigid rafts supported by granular piles. International Journal for Numerical and Analytical Methods in Geomechanics, 5, 379-403.

BALAAM, N. & BROWN, P. 1977. Settlement analysis of soft clay reinforced with granular piles.

BALAAM, N. & POULOS, H. 1978. Methods of analysis of single stone columns.

BALAAM, N. P. and Poulos, H. G. (1983). 'The behaviour of foundations supported by clay stabilised by stone columns', Proceedings of the Eighth European Conference on Soil Mechanics and Foundation Engineering, Helsinki, Vol. 1, pp. 199-204.

BALAAM, N. P. 1978. Load settlement behaviour of granular piles.

BARKSDALE, R. D. and BACHUS, R. C. (1983). 'Design and construction of stone columns, Volume 1', Report No. FHWA/RD-83/026. U.S. Federal Highway Administration.

BAUMANN, V. & BAUER, G. 1974. The performance of foundations on various soils stabilized by the vibro-compaction method. Canadian Geotechnical Journal, 11, 509-530.

BELL, A. L. THE LATERAL PRESSURE AND RESISTANCE OF CLAY AND THE SUPPORTING POWER OF CLAY FOUNDATIONS. Minutes of the Proceedings, 1915. Thomas Telford, 233-272.

BIAREZ, J., GAMBIN, M., GOMES-CORREIA, A., FLAVIGNY, E. & BRANQUE, D. 1998. Using pressuremeter to obtain parameters to elastic-plastic models for sands. Geotechnical Site Characterization, Roberton & Mayne, Balkerna, Rotterdam.

BIOT, M.A. (1941). 'General theory of three-dimensional consolidation', Journal of Applied Physics, 12(2), 155-164.

BLACK, J., SIVAKUMAR, V., MADHAV, M. R. & MCCABE, B. 2006. An improved experimental test set-up to study the performance of granular columns. Geotechnical Testing Journal, 29, 193-199.

BRAUNS, J. Initial bearing capacity of stone column and sand piles. Proc. Symp.„Soil Reinforcing and Stabilizing Techniques in Engineering Practise", Sydney, 1978.

BRINKGREVE, R. & BROERE, W. 2006. Plaxis 3D Foundation manual, Version 1.5. Delft University of Technology and PLAXIS bv, The Netherland.

BRINKGREVE, R., SWOLFS, W. & ENGIN, E. 2011. PLAXIS 2D Reference manual. Delft University of Technology and PLAXIS bv The Netherlands.

BRINKGREVE, R. B. J., ENGIN, E AND SWOLFS, W. M 2014. PLAXIS 2D AE.02 Foundation Manual version 2.1. PLAXIS BV.

BURLAND, J. B. 1987. Nash Lecture: The Teaching of Soil Mechanics - a Personal View. 9th ECSMFE. Dublin.

BURLAND, J. B. and ROSCOE, K. H. (1969). 'Local strains and pore pressures in a normally consolidation clay layer during one-dimensional consolidation', Geotechnique, 19(3), 335-356.

CASTRO, J. & SAGASETA, C. 2007. Consolidation around stone columns. Influence of column deformation. International Journal for Numerical and Analytical Methods in Geomechanics, 33, 851-77.

CASTRO, J. & SAGASETA, C. 2009. Consolidation around stone columns. Influence of column deformation. International Journal for Numerical and Analytical Methods in Geomechanics, 33, 851-877.

CHARLES, J. & WATTS, K. Compressibility of soft clay reinforced with granular columns. Proceedings of the 8th European conference on soil mechanics and foundation Engineering, Helsinki, 1983. 347-352.

CHRISTOULAS, S., BOUCKOVALAS, G. & GIANNAROS, C. 2000. An Experimental Study on Model Stone Columns. 地盤工学会論文報告集, 40, 11-22.

CLARKE, B. G. 1990. Pressuremeter in Geotechnical Engineering, Glasgow, Blackie Academic and Professional.

CLAYTON, C., HIGHT, D. & HOPPER, R. 1992. Progressive destructuring of Bothkennar clay. implications for sampling and reconsolidation procedures. Géotechnique, 42, 219-239.

COOPER, M. & ROSE, A. 1999. Stone column support for an embankment on deep alluvial soils. Proceedings of the ICE-Geotechnical Engineering, 137, 15-25.

CUNDALL, P. A. & STRACK, O. D. L. 1979. A discrete numerical model for granular assemblies. Geotechnique, 29, 47-65.

DATYE, K. R. SETTLEMENT AND BEARING CAPACITY OF FOUNDATION SYSTEM WITH STONE COLUMNS. 1985 Bangkok, Thail. A. A. Balkema, 85-103.

DESAI, C. S. & ABEL, J. F. 1972. Introduction to the Finite Element Method, New York, Van Nostrand Reinhold Company.

DOMINGUES, T. S., BORGES, J. L. AND CARDOSO, A. S. (2007b). Stone columns in embankments on soft soils. Analysis of the effect of the gravel deformability. 14th European Conf. on Soil Mechanics and Geotechnical Engineering, Madrid, Vol. 3, 1445–1450

DU YANJUN, Y. Y. L. S. & NENGHE, J. F. G. 2010. Field tests on bearing capacity of single diameter-varied soil-cement deep mixed column [J]. Journal of Southeast University (Natural Science Edition), 2, 027.

DUNCAN, J. M. & CHANG, C.-Y. 1970. Nonlinear analysis of stress and strain in soils. Journal of the soil mechanics and foundations division, 96, 1629-1653.

EGAN, D., SCOTT, W. & MCCABE, B. Installation effects of vibro replacement stone columns in soft clay. 2nd International Workshop on Geotechnics of Soft Soils, September 3, 2008 - September 5, 2008, 2009 Glasgow, Germany. CRC Press, 23-29.

ELSHAZLY, H., ELKASABGY, M. & ELLEBOUDY, A. 2008a. Effect of inter-column spacing on soil stresses due to vibro-installed stone columns: Interesting findings. Geotechnical and Geological Engineering, 26, 225-36.

ELSHAZLY, H., HAFEZ, D. & MOSSAAD, M. 2006. Back-calculating vibro-installation stresses in stone-column-reinforced soils. Ground Improvement, 10, 47-53.

ELSHAZLY, H., HAFEZ, D. & MOSSAAD, M. 2007. Settlement of circular foundations on stone column-reinforced grounds. Ground Improvement, 11, 163-70.

ELSHAZLY, H. A., HAFEZ, D. H. & MOSSAAD, M. E. 2008b. Reliability of conventional settlement evaluation for circular foundations on stone columns. Geotechnical and Geological Engineering, 26, 323-334.

ETEZAD-BOROJERDI, M. 2007. Geotechnical performance of group of stone columns. Concordia University.

FANG, Q., TSUCHIYA, T. & YAMAMOTO, T. 2002. Finite difference, finite element and finite volume methods applied to two-point boundary value problems. Journal of Computational and AppliedMathematics, 139, 9-19.

FORD, A. 1999. Modeling the Environment: An Introduction to System Dynamics Models of Environmental Systems, Washington D.C., Island Press.

GÄB, M., SCHWEIGER, H., THURNER, R. & ADAM, D. Field trial to investigate the performance of a floating stone column foundation. Proceedings of the 14th European Conference on Soil Mechanics and Geotechnical Engineering, Madrid, Spain, 2007. 24-27.

GAB, M., SCHWEIGER, H. F., KAMRAT-PIETRASZEWSKA, D. & KARSTUNEN, M. Numerical analysis of a floating stone column foundation using different constitutive models. 2nd International Workshop on Geotechnics of Soft Soils, September 3, 2008 - September 5, 2008, 2009 Glasgow, Germany. CRC Press, 137-142.

GERRARD, C., PANDE, G. & SCHWEIGER, H. 1984. Modelling the behaviour of soft clays reinforced with stone columns. Proc. Coll. Int. sur le renforcement en place des sols et des roches, 145.

GIBSON, R. & ANDERSON, W. 1961. In situ measurement of soil properties with the pressuremeter. Civil engineering and public works review, 56, 615-618.

GILL, D. R. & LEHANE, B. M. 2001. An optical technique for investigating soil displacement patterns. ASTM geotechnical testing journal, 24, 324-329.

GREENWOOD, D. Mechanical improvement of soils below ground surface. Inst Civil Engineers Proc, London/UK/, 1970.

GREENWOOD, D. 1975. Vibroflotation: Rationale for design and practice. Methods of treatment of unstable ground, 189-209.

GREENWOOD, D. & KIRSCH, K. Specialist ground treatment by vibratory and dynamic methods. Proceedings of the International Conference on Advances in Piling and Ground Treatment for Foundations, 1983. 17-45.

GREENWOOD, D. A. 1991a. Load tests on stone columns. Deep Foundation Improvements: Design, Construction, and Testing, 1089, 148.

GREENWOOD, D. A. 1991b. Load tests on stone columns. Deep Foundation Improvements: Design, Construction, and Testing, 148.

GUETIF, Z., BOUASSIDA, M. & DEBATS, J. 2007a. Improved soft clay characteristics due to stone column installation. Computers and Geotechnics, 34, 104-111.

GUETIF, Z., BOUASSIDA, M. & DEBATS, J. M. 2007b. Improved soft clay characteristics due to stone column installation. Computers and Geotechnics, 34, 104-111.

HAFEZ, D. H. (2003). Finite element study of the behaviour of stone columns (M.Sc. Thesis). Cairo University.

HAN, J. & YE, S. L. 2001. Simplified method for consolidation rate of stone column reinforced foundation. Journal of Geotechnical and Geoenvironmental Engineering, 127, 597-603.

HASSEN, G., BUHAN, P. D. & ABDELKRIM, M. 2010. Finite element implementation of a homogenized constitutive law for stone column-reinforced foundation soils, with application to the design of structures. Computers and Geotechnics, 37, 40-49.

HAWKINS, A., LARNACH, W., LLOYD, I. & NASH, D. 1989. Selecting the location, and the initial investigation of the SERC soft clay test bed site. Quarterly Journal of Engineering Geology and Hydrogeology, 22, 281-316.

HIGHT, D., BOND, A. & LEGGE, J. 1992. Characterization of the Bothkennaar clay: an overview. Géotechnique, 42, 303-347.

Holm, G. (2001). 'Deep mixing', American Society of Civil Engineering, Geotechnical Special Publication 112, pp 105-122.

Hu, W. (1993) Analysis of regular inhomogeneous soils: Application to stone column reinforced foundation (First year research report). Civil Engineering Department, University of Glasgow.

HU, W. 1995. Physical modelling of group behaviour of stone column foundations. University of Glasgow.

HUGHES, J. & WITHERS, N. 1974. Reinforcing of soft cohesive soils with stone columns. Ground engineering, 7.

HUGHES, J., WITHERS, N. & GREENWOOD, D. 1975. A field trial of the reinforcing effect of a stone column in soil. Geotechnique, 25, 31-44.

INDRARATNA, B., BASACK, S. & RUJIKIATKAMJORN, C. 2013. Numerical Solution of Stone Column-Improved Soft Soil Considering Arching, Clogging, and Smear Effects. Journal of Geotechnical & Geoenvironmental Engineering, 139, 377-94.

GOUGHNOUR, R. R. AND BAYUK, A. A. (1979). Analysis of stone column-soil matrix interaction under vertical load. Proc. Int. Conf. on Soil Mechanics Reinforcement, Paris, 271–277

JEBE, W. & BARTELS, K. The development of compaction methods with vibrators from 1976 to 1982. 8th European Conference on Soil Mechanics and Foundation Engineering, 1983.

JURAN, I. & GUERMAZI, A. 1988. Settlement response of soft soils reinforced by compacted sand columns. Journal of geotechnical engineering, 114, 930-943.

KALALA, J. T. & MOYS, M. H. 2004. Discrete element method modelling of liner wear in dry ball milling. School of Process and Materials Engineering, University of the Witwatersrand, Johannesburg.

KELLER FOUNDATION GROUP – Stone Column Installation <http://kellerfoundations.co.uk/technique/vibro-stone-columns> (Accessed 25 June 2011).

KEZDI, A. (1979). Stabilization with Lime. Development in Geotechnical Engineering. Vol. 19, Elsevier Scientific: Amsterdam. Pp 163-174.

KILLEEN, M. A. M., BRYAN. 2012. Numerical modelling of small groups of stone columns. National University of Ireland.

KILLEEN, M. M. & MCCABE, B. A. A numerical study of factors governing the performance of stone columns supporting rigid footings on soft clay. 7th European Conference on Numerical Methods in Geotechnical Engineering, NUMGE 2010, June 2, 2010 - June 4, 2010, 2010 Trondheim, Norway. Taylor & Francis - Balkema, 833-838.

KILLEEN, M. M. & MCCABE, B. A. 2014. Settlement performance of pad footings on soft clay supported by stone columns: A numerical study. Soils and Foundations, 54, 760-776.

Kimura, T., Nakase, A., Saitoh, K. And Takemura, J. (1983) "Centrifuge tests on sand compaction piles", Proc. 7th Asian Regional Conf. On Soil Mechanics and Foundation Engineering, Vol. 1, 255-260.

KIRSCH, F. (2004) vibro stone column installation and its effect on ground improvement. Vortrage der Bavgrundtagung, Leipzin. 149-156 Essen VGE.

KIRSCH, F. & SONDERMANN, W. Field measurements and numerical analysis of the stress distribution below stone column supported embankments and their stability. Workshop on Geotechnics of Soft Soils-Theory and Practice, Essen, 2003. 595-600.

KONDNER, R. 1963. Hyperbolic stress-strain response: cohesive soils. Proceedings of the Journal of Soil Mechanics and Foundation Division (ASCE), 98, 115-143.

LEE J.S. and Pande G.N. (1994) " Analysis of stone column reinforced foundations" Departmental Research Report CR1835194, University College of Swansea.

LEROUEIL, S., LEART, P., HIGHT, D. & POWELL, J. 1992. Hydraulic conductivity of a recent estuarine silty clay at Bothkennar. Geotechnique, 42, 275-288.

MADHAV, M. R., and Vitkar, P. P. _1978_. "Strip footing on weak clay stabilized with a granular trench or pile." Can. Geotech. J., 15_4_, 605–609.

MAGNIER, S. A. & DONZE, F. V. 1998. Numerical simulation of impacts using a discrete element method. Mechanics of Cohesive-Frictional Materials, 3, 257-276.

MARFURT, K. J. 1984. Accuracy of finite-difference and finite-element modelling of the scalar and elastic wave equation. Geophysics, 49, 533-549.

MCCABE, B. A., NIMMONS, G. J. & EGAN, D. 2009. A review of field performance of stone columns in soft soils. Proceedings of the Institution of Civil Engineers: Geotechnical Engineering, 162, 323-334.

MCDOWELL, C. (1966). Evaluation of Soil-Lime stabilization Mixtures. Highway Research Broad, Highway Research Record No. 139, 15-41.

MCKELVEY, D., Sivakumar, V., Bell, A., and Graham, J., 2004, "A Laboratory Model Study of the Performance of Vibrated Stone Columns in Soft Clay," J. Geotech. Eng., Vol. 152, pp. 1–13.

MCKELVEY, D. 2002. The performance of vibro stone column reinforced foundations in deep soft ground. Queen's University of Belfast.

MCKELVEY, D., SIVAKUMAR, V., BELL, A. & GRAHAM, J. 2004. Modelling vibrated stone columns in soft clay. Proceedings of the Institution of Civil Engineers: Geotechnical Engineering, 157, 137-149.

MEYERHOF, G. 1961. The ultimate bearing capacity of wedge-shaped foundations-La force portante des fondations en coins. Technical Memorandum, Division of Building Research, National Research Council Canada, 1-5.

MITCHELL, J. K. 1981. Soil improvement: state-of-the-art, Department of Civil Engineering, University of California.

MITCHELL, J. K. & HUBER, T. R. 1985a. PERFORMANCE OF A STONE COLUMN FOUNDATION. Journal of geotechnical engineering, 111, 205-223.

MITCHELL, J. K. & HUBER, T. R. STONE COLUMN FOUNDATIONS FOR A WASTEWATER TREATMENT PLANT: A CASE HISTORY. 1985b Bangkok, Thail. A. A. Balkema, 573-587.

MOSELEY M. P. and PRIEBE H. J. (1993) Vibro techniques. Ground Improvement, Chapman and Hall, UK.

MUNFAKH, G. A., SARKAR, S. K. & CASTELLI, R. J. PERFORMANCE OF A TEST EMBANKMENT FOUNDED ON STONE COLUMNS. 1984 London, Engl. Engl, 259-265.

MUIR WOOD, D., HU, W. AND NASH, D. F. T. (2000). Group effects in stone column foundations: model tests. Geotechnique 50(6): 689–698.

NARASIMHA RAO, S., MADHIYAN, M. & PRASAD, Y. Influence of bearing area on the behavior of stone columns. Proc., Indian Geotech. Conf, 1992. 235-237.

NASH, D., POWELL, J. & LLOYD, I. 1992a. Initial investigations of the soft clay test site at Bothkennar. Geotechnique, 42, 163-181.

NASH, D., SILLS, G. & DAVISON, L. 1992b. One-dimensional consolidation testing of soft clay from Bothkennar. Geotechnique, 42, 241-256.

PLAXIS (2008) Plaxis Finite Element Code for Soil and Rock Analyses, 2D-Version 9. Plaxis BV, Delft, The Netherlands.

PENNINE Vibro Piling - Stone Column Construction <http://www.penninevibropiling.com/library.html> (Accessed 24 June 2011).

POOROOSHASB, H. B and MEYERHOF, C. G (1997). Analysis of behaviour of stone columns and line columns computers and Geotechnics, vol 20 No 1, P 47-70.

Potts, D.M. and Zdravkovic, L. (1999). Finite element analysis in geotechnical engineering: theory. Thomas Telford

PRIEBE, H. 1976. Evaluation of the settlement reduction of a foundation improved by Vibro-Replacement. Bautechnik, 5, 160-162.

PRIEBE, H. Design criteria for ground improvement by stone columns. Proceedings of the Fourth National Conference on Ground Improvement, 1993.

PRIEBE, H. J. 1991. Vibro-replacement–design criteria and quality control. Deep Foundation Improvements: Design, Construction, and Testing, ASTM STP, 1089, 62-72.

PRIEBE, H. J. & GRUNDBAU, K. 1995. Design of vibro replacement. Ground Engineering, 28, [d]31-37.

PULKO, B. & MAJES, B. Simple and accurate prediction of settlements of stone column reinforced soil. 16th International Conference on Soil Mechanics and Geotechnical Engineering: Geotechnology in Harmony with the Global Environment, ICSMGE 2005, September 12, 2005 - September 16, 2005, 2005 Osaka, Japan. Millpress Science Publishers, 1401-1404.

RANDOLPH, M. F., CARTER, J. & WROTH, C. 1979. Driven piles in clay—the effects of installation and subsequent consolidation. Geotechnique, 29, 361-393.

RAO, S. S. 2005. The Finite Element Method in Engineering, Butterworth-Heinemann.Hill.

REDDY, J. N. 1993. An Introduction to the Finite Element Method, New York, McGraw-

ROWE, P. W. (1962). The stress-dilatancy relation for static equilibrium of an assembly of particles in contact. Proc. Royal Society A, Vol. 269, No. 1339, 500–527

SAADI, A. 1995. The behaviour of strip footings on stone columns. Ph.D, South Bank University.

SCHANZ, T. & VERMEER, P. A. 1998. Special Issue on Pre-Failure Deformation Behavior of Geomaterials. Geotechnique, 48, 383-387.

SCHANZ, T., VERMEER, P. & BONNIER, P. 1999. The hardening soil model: formulation and verification. Beyond 2000 in computational geotechnics, 281-296.

Schweiger, H.F. and Pande, G.N. (1986), "Modelling behaviour of stone column reinforced soft clays", Proc. 2nd Int. Symp. Num. Models in Geomechanics, Ghent, M. Jackson & Son, Publishers Ltd., pp 171-77.

Schweiger, H.F. and Pande, G.N. (1986), "Numerical analysis of stone column supported foundations", Computers & Geotechnics, Vol. 2, pp. 347-372.

SCHWEIGER, H. & PANDE, G. 1988. Numerical analysis of a road embankment constructed on soft clay stabilised with stone columns. Proceedings, numerical method in geomechanics, Innsbruck, 1329-1333.

SHAHU, J. T. & REDDY, Y. R. 2012. Clayey soil reinforced with stone column group: Model tests and analyses. Journal of Geotechnical and Geoenvironmental Engineering, 137, 1265-1274.

SHUI-LONG, S, YONG-GIN, J, FENG-XI, C and YE-SHUANG, X. (2005). Mechanism of property changes of soft clays around deep mixing column, Chinese Journal of Rock Mechanics and Engineering, Vol. 24, No. 23.

SHEN, S.-L., JIANG, Y.-Q., CAI, F.-X. & XU, Y.-S. 2005. Mechanisms of property changes of soft clays around deep mixing column. 岩石力学与工程学报, 24.

SHIEN, N. K. 2011. Cavity Expansion Approach In Modelling Stone Column Installation Effect. International Journal of Advances in Engineering Science and Technology, V2, 252-260.

SIMPSON, B. & TATSUOKA, F. 2008. Geotechnics: the next 60 years.

SLOCOMBE, B., BELL, A. & BAEZ, J. 2004. The densification of granular soils using vibro methods. Ground and Soil Improvement, 153.

SMITH, P., JARDINE, R. & HIGHT, D. 1992. The yielding of Bothkennar clay. Géotechnique, 42, 257-274.

SONDERMANN, W. AND WEHR, W. (2004). Deep vibro techniques, Ground Improvement, 2nd Edition, edited by M.P. Moseley and K. Kirsch, 57–92, Spon Press

STEWART, W.M. and HU, W. (1993), "Analysis of regular inhomogeneous soils-report on pilot tests", Departmental Research Report CE-GE93-27, Glasgow University.

TERASHI, M. & KITAZUME, M. 1990. Bearing capacity of clay ground improved by sand compaction piles of low replacement area ratio. Report of the Port and Harbour Research Institute, 29.

THORBURN, S. 1975. Building structures supported by stabilized ground. Geotechnique, 25, 83-94.

THORBURN, S. & MACVICAR, R. 1968. Soil stabilization employing surface and depth vibrators. The Structural Engineer, 46.

VANIMPE, W. F. MADHAV, M. R. and VANDERCRUYSSEN, J. P. (1997) Considerations in stone column design. Proceedings of the 3rd.

VAUTRAIN, J. 1977. Reinforced earth wall on stone column in soil. Symposium on soft clay. Bangkok.

VESIC, A. S. 1972. Expansion of cavities in infinite soil mass. Journal of Soil Mechanics & Foundations Div, 98.

VIBROFLOTATION GROUP "Vibratory ground improvement manual" , <http://www.vibroflotation.com/vibroflotation6.htm> (Accessed 20 June 2011).

WATTS, F. 2000. Specifying vibro stone columns. British Research Establishment (BRE) Report, Watford, UK.

WATTS, K. S., CHARLES, J. A. & BUTCHER, A. P. 1989. Ground improvement for low-rise housing using vibro at a site in Manchester. Municipal engineer, 6, 145-157.

WEBER, T. M., SPRINGMAN, S. M., GAB, M., RACANSKY, V. & SCHWEIGER, H. F. Numerical modelling of stone columns in soft clay under an embankment. 2nd International Workshop on Geotechnics of Soft Soils, September 3, 2008 - September 5, 2008, 2009 Glasgow, Germany. CRC Press, 305-311.

WEHR, W. 1999. Schottersäulen–das Verhalten von einzelnen Säulen und Säulengruppen. Geotechnik, 22, 40-47.

WOOD, D. M. (1990) "Soil Behaviour and Critical State Soil Mechanics" Cambridge University Press.

WOOD, D. M., HU, W. & NASH, D. 2000. Group effects in stone column foundations: model tests. Geotechnique, 50, 689-698.

YASUI, S., YOKOZAWA, K., YASUOKA, N. AND KONDO, H. (2005). Recent technical trends in Dry Mixing (DJM) in Japan. Proceedings of International Conference on Deep Mixing - Best Practice and Recent Advances (Deep Mixing 05), Sweden, 15-22.

YU, H. (2000). Cavity expansion methods in geomechanics. Kluwer Academic Publishers BV, Dordrecht, NL

ZAHMATKESH, A. & CHOOBBASTI, A. 2012. Settlement evaluation of soft clay reinforced with stone columns using the equivalent secant modulus. Arabian Journal of Geosciences, 5, 103-9.

ZIENKIEWICZ, O. C., KELLY, D. W. & BETTESS, P. 1977. The Coupling of the Finite Element Method and Boundary Solution Procedures. International Journal for Numerical Methods in Engineering, 11, 377-375.